UNIVERSIDADE FEDERAL DE SANTA CATARINA
CENTRO DE CIÊNCIAS AGRÁRIAS
PROGRAMA DE PÓS-GRADUAÇÃO EM RECURSOS GENÉTICOS VEGETAIS

Daniel Ferreira Holderbaum

Um modelo *in vitro* para identificação de propriedades emergentes da transformação genética de plantas

Florianópolis
2019

Daniel Ferreira Holderbaum

Um modelo *in vitro* para identificação de propriedades emergentes da transformação genética de plantas

Tese submetida ao Programa de Pós-Graduação em Recursos Genéticos Vegetais da Universidade Federal de Santa Catarina para a obtenção do título de Doutor em Ciências.
Orientador: Prof. Miguel Pedro Guerra, Dr.

Florianópolis
2019

Ficha de identificação da obra elaborada pelo autor,
através do Programa de Geração Automática da Biblioteca Universitária da UFSC.

Holderbaum, Daniel Ferreira
Um modelo in vitro para identificação de propriedades emergentes da transformação genética de plantas / Daniel Ferreira Holderbaum ; orientador, Miguel Pedro Guerra, 2018.
202 p.

Tese (doutorado) - Universidade Federal de Santa Catarina, Centro de Ciências Agrárias, Programa de Pós Graduação em Recursos Genéticos Vegetais, Florianópolis, 2018.

Inclui referências.

1. Recursos Genéticos Vegetais. 2. Plantas transgênicas. 3. Milho (Zea mays spp. mays). 4. Modelos. 5. Propriedades emergentes. I. Guerra, Miguel Pedro. II. Universidade Federal de Santa Catarina. Programa de Pós Graduação em Recursos Genéticos Vegetais. III. Título.

Daniel Ferreira Holderbaum

Um modelo *in vitro* para identificação de propriedades emergentes da transformação genética de plantas

O presente trabalho em nível de doutorado foi avaliado e aprovado por banca examinadora composta pelos seguintes membros:

Prof. Marcelo Rogalski, Dr.
Universidade Federal de Viçosa

Prof[a]. Neusa Steiner, Dr[a].
Universidade Federal de Santa Catarina

Prof. Rubens Onofre Nodari, Dr.
Universidade Federal de Santa Catarina

Certificamos que esta é a **versão original e final** do trabalho de conclusão que foi julgado adequado para obtenção do título de doutor em Ciências.

Assinado de forma digital por Claudio Roberto Fonseca Sousa Soares:50108557553
Dados: 2019.10.12 09:53:45 -03'00'

Prof. Cláudio Roberto Fonsêca Sousa Soares, Dr.
Coordenador(a) do Programa

Miguel Pedro Guerra:23245174004
Assinado de forma digital por Miguel Pedro Guerra:23245174004
Dados: 2019.10.11 15:28:37 -03'00'

Prof. Miguel Pedro Guerra, Dr.
Orientador

Florianópolis, 2019

Dedico este trabalho aos que perseveram.

AGRADECIMENTOS

Esta tese é fruto de intensa dedicação e esforço na busca do conhecimento e da verdade, e, no fim das contas, na busca por si mesmo. Sua realização só foi possível devido à presença, atividade, serviço e cooperação de inúmeras pessoas. Gostaria de agradecer expressamente aos meus pais, Virson Holderbaum e Sonia Ferreira Holderbaum, por terem me criado e educado no melhor das suas capacidades, apoiado em todos os momentos, e estimulado em mim a curiosidade e a busca por conhecimento e sabedoria; aos meus irmãos, André, Flora e Saulo, que muito me apoiaram e ensinaram em múltiplos sentidos; à querida Denise Olkoski, que me apoiou incondicionalmente durante todo o doutorado, e com quem muito aprendi sobre ciência e sobre a vida; ao meu orientador, Professor Miguel Pedro Guerra, por todo conhecimento transmitido, responsabilidade e confiança depositada (e pela paciência); ao Professor Rubens Onofre Nodari, meu coorientador extra-oficial e líder da pesquisa sobre plantas transgênicas no PPG-RGV; aos membros da banca avaliadora desta Tese, Professores Marcelo Rogalski, Neusa Steiner e Rubens Nodari; ao Professor Terje Traavik, que sem saber (?) plantou a semente de um estudo que foi se desenvolvendo e mutando até chegar nesta tese; aos meus amigos e colegas do RGV/LFDGV/CCA/UFSC/Mundo, que de diferentes formas contribuíram para a minha reflexão, meu estudo e meu trabalho no laboratório: Thiago Ornellas, Yohan Fritche, Edison Cardona, Ramon Scherer, Dorival Almeida, Daniela Werner, Patrick Marques, Catarina Puttkamer, Liliana Pilla, Joseph Ree, Francis Dias, Caroline Zanatta, Jefferson Mota, Camilla Felippe, Gleison de Oliveira, Rodrigo Arndt, Angelo Heringer, Hugo Fraga, Leila Vieira, Anyela Rojas, Clarissa Caprestano, Sarah Agapito-Tenfen, Rafael Benevenuto, Vinicius Vilperte, Lilian Machado, Vanessa Petry, Gustavo Klabunde, Tiago Montagna, Raissa Guze, Newton Costa, Miguel Lauterjung, Rafael Ribeiro, Márcia Hoeltgebaum, Andréia Mattos, Alisson Bernardi, Mauricio dos Reis, Lírio Dal Vesco, Fernando Sanchez, Luciano Seifert, Juan Otallora, Lido Borsuk, Joel Donazollo, Morgana Lopes, Alison Nazareno, Ihangika Tchitchi, Joana Salvador, Renata Calixto, Lucilene de Abreu, Márcia Faita, Márcia Rossarola, Thiago Tomazeti, Lara Ribeiro, André Knopp, Diana Morales, Hanna Bjorgas, Charlotte Petersen, Heinrich Odendaal, Desi Fourie, Leonardo Garcia, Silvia Aquini, Miguel Dias, Ivo Fachini e Isadora Ribeiro; a todas as pessoas que se dedicaram e dedicam de coração ao ensino, à ciência e ao livre pensar; aos Professores do RGV, pelos ensinamentos transmitidos;

aos Professores do Departamento de Fitotecnia, a Bernadete Ribas e Newton, pela parceria; a todos os servidores da UFSC, cujo trabalho permite o acesso de milhares de pessoas a uma Universidade pública e de qualidade; aos graduandos dos cursos de Agronomia, Ciência e Tecnologia de Alimentos e Zootecnia, para quem transmiti algum conhecimento, seja como Professor Substituto ou Estagiário de Docência, e que me ensinaram mais do que imaginam; a Alexandra Elbakyan, pelo livre acesso a milhares de publicações acadêmicas; a Jordan Peterson, pelo estímulo à reflexão profunda, ao enfrentamento de dragões, e à responsabilidade individual; a Claudia Riecken, que nos aconselha a pisar nosso chão e respirar, que (ainda) é grátis; a Esther Vilar, pela honestidade radical e pelo desafio; a todos os músicos cujo talento e trabalho me acompanharam e inspiraram durante estes cinco anos de doutorado (Arcade Fire, Beatles, Bob Dylan, Bombino, David Bowie, Brian Eno, Broken Bells, Daft Punk, Daniel Lanois, Estas Tonne, Neil Young, Led Zeppelin, Norah Jones, Pink Floyd, Queen, Red Hot Chili Perppers, Tame Impala, The The, U2, Wintergatan, entre outros), seja no fone de ouvido à bancada, nas noites no laboratório a todo volume, ou embalando análise e escrita. Agradeço a Jesus de Nazaré e seus mensageiros, pela boa nova. Por fim, agradeço ao Pai, pela(s) graça(s) da Vida e pelo Amor que arde em nossos corações. Seja feita a vossa vontade.

"Dificilmente pode-se negar que o objetivo supremo de toda teoria é tornar os elementos básicos irredutíveis o mais simples e tão poucos quanto possível, sem renunciar à representação adequada de um único dado de experiência."

EINSTEIN (1933)

"Aqui, na semente, no mais profundo recolhimento e silêncio, o fim de todas as coisas se une a um novo começo."

I CHING - O livro das mutações (WILHELM, 1998)

"Eu lhes digo a verdade: se o grão de trigo não for plantado na terra e não morrer, ficará só. Sua morte, porém, produzirá muitos novos grãos."

JESUS DE NAZARÉ (BÍBLIA - JOÃO 12:24)

RESUMO

Esta tese elabora um modelo baseado em culturas de células, tecidos e órgãos vegetais como alternativa para detecção de propriedades emergentes em plantas geneticamente modificadas (GM). A avaliação de propriedades emergentes em culturas *in vitro* apresenta vantagens potenciais em comparação a plantas ex vitro, quais sejam: i) utilização de um modelo biológico de menor complexidade que o sistema real (i.e. culturas de um ou poucos tipos de células, tecidos ou órgãos vegetais vs. a planta inteira, com múltiplos órgãos, tecidos e células em interação); ii) alto controle ambiental, viabilizando comparações fidedignas entre plantas transgênicas e suas contrapartes convencionais; iii) alta resolução de propriedades emergentes em processos ontogenéticos e morfogenéticos; iv) altas taxas de crescimento/proliferação; e v) aplicabilidade para experimentação. Um modelo interativo *in vitro* foi desenvolvido utilizando o milho (*Zea mays* spp. *mays*) híbrido AG-5011, em suas versões transgênica (AG-5011YG - milho YieldGard®, evento GM MON810) e não-transgênica (AG-5011), aqui definidos como "híbridos quase-isogênicos" (HQIs). Foram avaliadas múltiplas fontes de explante, concentrações e combinações de fitorreguladores e outros suplementos no meio de cultura, quanto à eficiência de indução e proliferação de culturas *in vitro* e à sua ontogênese e morfogênese. Ficaram evidenciadas diferenças ontogenéticas e morfogenéticas significativas entre os HQIs nas respostas a fitorreguladores exógenos, particularmente 2,4-D e 2iP. O mapeamento do perfil protéico de culturas em fase de proliferação, via análise proteômica shotgun seguida de análise de enriquecimento de ontologias gênicas, permitiu elucidar múltiplos processos biológicos, funções moleculares e componentes celulares afetados pela regulação diferencial de proteínas, incluindo metabolismo de carboidratos e energia, metabolismo de proteínas e outras macromoléculas, respostas a estresse e a estímulos, metabolismo de fitorreguladores, entre outros. Com base nos resultados observados, conclui-se que o modelo interativo *in vitro* é uma ferramenta poderosa e de alta resolução para a identificação de efeitos não-intencionais da transformação genética de plantas, e que a presença do constructo recombinante do milho GM MON810 e a conseqüente expressão constitutiva da proteína Cry1Ab recombinante, está associada a múltiplos efeitos off-target nos níveis molecular, celular e morfogenético do milho híbrido GM AG-5011YG *in vitro*.

Palavras-chave: Organismo geneticamente modificado. Planta transgênica. Milho. *Zea mays*. Modelo. Efeitos não-alvo. Propriedades emergentes. Proteoma.

ABSTRACT

This thesis elaborates a model based on plant cell, tissue and organ culture as an alternative for investigation of unintended effects, or emergent properties, in genetically modified (GM) plants. The evaluation of unintended effects *in vitro* presents potential advantages to ex vitro approaches, including i) the use of a biological model of less complexity than the real system (i.e. cultures of one or a few cell, tissue or organ types, vs. the whole plant in cultivation, with multiple organs, tissues and cell types in interaction); ii) high environmental control, allowing for reliable comparisons between transgenic plants and their conventional counterparts; iii) high resolution of unintended effects in ontogenetic and morphogenetic processes; iv) high biomass growth and proliferation rates; and v) applicability to experimentation. An *in vitro* interactive model was established using maize (*Zea mays* spp. *mays*) hybrid AG-5011, in its transgenic (AG-5011YG - YieldGard® maize, GM event MON810) and non-transgenic (AG-5011) versions, herein defined as near-isogenic hybrids (NIHs). Multiple explant sources, concentrations and combinations of plant growth regulators and of other culture medium supplements were evaluated regarding effects on *in vitro* culture induction, proliferation, ontogenesis and morphogenesis. Significant ontogenetic and morphogenetic differences were observed between the tested NIHs in response to exogenous growth regulators, particularly 2,4-D and 2iP. Proteomic profiling of proliferation-stage callus cultures by means of shotgun proteomics and gene ontology enrichment analysis, pointed to a diverse set of biological processes, molecular functions and cellular components affected by differential protein regulation, including carbohydrate and energy metabolism, protein and other macromolecules metabolisms, responses to stress and stimuli, growth regulator metabolism, among others. Based on the observed results, we conclude the developed *in vitro* model, coupled to thorough experimental design and statistical modeling of developmental, morphogenetic, and biochemical variables, constitutes a powerful, high resolution tool for identification of unintended effects of plant genetic transformation, and that the presence of the recombinant gene construct of GM maize MON810, and the consequent constitutive expression of the recombinant Cry1Ab protein, is associated to multiple off-target effects at the molecular, cellular, ontogenetic and morphogenetic levels of GM maize AG-5011YG *in vitro*.

Keywords: Genetically modified organism. Transgenic plants. Maize. *Zea mays*. Model. Unintended effects. Off-target effects. Emergent properties. Proteome.

LISTA DE FIGURAS

LISTA DE TABELAS

LISTA DE ABREVIATURAS E SIGLAS

2,4-D - Ácido diclorofenoxiacético/diclorophenoxiacetic acid

2iP - Isopenteniladenina/isopenteniladenine

ABA - Ácido abscísico/abscisic acid

AG - Sementes Agroceres

AIA - Ácido indolacético/indolacetic acid

BAP - Benzilaminopurina/benzylaminopurine

Bt - Bacillus thuringiensisis

cAIC - Corrected Akaike Information Crierion

CaMV - Vírus-do-mosaico-da-couve-flor/ Cauliflower mosaic

CAMV P35S - Promotor 35S do vírus-do-mosaico-da-couve-flor

CBB - Comassie brilliant blue/Azul brilhante de Comassie

CCD - Charge-couple device/Dispositivo de carga acoplada

CEG - Cassete de expressão gênica

DIA - Data-independent aquisition/Aquisição independende-de-dados

DNA - Deoxyribonucleic acid/ácido desoxi-ribonucléico

DTT - Dithiothreitol/Ditiotreitol

E.C. - Enzyme code/Código de enzima

ESI- Electrospray Ionization/Ionização por eletrospray

FDA - Food and Drug Administration

GEC - Gene expression cassete

GLU - Glutathione/Glutationa

GM - Genetically modified/Geneticamente modificado(s)

GMO(s) - Genetically modified organism(s)

GO - Gene ontology/ontologia gênica

HDMS - High definition mass spectrometry/Espetrometria de massas de alta definição

HQI(s) - Híbrido(s) quase-isogênico(s)

hsp70 - heat shock protein 70 gene/gene da proteína de choque térmico 70

HT - Herbicide tolerant/tolerante a herbicidas

IMS - Ion mobility spectrometry/Espectrometria de mobilidade de íons

KIN - Kinetin/cinetina

LC - Liquid cromatography/Cromatografia líquida

LQI(s) - Linha(s) quase-isogênica(s)

mRNA - messenger ribonucleic acid/ácido ribonucléico mensageiro

MS - Mass spectrometry/Espectrometria de massas

NIH(s) - Near-Isogenic Hybrid(s)

NIL(s) - Near-isogenic line(s)

NM - Not genetically modified

NOS - nopaline synthase gene/gene de nopalina sintase

OGM(s) - Organismo(s) geneticamente modificado(s)

ONAs - Organismo(s) não-alvo

PAS - Periodic acid-Schiff/Ácido periódico-Schiff

PCR - Polimerase chain reaction/Reação de polimerase em cadeia

PMSF - Phenylmethylsulfonyl fluoride/Fluoreto de fenilmetilsulfonil

RR - Roundup Ready®

SAM - Shoot apical meristem/Meristema apical do caulinar

TB-O - Toluidine Blue/Azul de toluidina

TCL(s) - Thin cell layer(s)/Camada(s) fina(s) de célula(s)

TDZ - Thidiazuron

TOF - Time-of-flight/Tempo-de-vôo

YG - YieldGard®

SUMÁRIO

1 INTRODUÇÃO

Diferentemente da maioria dos animais, nos quais somente os gametas são haplóides, o ciclo de vida das plantas alterna entre gerações multicelulares haplóides e diplóides (ciclo haplodiplonte). O desenvolvimento embrionário ocorre na geração diplóide, sendo o embrião originado da fusão de gametas, que por sua vez são formados pela geração haplóide (Gilbert, 2000).

Gametas são produzidos nos gametófitos multicelulares haplóides, que podem ser femininos (saco embrionário) e masculinos (grão de pólen) (Gilbert, 2000). A fertilização (fusão de um gameta feminino e um masculino) origina um esporófito multicelular diplóide (o embrião/planta), que na vida adulta produz esporos haplóides via meiose (micrósporos masculinos e megásporos femininos); estes esporos passam por divisões mitóticas para originar um gametófito multicelular haplóide, e então divisões mitóticas no gametófito são necessárias para a produção de gametas (Gilbert, 2000).

O embrião resulta da fecundação da oosfera (n) por um núcleo espermático (n), com subseqüente formação e desenvolvimento do zigoto (2n) que, após divisões celulares consecutivas, origina um embrião pluricelular (Gilbert, 2000).

Nas espermatófitas, o embrião desenvolve-se dentro de uma estrutura denominada semente, que na maioria das angiospermas, como o milho, é constituída por uma casca protetora (tegumento), um tecido nutritivo, geralmente triplóide (endosperma, formado pela fusão de um segundo núcleo espermático do grão de pólen e dois núcleos polares do saco embrionário), e um embrião. O endosperma irá nutrir o embrião quando a semente iniciar a germinação, até que a plântula comece a obter seus nutrientes através da raiz e do processo de fotossíntese, por meio do qual ela utiliza água, ar e luz para gerar energia química, que será utilizada em seu metabolismo (Taiz & Zeiger, 2013).

Dentro do grão de milho - que parece e funciona como semente, mas botanicamente é um fruto seco (mais precisamente uma cariopse, cujas camadas exteriores derivam dos tecidos do ovário após a polinização da flor de uma gramínea, sendo tais tecidos pouco discerníveis, a olho nu, do tegumento da semente propriamente dita em seu interior) - existe uma planta inteira em potencial, com suas raízes, caule(s), folhas, flores e grãos. De fato, o embrião vegetal pode ser visto como uma planta em miniatura, constituindo um eixo bipolar onde um dos pólos corresponde ao meristema apical caulinar e outro ao meristema apical

radicular (Taiz & Zeiger, 2003), sendo os meristemas as zonas de crescimento ativo, divisão e diferenciação celular, dos quais se originam todos os diferentes tipos de células, tecidos e órgãos vegetais.

Plantas, como produtores primários, são elementos essenciais para a manutenção da vida no planeta, interagindo e coevoluindo com outros seres, incluindo, obviamente, o ser humano. Em grande parte, foi a semente que permitiu o desenvolvimento de nossa civilização, sendo peça chave no desenvolvimento da agricultura, quando, de acordo com evidências arqueológicas e arqueobotânicas (Tudge, 1999), o ser humano intensificou a sua atenção e determinação em cultivar e multiplicar sistematicamente plantas provedoras de alimentos, fibras e fármacos. Isto possibilitou a mudança da vida nômade dos caçadores-coletores para a vida sedentária, e a fixação de grupos humanos em vilas e proto-cidades, há mais de 10.000 anos (Tudge, 1999).

Portanto, ao longo de pelo menos dez milênios, o ser humano tem, em maior ou menor grau, sistematicamente selecionado, plantado, colhido e se alimentando de sementes ou das plantas que se desenvolvem a partir das sementes (Tudge, 1999), em um processo dinâmico e contínuo no qual milhares de variedades vegetais foram obtidas, constituindo atualmente um patrimônio da humanidade de valor imensurável.

A semente está intimamente atrelada à nossa sobrevivência como indivíduos e como espécie, bem como à soberania alimentar de qualquer grupo humano. Milhares de sementes e grãos têm o potencial para nutrir o ser humano e outros animais, sendo consumidas, digeridas, e assimiladas como carboidratos, lipídeos, proteínas, e vitaminas, e então transformadas em carne e sangue, e finalmente em planta e grão, mais uma vez, através do cultivo. A semente, então, representa a origem, a vida incipiente, mas também a morte e o renascimento. A semente precisa "morrer" como semente, deixar de ser semente, para "renascer", germinar, e tornar-se planta.

Há milhares de anos o ser humano vem domesticando diferentes espécies vegetais e animais visando à melhoria de caracteres de interesse agrícola (Pickersgill, 2009). No século XX, a domesticação progrediu para o melhoramento genético, através de avanços nos conhecimentos em biologia, genética e estatística (Clement *et al*.. 2009), e nas últimas décadas, avanços em cultura *in vitro* e biologia molecular possibilitaram o desenvolvimento de organismos geneticamente modificados (OGMs), como as plantas transgênicas (Gordon-Kamm *et al*., 1990; Quétier, 2016).

Plantas transgênicas são desenvolvidas pela introdução de seqüências de DNA (codificadoras de proteínas ou outros produtos difusíveis, como RNA e suas variantes) no

genoma vegetal, utilizando tecnologia do DNA recombinante (rDNA) e cultura de tecidos vegetais (Gordon-Kamm *et al*., 1990). Deste modo, caracteres agronomicamente benéficos, p.e., resistência a insetos-praga, oriundos de espécimes da mesma ou de outra espécie (mesmo de outros reinos biológicos), podem, mediante inserção e complexa regulação gênica, ser expressos em plantas de interesse, representando uma possível vantagem na produção agrícola.

De acordo com a lei brasileira, OGMs são definidos como organismos nos quais o material genético (DNA) foi alterado através de técnicas usualmente denominadas de "biotecnologia moderna", "engenharia genética" ou "tecnologia do DNA recombinante" (Brasil, 2005). Estas técnicas possibilitam que genes individuais selecionados sejam transferidos de um organismo para outro, inclusive entre espécies não relacionadas, permitindo que o receptor expresse traços ou características normalmente associadas somente ao doador (Brasil, 2005). Tais métodos são empregados na obtenção de plantas geneticamente modificadas (GM) com fins comerciais desde a década de 1980 (Pretty, 2001; OMS, 2010).

Nos últimos 60 anos a aplicação de novas tecnologias aumentou significativamente a produção agrícola, mas também mostrou relevantes efeitos adversos no ambiente (Tilman *et al*., 2001; Matson *et al*., 1997). Apesar da recente introdução dos cultivos GM na agricultura mundial, dentre seus efeitos em agroecossistemas já foram observados alguns efeitos negativos, tais como: o desenvolvimento de plantas daninhas resistentes ao glifosato (ingrediente ativo do Roundup®, herbicida comercializado em pacote com muitas plantas GM tolerantes a herbicidas (Powles, 2008)); desenvolvimento de resistência de pragas-alvo a cultivos Bt (Kruger *et al*., 2009); e substituição de pragas-chave por pragas secundárias (Lu *et al*., 2010). Estudos em laboratório também demonstraram efeitos de plantas GM ou tecnologias associadas em organismos não-alvo (ONAs) (Bøhn *et al*., 2008; Schmidt *et al*., 2009; Paganelli *et al*., 2010; Holderbaum *et al*., 2015).

Atualmente, o debate sobre a segurança das plantas transgênicas continua bastante acalorado. Apesar da existência de extensa pesquisa sobre o assunto, permanecem questionamentos sobre os riscos e a segurança do cultivo em larga escala espaço-temporal de plantas transgênicas, e mesmo características elementares destas plantas podem permanecer ainda desconhecidas, especialmente no que toca à ocorrência de propriedades emergentes ou efeitos não-intencionais da transformação genética, que podem ocorrer devido a imprecisões

inerentes às tecnologias empregadas na obtenção de plantas transgênicas (Franck-Oberaspach & Keller, 1997; Kuiper *et al*., 2001; Quétier, 2016).

A tecnologia de rDNA permite a manipulação e construção de seqüências específicas de DNA, enquanto a cultura de tecidos e células vegetais se embasa na totipotência de células vegetais - a habilidade de determinadas células somáticas vegetais, sob estímulos ambientais específicos, de se desdiferenciar até um estado embrionário/meristemático, e então se re-diferenciar para gerar qualquer tipo de célula, ou mesmo embriões completos (embriogênese somática) (Verdeil *et al*., 2017) - para obter alta produção de células, tecidos, órgãos ou embriões vegetais *in vitro*.

Células e massas celulares cultivadas *in vitro*, denominadas calos, podem ser transformadas geneticamente pela inserção e integração estável de seqüências de DNA no genoma vegetal (Gordon-Kamm *et al*., 1990), e então as células transformadas podem regenerar plantas por organogênese ou embriogênese somática, e ser empregadas em melhoramento vegetal convencional como fonte do novo traço transgênico.

Desde o advento da transformação genética de plantas até hoje, vários diferentes processos de transformação foram desenvolvidos para integrar estavelmente rDNA em genomas vegetais, incluindo transformação mediada por plasmídeo TI de Agrobacterium tumefasciens, biobalística (que consiste na aceleração de micropartículas de ouro ou tungstênio recobertas com rDNA, e seu disparo em culturas de células ou tecidos vegetais), e mais recentemente, edição genômica dirigida (Quétier, 2016). Excetuando-se a edição genômica, que é uma tecnologia ainda incipiente, todos os outros processos de transformação não são direcionados, o que significa que a maioria dos eventos GM atualmente comercializados foram transformados pela inserção aleatória de constructos de rDNA nos genomas vegetais. Cada evento de inserção aleatória gera um "transformante" diferente, tornando a inserção não direcionada passível de conseqüências genéticas e fenotípicas inesperadas, dependendo do número de inserções, sítio de inserção, integridade do(s) inserto(s), ocorrência de indels, e do "ambiente genômico" (Franck-Oberaspach & Keller, 1997; Kuiper *et al*., 2001; Quétier, 2016).

Quando a transformação genética é exitosa, a conseqüência intencional é a integração estável de uma fita de rDNA que codifica um novo traço de interesse no transformante ou evento de transformação; conseqüências não-intencionais ou efeitos não-alvo constituem possíveis propriedades emergentes, e podem incluir mutações genéticas e interações entre o cassete de expressão recombinante e o novo ambiente genômico, em ambos os casos podendo levar a efeitos genéticos e fenotípicos (Zolla *et al*., 2008; Agapito-Tenfen *et*

al., 2013; La Paz *et al*., 2014; Quétier, 2016). Possíveis efeitos não-alvo são evento-específicos, e podem ser influenciados pelo background genético no qual o lócus recombinante foi introgredido por melhoramento genético convencional, após a transgênese e regeneração do transformante original (i.e. diferentes híbridos comerciais de milho que contém o mesmo constructo genético recombinante) (Coll *et al*., 2008; 2009; 2010; La Paz *et al*., 2014).

O evento de milho (*Zea mays* spp. *mays*) GM MON810 (Monsanto, milho YieldGard® (CERA, 2016)) é um milho GM amplamente empregado para a produção de híbridos GM resistentes a pragas (James, 2016; CERA, 2016). Foi obtido pela inserção por biobalística de um constructo geneticamente engenheirado (CGE) no genoma do milho híbrido Hi-II, com alta capacidade regenerativa *in vitro* (fruto do cruzamento entre as linhas endogâmicas A188 e B73) (CERA, 2016).

Após transformação, seleção e regeneração, MON810 foi retrocruzado com Hi-II, e o evento MON810 utilizado na produção de milhos híbridos GM é proveniente da terceira geração de retrocruzamentos (CERA, 2016). Já que Hi-II é um híbrido simples (produto do cruzamento entre duas linhas endogâmicas homozigotas contrastantes), a incorporação do CGE recombinante em vários híbridos comerciais, sejam híbridos simples, duplos, ou triplos, depende da sua introgressão, em homozigose, em linhas endogâmicas parentais por meio de retrocruzamentos consecutivos. Adicionalmente, MON810 é utilizado em alguns dos chamados eventos GM "stack", que combinam mais de um evento GM por meio de cruzamentos e melhoramento convencional (Taverniers *et al*., 2008). Dentre centenas de eventos GM comerciais, MON810 tem o terceiro maior número de aprovações regulatórias no mundo (James, 2016).

Previamente à aprovação para cultivo e comercialização, normalmente um novo evento GM deve passar por uma avaliação de risco na qual não apenas a integração, estabilidade e expressão do constructo recombinante sejam demonstradas, mas também que possíveis efeitos genéticos e fenotípicos não-intencionais sejam escrutinados, em comparação à contraparte convencional mais similar disponível (Bartsch *et al*., 2010). Dependendo da espécie vegetal, a contraparte apropriada pode ser a variedade parental que foi transformada - no caso de espécies com propagação predominantemente vegetativa - ou linhas quase-isogênicas (LQIs), no caso de espécies de reprodução sexual (Cellini *et al*., 2004), como o milho.

LQIs são obtidas ao se cruzar duas linhagens contrastantes para um lócus-alvo (p.e. um constructo recombinante), e então realizar retrocruzamentos consecutivos da progênie com a linhagem parental receptora, até que o lócus-alvo seja introgredido; assim, após 6-8 retrocruzamentos, o genótipo das sementes produzidas será mais que 99% similar ao da linhagem parental receptora, além de conter o lócus de seleção (Allard, 1960; Brigs e Knowles, 1967). Baseado nisto, LQIs são definidas como duas ou mais linhas homozigotas que compartilham a mesma constituição genética, exceto por um lócus de seleção, e possivelmente alguns loci adicionais geneticamente ligados ao lócus de seleção (Zeven & Waninge, 1986). Assim, no caso da maioria das cultivares comerciais de milho, faz mais sentido definir as contrapartes transgênica e convencional como "híbridos quase-isogênicos" (HQIs), uma vez que são híbridos 99% similares - e não linhagens puras - que diferem entre si por um ou poucos loci.

Neste contexto, uma planta é um organismo multicelular complexo, constituído por uma variedade de tipos celulares, organizados em tecidos altamente regulados que diferem em seu perfil de expressão gênica e funções (Cavez *et al*., 2009), que por sua vez são organizados nos diferentes órgãos vegetais. Em contraste, a despeito de sua complexidade técnica/tecnológica, culturas de células, tecidos e órgãos vegetais consistem de um ou poucos tipos celulares, de tecidos ou órgãos, e podem neste sentido ser empregados como sistemas de menor complexidade biológica do que a planta completa em cultivo. Tais culturas *in vitro*¬ possuem vantagens como altas taxas de crescimento, alta reprodutibilidade experimental e alto rendimento de biomassa vegetal (Cavez *et al*., 2009). Estas características tornam a cultura de células, tecidos e órgãos vegetais um potencial modelo para a avaliação de propriedades emergentes em plantas transgênicas, pela comparação da ontogênese, morfogênese e caracteres bioquímicos destas com suas contrapartes convencionais *in vitro*.

Com base no exposto, o objetivo deste estudo foi desenvolver e avaliar um modelo para o estudo de propriedades emergentes derivadas da transformação genética de plantas. Tal modelo baseia-se na caracterização e comparação de aspectos ontogenéticos e morfogenéticos de um milho híbrido GM (AG-5011YG, evento MON810) e seu híbrido quase-isogênico convencional (AG-5011), sob variadas condições de cultura *in vitro*, incluindo indução de culturas, proliferação, morfogênese, embriogênese somática, e parâmetros associados, complementadas com análises histológicas, bioquímicas, proteômicas, estatísticas e gráficas. A hipótese central testada no modelo desenvolvido foi: a presença do cassete de expressão recombinante do evento GM MON810 gera propriedades emergentes que alteram as respostas ontogenéticas e morfogenéticas do milho híbrido AG-5011YG *in vitro*, em comparação a seu

híbrido quase-isogênico convencional AG-5011, no qual não há o cassete de expressão recombinante.

REFERÊNCIAS

AGAPITO-TENFEN, S.Z.; GUERRA, M.P.; WIKMARK, O.G.; NODARI, R.O. Comparative proteomic analysis of genetically modified maize grown under different agroecosystems conditions in Brazil. **Proteome Sci.**, v. 11, p. 46, 2013.

ALLARD, R.W. **Principles of Plant Breeding**. London: John Wiley & Sons Inc, 1960.

BARTSCH, D.; DEVOS Y.; HAILS, R.; KISS, J.; KROGH, P.H.; MESTDAGH, S.; NUTI, M.; SESSITSCH, A.; SWEET J.; GATHMANN, A. Environmental impact of genetically modified maize expressing Cry1 proteins. In: KEMPKEN, F.; Jung, C. (eds.). **Genetic Modification of Plants: Agriculture, Horticulture and Forestry**. Springer, 2010.

BØHN, T.; PRIMICERIO, R.; Traavik, T. Reduced Fitness of *Daphnia magna* Fed a Bt-Transgenic Maize Variety. Archives of Environmental Contamination and Toxicology, v. 55, p. 584-592, 2008.

BRASIL. **Lei Nº 11.105, de 24 de Março de 2005**. Regulamenta os incisos II, IV e V do § 1º do art. 225 da Constituição Federal, estabelece normas de segurança e mecanismos de fiscalização de atividades que envolvam organismos geneticamente modificados – OGM e seus derivados, cria o Conselho Nacional de Biossegurança – CNBS, reestrutura a Comissão Técnica Nacional de Biossegurança – CTNBio, dispõe sobre a Política Nacional de Biossegurança – PNB, revoga a Lei nº 8.974, de 5 de janeiro de 1995, e a Medida Provisória nº 2.191-9, de 23 de agosto de 2001, e os arts. 5º , 6º , 7º , 8º , 9º , 10 e 16 da Lei nº 10.814, de 15 de dezembro de 2003, e dá outras providências. Brasília, DF: Presidência da República, 2005. Disponível em: http://www.planalto.gov.br/ccivil_03/_ato2004-2006/2005/Lei/L11105.htm. Acesso em: 03 out. 2019.

BRIGGS, F.N.; KNOWLES, P.F. **Introduction to Plant Breeding**. Reinhold Publishing Corporation. 1967.

CAVEZ, D.; HATCHES, C.; CHAUMONT, F. Maize black Mexican sweet suspension cultured cells are a convenient tool for studying aquaporin activity and regulation. **Plant Signal. Behav.**, **v.** 9, p. 890-892, 2009.

CELLINI, F.; CHESSON, A.; COLQUHOUN, I.; CONSTABLE, A; DAVIES, H.V.; ENGEL, K.H.; GATEHOUSE, A.M.; KÄRENLAMPI, S.; KOK, E.J.; LEGUAY, J.J.; LEHESRANTA, S.; NOTEBORN, H.P.; PEDERSEN, J.; SMITH, M. Unintended effects and their detection in genetically modified crops. **Food and Chemical Toxicology**, v. 42, p. 1089-1125, 2004.

CERA, Center for Environmental Risk Assessment. **GM Crop Database, MON-ØØ81Ø-6 (MON810)**. ILSI Research Foundation, Washington D.C., 2016. Disponível em: http://cera-gmc.org/GmCropDatabaseEvent/MON810/short. Acesso em: 03 dez. 2016.

CLEMENT, C.R.; BORÉM, A.; LOPES, M.T.G. **Da domesticação ao melhoramento de plantas**. In: BORÉM, A.; LOPES, M.T.G.; CLEMENT, C.R. (eds.). Domesticação e melhoramento: espécies amazônicas. Editora da Univ. Fed. Viçosa, Viçosa, MG. pp.11-38, 2009.

COLL, A.; NADAL A.; COLLADO, R.; CAPELLADES, G.; KUBISTA, M.; MESSEGUER, J; PLA, M. Natural variation explains most transcriptomic changes among maize plants of MON810 and comparable conventional varieties subjected to two N-fertilization farming practices. **Plant Mol. Biol.**, v. 73, p. 349–362, 2010.

COLL, A.; NADAL, A.; COLLADO, R.; CAPELLADES, G.; MESSEGUER, J.; MELÉ, E.; PALAUDELMÀS, M.; PLA, M. Gene expression profiles of MON810 and comparable conventional maize varieties cultured in the field are more similar than are those of conventional lines. **Transgenic Res.**, v. 18, p. 801–8. 2009.

COLL, A.; NADAL, A.; PALAUDELMÀS, M.; MESSEGUER, J.; MELÉ, E.; PUIGDOMÈNECH, P.; PLA, M. Lack of repeatable differential expression patterns between MON810 and comparable commercial varieties of maize. **Plant Mol Biol.**, v. 68, p. 105-117, 2008.

FRANCK-OBERASPACH, S.L.; KELLER, B. Consequences of classical and biotechnological resistance breeding for food toxicology and allergenicity. **Plant Breeding**, v. 116, p. 1-17, 1997.

GILBERT, S.F. **Developmental Biology**. 6th edition. Sunderland (MA): Sinauer Associates, 2000. Plant Life Cycles. Disponível em: https://www.ncbi.nlm.nih.gov/books/NBK9980/

GODDIJN, O.J.M.; LINDSEY, K.; VAN DER LEE, F.M.; KLAP, J.C.; SIJMONS, P.C. Differential gene expression in nematode induced feeding structures of transgenic plant harbouring promoter-gusA fusion constructs. **Plant Journal**, v. 4, p. 863-73, 1993.

GORDON-KAMM, W.J.; SPENCER, T.M.; MANGANO, M.L.; ADAMS, T.R.; DAINES, R.J.; START, W.G.; O'BRIEN, J.V.; CHAMBERS, S.A.; ADAMS JR, W.R.; WILLETS, N.G.; RICE, T.B.; MACKEY, C.J.; KRUEGER, R.W.; KAUSCH, A.P.; LEMAUX, P. Transformation of maize cells and regeneration of fertile transgenic plants. **The Plant Cell**, v. 2, p. 603-618, 1990.

HOLDERBAUM, D.F.; CUHRA, M.; WICKSON, F.; ORTH, A.I.; NODARI, O.R.; BØHN, T. Chronic responses of *Daphnia magna* under dietary exposure to leaves of a transgenic (event MON810) Bt–maize hybrid and its conventional near-isoline. **Journal of Toxicology and Environmental Health, Part A**, v. 78, p. 993-1007, 2015.

JAMES, C. **Executive Summary of Global Status of Commercialized Biotech/GM Crops: 2016**. ISAAA Brief, 52. Ithaca, NY, 2016.

KRUGER, M.; VAN RENSBURG, J.B.J.; VAN DEN BERG, J. Perspective on the development of stem borer resistance to Bt maize and refuge compliance at the Vaalharts irrigation scheme in South Africa. **Crop Protection**, v. 28, p. 684-689, 2009.

KUIPER, H.A.; KLETER, G.A.; NOTEBORN, H.P.; KOK, E.J. Assessment of the food safety issues related to genetically modified foods. **The Plant Journal,** v. 27, p. 503-528, 2001.

LA PAZ, J.L.; PLA, M.; CENTENO, E.; VICIENT, C.M.; PUIGDOMÈNECH, P. The use of massive sequencing to detect differences between immature embryos of MON810 and a comparable conventional maize variety. **PLoS ONE**, v. 9(6), e100895. Disponível em: https://doi.org/10.1371/journal.pone.0100895.

LU, Y.; WU, K.; JIANG, Y.; XIA, B.; LI, P.; FENG, H.; WYCKHUYS, K.A.G.; GUO, Y. Mirid Bug Outbreaks in Multiple Crops Correlated with Wide-Scale Adoption of Bt Cotton in China. **Science**, v. 328, n. 5982, p. 1151-11542010.

MATSON, P.A.; PARTON, W.J.; POWER, A.G.; SWIFT, M.J. Agricultural Intensification and Ecosystem Properties. **Science**, v. 277, p. 504–509, 1997.

PAGANELLI, A.; GNAZZO, V.; ACOSTA, H.; LOPEZ, S.L.; CARRASCO, A.E. Glyphosate-based herbicides produce teratogenic effects on vertebrates by impairing retinoic acid signaling. **Chemical Research in Toxicology**, v. 23(10), p. 1586-1595, 2010.

PICKERSGILL, B. Domestication of plants revisited – Darwin to the present day. **Botanical Journal of the Linnean Society**, v. 161, p. 203-212, 2009.

POWLES, S.B. Evolved glyphosate-resistant weeds around the world: lessons to be learnt. **Pest Management Science**, v. 64, p. 360-365, 2008.

PRETTY, J.N. The rapid emergence of genetic modification in world agriculture: contested risks and benefits. **Environmental Conservation**, v. 28, n. 3, p. 248-62, 2001.

QUÉTIER, F. The CRISPR-Cas9 technology: Closer to the ultimate toolkit for targeted genome editing. **Plant Science**, v. 242, p. 65-76, 2016.

SCHMIDT, J.E.U. Effects of activated Bt transgene products (Cry1Ab, Cry3Bb) on immature stages of the ladybird Adalia bipunctata in laboratory ecotoxicity testing. **Archives of Environmental Contamination and Toxicology**, v. 56, n. 2, p. 221-228, 2009.

TAIZ, L.; ZEIGER, E. (eds). **Plant Physiology**, 2nd Ed. Sunderland, Mass: Sinauer Assc. Inc., 2013.

TAVERNIERS, L.; PAPAZOVA, N.; BERTHEAU, Y., DE LOOSE, M.; HOLST-JENSEN, A. Gene stacking in transgenic plants: towards compliance between definitions, terminology, and detection within the EU regulatory framework. **Environ. Biosafety Res.**, v. 7, p. 197-218, 2008.

TILMAN, D.; FARGIONE, J.; WOLFF, B.; D'ANTONIO, C.; DOBSON, A.; HOWARTH, R.; SCHINDLER, D.; SCHLESINGER, W.H.; SIMBERLOFF, D.; SWACKHAMER, D. Forecasting Agriculturally Driven Global Environmental Change. **Science**, v. 292, p. 281-284, 2001.

TUDGE, C. **Neanderthals, bandits and farmers – How agriculture really began**. London: Weidenfeld & Nicolson, 1998.

VERDEIL, J.L.; ALEMANNO, L.; NIEMENAK, N.; TRANBARGER, T.J. Pluripotent versus totipotent plant stem cells: dependence versus autonomy? **Trends Plant Sci.**, v. 12, p. 245-252, 2007.

OMS/WHO (WORLD HEALTH ORGANIZATION). **20 questions on genetically modified foods**, 2010. Disponível on-line em: www.who.int/foodsafety/publications/biotech/20questions/en/.

ZEVEN, A.C.; Waninge, J. The degree of phenotypic resemblance of the near-isogenic lines of the wheat cultivar Thatcher with their recurrent parent. **Euphytica**, v. 35, p. 665-676, 1986.

ZOLLA, L.; RINALDUCCI, S.; ANTONIOLI, P.; RIGHETTI, P.G. Proteomics as a complementary tool for identifying unintended side effects occurring in transgenic maize seeds as a result of genetic modifications. **J. Proteome Res.**, v. 7, p. 1850-1861, 2008.

2 OBJETIVOS

2.1 OBJETIVO GERAL

Desenvolver um novo modelo de estudo sobre propriedades emergentes da transformação genética de plantas, utilizando culturas *in vitro* como modelo interativo, e comparando o milho híbrido GM AG-5011YG (evento MON810) à sua contraparte convencional, AG-5011, quanto a parâmetros ontogenéticos, morfogenéticos, histoquímicos, e de perfil protéico das culturas, com o auxílio de técnicas de modelagem estatística avançada e modelos gráficos como ferramentas complementares de investigação do modelo *in vitro*. A hipótese central testada no modelo é: a presença e atividade do cassete de expressão recombinante de MON810 gera propriedades emergentes não intencionais no milho GM, em comparação à sua contraparte convencional quase-isogênica.

2.2 OBJETIVOS ESPECÍFICOS

1) Justificar e idear um modelo interativo *in vitro* como alternativa para investigação de propriedades emergentes da transformação genética de plantas, baseado na detecção de alterações moleculares, celulares, ontogenéticas e morfogenéticas em múltiplas condições ambientais e temporais *in vitro* (Introdução).

2) Compilar um referencial teórico relevante à contextualização e ao desenvolvimento de um modelo *in vitro* para o estudo de propriedades emergentes em milho GM MON810 (Referencial Teórico).

3) Avaliar a capacidade de iniciação de culturas *in vitro* e características qualitativas de uma cultivar de milho transgênico (híbrido AG-5011YG, evento MON810), considerando diferentes fontes de explante, condições de luminosidade e gradientes de concentração de 2,4-D no meio de cultura (Capítulo I).

4) Estabelecer culturas *in vitro* de milho GM AG-5011YG e de sua contraparte convencional quase-isogênica AG-5011, comparando as freqüências de indução e

características qualitativas das culturas induzidas utilizando diferentes fontes de explante, condições de luminosidade e gradientes de concentração de 2,4-D (Capítulo II).

5) Avaliar condições de manutenção/proliferação de culturas *in vitro* de milho GM AG-5011YG e de sua contraparte convencional quase-isogênica AG-5011, comparando as culturas quanto à ontogênese e capacidade morfogenética em resposta ao sistema de cultivo, tempo de subcultivo, alterações nas concentrações de 2,4-D, 2iP e ABA (Capítulo III).

6) Avaliar e comparar as culturas de milho GM AG-5011YG e de sua contraparte convencional quase-isogênica AG-5011, mantidas *in vitro* por mais de 3 anos, quanto ao potencial para indução de embriogênese somática sob a influência de diferentes regimes de iluminação e concentrações de ácido abscísico, TDZ, e glutationa no meio de cultura (Capítulo IV).

7) Analisar características histoquímicas e o perfil proteômico de culturas de calos *in vitro* dos HQIs transgênico e convencional, e cruzar os resultados ontogenéticos e morfogenéticos das culturas com as análises histoquímicas e do proteoma, visando compreender as bases fisiológicas e bioquímicas de possíveis respostas ontogenéticas e morfogenéticas diferenciais em *Zea mays* geneticamente modificado (Capítulo V).

8) A partir da literatura especializada e da compilação dos resultados obtidos neste estudo, i) avaliar a adequação do modelo desenvolvido para identificação de propriedades emergentes em plantas GM; ii) responder se existem propriedade emergentes em culturas de milho GM AG-5011YG, em comparação a seu HQI convencional AG-5011; e iii) definir parâmetros de interesse relacionados a possíveis propriedades emergentes no milho GM para posterior validação do modelo, tais como processos biológicos-chave e indicadores bioquímicos, ontogenéticos e morfogenéticos identificados nas culturas de milho *in vitro* (Conclusão).

3 REFERENCIAL TEÓRICO

3.1 MILHO: DA DOMESTICAÇÃO À TRANSGENIA

O milho começou a ser domesticado por populações humanas no que é atualmente o México central, cerca de 9000 anos antes do presente (AP), à partir do teosinte silvestre (*Zea mays* ssp. parviglumis); carregado por migrantes humanos, a cerca de 7500 anos AP o milho havia atravessado a America Central, e há ~6500 anos se distribuído em cultivos pela América do Sul (Kistler *et al*., 2018).

Dados genômicos, linguísticos, arqueológicos e paleoecológicos sugerem que um milho parcialmente domesticado foi levado para a América do Sul, antes da fixação dos traços característicos do milho domesticado, ocasionando um possível efeito fundador ao se isolar o milho do pool gênico do teosinte no centro de domesticação original, bem como a formação de linhagens altamente estruturadas na América do Sul, o que denotaria um caso de domesticação estratificada para a espécie (Kistler *et al*., 2018).

Desde o início do século XX, o milho tem sido utilizado como organismo modelo em biologia e genética de monocotiledôneas, sendo um dos sistema genéticos mais estudados (Strable e Scanlon, 2009). O milho é um exemplo clássico da domesticação de plantas, tendo sofrido, entre outras mudanças morfológicas, uma reestruturação radical de sua inflorescência feminina, resultando na produção de centenas de grãos em uma ou poucas inflorescências, maturação sincrônica destas inflorescências, e indeiscência de grãos e espigas, tornando o milho acentuadamente dependente dos humanos para sua propagação e perpetuação (Stitzer & Ross-Ibarra, 2018).

Atualmente o milho é largamente cultivado ao redor do mundo, consistindo muitas vezes da base energética alimentar de populações humanas (FAO, 2018), sendo um elemento de grande relevância alimentícia, ambiental e cultural em muitas regiões onde é cultivado.

A partir de meados da década de 1990, variedades de milho GM têm sido desenvolvidas e cultivadas em larga escala, com a maioria delas possuindo transgenes que conferem resistência a alguns insetos-praga (p.e. milho Bt (Bacillus thuringiensis) com genes da bactéria B. thuringiensis para expressão de proteínas inseticidas), tolerância a herbicidas (milho HT - herbicide tolerant - p.e. milho RR (Roudup Ready®), com genes bacterianos de resistência ao glifosato), ou ambos os traços juntos (James, 2016).

3.2 MILHO BT E O EVENTO MON810

O milho GM é o segundo maior cultivo GM em área plantada no mundo, com 50 milhões de hectares (34% da área mundial com cultivos GM) (James, 2016). No Brasil o plantio e comercialização de variedades de milho GM YieldGard® (evento MON810), que contém um gene codificador da proteína inseticida Cry1Ab de B. thuringiensis (Bt), foram autorizados em 2007 (Brasil, 2007). Ao lado do evento NK603 (milho HT RR), o evento de transformação MON810 é o evento com o segundo maior número de aprovações no mundo (20 países), atrás do evento GTS-40-3-2 (soja HT RR) (James, 2016).

O desenvolvimento do evento MON810 requereu diversas modificações e rearranjos genéticos dos componentes do cassete de expressão gênica, para que este se tornasse funcional mediante integração estável no genoma do milho (Goddijn *et al*. 1993; Urwin *et al*. 1997; Bogdanova *et al*., 2012). Portanto, a expressão do gene cry1Ab recombinante em híbridos de milho MON810 deriva da integração estável de um cassete de expressão detalhadamente engenheirado, de modo a permitir a expressão constitutiva do transgene e produção constante de proteína recombinante em altos níveis (Bogdanova *et al*., 2012).

A introdução de um traço de resistência a insetos em plantas vasculares demanda modificações significativas das seqüências codificadoras de toxinas Cry de Bt para sua expressão em plantas (Koziel *et al*., 1993; Fujimoto *et al*., 1993; Perlak *et al*., 1990, 1991, 1993; Sutton *et al*., 1992; Adang *et al*., 1993). Além disso, a transcrição eficiente de genes cry recombinantes no núcleo de células vegetais requer a remoção de seqüência ricas em A-T, que podem causar instabilidade do mRNA (Perlak *et al*., 1991; 1993; Sutton *et al*., 1992; Adang *et al*., 1993) ou aberrações de splicing (van Aarssen *et al*., 1995). A tradução de mRNAs também pode ser aumentada pela modificação de códons redundantes, de modo a incorporar códons mais utilizados pela planta (Perlak *et al*., 1991; Koziel *et al*.1993).

O maior grupo de toxinas Cry, o grupo das proteínas Cry1, é constituído por proteínas globulares com três domínios estruturais, tendo como característica particular a presença de pro-toxinas com duas diferentes classes de tamanho (curtas e longas) (Bravo *et al*., 2007). A extensão carboxi-terminal encontrada nas pro-toxinas longas, como Cry1Ab, é dispensável para a toxicidade e acredita-se que exerça função na formação de corpos de inclusão cristalinos dentro da bactéria (de Maagd *et al*., 2001).

Quando ingeridas por larvas suscetíveis, as inclusões cristalinas bacteriais dissolvem-se no ambiente intestinal alcalino do inseto, e as pro-toxinas solubilizadas inativas são

clivadas por proteases das células epiteliais do intestino do hospedeiro, dando origem a toxinas ativas de 60-70 kDa, resistentes à proteases (Bravo *et al*., 2005). Ao se inserirem especificamente na membrana gastrointestinal, as toxinas ativas causam a perda de íons e lise celular (Bravo *et al*., 2005). A inserção da toxina na membrana leva à formação de poros líticos em microvilosidades das membranas apicais (Aronson & Shai, 2001; Bravo *et al*., 2005), e a lise celular e o rompimento do epitélio intestinal liberam o conteúdo celular, provendo aos esporos da bactéria um meio germinativo, por fim ocasionando septicemia severa e morte do inseto (de Maagd *et al*., 2001; Bravo *et al*., 2005).

O evento de transformação MON810 foi obtido por bombardeamento de partículas recobertas com um cassete de expressão do gene Bt cry1Ab em células do milho híbrido Hi-II (CERA, 2016). O cassete de expressão desenvolvido continha o promotor viral 35s (oriundo do vírus-do-mosaico-da-couve-flor, CaMV) modificado para alta expressão gênica em monocotiledôneas (Goddijn *et al*. 1993; Urwin *et al*. 1997), uma seqüência codificadora de Cry1Ab truncada na extremidade 3', para possibilitar a expressão da proteína em uma forma já ativada e solúvel no meio celular vegetal (Bogdanova *et al*., 2012); um íntron de uma proteína de choque térmico (hsp70) nativa de milho, necessário para incrementar a expressão do transgene (Bogdanova *et al*., 2012); e o terminador do gene de nopaline synthase (NOS), que foi perdido por ocasião da inserção do constructo no genoma do milho (CERA, 2016), fato que também levou à perda de parte da seqüência codificadora de Cry1Ab (já prévia e intencionalmente truncada), o que não impediu a produção e atividade da proteína transgênica, ou afetou as características fenotípicas e agronômicas de MON810 e híbridos comerciais contendo seu cassete de expressão recombinante (Rosati *et al*., 2008; CERA, 2016). Adicionalmente, MON810 foi gerado pela inserção do cassete de expressão recombinante no DNA nuclear, sem adição de seqüências que codifiquem peptídeos de sinal/trânsito, que poderiam direcionar a proteína Cry1Ab recombinante para compartimentos sub-celulares específicos (Bogdanova *et al*., 2012),

Para a comercialização de plantas transgênicas resistentes a insetos, são requeridas informações das empresas de agro-biotecnologia acerca da expressão de proteínas inseticidas no nível dos órgãos ou estruturas reprodutivas (folhas, raízes, sementes, pólen) (US EPA, 2010), além de estudos sobre a ocorrência de efeitos não-intencionais (Cellini *et al*., 2004). Estudos sobre os níveis de expressão gênica e tradução de proteínas Cry em plantas GM são abundantes na literatura (ver Széckacks *et al*., 2010), e estratégias *untargetet* de avaliação de

perfis genômicos, transcriptômicos, proteômicos ou metabolômicos têm sido empregadas para responder perguntas sobre a ocorrência de mutações induzidas pela transformação genética de plantas, com possíveis propriedades emergentes não-intencionais (Franck-Oberaspach & Keller, 1997; Kuiper *et al*., 2001; Latham *et al*., 2006). Diversos estudos com milhos GM Bt já foram realizados neste sentido (ver Latham *et al*., 2006; Pechanova *et al*., 2013), embora ainda permaneçam muitas incógnitas sobre interações entre a nova proteína recombinante (p.e. Cry1Ab) e o metabolismo vegetal.

Efeitos ambientais e a grande variabilidade natural do milho são dois importantes fatores em avaliações de risco de milho GM (Anttonen *et al*., 2010), de modo que o controle ambiental e cuidados no desenho experimental são necessários para a aquisição de dados confiáveis (Pechanova *et al*., 2013).

3.3 MODELOS E MODELAGEM

Um modelo é um substituto para um sistema real. Modelos são utilizados quando é mais fácil trabalhar com um substituto do que com o sistema de fato. São úteis quando nos ajudam a aprender algo novo sobre os sistemas que representam. Do mesmo modo, modelos matemáticos ou estatísticos utilizam equações para representar as interconexões em um sistema (Ford, 1999).

Modelos revelam nossa habilidade de formar teorias para explicar o mundo à nossa volta. Entretanto, esta tarefa torna-se incrivelmente complicada quando pensamos sobre sistemas complexos, desde problemas locais como poluição aérea urbana, até problemas globais como a acumulação de gases estufa na atmosfera (Ford, 1999), ou mesmo problemas moleculares e genéticos como os efeitos da introdução de um gene exógeno no genoma de uma planta. Podemos gerar múltiplas e conflitantes explicações para o problema, e não ter certeza sobre qual explicação é a mais correta (Ford, 1999).

Modelos podem ter muitas formas, tamanhos e estilos. É importante enfatizar que um modelo não é o mundo real, mas somente um constructo humano com o objetivo de ajudar no melhor entendimento dos sistemas do mundo real (Ford, 1999). De modo geral, todos modelos possuem uma entrada de informação, um processador de informação, e uma saída de resultados. Aspectos-chave comuns no desenvolvimento de qualquer modelo incluem: i) suposições simplificadoras devem ser feitas; ii) condições de limite e/ou condições iniciais devem ser identificadas; iii) a escala de aplicabilidade do modelo deve ser entendida (Ford, 1999).

Existem vários tipos diferentes de modelos, dentre os quais se podem citar "modelos conceituais", "modelos interativos", "modelos matemáticos e estatísticos", e "modelos visuais"; um bom modelo de um sistema real irá provavelmente conter aspectos de cada tipo dos modelos descritos a seguir (Ford, 1999):

i) Modelos conceituais: são modelos qualitativos que ajudam a ressaltar conexões importantes em sistemas e processos reais. São utilizados como um passo inicial no desenvolvimento de modelos mais complexos.

ii) Modelos interativos: são modelos físicos de sistemas que podem ser facilmente observados e manipulados e que possuem características similares a sistemas mais complexos no mundo real. Tais modelos podem ajudar na conexão entre modelos conceituais e um sistema real.

iii) Modelos matemáticos e estatísticos: envolvem a solução de equações relevantes de um sistema ou a caracterização de um sistema baseado em seus parâmetros estatísticos, como média, moda, variância ou coeficientes de regressão. Modelos estatísticos são úteis na identificação de padrões e relações subjacentes entre conjuntos de dados.

iv) Modelos visuais: qualquer recurso que auxilie na visualização de como um sistema funciona. Um modelo visual pode ser uma representação direta de dados ou pode estar conectado a outro tipo de modelo (conceitual, interativo ou estatístico) de modo a converter a "saída" ou resultados em um formato visualmente útil. Exemplos incluem gráficos, mapas, animações, manipulação de imagens e análise de imagens.

3.4 CULTURA DE CÉLULAS, TECIDOS E ÓRGÃOS VEGETAIS

Técnicas de micropropagação de plantas baseiam-se na totipotência de células vegetais - a competência de determinadas células somáticas vegetais, sob estímulos ambientais específicos, de se desdiferenciar até um estado embrionário/meristemático, e então se re-diferenciar para gerar qualquer tipo de célula, ou mesmo embriões somáticos (Verdeil *et al*., 2017). Usualmente, três principais rotas morfogenéticas são definidas: organogênese,

embriogênese somática, e culturas nodulares (George *et al*., 2008; Dal Vesco, 2010), e todas elas tem potencial para propagação massal, facilitando a captura e fixação de ganhos genéticos para fins de melhoramento genético, e/ou a conservação de germoplasma (Dal Vesco, 2011).

A iniciação de culturas de tecidos vegetais *in vitro* demanda meios de cultura especializados, cuja composição básica deve incluir sais - que irão prover os elementos essenciais para o desenvolvimento de plantas - e uma fonte de carbono (p.e. sacarose), além de geralmente incluírem vitaminas e aminoácidos (George *et al*., 2008). Adicionalmente, fitorreguladores como auxinas, citocininas, ácido giberélico e ácido abscísico, são geralmente suplementados ao meio de cultura para induzir desdiferenciação/diferenciação, divisão e crescimento celular, e estabelecer pontos de controle de diferentes rotas morfogenéticas *in vitro* (George *et al*., 2008).

Células vegetais competentes podem ser cultivadas como massas de tecido agregado (calos) em meio semi-sólido contendo uma mistura apropriada de fitorreguladores, ou podem ser livremente dispersas em meio liquido contendo os mesmos hormônios para promover crescimento rápido e prevenir a diferenciação (George *et al*., 2008; Hellwig *et al*., 2004). Culturas ou suspensões celulares são usualmente iniciadas pela introdução de um inoculo de calo friável em meio líquido; sob agitação, células individuais se separam e, através de divisão, formam cadeias e aglomerados celulares que se fracionam novamente em células individuais e pequenos grupos de células (Hellwig *et al*., 2004).

Muitos órgãos/tecidos de uma planta têm células com potencial para proliferar *in vitro*, mas é freqüentemente verificado que culturas de calos são mais facilmente estabelecidas a partir de alguns órgãos/tecidos do que de outros: tecidos meristemáticos jovens são mais aptos, mas áreas meristemáticas em partes mais velhas de uma planta, como o cambio, também podem dar origem a calos (George *et al*., 2008). Diferenças na capacidade de tecidos de dar origem a calos são particularmente aparentes em monocotiledôneas; na maioria dos cereais, o crescimento de calos somente pode ser obtido a partir de explantes como embriões zigóticos, sementes germinadas, endosperma, bases foliares, mesocótilo de plântulas, e folhas ou laminas foliares muito jovens (George *et al*., 2008).

3.5 CULTURA *IN VITRO* DE MILHO (*ZEA MAYS* SPP. *MAYS*)

A morfogênese *in vitro* e regeneração de plantas através de embriogênese somática foi previamente obtida em Z. *mays* spp. *mays*, inicialmente a partir de embriões zigóticos

imaturos (Green & Phillips 1975; Springer *et al*., 1979; Duncan *et al*., 1985; Vasil *et al*., 1985; Hodges *et al*., 1986). Até recentemente, embriões imaturos de milho têm sido amplamente utilizados como explante regenerativo (Frame *et al*.. 2002). Entretanto, além da dificuldade inerente de manter um suprimento contínuo de embriões imaturos, que requer estufas de alta qualidade e cuidado intensivo, a resposta regenerativa é fortemente dependente do genótipo utilizado para indução das culturas (Vasil 1987; Zhong *et al*., 1992).

Diferentes tipos de explante já foram testados para superar a genótipo-dependência da morfogênese *in vitro* de milho. Culturas que empregaram primórdios de pendão (Rhodes *et al*.., 1986), segmentos foliares (Conger *et al*., 1987), gema apical de seedlings (Zhong *et al*., 1992) e embriões zigóticos maduros (Wang, 1987; Huang & Wei 2004; Al-Abed *et al*., 2006) também foram capazes de regenerar plantas de milho através de embriogênese somática ou morfogênese de microbrotos (organogênese).

Diferenças de origem genotípica na capacidade regenerativa de culturas *in vitro* de milho também podem ser contornadas pela manipulação da concentração de reguladores de crescimento no meio de cultura (Vasil 1987; Zhong *et al*., 1992). A combinação de diferentes auxinas e citocininas tem o potencial de induzir embriogênese somática a partir de culturas de calos em cereais (Bhaskaran & Smith, 1990). De modo similar, o uso de citocininas, tais como benzilaminopurina (BAP), cinetina (KIN) e *zea*tina, tem mostrado potencial para a indução de culturas de microbrotos (organogênese), tanto diretamente a partir de células diferenciadas do explante (organogênese direta), quanto após a formação de calos morfocompetentes (organogênese indireta) (Chang 1983; Zhong *et al*.. 1992; Sairam *et al*.. 2003; Al-Abed *et al*., 2006).

A concentração de ácido abscísico (ABA) no meio de cultura inibe a germinação precoce de embriões imaturos de milho *in vitro* (Emons *et al*., 1993). O tipo e concentração da fonte de carbono também estão relacionados à eficiência de formação de calos morfogênicos em cereais (Emons *et al*., 1993). Carboidratos servem não apenas como suprimento energético, mas também influenciam na osmolaridade do meio de cultura. A importância de um maior valor osmótico para evitar a germinação de embriões imaturos e maduros, bem como para aumentar a capacidade morfogênica e sua manutenção, foram demonstradas em diversos cereais, incluindo milho (Lu *et al*., 1983).

REFERÊNCIAS

ADANG, M.J.; BRODY, M.S.; CARDINEAU, G.; EAGAN, N.; ROUSH, R.T.; SHEWMAKER, C.K.; JONES, A.; OAKES, J.V.; MCBRIDE, K.E. The reconstruction and expression of a Bacillus thuringiensis cryIIIA gene in protoplasts and potato plants. **Plant Mol. Biol.**, v. 21, p. 1131-1145, 1993.

AL-ABED, D.; RUDRABHATLA, S.; TALLA, R.; GOLDMAN, S. Split-seed: a new tool for maize researchers. **Planta**, v. 223, p. 1355-1360, 2006.

ALTIERI, M.A. Modern Agriculture: Ecological impacts and the possibilities for truly sustainable farming. 2000. Disponível em: http://nature.berkeley.edu/~agroeco3/modern_agriculture.html

ANTTONEN, M.J.; LEHESRANTA, S.; AURIOLA, S.; RICHARD, M.; ENGEL, K-H.; Kärenlampi, S.O.Genetic and environmental influence on maize kernel proteome. **J. Proteome Res.**, v. 9, p. 6160-6168, 2010.

ARONSON, A.I.; SHAI, Y. Why Bacillus thuringiensis insecticidal toxins are so effective: unique features of their mode of action. **FEMS Microbiol. Lett.**, v. 195, p. 1–8, 2001.

BHASKARAN, S.; SMITH, R.A. Regeneration in cereal tissue culture a review. **Crop Sci**., v. 30, p. 1328-1336, 1990.

BOGDANOVA, N.N.; CORBIN, D.R.; MALVAR, T.M.; PERLAK, F.J.; ROBERTS, J.K.; ROMANO, C.P. **U.S. Patent Application No. 13/686,320**, 2012.

BRASIL. Comissão Técnica Nacional de Biossegurança (CTNBio). Parecer Técnico Nº 1.100/2007, 2007. Disponível em http://ctnbio.mcti.gov.br/documents/566529/1462561/Parecer+T%C3%A9cnico+1100-2007.doc/e5fae84d-abde-46be-8939-9ff2bdc1d119;jsessionid=B1D9978EBC671C1C4AE3A5020E5D588D.rima?version=1.0;

BRAVO, A.; GILL, SS.; SOBERÓN, M. Bacillus thuringiensis mechanisms and use. In: GILBERT, L.I.; IATROU, K.; GILL, S.S. (eds). **Comprehensive Molecular Insect Science**. Oxford: ELSEVIER, 2005. pp. 175–206.

BRAVO, A.; SARJEET, S.G.; SOBERÓN, M. Mode of action of Bacillus thuringiensis Cry and Cyt toxins and their potential for insect control. **Toxicon**, v. 49. n. 4, p. 423-435, 2007.

CELLINI, F.; CHESSON, A.; COLQUHOUN, I.; CONSTABLE, A; DAVIES, H.V.; ENGEL, K.H.; GATEHOUSE, A.M.; KÄRENLAMPI, S.; KOK, E.J.; LEGUAY, J.J.; LEHESRANTA, S.; NOTEBORN, H.P.; PEDERSEN, J.; SMITH, M. Unintended effects and their detection in genetically modified crops. **Food and Chemical Toxicology**, v. 42, p. 1089-1125, 2004.

CERA, Center for Environmental Risk Assessment. **GM Crop Database, MON-ØØ81Ø-6 (MON810)**. ILSI Research Foundation, Washington D.C., 2016. Disponível em: http://cera-gmc.org/GmCropDatabaseEvent/MON810/short. Acesso em: 03 dez. 2016.

CHANG, W.F. Plant regeneration *in vitro* from leaf tissues derived from cultured immature embryos of *Zea mays* L. **Plant Cell Rep.**, v. 2, p. 183-185, 1983.

CONGER, B.V.; NOVAK, F.J.; AFZA, R.; ERDELSKY, K. Somatic embryogenesis from cultured leaf segments of *Zea mays*. **Plant Cell Rep.**, v. 6, p. 345-347, 1987.

DAL VESCO, L.L.; GUERRA, M.P. *In vitro* morphogenesis and adventitious shoot mass regeneration of Vriesea reitzii from nodule cultures. **Scientia Horticulturae**, v. 125, p. 748-755, 2010.

DAL VESCO, L.L.; STEFENON, V.M.; WELTER, L.J.; SCHERER, R.F.; GUERRA, M.P. Induction and scale-up of Billbergia zebrina nodule cluster cultures: implications for mass propagation, improvement and conservation. **Scientia Horticulturae**, v. 128, p. 515-522, 2011.

DE MAAGD, R.A.; BRAVO, A.; CRICKMORE, N. How Bacillus thuringiensis has evolved specific toxins to colonize the insect world. **Trends in Genetics**, v. 17, p. 193-199, 2001.

DUNCAN, D.R.; WILLIAMS, M.E.; ZEHR, B.E.; WIDHOLM, J.M. The production of callus capable of regeneration from immature embryos of numerous *Zea mays* genotypes. **Planta**, v. 165, p. 322-332, 1985.

FAO of the United Nations, **FAOSTAT statistics database, 2018**. Disponível em www.fao.org/faostat/.

FORD, A. Modeling the Environment (2nd edition). Washington DC: Island Press, 2009.

FRAME, B.R.; SHOU, H.; CHIKWAMBA, R.K.; ZHANG, Z.; XIANG, C.; FONGER, T.M.; PEGG, S.E.E.; LI, B.; NETTLETON, D.S.; PEI, D.; WANG, K. Agrobacterium tumefaciens-mediated transformation of maize embryos using a standard binary vector system. **Plant Physiol.**, v. 129, p. 13-22, 2002.

FUJIMOTO, H.; ITOH, K.; YAMAMOTO, M.; KYOZUKA, J.; SHIMAMOTO, K. Insect resistant rice generated by introduction of a modified δ-endotoxin gene of Bacillus thuringiensis. **Nature Biotechnology**, v. 11, n. 10, p. 1151-1155, 1993.

GEORGE, E.F.; HALL, M.A.; DE KLERK, G.J. (eds.). **Plant Propagation by Tissue Culture**. Dordrecht, The Netherlands: Springer, 2008. 464p.

GODDIJN, O.J.M.; LINDSEY, K.; VAN DER LEE, F.M.; KLAP, J.C.; SIJMONS, P.C. Differential gene expression in nematode induced feeding structures of transgenic plant harbouring promoter-gusA fusion constructs. **Plant Journal**, v. 4, p. 863-73, 1993.

GORDON-KAMM, W.J.; SPENCER, T.M.; MANGANO, M.L.; ADAMS, T.R.; DAINES, R.J.; START, W.G.; O'BRIEN, J.V.; CHAMBERS, S.A.; ADAMS JR, W.R.; WILLETS, N.G.; RICE, T.B.; MACKEY, C.J.; KRUEGER, R.W.; KAUSCH, A.P.; LEMAUX, P.

Transformation of maize cells and regeneration of fertile transgenic plants. **The Plant Cell**, v. 2, p. 603-618, 1990.

GREEN, C.E.; PHILIPS, R.L. Plant regeneration from tissue culture of maize. **Crop. Sci.**, v. 15, p. 417-421, 1975.

HELLWIG, S.; DROSSARD, J.; TWYMAN, R.M.; FISCHER, R. Plant cell cultures for the production of recombinant proteins. **Nature Biotechnology**, v. 22, n. 11, p. 1415-1422, 2004.

HODGES, T.K.; KAMO, K.K.; IMBRIE, C.W.; BECWAR, M.R. Genotype specificity of somatic embryogenesis and regeneration in maize. **BioTechnology**, v. 4, p. 219-223, 1986.

HUANG, X.Q.; WEI, Z.M. High-frequency plant regeneration through callus initiation from mature embryos of maize (*Zea Mays* L.). **Plant Cell Rep.**, v. 22, p. 293-800, 2004.

JAMES, C. **Executive Summary of Global Status of Commercialized Biotech/GM Crops: 2016**. ISAAA Brief 52. Ithaca, NY, 2016.

KISTLER, L.; MAEZUMI, S.Y.; DE SOUZA, G.J.; PRZELOMSKA, N.A.S.; MALAQUIAS COSTA, F.; SMITH, O.; LOISELLE, H.; RAMOS-MADRIGAL, J.; WALES, N.; RIBEIRO, E.R.; MORRISON, R.R.; GRIMALDO, C.; PROUS, A.P.; ARRIAZA, B.; GILBERT, M.T.P.; FREITAS, F.O.; ALLABY, R.G. Multiproxy evidence highlights a complex evolutionary legacy of maize in South America. **Science**, v. 362(6420), p. 1309-1313., 2018. doi:10.1126/science.aav0207

KOZIEL, M.G.; BELAND, G.L.; BOWMAN, C.; CARROZI, N.B.; CRENSHAW, R. CROSSLAND, L.; DAWSON, J.; DESAI, N.; HILL, M.; KADWELL, S.; LAUNIS, K.; LEWIS, K.; MADDOX, D.; MCPHERSON, K.; MEGHJI, M.R.; MERLIN, E.; RHODES, R.; WARREN, G.W.; WRIGHT, M; EVOLA, S.V. Field performance of elite transgenic maize plants expressing an insecticidal protein derived from Bacillus thuringiensis. **Bio/Technology**, v. 11, p. 194-200, 1993.

LATHAM, J.R.; WILSON, A.K.; STEINBRECHER, R.A. The mutational consequences of plant transformation. **J. Biomed. Biotech.**, 25376, 1–7, 2006

LU, C.; VASIL, V.; Vasil, I.K. Improved efficiency of somatic embryogenesis and plant regeneration in tissue cultures of maize (*Zea mays* L.). **Theoret. Appl. Genet.**, 66: 285, 1983. Disponível em: https://doi.org/10.1007/BF00251161.

PECHANOVA, O.; TAKÁ, T.; SAMAJ, J.; PECHAN, T. Maize proteomics: an insight into the biology of an important cereal crop. **Proteomics**, v. 13, p. 637-662, 2013.

PERLAK, F.J.; FUCHS, R.L.; DEAN, D.A.; MCPHERSON, S.L.; FISCHHOFF, D.A. Modification of the coding sequence enhances plant expression of insect control protein genes. **Proc. Natl. Acad. Sci. USA**. v. 88, n.8, p. 3324-3328, 1991.

PERLAK, F.J.; DEATON, R.W.; ARMSTRONG, T.A.; FUCHS, R.L.; SIMS, S.R.; GREENPLATE, J.T.; FISCHHOFF, D.A. Insect resistant cotton plants. **Biotechnology**, v. 8, n. 10, p. 939-943, 1990.

PERLAK, F.J.; STONE, T.B.; MUSKOPF, Y.M.; PETERSEN, L.J.; PARKER, G.B.; MCPHERSON, S.A.; WYMAN, J.; LOVE, S.; REED, G.; BIEVER, D.; Fischhoff, D.A. Genetically improved potatoes: protection from damage by Colorado potato beetles. **Plant Mol. Biol.**, v. 22, n. 2, p. 313-321, 1993.

PIPERNO, D.R.; RANERE, A.J.; HOLST, I.; IRIARTE, J.; DICKAU, R. Starch grain and phytolith evidence for early ninth millennium B.P. maize from the Central Balsas River Valley, Mexico. **Proceedings of the National Academy of Sciences USA**, v. 106, p. 5019-5024, 2009.

R CORE TEAM. **R: A Language and Environment for Statistical Computing**. R Foundation for Statistical Computing. Vienna, Austria, 2017.

RHODES, C.R.; GREEN, C.E.; PHILLIPS, R.L. Factors affecting tissue culture initiation from maize tassels. **Plant Science**, v. 46, p. 225-232, 1986.

ROSATI A.; BOGANI, P.; SANTARLASCI, A.; BUIATTI, M. Characterization of 3′ transgene insertion site and derived mRNAs in MON810 Yieldgard maize. **Plant Mol. Biol.**, v. 67, p. 271-281, 2008.

SAIRAM, R.V.; PARANI, M.; FRANKLIN, G.; LIFENG, Z.; SMITH, B.; MACDOUGALL, J.; WILBER, C.; SHEIKHI, H.; KASHIKAR, N.; MEEKER, K.; AL-ABED, D.; BERRY, K.; VIERLING, R.; GOLDMAN, S.L. Shoot meristem: an ideal explant for *Zea mays* L. transformation. **Genome**, v. 46, p. 323-329, 2003.

SPRINGER, W.D.; GREEN, C.E.; KOHN, K.A. A histological examination of tissue culture initiation from immature embryos of maize. **Protoplasma**, v. 101, p. 269-281, 1979.

STITZER, M.C.; ROSS-IBARRA, J. Maize domestication and gene interaction. **New Phytol.**, 2018. Disponível em: https://doi.org/10.1111/nph.15350.

STRABLE, J.; SCANLON, M.J. Maize (*Zea mays*): a model organism for basic and applied research in plant biology. **Cold Spring Harb. Protoc.**, v. 10, 2009. Disponível em: http:// doi:10.1101/pdb.emo132

SUTTON, D.W.; HAVSTAD, P.K.; KEMP, J.D. Synthetic cryIIIA gene from Bacillus thuringiensis improved for high expression in plants. **Transgenic Res.**, v. 1, n. 5, p. 228-236, 1992.

URWIN, P.E.; MOLLER, S.G.; LILLEY, C.J.; MCPHERSON, M.J.; ATKINSON, H.J. Continual green fluorescent protein monitoring of Cauliflower mosaic virus 35S promoter activity in nematode-induced feeding cells in Arabidopsis thaliana. **Mol. Plant Microbe Interact.**, v. 10. p. 394-400, 1997.

US EPA (United States of America Environmental Protection Agency). **Biopesticides Registration Action Document (BRAD): Cry1Ab and Cry1F Bacillus thuringiensis (Bt) Corn Plant-Incorporated Protectants**. US EPA Office of Pesticide Programs, Biopesticides

and Pollution Prevention Division, 2010. Disponível em: https://www3.epa.gov/pesticides/chem_search/reg_actions/pip/cry1f-cry1ab-brad.pdf.

VAN AARSSEN, R.; SOETAERT, P.; STAM, M.; DOECKX, J.; GOSSELÉ, V.; REYNAERTS, A.; CORNELISSEN, M. cryIA(b) transcript formation in tobacco is inefficient. **Plant Mol. Biol.**, v. 28, n. 3, p. 513–524, 1995.

VASIL, V.; LU, C.; VASIL, I.K. Histology of somatic embryogenesis in cultured immature embryos of maize (*Zea mays* L.). **Protoplasma**, v. 127, p. 1–8, 1985.

VASIL, L.K. Developing cell and tissue culture systems for the improvement of cereal and grass crops. **Journal of Plant Physiology**, v. 128, p. 193-218, 1987.

WANG, A.S. Callus induction and plant regeneration from maize mature embryos. **Plant Cell Rep.**, v. 6. p. 360-362, 1987.

ZHONG, H.; SRINIVASAN, C.; STRICKLEN, M.B. In-vitro morphogenesis of corn (*Zea mays* L.). I. Differentiation of multiple shoot clumps and somatic embryos from shoot tips. **Planta**, v. 187, p. 483-48, 1992.

4. CAPÍTULO I - INDUCTION AND ESTABLISHMENT OF *IN VITRO* CULTURES OF TRANSGENIC MAIZE AG-5011YG (MON810).

ABSTRACT

MON810 is a genetically modified (GM) maize event which expresses an insecticidal recombinant Cry1Ab protein, and MON810's recombinant gene expression cassette is present in several insect resistant GM maize hybrids. GM events obtained by biolistics, such as MON810, are generated by insertion of a recombinant DNA sequence in a random *locus* of the plant genome, and this process may produce emergent properties, in greater or lesser extent, depending on each transformation event. In order to initiate the development of an *in vitro* model for the study of emergent properties of plant transformation, a MON810 GM maize hybrid (AG-5011YG) was tested regarding *in vitro* callus induction, and callogenesis frequency, callus friability rate, explant oxidation rate, and rhizogenesis rate were evaluated, comparing different explant sources (light- or dark-germinated seedlings), explant types (thin cell layers (TCLs) from the coleoptilar node - controlling for the distance (mm) of the TCL to the coleoptilar node center - and root segments), culture lighting regimes (24 h dark and 16 h light/8 h dark), and 2,4-D concentrations in the culture medium (0, 5, 10 or 20 μM). 2,4-D effectively modulated the *in vitro* responses of AG-5011YG, increasing callus induction in a quadratic trend ($p<0.001$). Seedlings used as explant source for callus induction should be germinated in complete darkness, especially if coleoptilar node thin cell layers - which are most responsive within 1mm of the seedling coleoptilar node - are to be employed as explant. Culture induction should also occur in complete darkness. Both tested explants excised from seedlings germinated in complete darkness showed good potential for culture initiation *in vitro* (60-80% success in the best treatments), but root segments, which are available in greater numbers, presented higher and significant linear increases ($p<0.001$) in callus friability rate with increasing 2,4-D concentrations, indicating greater suitability for *in vitro* culture initiation. In conclusion, excellent callus induction rates (~80%) and callus friability rates (~70%) were achieved in cultures kept in constant darkness, using root segments from seedlings germinated in the dark, cultured in MS medium supplemented with 20 μM 2,4-D. These findings represent the first step towards the development of an *in vitro* model for the identification of emergent properties in GM plants.

4.1 INTRODUCTION

Maize (*Zea mays spp. mays*) GM event MON810 (Monsanto Company, YieldGard® maize, unique identifier MON-ØØ81Ø-6 (CERA, 2016)) is a GM maize widely employed for the production of insect resistant GM maize hybrids (James, 2016; CERA, 2016). It was obtained by biolistic insertion of a recombinant genetically engineered construct (GEC) in the genome of highly *in vitro* regenerable maize hybrid Hi-II (CERA, 2016).

In most countries, before approval for cultivation and commercialization, a new GM event must undergo a risk assessment where not only the recombinant construct integration, stability and expression must be demonstrated, but also possible genetic and phenotypic unintended effects must be evaluated, in comparison to the most similar conventional counterpart available (Bartsch *et al.*, 2010).

For Bt-maize events such as MON810, several studies (Zolla *et al.*, 2008; Agapito-Tenfen *et al.*, 2013; La Paz *et al.*, 2014; Holderbaum *et al.*, 2015) point to a lack of certainty regarding how similar pairs of near-isogenic hybrids truly are in phenotypical terms, considering they share more than 99% of their genetic makeup, with exception of the recombinant GEC and possibly some genetically linked DNA sequences (Zeven and Waninge, 1986).

Plant cell, tissue and organ cultures comprise a valuable tool in multiple fronts, from developmental physiology studies, to plant mass propagation, fixation of genetic gains, germplasm conservation, and the generation of transgenic plants (Dal Vesco *et al*., 2011). Additionally, the highly controllable and contained environment of plant *in vitro* cultures allows for several advantages from an experimental point of view: minimization of "random" environmental effects, high reproducibility, and scalability (Cavez *et al*., 2009). Thus, plant *in vitro* cultures would be an ideal model to evaluate the occurrence of unintended effects/emergent properties of plant transformation.

In maize tissue culture, classical explants are immature zygotic embryos, for which the *in vitro* morphogenic potential was thoroughly established (Green and Phillips 1975; Springer *et al.* 1979; Vasil *et al.* 1985; Hodges *et al.* 1986; Emons *et al.*, 1993; Frame *et al.,* 2002). However, the use of immature embryos as explants for *in vitro* establishment of a commercial GM maize hybrid is mostly unpractical, because it requires keeping the parent lines, which are not normally accessible. This emphasizes the need to optimize the *in vitro* response of other explant types for this purpose.

Known differences in the regenerative capacity of maize genotypes can be overcome by manipulation of growth regulator concentration in the culture medium (Vasil 1987; Zhong *et al.*, 1992). The potential of the synthetic auxin 2,4-D in combination with cytokinins for maize *in vitro* morphogenesis was previously demonstrated, allowing the establishment of cell and tissue cultures and plant regeneration, independently of the explant genotype (Zhong *et al.*, 1992).

The objective of this study was to evaluate induction success, callus quality and morphogenesis of a GM maize hybrid (AG-5011YG), using two main explant sources - seedling root segments and seedling coleoptilar node thin cell layers (TCLs), from seedlings germinated in the dark or in 16 h light/8 h dark photoperiod - cultured with a range of 2,4-D concentrations in the culture medium and on the same two lighting regimes used for seed germination. The main hypotheses tested were: explant source, germination lighting regime, culture lighting regime and 2,4-D concentration affect callus induction, friability and morphogenic potential, either independently or in an interactive fashion.

4.2 MATERIAL AND METHODS

4.2.1 Plant material

Seeds of GM maize hybrid AG-5011YG (MON810) were purchased in the seed market in Erval do Oeste, Santa Catarina, south Brazil. Seeds were analyzed to confirm their GM status, using a lateral flow strip kit for detection of Cry1Ab protein (Envirologix Quickstix AS-003-CRLS kit) and qualitative PCR for detection of the CAMV-35S promoter and the *cry1Ab* gene, using *zein* as endogenous control (Data not shown).

4.2.2 Seed preparation

Seeds (n=40) were separately and thoroughly washed in glass beakers under tap water for 5 min, in order to remove the seed fungicide coat and excess bacteria; seeds were then immersed in distilled water with Tween 20 (40 µl 100 ml^{-1}) for 5 min under hand shaking; the water was drained, seeds were taken to an aseptic laminar flow hood, surface sterilized with 70% alcohol for 3 min, NaClO 1% with Tween 20 (40 µl/100 ml) for 30 min,

washed five times with sterile distilled water, and immersed in sterile distilled water for 72 h to soften and facilitate subsequent embryo excision. All subsequent manipulations of seeds, embryos, seedlings and cultures took place in aseptic conditions in a laminar flow hood, using aseptic technique and sterilized tools and materials.

4.2.3 Zygotic embryo excision and in vitro germination

Mature zygotic embryos (Figure 1) were excised from softened seeds placed on paper plates, using forceps and scalpels under a stereomicroscope. Excised embryos were placed in glass flasks with sterile distilled water to prevent dehydration, and after the procedure embryos were inoculated in test tubes containing 15 ml germination medium (MS salts (Murashige and Skoog, 1962) supplemented with Morel vitamins (Morel and Wetmore, 1951) and 3% sucrose). Inoculated embryos were divided in two groups of 20, kept at 25±2 ºC in the dark or under 16 h light/8 h dark photoperiod, with light intensity of 60 $\mu mol.m^{-2}.s^{-1}$ from cool white fluorescent lamps (Sylvania®), for 3 weeks. Contamination-free plantlets were used as source of different explants for callus induction.

Figure 1: Diagram of maize grain (left: whole grain; right: radial cross section).

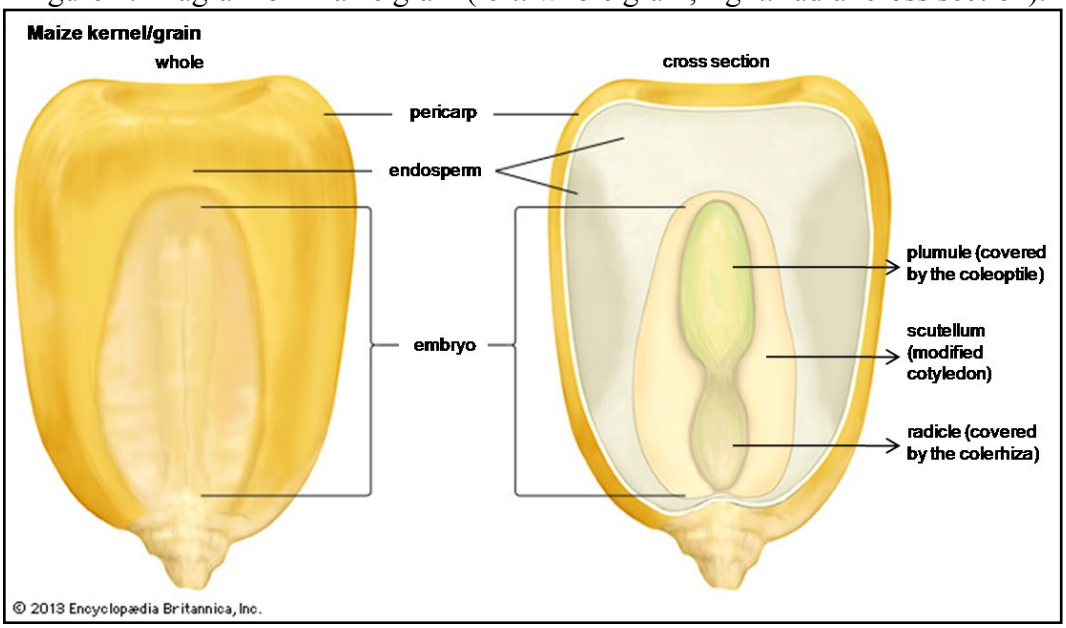

Fonte: Image adapted from Encyclopedia Britannica 'corn anatomy', available at: https://www.britannica.com/science/endosperm#/media/1/187065/232608, access date september 22nd 2018.

4.2.4 Culture induction

The basal nutrient medium used for maize *in vitro* cultures consisted of MS salts supplemented with Morel vitamins, 3% sucrose, enzymatic casein hydrolisate (200 mg/L) and adenine (40 mg/L) (modified from O'Connor-Sanchez *et al.* (2002)). All culture media had pH adjusted to 5.8 prior to sterilization at 121 ºC and 1.5 atm for 20 min; media were gelled with 0.2% Phytagel. Contaminant-free maize plantlets (Figure 2) (n = 16 for both dark- and light-germinated seedlings) were used to obtain two types of explants: root segments (~2 cm) (10-16 segments per seedling, including primary root and seminal roots, and excluding nodal roots), and TCLs (~1 mm) of tissues directly bellow, over, and above the coleoptilar node. Five TCLs were excised per plantlet, including one TCL centered on the coleoptilar node (position 0), two TCLs above it (positions +1 and +2 mm), and two TCLs under it (positions -1 and -2 mm). This sectioning of seedlings' mesocotile/node/epicotile region was intended to include the shoot apical meristem (SAM), and determine quantitatively if the distance to the coleoptilar node (as an indicator of SAM position) had an influence in callus induction capacity. Similar procedures were carried out in studies using TCLs of seedling tissues for other monocot species (Van Le *et al*., 1997; Steinmacher *et al*., 2007).

Figure 2: Diagram of maize seedling.

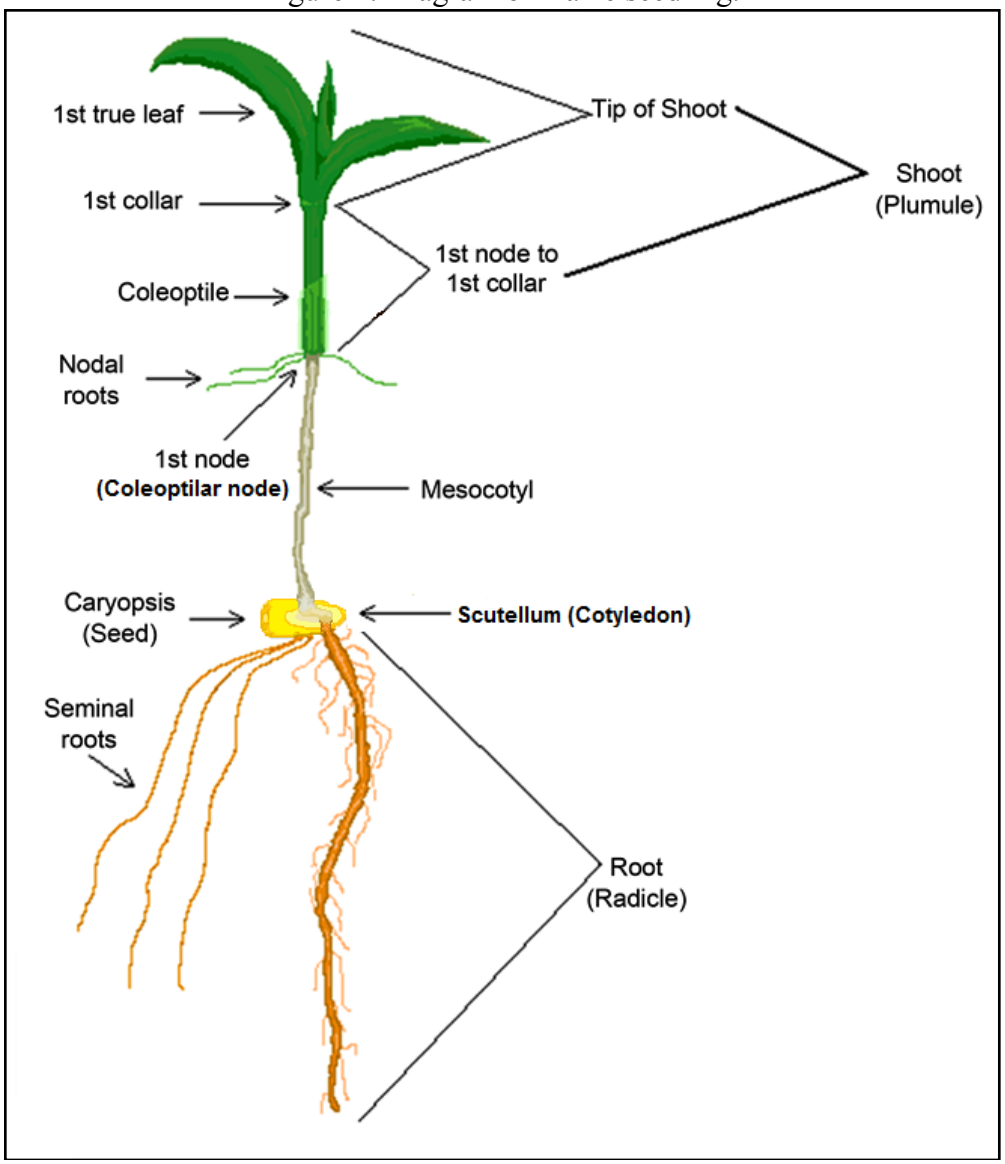

Fonte: Image adapted from Bousselot *et al*. (2017).

Here, callus is defined as an unorganized cell mass (Ikeuchi *et al.*, 2013). In order to assess effects of germination lighting regime, culture lighting regime, explant type and 2,4-D on callus induction and qualitative traits, explants were excised from plantlets on paper plates using scalpels and forceps, and immediately inoculated in plastic Petri dishes containing 25 ml basal nutrient media supplemented with a gradient of 2,4-D concentrations (0, 5 10 and 20 μM).

All cultures were kept at 25 ºC. For the experiment with root segments, half of the seedlings germinated in the dark, and half of the seedlings germinated in 16 h light/8 h dark photoperiod were used to initiate cultures in each lighting condition. For the TCL experiment, seedlings of both lighting regime conditions were used to initiate cultures in the dark only. A total of 160 TCLs and 385 root segments were inoculated.

For root segments and TCLs, callogenesis and callus friability were evaluated four weeks after induction. Frequency of explant blackening/oxidation was recorded for TCLs only. All endpoints were recorded by visual inspection under the stereomicroscope. Callus samples were photographed inside Petri dishes in an Olympus stereomicroscope attached to an Olympus DP-71 image capture system.

4.2.5 Statistical Analysis

Data were analyzed in a generalized linear mixed model framework (Mccullagh and Nelder, 1989; Bolker *et al.*, 2009). Data on callus induction, callus friability and TCL oxidation were evaluated as binary outcomes (yes = 1; no = 0) and analyzed with logistic regression. For every analysis, the initial statistical models included all explanatory variables, interactions, and quadratic terms for quantitative variables (e.g. 2,4-D concentration and TCL distance from coleoptilar node). Model selection was carried out by means of stepwise elimination of variables followed by inspection of the small sample-corrected Akaike Information Criterion (cAIC) (Hurvich and Tsai, 1989; Burnham and Anderson, 2004). When significant, plantlet was treated as a random effect in all models to account for correlations between calli derived from the same plantlet. Model assumptions about residual variance and distribution were evaluated graphically for all models, and the dispersion parameter - Chi-square/degrees of freedom - was additionally used to assess model fit, when applicable (Mccullagh and Nelder, 1989; Bolker *et al.*, 2009). Effects were considered significant when $P < 0.05$. Significant trend- and point-wise differences were detected by comparison of 95% confidence intervals/envelopes (Cumming and Finch, 2005; Cumming *et al.*, 2007). Analyses were carried out in the R language/software (R Core Team, 2017).

4.3 RESULTS AND DISCUSSION

4.3.1 Explant: thin cell layers of the seedling coleoptilar-node region

4.3.1.1 Callus induction

All three evaluated factors - lighting regime of seedling germination prior to callus induction, TCL distance to the coleoptilar node and 2,4-D concentration in the medium - affected callus induction in marked ways.

The majority of seedlings germinated in 16 h light/8 h dark photoperiod grew normally, presenting bright-green, well developed leaves. Seedlings germinated in the dark were etiolated, with a lengthy mesocotyl and pale-green leaves. Explant source lighting regime presented a highly significant effect ($p<000.1$) where only TCLs from seedlings germinated in the dark were responsive to *in vitro* callus induction treatments, regardless of TCL topological position and 2,4-D concentration (Figures 3, 4, 5 and 6), indicating that, compared to germination in the dark, germination in the light ultimately renders TCLs from the coleoptilar-node region of seedlings unsuitable for maize *in vitro* culture initiation.

According to George *et al*. (2008), plants can follow different developmental strategies when grown in the dark (skotomorphogenesis) or in the light (photomorphogenesis); plants grown in the dark become etiolated, with rapid stem elongation, limited or no leaf expansion, and a lack of functional photosynthetic apparatus; when exposed to light, however, rapid changes in gene expression occur, leading to the normal pattern of development.

The distance from the coleoptilar node showed a significant curvilinear trend ($p<0.001$) for TCL induction capacity, with TCLs excised directly over (position 0) or slightly above (position +1) the coleoptilar node showing the highest induction rates, and induction decreasing continuously in both directions (Figures 3, 4 and 5). It is likely this result reflects the fact that the shoot apical meristem (SAM), a reliable explant source for induction of *in vitro* maize cultures (Zhong *et al.*, 1992; O'Connor-Sanchez *et al.*, 2002), is positioned slightly above the coleoptilar node.

Here, the concentration of 2,4-D in the medium also influenced the induction response of TCLs, evidencing a significant curvilinear dose-response ($p<0.01$) (Figures 4 and 6). Overall, increasing 2,4-D up to ~10 μM corresponded to continually increasing induction rates in a range between 40% and 80%, depending on TCL distance to the coleoptilar node (60% on average), and from 10 μM to 20 μM a tendency for stabilization (or even a slight decrease) in induction rates was observed.

Figure 3: Maize callus induction as a function of TCL topological position (-2,-1, 0, 1 and 2 mm from the coleoptilar node) from seedlings germinated in 24 h darkness (Escuro) or in a 16 h light/8 h dark photoperiod (Luz), and cultured in complete darkness, on media containing 0, 5, 10 or 20 μM 2,4-D. Blue lines depict estimated trends, grey shaded bands represent 95% confidence intervals and black dots represent observations (slightly dislocated vertically and horizontally to improve visualization).

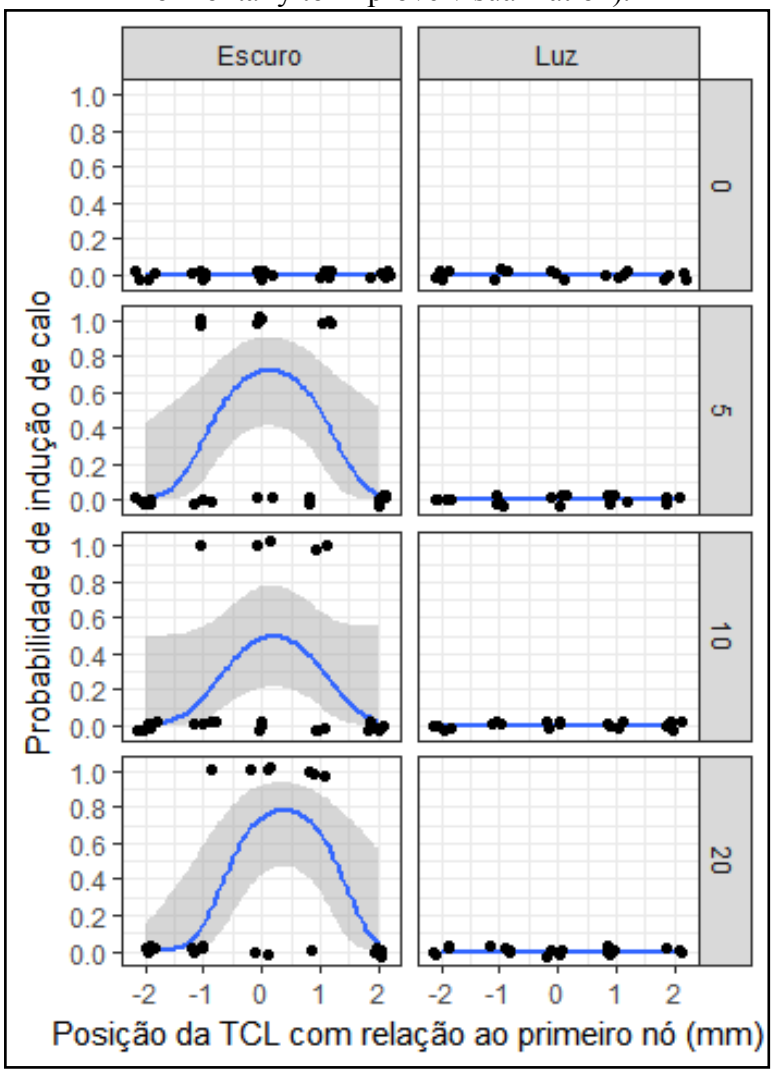

Fonte: Daniel Ferreira Holderbaum (2019).

Steinmacher *et al*. (2007) obtained similar results for peach-palm (*Bactris gasipaes*) somatic embryogenesis, where *in vitro* seedlings' root-shoot axes, including the SAM, were used as source of TCLs for culture initiation. Likewise, these authors found that callus induction on TCLs from seedlings' SAM region was significantly superior to other tissues, when combined with the correct auxin (Picloram) concentration (between 150 and 600 μM) in the medium.

Figure 4: Maize callus induction as a function of 2,4-D concentration in the media, faceted by TCL topological position (-2,-1, 0, 1 and 2 mm from the coleoptilar node) and seedling (explant source) germination lighting regime (24 h dark - Escuro - and 16 h light/8 h dark photoperiod - Luz). Blue lines depict estimated trends, grey shaded bands represent 95% confidence intervals and black dots represent observations (slightly dislocated vertically and horizontally to improve visualization).

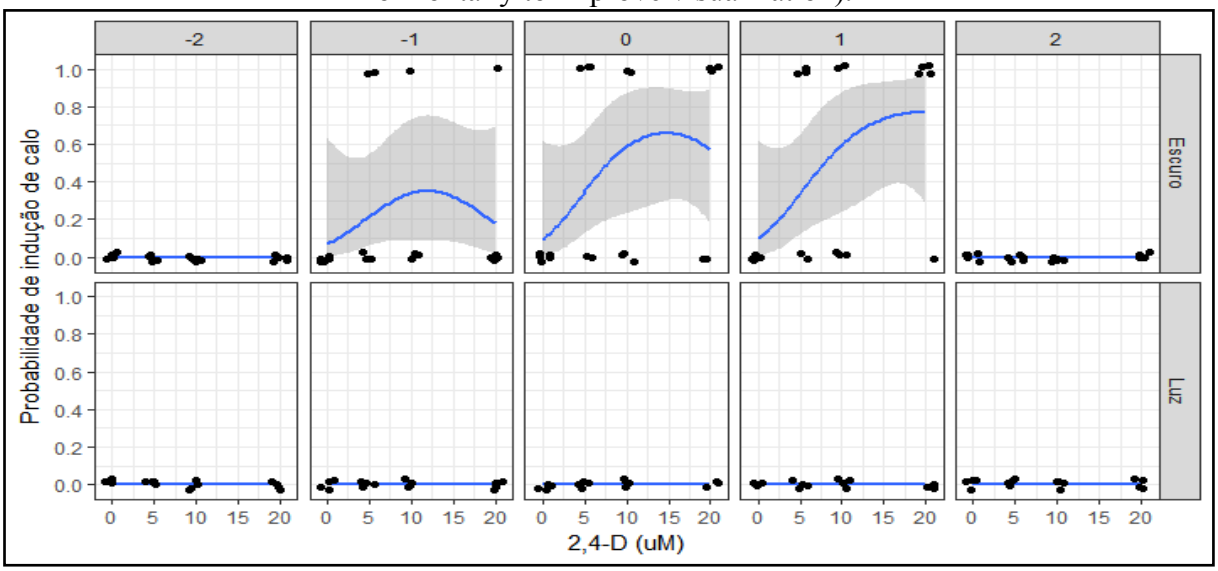

Fonte: Daniel Ferreira Holderbaum (2019).

Figure 5: Maize callus induction as a function of TCL topological position (-2,-1, 0, 1 and 2 mm from the coleoptilar node) and seedling germination lighting regime (24 h dark - Escuro - and 16 h light/8 h dark photoperiod - Luz), averaged for all tested 2,4-D concentrations. Lines depict estimated trends, shaded bands represent 95% confidence intervals and black dots represent observations (dislocated vertically and horizontally to improve visualization).

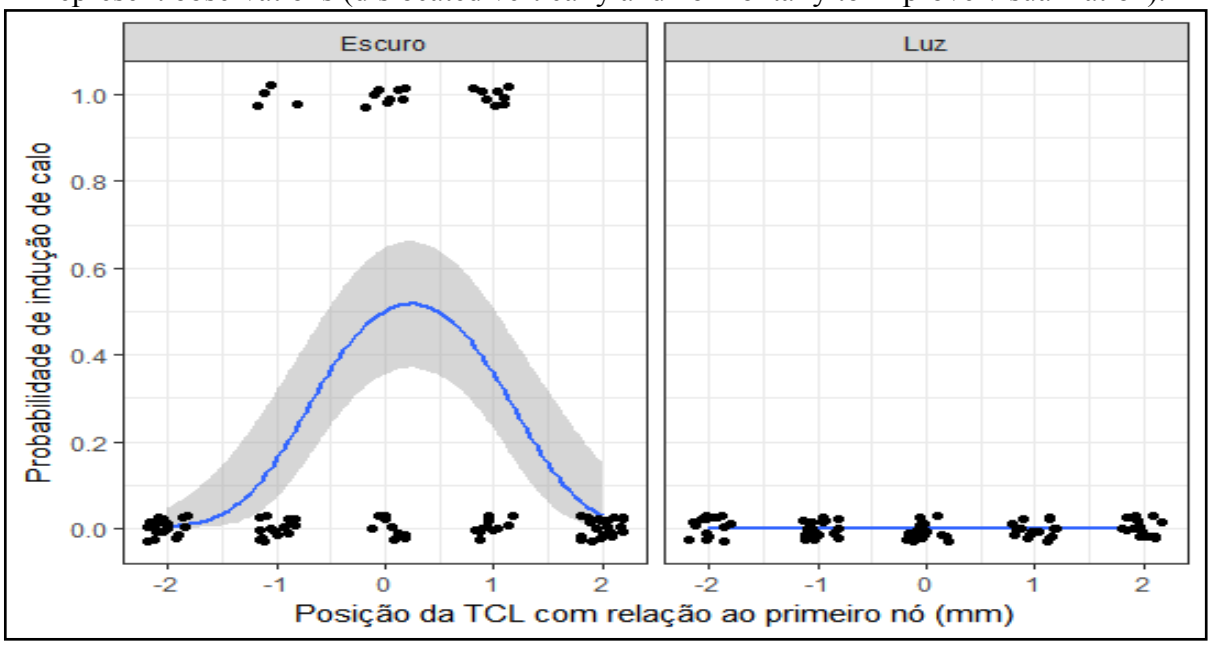

Fonte: Daniel Ferreira Holderbaum (2019).

Figure 6: Maize callus induction as a function of 2,4-D concentration in the media, faceted by seedling (explant source) germination lighting regime (24 h dark - Escuro - and 16 h light/8 h dark photoperiod - Luz), and averaged between responsive TCL topological positions (-1, 0 and 1 mm from coleoptilar node). Lines depict estimated trends, grey shaded bands represent 95% confidence intervals and black dots represent observations (slightly dislocated vertically and horizontally to improve visualization).

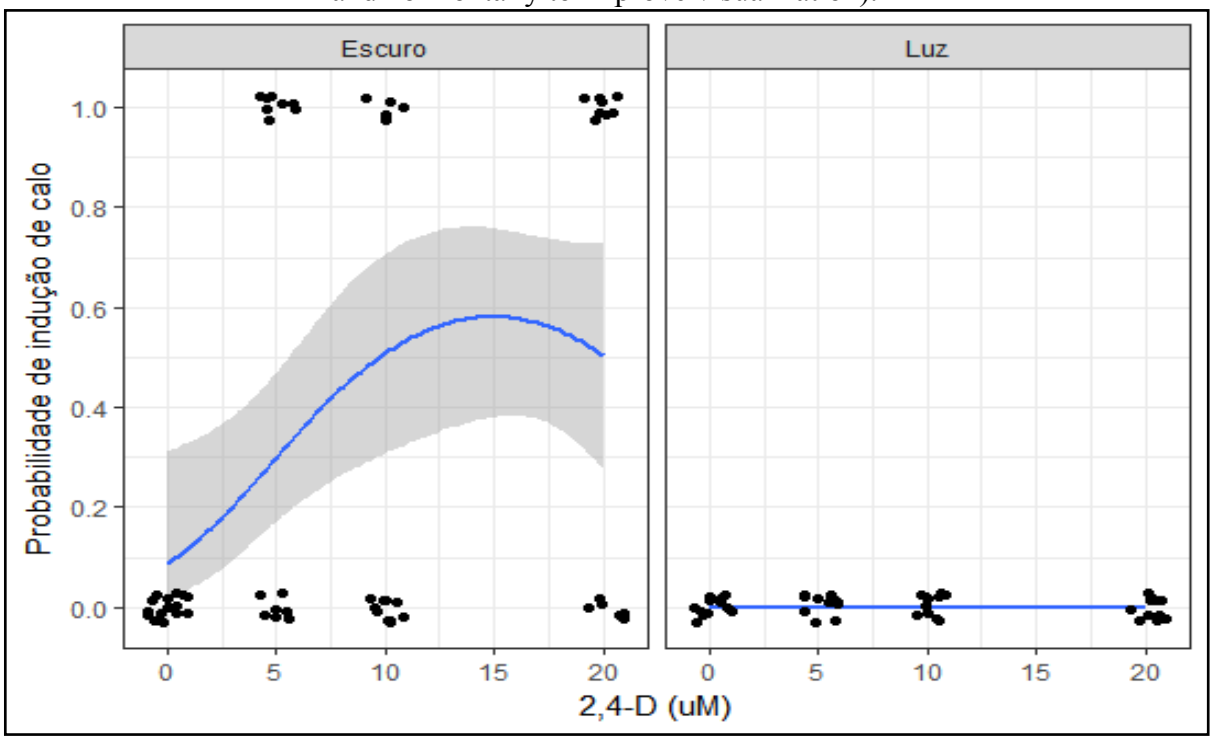

Fonte: Daniel Ferreira Holderbaum (2019).

4.3.1.2 Callus friability

Callus friability is desirable in maize *in vitro* callus induction, insofar as friable calli tend to be more amenable to initiation of suspension cultures (Songstad *et al*, 1992). No evidence was found for a significant effect of either TCL position (p=0.62, Figure 7) or 2,4-D concentration (p=0.39, Figure 8) on callus friability, and seedling germination lighting regime could not be assessed, since TCLs from seedlings germinated in the light did not induce any callus growth. It should be noted, moreover, that the analysis of frequency of friable calli was hampered in this initial experiment by a reduced sample size, given that only induced calli can be included in this analysis. The estimated trends point, however, to a linear increase in the frequency of friable calli from TCL positions -1 to 1, and from 5 to 20 μM 2,4-D, although slopes were not significantly different from 0. Also, there was no evidence for interaction between TCL position and 2,4-D concentration regarding the frequency of friable calli.

Figure 7: Frequency of friable maize calli as a function of TCL topological position (-2,-1, 0, 1 and 2 mm from the coleoptilar node), from seedlings (explant source) germinated in 24 h darkness, averaged for all tested 2,4-D concentrations. Blue lines depict estimated trends, grey shaded bands represent 95% confidence intervals and black dots represent observations (slightly dislocated vertically and horizontally to improve visualization).

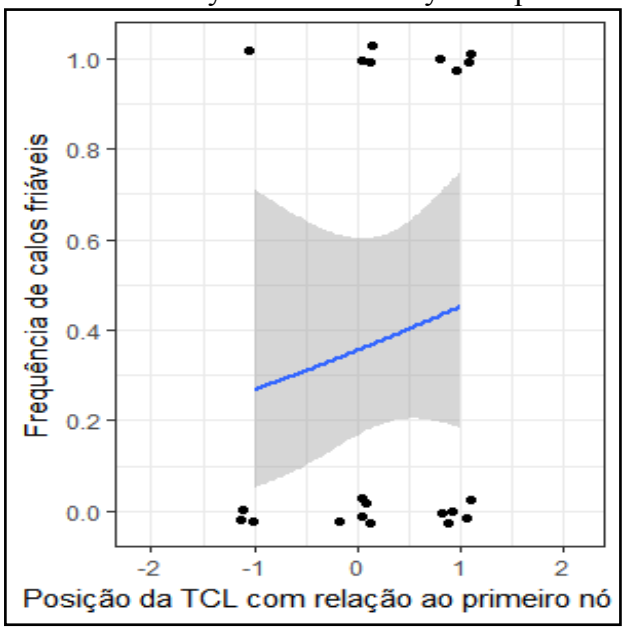

Fonte: Daniel Ferreira Holderbaum (2019).

Figure 8: Frequency of friable maize calli as a function of 2,4-D concentration in the media, from seedlings (explant source) germinated in 24 h darkness, and averaged between responsive TCL topological positions (-1, 0 and 1 mm from the coleoptilar node). Blue lines depict estimated trends, grey shaded bands represent 95% confidence intervals and black dots represent observations (slightly dislocated vertically and horizontally to improve visualization).

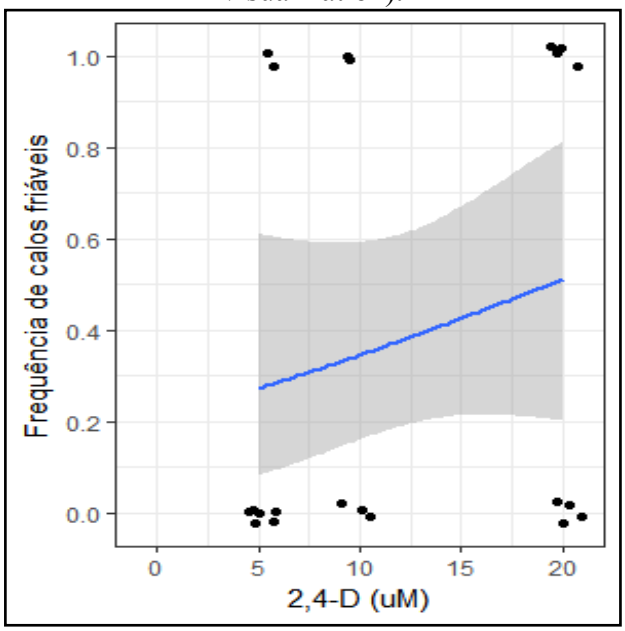

Fonte: Daniel Ferreira Holderbaum (2019).

4.3.1.3 Explant blackening/oxidation

During data collection, several TCL explants showed a marked browning or blackening of the tissues. In many cases, tissue blackening derives from the oxidation of phenolic compounds, a common phenomenon in injured plant tissues (Holderbaum *et al*., 2010), and is often related to cell death and explant loss in tissue culture (George *et al*., 2008; Taiz & Zeiger, 2013). Thus, we recorded the frequency of blackening in TCL explants. TCL blackening was significantly affected by the seedling germination lighting regime ($p<0.001$, Figures 9 and 10), where all TCL explants derived from light-exposed seedlings presented browning/blackening, and none induced callus, regardless of TCL distance from the coleoptilar node (Figure 9) or 2,4-D concentration (Figure 10), whereas TCLs from dark-germinated seedlings showed ~60% browning/blackening in medium free of 2,4-D, and a linear increase in explant browning from 0 μM to 20 μM (up to ~80% TCL browning).

Figure 9: TCL blackening as a function of TCL topological position (-2,-1, 0, 1 and 2 mm from the coleoptilar node) and seedling (TCL source) germination lighting regime (24 h darkness - Escuro - and 16 h light/8 h dark photoperiod - Luz), averaged for all tested 2,4-D concentrations. Blue lines depict estimated trends, grey shaded bands represent 95% confidence intervals and black dots represent observations (slightly dislocated vertically and horizontally to improve visualization).

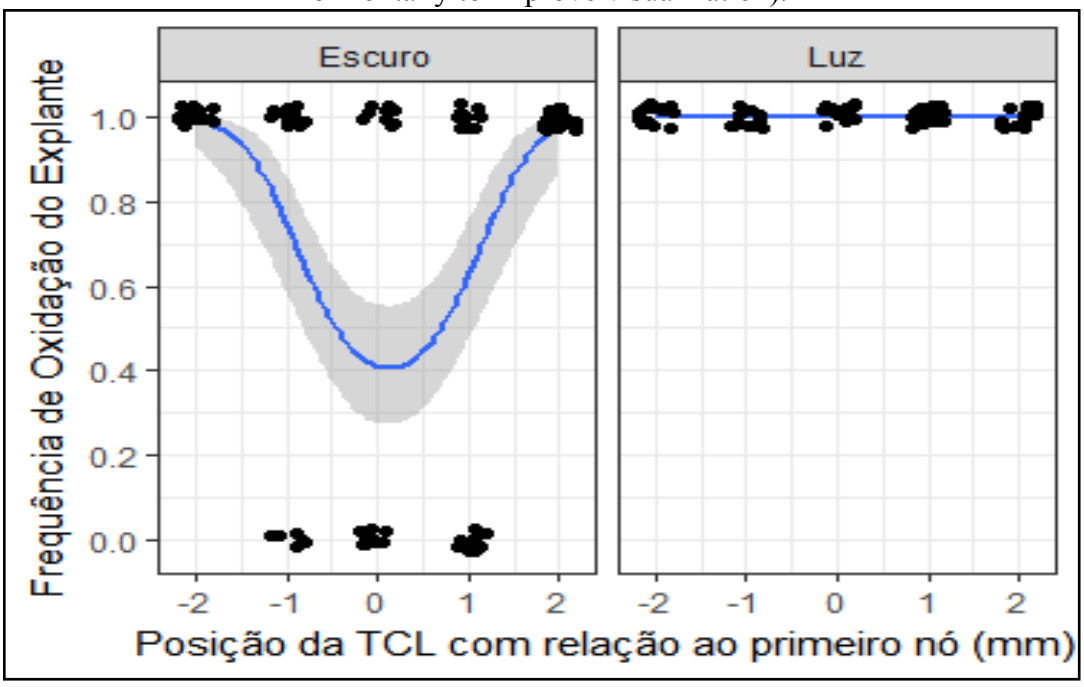

Fonte: Daniel Ferreira Holderbaum (2019).

The distance from the coleoptilar node presented a significant quadratic effect on TCL tissue blackening ($p<0.001$), with TCLs closer to the SAM position (positions 0 and 1) showing significantly less oxidation than TCLs from other positions. The further removed from the SAM, the higher are explant blackening rates. This result, coupled to the evidence that TCLs excised from positions 0 and 1 are the most responsive to induction by 2,4-D, further suggest the greater potential tissues located close to or including the SAM have for *in vitro* culture initiation (Zhong *et al.*, 1992; O'Connor-Sanchez *et al.*, 2002).

2,4-D also had a significant effect on TCL blackening/oxidation ($p=0.018$), but this effect was linear, and less pronounced than the TCL topological position effect. It is estimated that TCL oxidation increases linearly from ~60% to ~85% concomitant to an increase in 2,4-D from 0 to 20 μM.

Figure 10: TCL blackening as a function of 2,4-D concentration in the media, faceted by seedling (TCL source) germination lighting regime (24 h darkness - Escuro - and 16 h light/8 h dark photoperiod - Luz), and averaged between TCL topological positions. Blue lines depict estimated trends, grey shaded bands represent 95% confidence intervals and black dots represent observations (slightly dislocated vertically and horizontally to improve visualization.

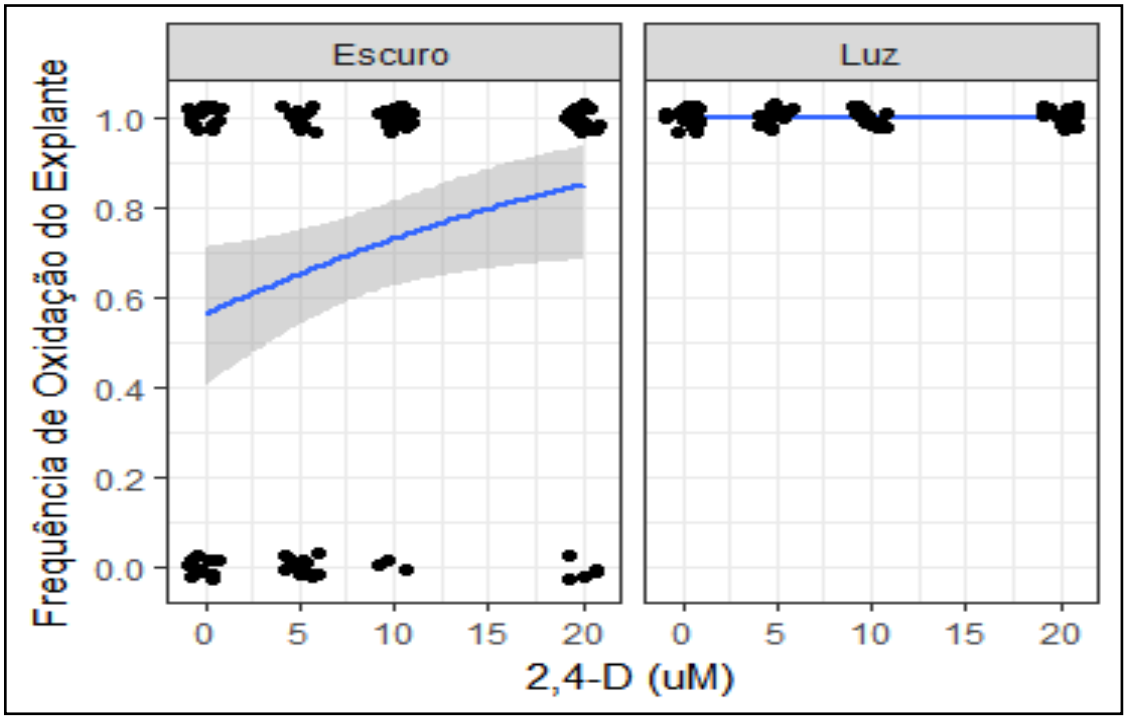

Fonte: Daniel Ferreira Holderbaum (2019).

4.3.2 Explant: Seedling root segments

4.3.2.1 Callus induction

The inspected variables of seedling germination lighting regime, callus induction lighting regime, and 2,4-D concentration significantly affected callus induction in root segments in a complex manner (Figure 11). 2,4-D showed a quadratic effect ($p<0.001$) and significant two-way interactions with seedling germination lighting regime ($p=0.018$) and callus induction lighting regime ($p=0.031$), while weaker evidence ($p=0.068$) was obtained for an interaction between seedling germination lighting regime and callus induction lighting regime.

Figure 11: Maize callus induction in seedling root segments, as a function of 2,4-D concentration in the medium, seedling germination lighting regime (24 h darkness - Escuro - and 16 h light/8 h dark photoperiod - Luz), and callus induction lighting regime (solid line: 24 h darkness; dashed line: 16 h light/8 h dark photoperiod). Lines depict estimated trends, grey shaded bands represent 95% confidence intervals and black dots represent observations (slightly dislocated vertically and horizontally to improve visualization).

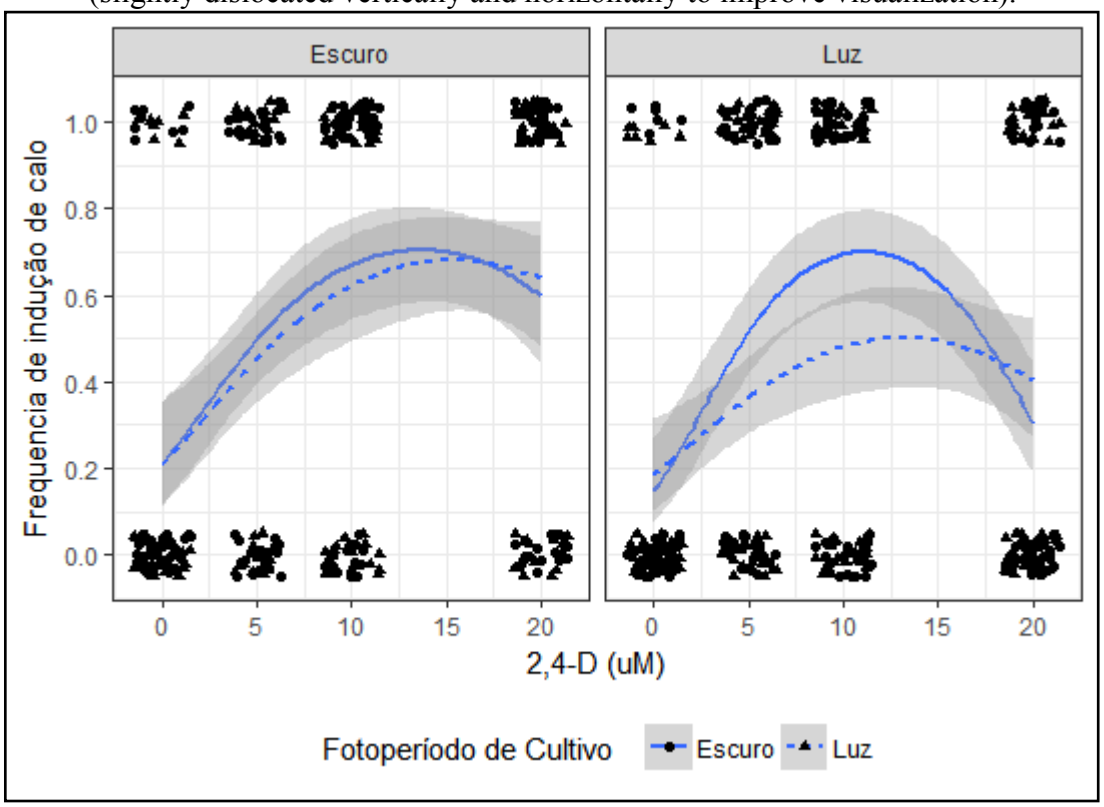

Fonte: Daniel Ferreira Holderbaum (2019)

The observed interactions mean callus induction increases curvilinearly from 0 to 20 µM 2,4-D, but the estimated curves are significantly different depending on seedling germination lighting regime and callus induction lighting regime. Specifically, root segments excised from seedlings germinated either in the light or dark show similar estimated induction

values from 0 to ~15 µM 2,4-D, but on higher concentrations explants from dark-germinated seedlings present higher induction rate (Figure 12). This is also reflected on inflection points (where induction is at its estimated maximum) occurring at a higher 2,4-D concentration for explants from dark-germinated seedlings. Likewise, roots segments induced in either light or dark show quadratic curvilinear trends with increasing 2,4-D concentration, but the trends are significantly different and have different inflection points, although 95% confidence bands overlap throughout the 2,4-D gradient (Figure 13).

Figure 12: Maize callus induction on seedling root segments, as a function of 2,4-D concentration in the medium and seedling germination lighting regime (solid line: 24 h darkness - Escuro; dashed line: 16 h light/8 h dark photoperiod - Luz), averaged between callus induction lighting conditions. Lines depict estimated trends, grey shaded bands represent 95% confidence intervals and black dots represent observations (slightly dislocated vertically and horizontally to improve visualization).

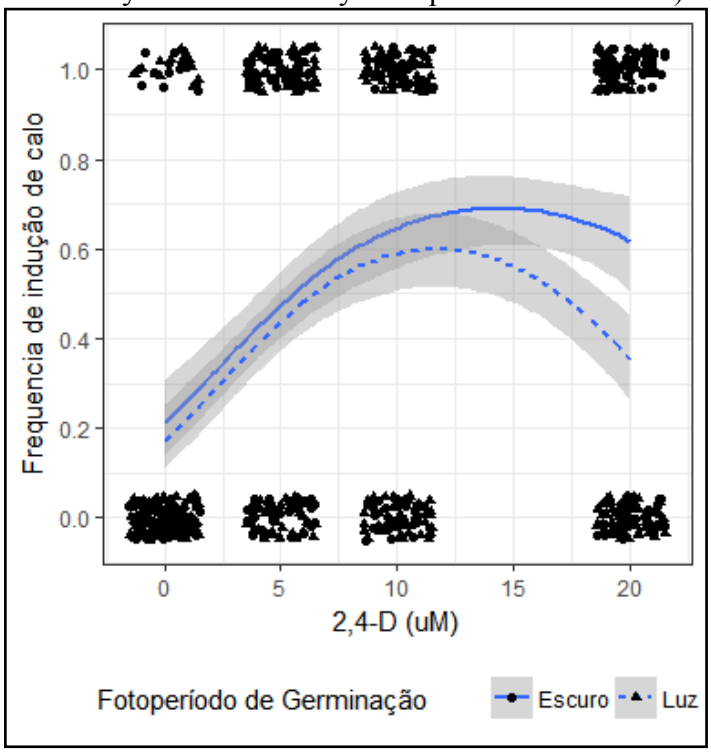

Fonte: Daniel Ferreira Holderbaum (2019).

The growth of organized plant tissues *in vitro* is not generally inhibited by light, but initial cell divisions of explants and growth of callus tissues are prevented by light in some cases (George *et al*., 2008). Fraser *et al*. (1967) showed that light suppresses the initial cell divisions of *in vitro* cultured artichoke explants, and Yeoman and Davidson (1971) further demonstrated that cells were sensitized to light by 2,4-D *in vitro*.

In the current study, depending on explant type, maize callus induction presented different responses to light-regime, considering both indirect effects in the explant source (*in vitro* grown seedlings), and direct effects in cultures.

Figure 13: Maize callus induction on seedling root segments, as a function of 2,4-D concentration in the medium and callus induction lighting regime (solid line: 24 h darkness - Escuro; dashed line: 16 h light/8 h dark photoperiod - Luz), averaged between seedling germination lighting conditions. Blue lines depict estimated trends, grey shaded bands represent 95% confidence intervals and black dots represent observations (slightly dislocated vertically and horizontally to improve visualization).

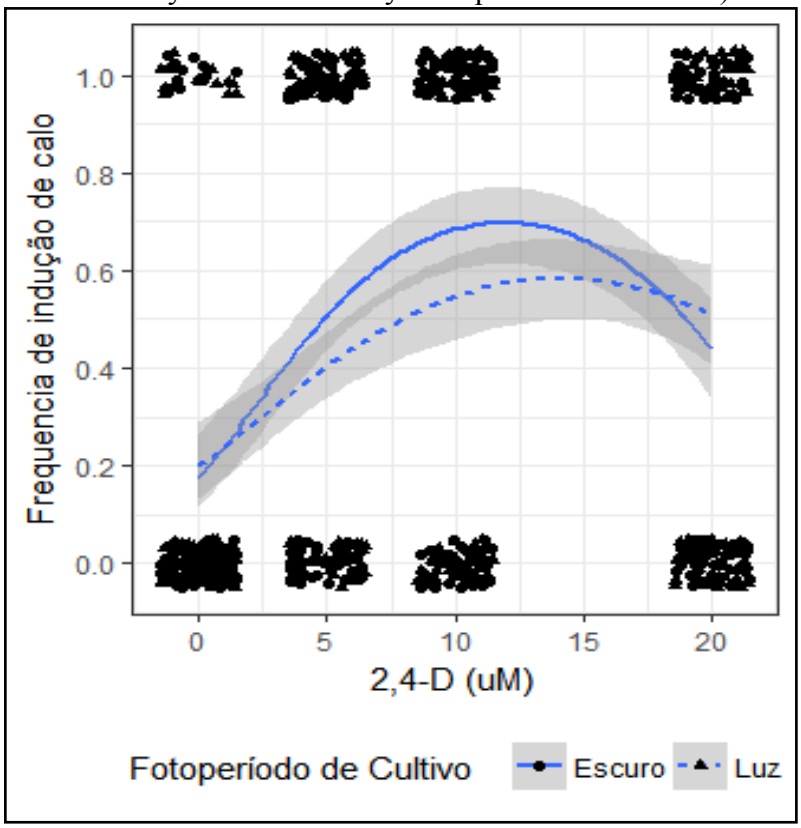

Fonte: Daniel Ferreira Holderbaum (2019).

Callus induction in TCLs from the coleoptilar node of maize seedlings was completely inhibited when seedlings were grown under fluorescent cool-white lamps in a 16 h light/8 h dark photoperiod, regardless of 2,4-D concentration in induction medium. However, callus induction on TCLs from seedlings grown in the dark was responsive to 2,4-D, showing a curvilinear response from 0 μM to 20 μM.

Light affected callus induction in seedlings' root segments in a different way, as compared to coleoptilar-node TCLs. Growing seedlings in the light did not inhibit callus formation in seedling root segments, but it did alter the response to 2,4-D, depending on an

additional factor: culture lighting-regime. If explant-source seedlings are grown in the dark, callus induction in seedling root segments shows a curvilinear response to increasing 2,4-D concentration, and this is not affected by the light regime during callus induction; however, growing explant-source seedlings under fluorescent cool-white lamps in a 16 h light/8 h dark photoperiod alters callus induction responses to 2,4-D, with a significant decrease specifically at the highest 2,4-D concentration (20 μM) in root segments cultured in the dark, and an overall decrease in root segments cultured in the light.

According to Stickland and Sunderland (1972), light can alter IAA oxidation by peroxidase enzymes, via regulation of levels of cofactors and enzyme inhibitors. Additionally, reductants like ascorbic acid and polyphenols can inhibit the oxidation of IAA by riboflavin, which could contribute to the ability of some plant cells/tissues to grow and divide *in vitro* under light (George *et al*., 2008). Regarding a protective effect of polyphenols against IAA oxidation, in many cases polyphenol oxidation leads to the formation of brown pigments which are associated to macroscopic plant tissue browning/blackening (Holderbaum *et al*., 2010).

4.3.2.2 Callus friability

All three factors tested influenced the frequency of friable calli among calli induced on root segments, but no interaction was observed between factors (Figure 14). On average, root segments from seedlings germinated in the dark showed higher frequency of friable calli ($p=0.021$) than root segments from light-germinated seedlings, regardless of induction lighting regime and 2,4-D concentration, while root segments cultured in the dark showed higher average frequency of friable calli than root segments cultured in 16 h light/8 h dark photoperiod ($p<0.001$), regardless of seedling germination lighting regime and 2,4-D concentration. 2,4-D concentration showed a significant tendency for linear increase ($p<0.001$) in the frequency of friable calli (Figure 15), and although this tendency was higher for explants induced in the dark, the difference in the rate of increase was not significant.

Figure 14: Frequency of maize friable calli derived from seedling root segments, as a function of 2,4-D concentration, callus induction lighting regime (24 h darkness - Escuro - and 16 h light/8 h dark photoperiod - Luz), and seeding germination lighting regime (solid line: 24 h darkness - Escuro; dashed line: 16 h light/8 h dark photoperiod - Luz). Lines depict estimated, grey shaded bands represent 95% confidence intervals and black dots represent observations (slightly dislocated vertically and horizontally to improve visualization).

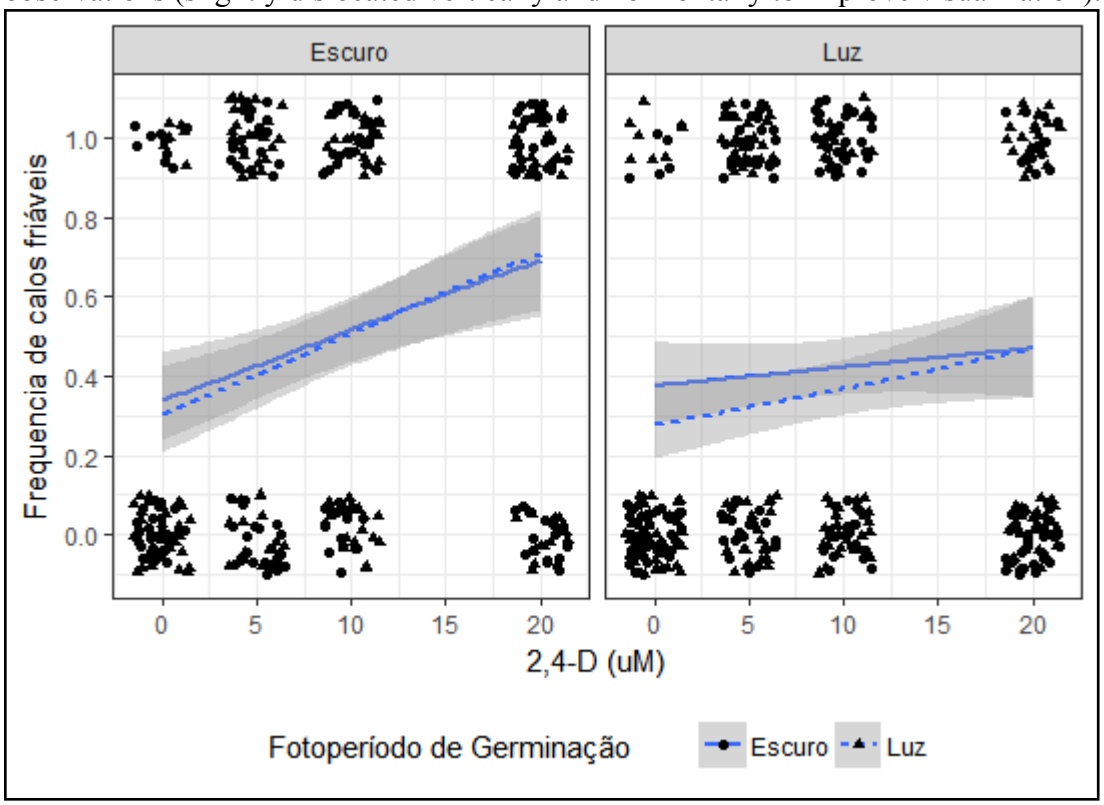

Fonte: Daniel Ferreira Holderbaum (2019).

This study reports an experimental attempt to initiate *in vitro* callus cultures of a commercial GM maize hybrid (AG-5011YG), with the intent of setting up the foundation for the establishment of an *in vitro* interactive model for the study of emergent properties of plant genetic transformation. Though far from trivial, *in vitro* plant cell, tissue and organ culture represent a low complexity model for plant developmental studies, as opposed to whole plants, which are more complex systems of multiple cells, tissues and organs with specific genetic regulation and metabolisms (Cavez *et al.*, 2009).

Previously, different types of explants were employed to induce maize callogenesis, organogenesis or somatic embryogenesis *in vitro*, including tassel primordia (Rhodes *et al.*, 1986), leaf segments (Conger *et al.*, 1987), seedlings' SAMs (Zhong *et al.*, 1992; O'Connor-Sanchez *et al.*, 2002), mature zygotic embryos (Wang, 1987; Huang and Wei 2004; Al-Abed *et al.*, 2006) and immature zygotic embryos (Green and Phillips 1975; Vasil *et al.* 1985;

Hodges *et al.* 1986; Emons *et al.*, 1993; Frame *et al.* 2002), the latter being the most common and amenable for *in vitro* establishment.

Figure 15: Frequency of maize friable calli derived from seedling root segments as a function of 2,4-D concentration, and averaged all conditions of seedling germination lighting regime and callus induction lighting regime. The line depicts the average estimated trend, the grey shaded band represents 95% confidence intervals, and black dots represent observations (dislocated vertically and horizontally to improve visualization).

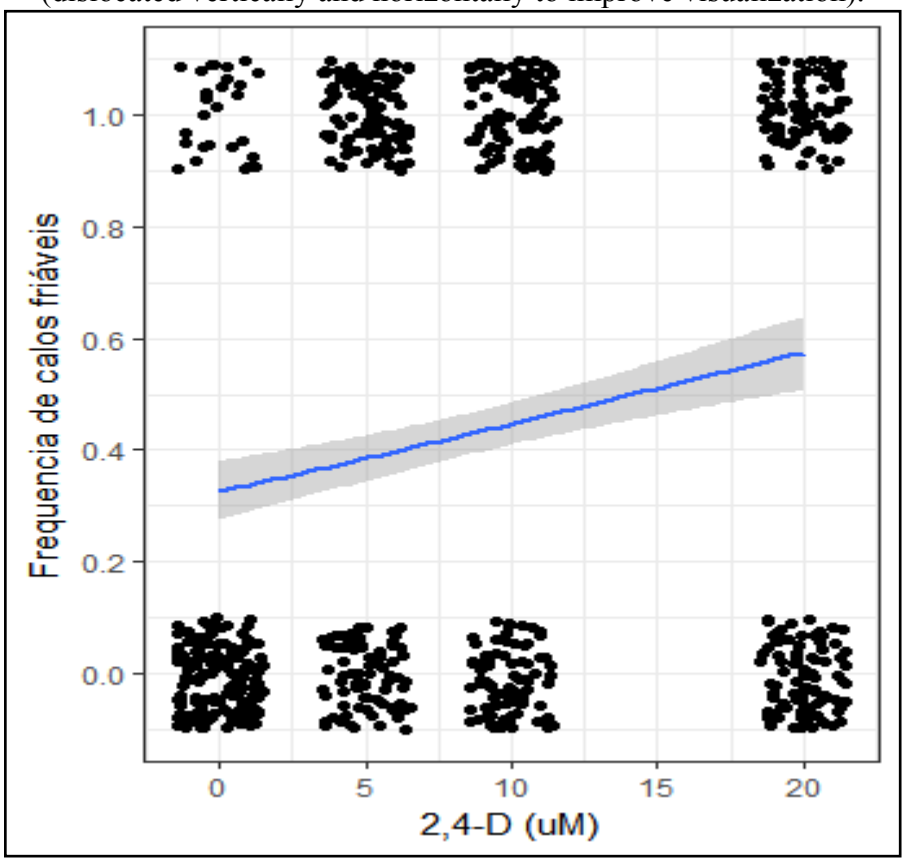

Fonte: Daniel Ferreira Holderbaum (2019).

However, in addition to expensive facilities, equipment and labor, the use of immature embryos of GM and conventional near-isogenic hybrids requires access to the GM and conventional parent lines, which is not common. Thus, we tested two alternative and easily obtained explant types for callogenesis induction: SAM TCLs (controlling for the TCL position in relation to the coleoptilar node) and root segments of *in vitro* germinated plantlets. Furthermore, we compared seedlings germinated in 24 h dark and 16 h light/8 h dark photoperiod as explant sources, crossed with the same two lighting conditions for callus induction. SAM explants were previously shown to be amenable to maize callus induction (Zhong *et al.*, 1992; O'Connor-Sanchez *et al.*, 2002), while the use of root segments, which previously showed good responses *in vitro* for other monocot species (Kerbauy and Estelita, 1996; Park *et al.*, 2003) is a novel approach in maize. We carried out another experiment

testing the induction potential of split maize kernels, mature zygotic embryos and split mature zygotic embryos as explants (Wang, 1987; Huang and Wei 2004; Al-Abed *et al.*, 2006), in a range of 2,4-D concentrations, but the induction frequency and especially callus maintenance capability and quality were inferior to SAM TCLs and roots segments (data not shown).

Overall, using seedlings germinated in the light as explant source proved to be detrimental for culture induction, and markedly so when using SAM TCL explants, for which exposing germinating seedlings to light completely prevented callus induction, while root segments were not as affected. For root segments, induction capacity was maintained in explants derived from light-germinated seedlings, as well as in explants cultured under light exposition, although complete darkness for both seedling germination and callus induction still rendered the highest estimated induction values.

In a very practical sense, it was possible to determine the exact location of responsive tissue within the coleoptilar-node of maize seedlings. Only TCLs (1 mm) excised directly from the coleoptilar-node or 1 mm below or above it showed capacity for callus induction.

In all conditions where callus induction was achieved, a quadratic dose-response to 2,4-D concentration was evidenced, with the growth regulator significantly improving callogenesis and showing the highest induction rates between 10 and 20 μM, depending on other factors.

Maize callus friability is an indicator of a low degree of differentiation, and usually friability is associated with high regeneration capacity through somatic embryogenesis (Emons and Kieft, 1995). However, some friable maize calli are also known to be highly determined to rhizogenesis (Emons *et al.,* 1993).

Embryogenic maize callus is generally classified as: i) Type I callus, characterized as a compact, morphologically complex and organized callus (Armstrong and Green, 1985); ii) Type II callus, characterized as a friable callus where the somatic embryos are discretely arranged throughout the structure (Armstrong and Green, 1985); and iii) Type III callus, similar to Type II callus in appearance, but more strongly determined to rhizogenesis (Emons & Kieft, 1995).

Two predominant callus types were identified in this study: a friable, cream-yellowish callus capable of producing globular structures, that over time in the same medium or in low 2,4-D concentrations would turn rhizogenic - the globular structures in this callus type are possibly globular immature embryos, that would germinate before maturity, thus

developing only roots - (Emons *et al.*, 1993; Emons and Kieft, 1995), and non-friable, spongy, translucent to brown callus that did not produce globular structures but were also capable of producing a few roots.

In this study, callus friability was significantly affected by 2,4-D only for root segment explants, with the frequency of friable calli showing a clear tendency to increase linearly with increasing 2,4-D concentration. A similar trend was observed for calli derived from TCLs, but the trend was not significant, what could be a consequence of a smaller sample size, since friability can only be recorded on induced calli, and the number of induced calli on TCLs (as well as the number of explants per se) was lower than for root segments.

Combining the results of callus induction and callus friability, it can be observed that the 2,4-D concentration which maximizes callus induction does not correspond to the concentration that maximizes callus friability, since models estimated a decrease in induction towards the higher end of the tested 2,4-D gradient, while the frequency of friable calli maintained an increasing trend throughout the whole gradient.

A marked occurrence of blackening/browning of explant tissues was observed in TCL explants, but not in root segments. This tendency for TCL oxidation was influenced by seedling germination lighting regime (100% of TCLs from light-germinated seedlings showed browning, and none induced callus), by TCL distance from the first-node (TCLs from directly over or 1mm above or below the node showed decreased oxidation), and by 2,4-D concentration, with an increasing linear trend for oxidation following increasing 2,4-D concentration.

According to these results, the best evaluated conditions for maize callus induction based on *in vitro* germinated seedlings as explant source, include: i) maize seedlings should be germinated and grown in complete darkness prior to explant excision; ii) callus should be induced in complete darkness, and high induction frequencies can be achieved in TCLs of a ~3 mm region centered on the coleoptilar node, or in seedling root segments; iii) high induction rates associated with high callus friability rates can be achieved with 20 μM 2,4-D.

4.4 CONCLUSIONS

This is the first study to evaluate the induction capacity and morphogenic aspects of induced calli from a MON810 GM maize hybrid (AG-5011YG), using different explant sources, explant types, culture lighting regimes, and 2,4-D concentrations in culture media. This constitutes the first step in the development of an *in vitro* model-system for the study of

emergent properties of plant genetic modification. The best combined results for callus induction and friability were achieved using root segments from seedlings germinated in complete darkness as explants, cultured also in complete darkness, in MS medium containing 20 μM 2,4-D. The synthetic auxin 2,4-D effectively modulated the *in vitro* responses of the tested GM maize hybrid, increasing induction in a curvilinear fashion and friability in a linear fashion, but also showing interactions with seedling germination lighting regime and culture lighting regime. The induction experiments herein reported indicate the viability of *in vitro* cultures as a novel and feasible approach for the study of GM maize responses to diverse environmental stimuli, and further *in vitro* studies including GM and conventional counterparts (near-isogenic hybrids) are expected to expand the *in vitro* model for the study of emergent properties of plant genetic transformation.

REFERENCES

AGAPITO-TENFEN, S.Z.; GUERRA, M.P.; WIKMARK, O.G.; NODARI, R.O. Comparative proteomic analysis of genetically modified maize grown under different agroecosystems conditions in Brazil. **Proteome Sci.**, v. 11, p. 46, 2013.

AL-ABED, D.; RUDRABHATLA, S.; TALLA, R.; GOLDMAN, S. Split-seed: a new tool for maize researchers. **Planta**, v. 223, p. 1355-1360, 2006.

BARTSCH, D.; DEVOS Y.; HAILS, R.; KISS, J.; KROGH, P.H.; MESTDAGH, S.; NUTI, M.; SESSITSCH, A.; SWEET J.; GATHMANN, A. Environmental impact of genetically modified maize expressing Cry1 proteins. In: KEMPKEN, F.; Jung, C. (eds.). **Genetic Modification of Plants: Agriculture, Horticulture and Forestry**. Springer, 2010.

BOLKER, B.M.; BROOKS, M.E.; CLARK, C.J.; GEANGE, S.W.; POULSEN, J.R.; STEVENS, M.H.H.; WHITE, J.S.S. Generalized linear mixed models: A practical guide for ecology and evolution. **Trends Ecol. Evol.**, v. 24, p. 127-135, 2009.

BOUSSELOT, J.; MUENCHRATH, D.; KNAPP, A.; REEDER, J. Emergence and Seedling Characteristics of Maize Native to the Southwestern US. **American Journal of Plant Sciences**, v. 8, p. 1304-1318, 2017. Disponível em: http://doi.org/10.4236/ajps.2017.86087.

BURNHAM, K.P.; ANDERSON, D.R. Multimodel inference: understanding AIC and BIC in model selection. **Sociological Methods & Research**, v. 33, p. 261-304, 2004. Disponível em: https://doi.org/10.1177/0049124104268644.

CAVEZ, D.; HATCHES, C.; CHAUMONT, F. Maize black Mexican sweet suspension cultured cells are a convenient tool for studying aquaporin activity and regulation. **Plant Signal. Behav.**, **v.** 9, p. 890-892, 2009.

CERA, Center for Environmental Risk Assessment. **GM Crop Database, MON-ØØ81Ø-6 (MON810)**. ILSI Research Foundation, Washington D.C., 2016. Disponível em: http://cera-gmc.org/GmCropDatabaseEvent/MON810/short. Acesso em: 03 dez. 2016.

CONGER, B.V.; NOVAK, F.J.; AFZA, R.; ERDELSKY, K.E. Somatic embryogenesis from cultured leaf segments of *Zea mays*. **Plant Cell Rep.**, v. 6, p. 345-347, 1987.

CUMMING, G.; FINCH, S. Inference by eye: Confidence intervals, and how to read pictures of data. **American Psychologist**, v. 60, p. 170-180, 2005.

CUMMING, G.; FIDLER, F.; VAUX, D.L. Error bars in experimental biology. **Journal of Cell Biology**, v. 177, p. 7-11, 2007. Disponível em: http://doi.org/10.1083/jcb.200611141.

DAL VESCO, L.L.; STEFENON, V.M.; WELTER, L.J.; SCHERER, R.F.; GUERRA, M.P. Induction and scale-up of Billbergia zebrina nodule cluster cultures: implications for mass propagation, improvement and conservation. **Scientia Horticulturae**, v. 128, p. 515-522, 2011.

EMONS, A.M.C.; SAMALLO-DROPPERS, A.; VAN DER TOOM, C. The influence of sucrose, mannitol. L-proline, abscisic acid and gibberellic acid on the maturation of somatic embryos of *Zea mays* L. from suspension cultures. **Plant Physiol.**, v. 142, p. 597-604, 1993.

EMONS, A.M.C.; KIEFT, H. Somatic embryogenesis in maize (*Zea mays* L.), in: BAJAJ, Y.P.S. (ed), **Biotechnology in Agriculture and Forestry**, v. 31. Berlin: Springer, 1995, p. 24-39.

FRAME, B.R.; SHOU, H.; CHIKWAMBA, R.K.; ZHANG, Z.; XIANG, C.; FONGER, T.M.; PEGG, S.E.E.; LI, B.; NETTLETON, D.S.; PEI, D.; WANG, K. Agrobacterium tumefaciens-mediated transformation of maize embryos using a standard binary vector system. **Plant Physiol.**, v. 129, p. 13-22, 2002.

FRASER R.S.S., LOENING U.E. & YEOMAN M.M. 1967 Effect of light on cell division in plant tissue cultures. Nature 215, 873.

GEORGE, E.F.; HALL, M.A.; DE KLERK, G.J. (eds.). **Plant Propagation by Tissue Culture**. Dordrecht, The Netherlands: Springer, 2008.

GREEN, C.E.; PHILIPS, R.L. Plant regeneration from tissue culture of maize. **Crop. Sci.**, v. 15, p. 417-421, 1975.

HODGES, T.K.; KAMO, K.K.; IMBRIE, C.W.; BECWAR, M.R. Genotype specificity of somatic embryogenesis and regeneration in maize. **BioTechnology**, v. 4, p. 219-223, 1986.

HOLDERBAUM, D.F.; CUHRA, M.; WICKSON, F.; ORTH, A.I.; NODARI, O.R.; BØHN, T. Chronic responses of *Daphnia magna* under dietary exposure to leaves of a transgenic (event MON810) Bt–maize hybrid and its conventional near-isoline. **Journal of Toxicology and Environmental Health, Part A**, v. 78, p. 993-1007, 2015.

HOLDERBAUM, D.F.; KON, T.; KUDO, T.; GUERRA, M.P. Enzymatic Browning, Polyphenol Oxidase Activity, and Polyphenols in Four Apple Cultivars: Dynamics during Fruit Development. **Hortscience**, v. 45, n. 8, p. 1150-1154, 2010.

HUANG, X.Q.; WEI, Z.M. High-frequency plant regeneration through callus initiation from mature embryos of maize (*Zea Mays* L.). **Plant Cell Rep.**, v. 22, p. 293-800, 2004.

HURVICH, C.M.; TSAI, C-L. Regression and Time Series Model Selection in Small Samples. **Biometrika**, v. 76, p. 297-307.

IKEUCHI, M.; SUGIMOTO, K.; IWASE, A. Plant callus: mechanisms of induction and repression. **Plant Cell**, v. 25, n. 9, p. 3159-3173, 2013.

JAMES, C. **Executive Summary of Global Status of Commercialized Biotech/GM Crops: 2016**. ISAAA Brief, 52. Ithaca, NY, 2016.

KERBAUY, G.B.; ESTELITA, M.E.M. Formation of protocorm-like bodies from sliced root apexes of Clowesia warscewiczii. **Revista Brasileira de Fisiologia Vegetal**, v. 8, p. 157-159.

LA PAZ, J.L.; PLA, M.; CENTENO, E.; VICIENT, C.M.; PUIGDOMÈNECH, P. The use of massive sequencing to detect differences between immature embryos of MON810 and a comparable conventional maize variety. **PLoS ONE**, v. 9, n. 6, e100895, 2014. Disponível em: https://doi.org/10.1371/journal.pone.0100895.

MCCULLAGH, P.; NELDER, J.A. **Generalized Linear Models**, Second Edition, London: Chapman and Hall, 1989.

MOREL, G.; WETMORE, R.H. Fern callus tissue culture. **American Journal of Botany**, v. 38, n. 2, p.141-143, 1951.

MURASHIGE, T.; SKOOG, F. A revised medium for rapid growth and bio assays with tobacco tissue cultures. **Physiologia Plantarum**, v. 15, p. 473-497, 1962.

O'CONNOR-SANCHEZ, A.; CABRERA-PONCE, J.L.; VALDEZ-MELARA, M.; TÉLLEZ-RODRÍGUEZ, P.; PONS-HERNÁNDEZ, J.L.; HERRERA-ESTRELLA, L. Transgenic maize plants of tropical and subtropical genotypes obtained from calluses containing organogenic and embryogenic-like structures derived from shoot tips. **Plant Cell Reports**, v. 21, p. 302-312, 2002.

PARK, S.Y.; MURTHY, H.N.; PAEK, K.Y. Protocorm-like body induction and subsequent plant regeneration from root tip cultures of Doritaenopsis. **Plant Science**, v. 164, p. 919-923, 2003. Disponível em: http://doi.org/10.1016/S0168-9452(03)00019-0.

RHODES, C.R.; GREEN, C.E.; PHILLIPS, R.L. Factors affecting tissue culture initiation from maize tassels. **Plant Science**, v. 46, p. 225-232, 1986.

SONGSTAD, D.D.; PETERSEN, W.L.; ARMSTRONG, C.L. Establishment of Friable Embryogenic (Type II) Callus from Immature Tassels of *Zea mays* (Poaceae). **American Journal of Botany**, v. 79, n. 7, p. 761-764, 1992.

SPRINGER, W.D.; GREEN, C.E.; KOHN, K.A. A histological examination of tissue culture initiation from immature embryos of maize. **Protoplasma**, v. 101, p. 269-281, 1979.

STEINMACHER, D.A.; KROHN, N.G.; DANTAS, A.C.M.; STEFENON, V.M.; CLEMENT, C.R.; GUERRA, M.P. Somatic Embryogenesis in Peach Palm Using the Thin Cell Layer Technique: Induction, Morpho-histological Aspects and AFLP Analysis of Somaclonal Variation. **Annals of Botany**, v. 100, p. 699-709, 2007.

STICKLAND, R.G.; SUNDERLAND, N. Photocontrol of growth, and of anthocyanin and chlorogenic acid production in cultured callus tissues of Happlopappus gracilis. **Ann. Bot.**, v. 36, p. 671-685, 1972.

TAIZ, L.; ZEIGER, E. (eds). **Plant Physiology**, 23d Ed. Sunderland, Mass: Sinauer Assc. Inc., 1998.

R CORE TEAM. **R: A Language and Environment for Statistical Computing**. R Foundation for Statistical Computing. Vienna, Austria, 2017.

VAN LE, B.; MY NGHIENG THAO, D.; GENDY, C.; VIDAL, J.; TRAN THANH VAN, K. Somatic embryogenesis on thin cell layers of a C4 species, Digitaria sanguinalis (L.) Scop. **Plant Cell, Tissue and Organ Culture**, v. 49, p. 201-208, 1997.

VASIL, V.; LU, C.; VASIL, I.K. Histology of somatic embryogenesis in cultured immature embryos of maize (*Zea mays* L.). **Protoplasma**, v. 127, p. 1–8, 1985.

VASIL, L.K. Developing cell and tissue culture systems for the improvement of cereal and grass crops. **Journal of Plant Physiology**, v. 128, p. 193-218, 1987.

WANG, A.S. Callus induction and plant regeneration from maize mature embryos. **Plant Cell Rep.**, v. 6. p. 360-362, 1987.

YEOMAN, M.M.; DAVIDSON, A.W. Effect of light on cell division in developing callus cultures. **Ann. Bot.**, v. 35, p. 1085-1100, 1971.

ZEVEN, A.C.; Waninge, J. The degree of phenotypic resemblance of the near-isogenic lines of the wheat cultivar Thatcher with their recurrent parent. **Euphytica**, v. 35, p. 665-676, 1986.

ZHONG, H.; SRINIVASAN, C.; STRICKLEN, M.B. In-vitro morphogenesis of corn (*Zea mays* L.). I. Differentiation of multiple shoot clumps and somatic embryos from shoot tips. **Planta**, v. 187, p. 483-489, 1992.

ZOLLA, L.; RINALDUCCI, S.; ANTONIOLI, P.; RIGHETTI, P.G. Proteomics as a complementary tool for identifying unintended side effects occurring in transgenic maize seeds as a result of genetic modifications. **J. Proteome Res.**, v. 7, p. 1850-1861, 2008.

5. CAPÍTULO II - INDUCTION, ESTABLISHMENT AND COMPARISON OF *IN VITRO* CALLUS CULTURES OF A TRANSGENIC MAIZE (AG-5011YG - MON810) AND ITS CONVENTIONAL NEAR-ISOGENIC MAIZE (AG-5011)

ABSTRACT

Genetically modified plant events obtained by biolistics, such as the MON810 maize, are generated by insertion of a recombinant DNA sequence in a random *locus* of the plant genome, and this process may produce unintended emergent properties that can alter the transformed cell phenotype. This study aimed at evaluating morphophysiological parameters of a MON810 GM maize hybrid (AG-5011YG) and its conventional near-isogenic hybrid (NIH) (AG-5011), using *in vitro* cultures as an interactive model. Callus cultures of both NIHs were induced and proliferated using two explant types (thin cell layers of shoot apical meristem (SAM TCLs), and root segments), and varying 2,4-D concentrations (from 0 to 25 μM) in nutrient medium. Callogenesis frequency, callus friability rate and morphogenesis were evaluated. Seedling root segments provided optimal callogenesis and friability rates, especially when combined with high concentrations of 2,4-D. 2,4-D effectively modulated the morphophysiological responses of the GM and conventional NIHs, but overall the GM hybrid presented weaker trends and lower maximum values for callus induction and friability rates than the conventional hybrid, indicating altered cell response to 2,4-D. Further research efforts are required to elucidate the specific molecular mechanisms behind the altered response of the GM hybrid's cells. The use of *in vitro* cultures is a novel approach to perform comparisons between GM maize and conventional counterparts, potentially providing a sensitive, low complexity model for detection of emergent properties or off-target effects of genetic transformation, as reflected on altered phenotypic responses of GM maize cells to environmental stimuli *in vitro*.

5.1 INTRODUCTION

Genetically modified (GM) maize (*Zea mays spp. mays*) event MON810 (Monsanto Company, YieldGard® maize, unique identifier MON-ØØ81Ø-6 (CERA, 2016)) is a GM

maize widely employed for the production of insect resistant GM maize hybrids (CERA, 2016), having the third highest number of regulatory approvals in the world among commercial GM events (James, 2016).

Previously (Capítulo I), we tested various experimental conditions for the initiation of *in vitro* cultures of GM maize hybrid AG-5011YG, as the initial benchmark for the application of *in vitro* cell, tissue and organ culture as a model for the study of unintended effects of plant transformation. Here we build upon those results and expand the conceptual/interactive model by testing the same GM hybrid (AG-5011YG) alongside its conventional near isogenic hybrid (AG-5011), and comparing their *in vitro* ontogenetic and morphogenetic responses to environmental stimuli during culture induction.

The establishment of maize *in vitro* cultures is known to be highly dependent growth regulators (Vasil 1987; Zhong *et al.*, 1992; Bhaskaran and Smith, 1990) and also explant source (Rhodes *et al.*., 1986; Conger *et al.*, 1987; Zhong *et al.*, 1992; Wang, 1987; Huang & Wei 2004; Al-Abed *et al.*, 2006). The classic maize explants are immature zygotic embryos, for which the *in vitro* morphogenic potential is well established (Green and Phillips 1975; Springer *et al.* 1979; Duncan *et al.* 1985; Vasil *et al.* 1985; Hodges *et al.* 1986; Emons *et al.*, 1993; Frame *et al.,* 2002). However, the use of immature embryos as explants for *in vitro* establishment of a commercial GM maize hybrid and its conventional near-isogenic hybrid is rare, because it requires access to the hybrid's parent lines, which are not common. Previously (Chapter I), we demonstrated the capacity of root segments and thin cell layers (TCLs) from the coleoptilar node (including the shoot apical meristem - SAM) of seedlings germinated in the dark, as reliable explants for GM maize hybrid AG-5011YG (MON810) *in vitro* culture initiation, as modulated by 2,4-D in the culture medium.

The objective of this study was to evaluate and compare induction rates, callus friability rates and morphogenesis of a GM maize hybrid (AG-5011YG) and its conventional near-isogenic hybrid (AG-5011) cultured *in vitro*, using two explant types (root segments and SAM TCLs), from seedlings germinated in the dark, cultured in a range of 2,4-D concentrations in culture media. The main hypotheses tested were: maize near-isogenic hybrid (transgenic and conventional), explant source (root segments and SAM TCLs) and 2,4-D concentration affect callus induction, friability and morphogenic potential, either in an interactive or independent fashion.

5.2 MATERIAL AND METHODS

5.2.1 Plant material

Seeds of GM maize hybrid AG-5011YG (MON810) and conventional near-isogenic hybrid AG-5011 were purchased in the seed market in Erval do Oeste, Santa Catarina, south Brazil. Seeds of both lines were analyzed to confirm their GM or conventional status, using a lateral flow strip kit for detection of Cry1Ab protein (Envirologix Quickstix AS-003-CRLS kit), and qualitative PCR for detection of the CAMV-35S promoter and the *cry1Ab* gene, using *zein* as endogenous control (Data not shown).

5.2.2 Seed preparation

Seeds of the GM and conventional near-isogenic maize hybrids (n=30) were thoroughly washed in glass beakers under tap water for 5 min, in order to remove the seed fungicide coat and excess bacteria; seeds were then immersed in distilled water with Tween 20 (40 µl 100 ml^{-1}) for 5 min under hand shaking, the water was drained, seeds were taken to an aseptic laminar flow hood, surface sterilized with 70% alcohol for 3 min, NaClO 1% with Tween 20 (40 µl/100 ml) for 30 min, washed five times with sterile distilled water, and immersed in sterile distilled water for 72 h to soften and facilitate subsequent embryo excision. All subsequent manipulations of seeds, embryos, seedlings and cultures took place in aseptic conditions in a laminar flow hood, using aseptic technique and sterilized tools and materials.

5.2.3 Zygotic embryo excision and in vitro germination

Mature zygotic embryos were excised from softened seeds placed on paper plates, using forceps and scalpels under a stereomicroscope. Excised embryos were placed in glass flasks with sterile distilled water to prevent dehydration, and lastly embryos were once again surface sterilized with 70% ethanol for 1 min, NaClO 1% for 10 min, washed five times with sterile distilled water, and inoculated in test tubes containing 15 ml germination medium (MS salts (Murashige and Skoog, 1962) supplemented with Morel vitamins (Morel and Wetmore,

1951) and 3% sucrose). Germinating embryos were and kept at 25±2 ºC in the dark for 3 weeks, and plantlets were used as source of different explants for callus induction.

5.2.4 Culture media and in vitro experimental practices

The basal nutrient medium used for maize *in vitro* cultures consisted of MS salts supplemented with Morel vitamins, 3% sucrose, enzymatic casein hydrolisate (200 mg/L) and adenine (40 mg/L); the basal medium was supplemented with a range of 2,4-D concentrations (detailed below). All culture media had pH adjusted to 5.8 prior to sterilization at 121 ºC and 1.5 atm for 20 min; media were gelled with 0.2% Phytagel prior to sterilization.

5.2.4 Callogenesis induction

Contaminant-free well developed plantlets of GM and conventional maize (n = 24 for GM and 28 for conventional) were used to obtain TCLs (~0.75 mm) (4 TCLs around the coleoptilar node per plantlet), and root segments (~2 cm) (10-16 segments per seedling), which were employed as explants in the callus induction experiment. Here, callus is defined as an unorganized cell mass (Ikeuchi *et al.*, 2013). In order to assess effects of maize NIH, explant type and 2,4-D on callus induction, friability and morphogenesis, explants were excised from plantlets placed on paper plates using scalpels and forceps, and immediately inoculated in plastic Petri dishes containing 25 ml basal nutrient medium supplemented with a gradient of 2,4-D concentrations (0, 4 and 17 μM for TCLs; 0, 13, 17 and 21 μM for root segments - ranges defined based on previous experiments). A total of 229 TCLs and 576 root segments were inoculated. Cultures were kept at 25 ºC in the dark. Callogenesis and callus friability were evaluated four weeks after induction, and morphogenesis was evaluated four and eight weeks after induction. All endpoints were recorded by visual inspection under the stereomicroscope. Callus samples were photographed inside Petri dishes in an Olympus stereomicroscope attached to an Olympus DP-71 image capture system.

5.2.5 Statistical Analysis

Data were analyzed in a generalized linear mixed model framework (Mccullagh and Nelder, 1989; Bolker *et al.*, 2009). Data on callus induction, callus friability and morphogenesis were evaluated as binary variables (yes = 1; no = 0) and analyzed with logistic

regression. For every analysis, the initial statistical models included all explanatory variables, interactions, and quadratic terms for quantitative variables (e.g. 2,4-D concentration). When significant, plantlet was treated as a random effect variable in all models to account for correlations between calli derived from the same plantlet. Model selection was carried out by means of stepwise elimination of variables followed by inspection of the small sample-corrected Akaike Information Criterion (cAIC) (Hurvich and Tsai, 1989; Burnham and Anderson, 2004). Model assumptions about residual variance and distribution were evaluated graphically for all models, and the dispersion parameter - Chi-square/degrees of freedom - was additionally used to assess model fit, when applicable (Mccullagh and Nelder, 1989; Bolker *et al.*, 2009). Effects were considered significant when $P < 0.05$. Significant trend- and point-wise differences were detected by comparison of 95% confidence intervals/envelopes (Cumming and Finch, 2005; Cumming *et al.*, 2007). Analyses were carried out in the R statistical language (R Core Team, 2017).

5.3 RESULTS AND DISCUSSION

5.3.1 Callogenesis Induction

Callogenesis was induced in both maize NIHs (GM and conventional), using TCLs (~0.75 mm) from the coleoptilar-node (Figure 16), as well as root segments (~2 mm) (Figure 17) of *in vitro* germinated plantlets. Curvilinear trends ($P < 0.001$) of callus induction were evidenced with increasing 2,4-D concentrations (0-21 μM), for both NIHs and types of explant (Figures 18 and 19). However, significant two-way interactions between NIHs and explant types ($P < 0.05$), explant type and 2,4-D concentration ($P < 0.001$) (Figure 20), and between NIH and 2,4-D concentration ($P < 0.001$) (Figure 21) were evidenced to affect *in vitro* callogenesis.

Figure 16: Calli of conventional (a-c) and GM (MON810) (d-f) near-isogenic maize hybrids induced on thin cell layers (0.75 mm) of the coleoptilar node of *in vitro* germinated plantlets, on media supplemented with 2,4-D at 0 µM (a and d), 4 µM (b and e) and 17 µM (c and f).

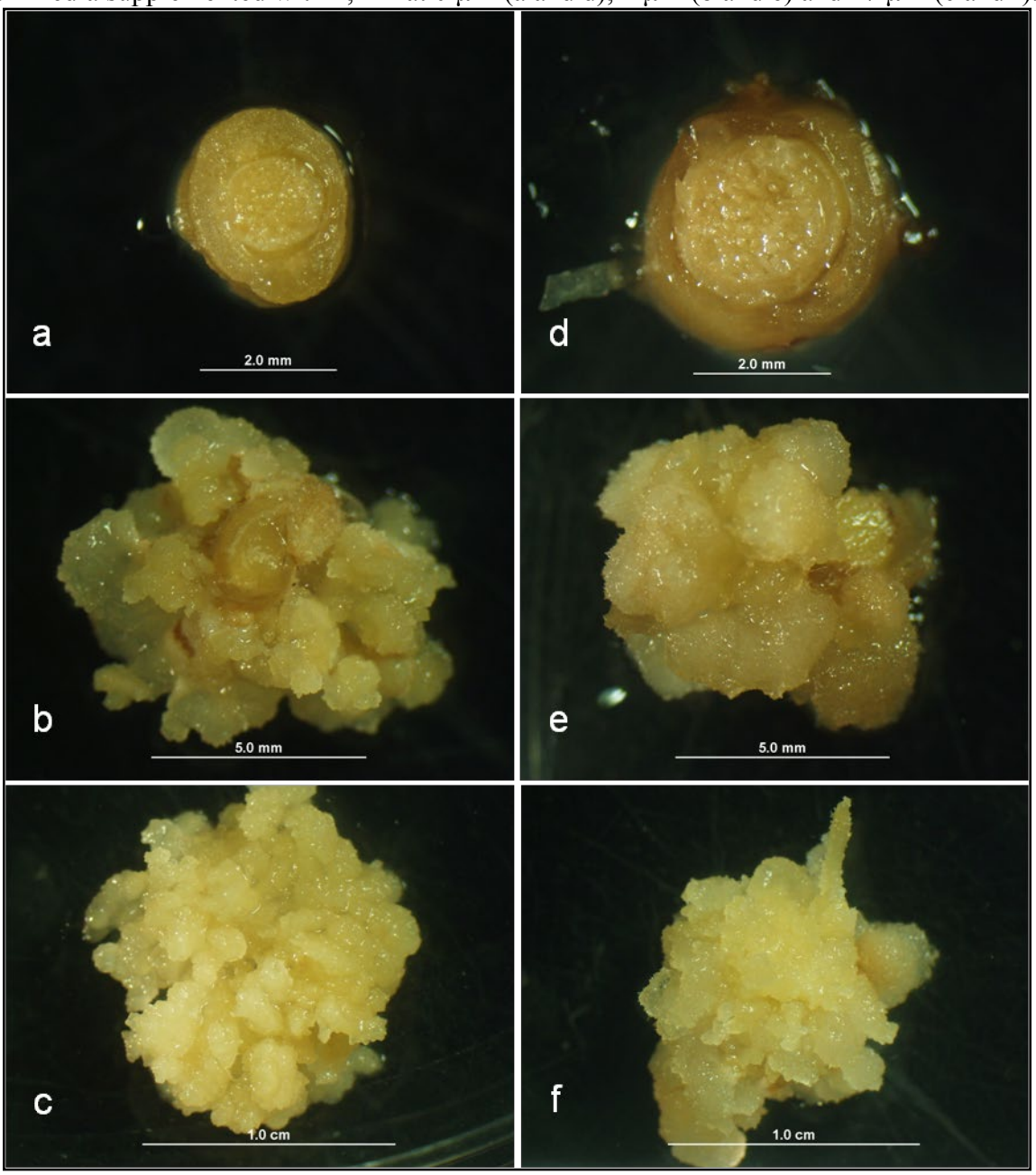

Fonte: Daniel Ferreira Holderbaum (2019).

Figure 17: Calli of conventional (a-d) and GM (MON810) (e-h) near-isogenic maize hybrids induced on root segments (2 mm) of *in vitro* germinated plantlets, on media supplemented with 2,4-D at 0 µM (a and e), 13 µM (b and f), 17 µM (c and g) and 21 µM (d and h).

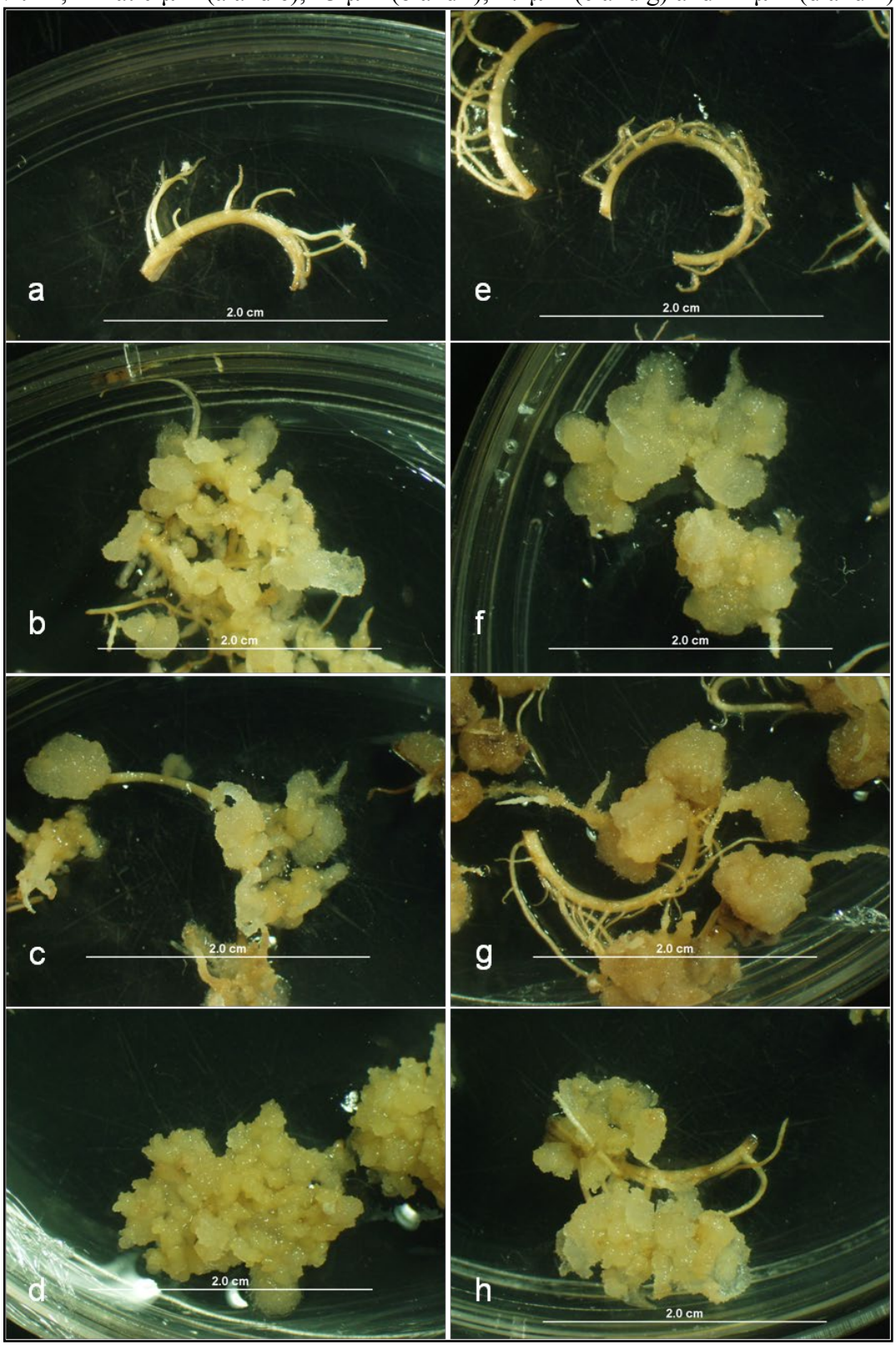

Fonte: Daniel Ferreira Holderbaum (2019)

Figure 18: Frequency of callus induction of GM (GM) and conventional (NM) near-isogenic maize hybrids 4 weeks after induction, using thin cell layers (0.75 mm) of shoot apical meristem (M - solid line) and root segments (2 cm) (R - dashed line) of *in vitro* germinated plantlets, cultured in media containing a gradient of 2,4-D concentrations in basal culture media. Shaded bands indicate 95% confidence envelopes.

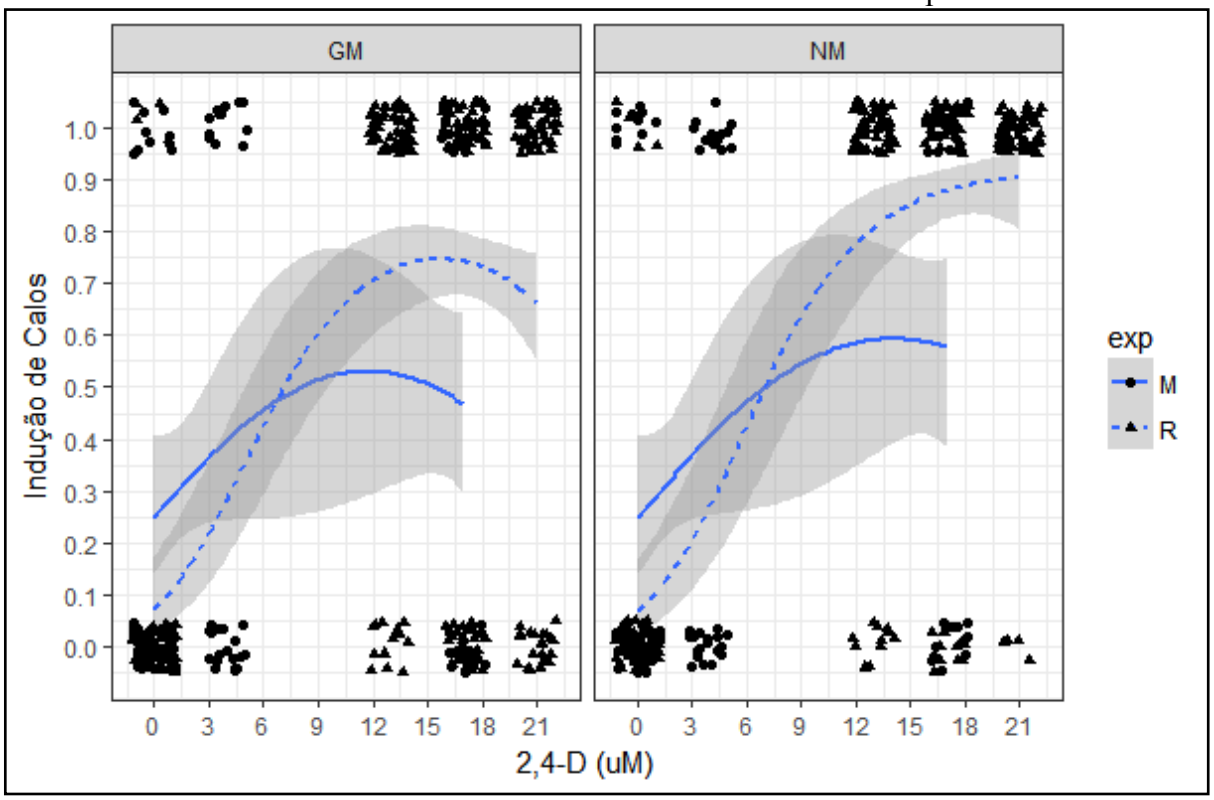

Fonte: Daniel Ferreira Holderbaum (2019).

The interaction between NIH and explant type indicates that SAM TCLs and root segments respond differently depending on the NIH: SAM TCLs show very similar induction trends for both NIHs throughout the tested 2,4-D gradient, with confidence envelopes including the means of GM and conventional, while root segments evidenced significantly different trends for GM and conventional, with the conventional NIH presenting overall higher induction frequencies by ~15%.

Figure 19: Frequency of callus induction on thin cell layers (0.75 mm) of shoot apical meristem (M) and root segments (2 cm) (R) of *in vitro* germinated plantlets of GM (GM - solid line) and conventional (NM - dashed line) near-isogenic maize hybrids, along a gradient of 2,4-D concentrations in basal culture media. Shaded bands indicate 95% confidence envelopes.

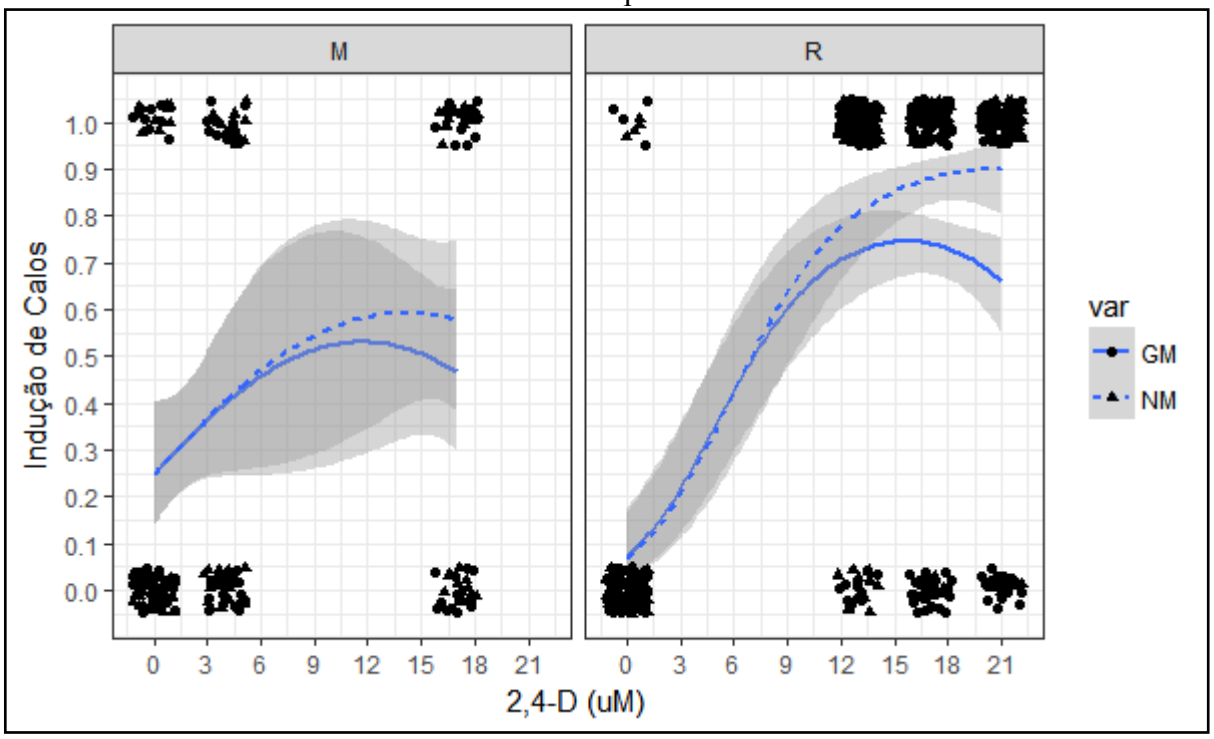

Fonte: Daniel Ferreira Holderbaum (2019).

The interaction between explant type and 2,4-D indicates that TCLs and root segments present significantly different induction trends across the 2,4-D gradient: quadratic trends were evidenced for both TCLs and root segments, but root segments show a steeper slope and require higher 2,4-D to attain maximum induction compared to TCLs (Figures 18 and 20). Likewise, the interaction between NIH and 2,4-D concentration suggests the effect of 2,4-D in culture induction is influenced by the NIH, with the conventional NIH showing significantly higher values at the highest 2,4-D levels (~20 µM).

Figure 20: Frequency of callus induction on thin cell layers (0.75 mm) of coleoptilar node (M - solid line) and root segments (2 cm) (R - dashed line) of *in vitro* germinated plantlets, averaged between GM and conventional near-isogenic hybrids, along a gradient of 2,4-D concentrations in basal culture media. Shaded bands indicate 95% confidence envelopes.

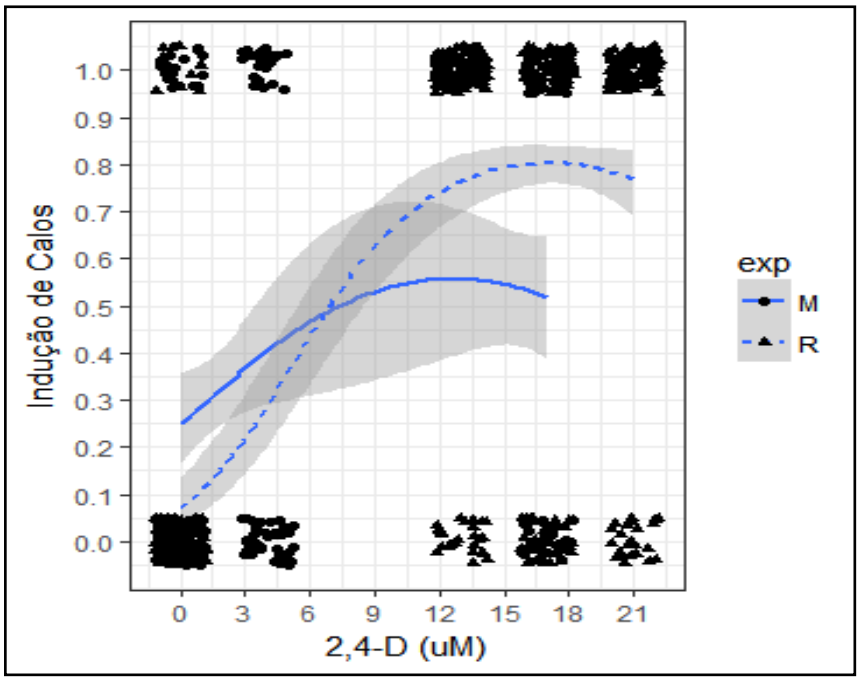

Fonte: Daniel Ferreira Holderbaum (2019).

Figure 21: Frequency of callus induction for GM (solid line) and conventional (dashed line) near-isogenic hybrids, averaged between explant types (thin cell layers (0.75 mm) of coleoptilar node and root segments (2 cm) of *in vitro* germinated plantlets), along a gradient of 2,4-D concentrations in culture media. Shaded bands indicate 95% confidence envelopes.

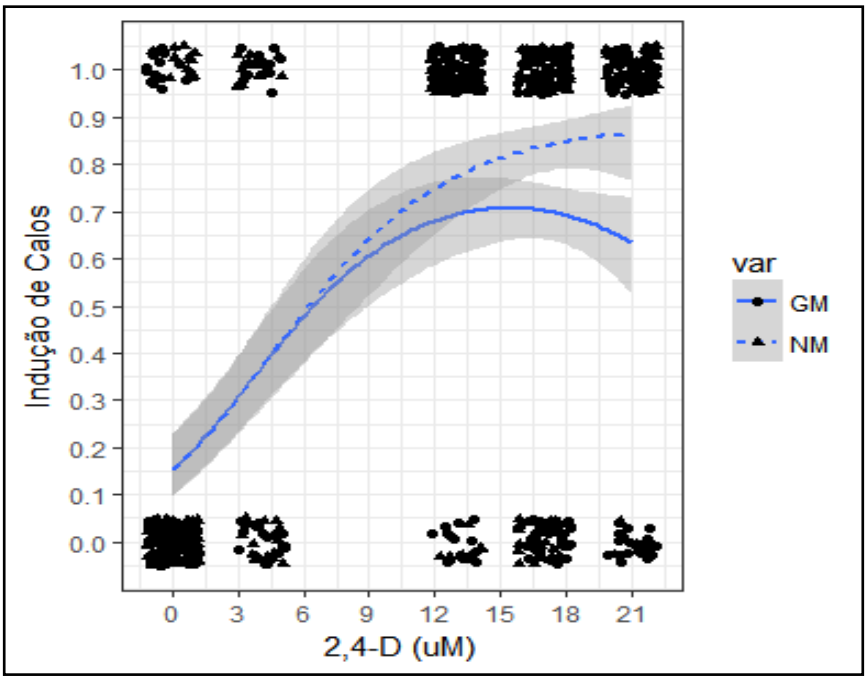

Fonte: Daniel Ferreira Holderbaum (2019).

5.3.2 Callus friability

Significant effects of 2,4-D concentration and NIH were detected for callus friability, while explant type did not affect this parameter. Increasing 2,4-D concentration in the culture medium increased the frequency of friable calli, with the highest frequencies achieved in the highest tested 2,4-D concentrations for GM and conventional NIHs, as well as for TCLs and root segments (Figure 22). Overall, the conventional NIH showed higher frequency of friable calli across the tested 2,4-D gradient (Figure 23), but the difference was more prominent in calli derived from root segments than from TCLs, although there was no evidence for a significant three-way interaction.

Figure 22: Frequency of friable calli of GM (GM - solid line) and conventional (NM - dashed line) near-isogenic maize hybrids, 4 weeks after induction, using thin cell layers (0.75 mm) of shoot apical meristem (M) or root segments (2 cm) (R) of *in vitro* germinated plantlets as explants, along gradients of 2,4-D concentrations in basal culture media. Shaded bands indicate 95% confidence envelopes.

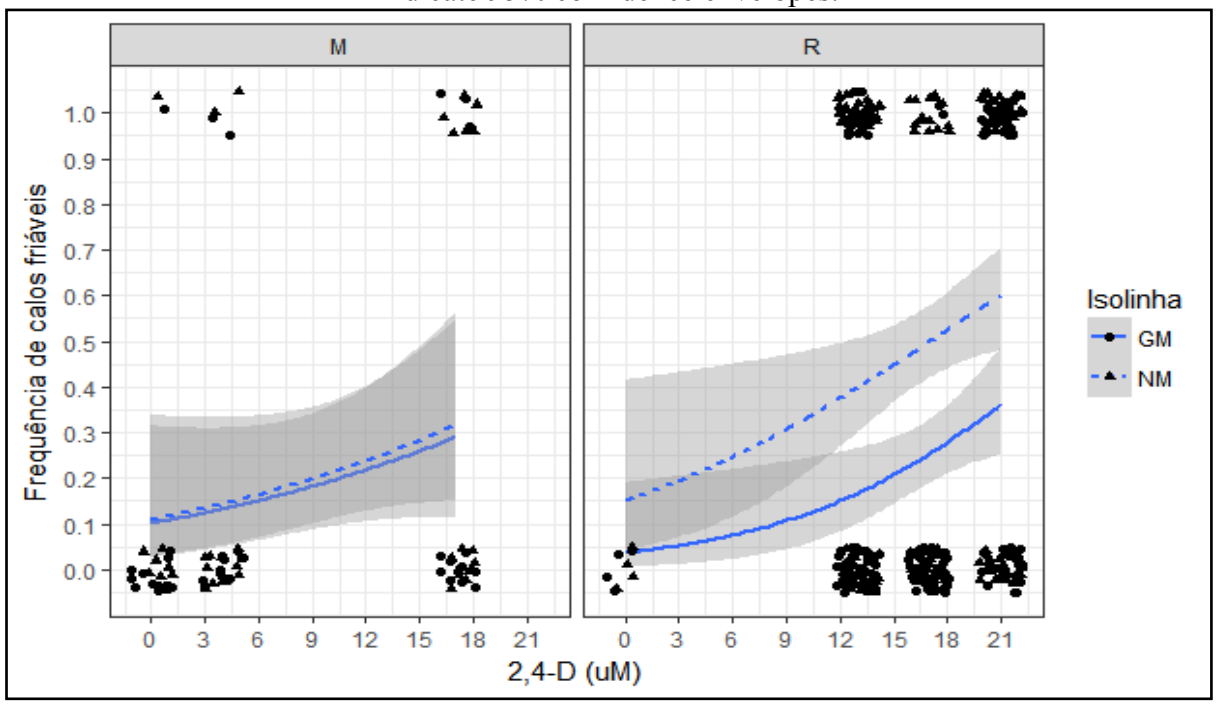

Fonte: Daniel Ferreira Holderbaum (2019).

Figure 23: Frequency of friable calli of GM (GM - solid line) and conventional (NM - dashed line) near-isogenic maize hybrids, 4 weeks after induction, averaged between the two employed explant types (thin cell layers (0.75 mm) of shoot apical meristem or root segments (2 cm) of *in vitro* germinated plantlets), along gradients of 2,4-D concentrations in basal culture media. Shaded bands indicate 95% confidence envelopes.

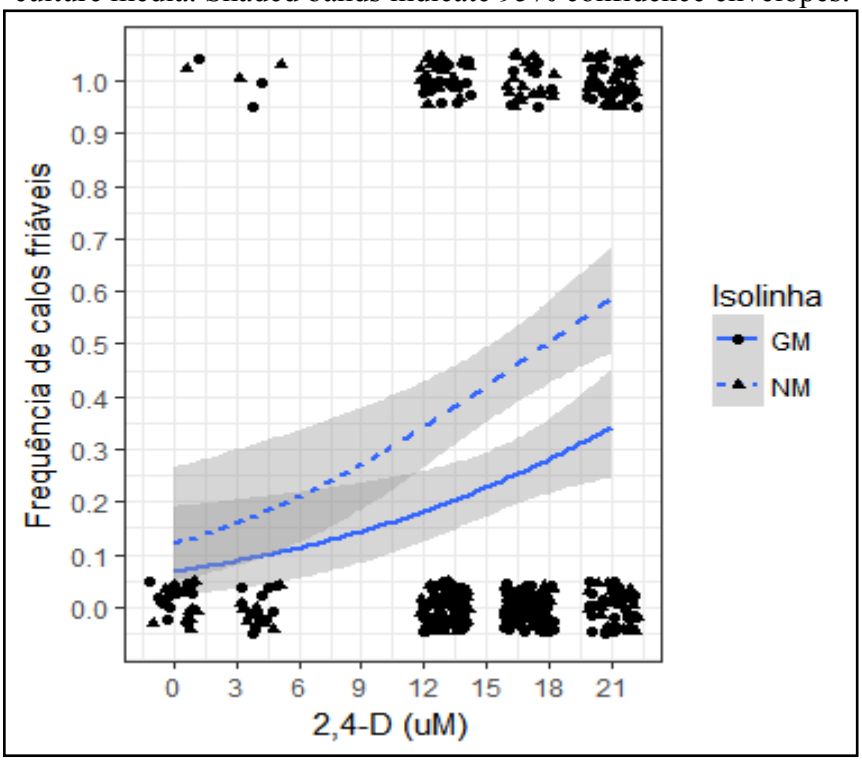

Fonte: Daniel Ferreira Holderbaum (2019).

5.3.3 Callus Rhizogenesis

Four weeks after callus induction the majority of morphogenic responses observed in calli were either to stay unorganized or become rhizogenic, depending on experimental conditions, especially 2,4-D concentration (Figure 24). 2,4-D induced curvilinear responses ($p<0.001$) with opposite signs (opposite curvatures) depending on explant type - denoting a significant interaction between explant type and 2,4-D concentration ($p<0.001$) (Figure 25). There was also evidence of a significant interaction between NIH and a quadratic trend for 2,4-D concentration ($p=0,008$) (Figure 26). The interaction between 2,4-D and NIH evidenced that, when averaging both explant types, 2,4-D had an almost constant effect in the conventional NIH, while a more pronounced curvilinear effect on the GM NIH (Figure 26).

Figure 24: Frequency of rhizogenic calli of GM (GM - solid line) and conventional (NM - dashed line) near-isogenic maize hybrids, 4 weeks after induction, using thin cell layers (0.75 mm) of shoot apical meristem (M) or root segments (2 cm) (R) of *in vitro* germinated plantlets as explants, along gradients of 2,4-D concentrations in basal culture media. Shaded bands indicate 95% confidence envelopes.

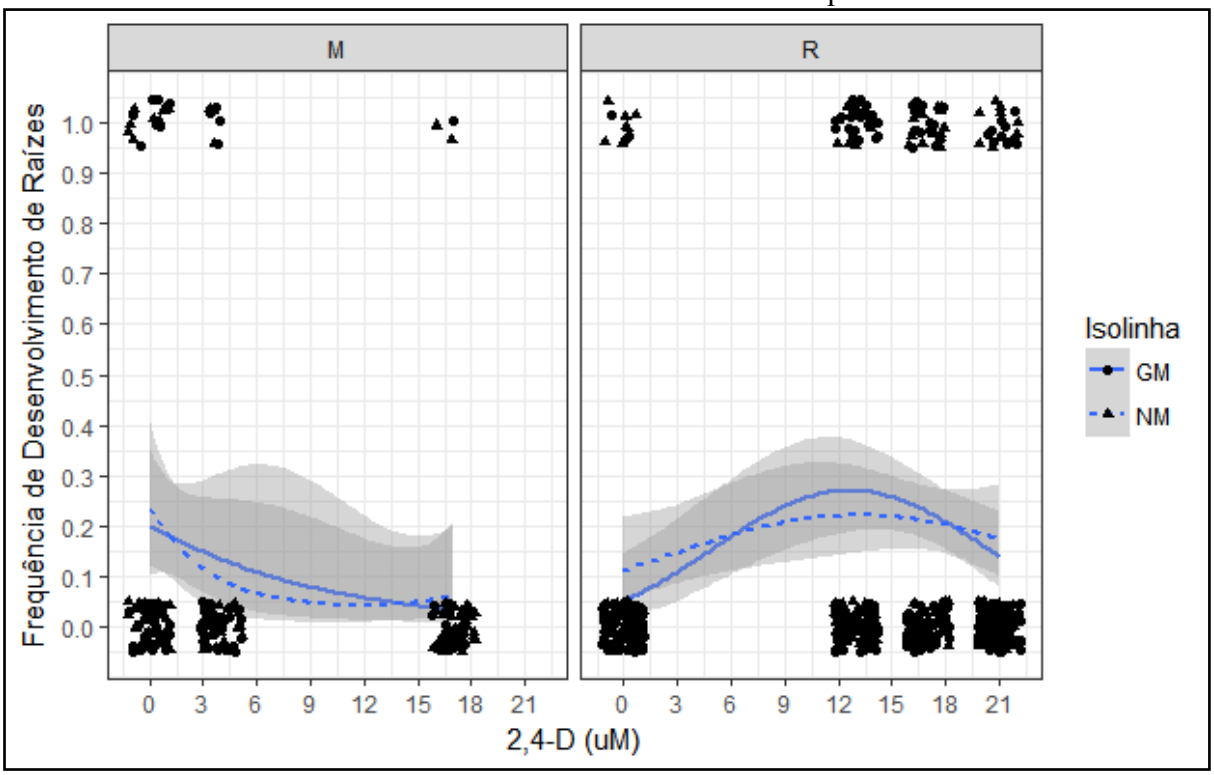

Fonte: Daniel Ferreira Holderbaum (2019).

However, callus rhizogenesis on the GM and conventional NIHs was also dependent on explant type: overall, averaging between both NIHs, root derived calli showed greater rhizogenic determination with a curvilinear trend and higher frequency of rhizogenic calli induced in mid-level 2,4-D concentrations, while TCL derived calli had their rhizogenic response more easily and continuously inhibited by increasing 2,4-D concentrations in induction medium.

Figure 25: Frequency of rhizogenic calli derived from thin cell layers (0.75 mm) of coleoptilar node (M-solid line) or root segments (2 cm) (R-dashed line) of *in vitro* germinated plantlets, averaged by near-isogenic maize hybrids, 4 weeks after induction along gradients of 2,4-D concentrations in basal culture media. Shaded bands indicate 95% confidence envelopes.

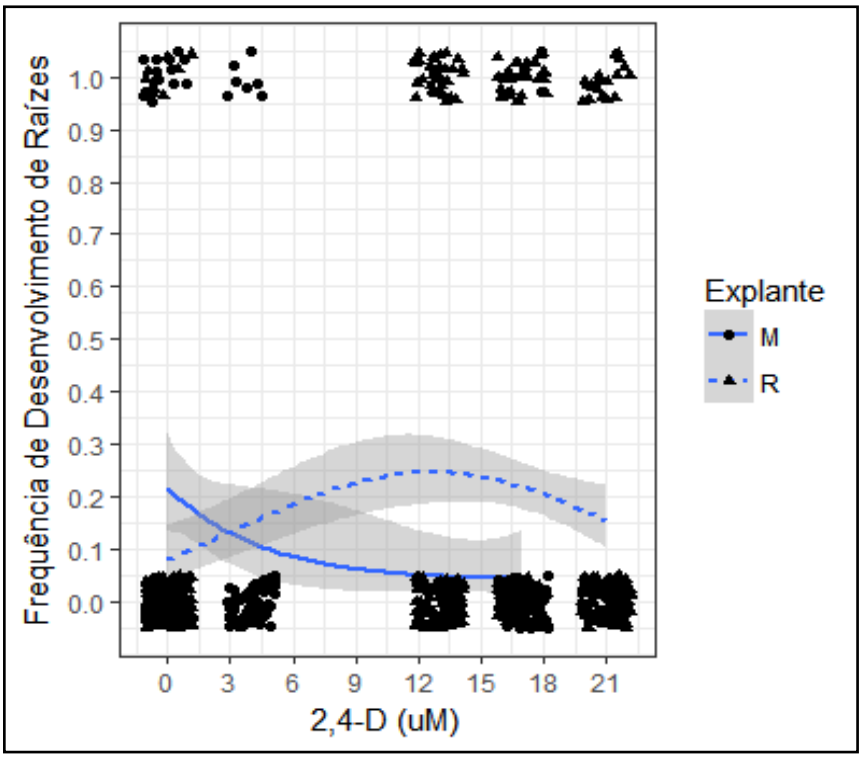

Fonte: Daniel Ferreira Holderbaum (2019).

This study reports the *in vitro* establishment of a commercial GM maize hybrid and its conventional NIH, allowing for the investigation of ontogenetic and morphogenetic parameters and comparisons between NIHs. *In vitro* plant cell, tissue and organ culture represents a model for plant developmental studies, and in this study the brazilian commercial maize hybrid AG-5011 was used in its conventional and GM (AG-5011YG - MON810) versions to assess emergent properties of genetic transformation, relating to *in vitro* maize ontogenesis and morphogenesis as modulated by controlled environmental factors.

Other authors employed a variety of explant types to induce maize callogenesis, organogenesis or somatic embryogenesis *in vitro*, including tassel primordia (Rhodes *et al.*, 1986), leaf segments (Conger *et al.*, 1987), seedlings' SAMs (Zhong *et al.*, 1992; O'Connor-Sanchez *et al.*, 2002), mature zygotic embryos (Wang, 1987; Huang and Wei 2004; Al-Abed *et al.*, 2006) and the "classic" immature zygotic embryos (Green and Phillips 1975; Duncan *et al.* 1985; Vasil *et al.* 1985; Hodges *et al.* 1986; Emons *et al.*, 1993; Frame *et al.* 2002).

Figure 26: Frequency of rhizogenic calli of GM (solid line) and conventional (dashed line) near-isogenic maize hybrids, 4 weeks after induction, averaged between explant types (thin cell layers (0.75 mm) of coleoptilar node or root segments (2 cm) of *in vitro* germinated plantlets), along gradients of 2,4-D concentrations in basal culture media. Lines depict estimated trends, and shaded bands indicate 95% confidence envelopes.

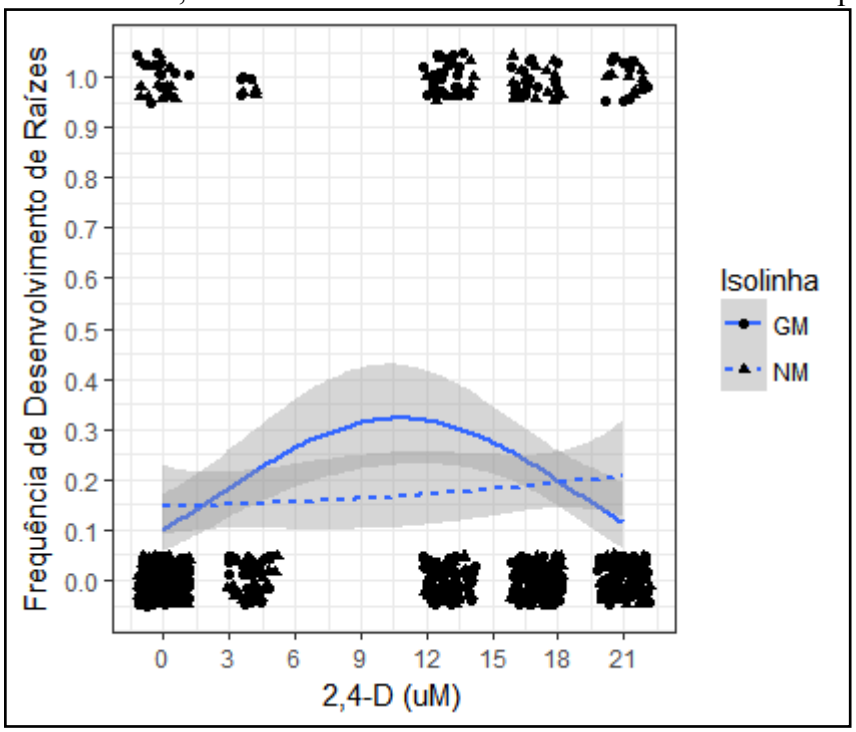

Fonte: Daniel Ferreira Holderbaum (2019).

Previously (Chapter I), we successfully established GM maize cultures *in vitro* using SAM TCLs and root segments of plantlets germinated *in vitro*, in the dark. SAM explants were previously shown to be competent for callus induction (Zhong *et al.*, 1992; O'Connor-Sanchez *et al.*, 2002), while the use of root segments is a novel approach in maize.

Calli were effectively induced by 2,4-D on both explant types, but root segments required higher 2,4-D concentration than SAM TCLs to reach maximum induction frequency. Since roots represent a more differentiated tissue than SAMs, the requirement of higher 2,4-D levels to induce cell dedifferentiation in root tissues is consistent with the plant tissue culture literature (George *et al*. 2008). Interestingly, induction frequencies on SAM TCLs and root segments was not only dependent on 2,4-D, but also on maize NIH: induction trends on SAM TCLs were similar for GM and conventional maize, but for root segments higher induction frequencies were observed in conventional compared to the GM maize, indicating a different cell response to auxin between the tested NIHs, which was only detectable when using explants that require higher 2,4-D concentration for dedifferentiation.

Maize callus friability is an indicator of a low degree of differentiation, and usually friability is associated with high regeneration capacity through somatic embryogenesis (Emons and Kieft, 1995). However, some friable maize calli are also known to be highly determined to rhizogenesis (Emons and Kieft, 1995).

In this study, callus friability was significantly affected by 2,4-D and NIH, but not by explant type. Increasing 2,4-D concentration continuously enhanced friable callus frequency in both NIHs, but the conventional NIH showed a stronger response to 2,4-D, producing significantly more friable calli. Combining the results of callus induction and callus friability, it can be observed that the 2,4-D concentration which maximizes callus induction does not correspond to the concentration that maximizes callus friability, since models estimated a decrease in induction towards the higher end of the tested 2,4-D gradient, while the frequency of friable calli maintained an increasing trend throughout the whole gradient.

After induction, calli were left in the same culture medium for 8 weeks, which is a considerably long time without subculture for maize callus (see Emons and Kieft, 1995). This was done for two reasons: detect possible late induction responses from inoculated explants, and allow for a full development of induced calli in the induction medium. Clearly, within this time there was 2,4-D uptake by explant cells, causing callus induction, and induced calli continued to grow, possibly leading to a decrease in the medium's 2,4-D concentration over time, that ultimately allowed calli to enter in a morphogenic pathway (Emons and Kieft, 1995). Several calli became rhizogenic (produced roots), as previously reported by other authors, and no development of shoots nor somatic embryos was observed. This means the obtained friable, yellowish calli, very similar to the known embryogenic Type II calli, have strong determination to form roots after a long time (8 weeks) in induction medium without subculture, suggesting they are actually Type III calli (Emons & Kieft, 1995).

5.4 CONCLUSIONS

This is the first study to establish *in vitro* cultures of a commercial GM maize hybrid and its near-isogenic hybrid, allowing for the evaluation of emergent properties of genetic transformation by employing *in vitro* cultures as a low complexity model. The synthetic auxin 2,4-D effectively modulated the morphophysiological responses of the GM and conventional NIHs, but overall, compared to the conventional the GM hybrid required higher 2,4-D concentrations to attain maximum observed effects, and the highest values for callogenesis, callus friability rate and rhizogenesis were significantly different between NIHs, indicating

altered cell response to 2,4-D. From the observed results, root segments are the most competent explant for *in vitro* establishment, although it requires higher 2,4-D doses (~20 μM) than SAM TCLs for combined maximum induction and friability rates, for both NIHs. Moreover, seedling roots are often profuse *in vitro*, making it an easily available explant source; and last, but not least, an emergent property related to the GM maize response to exogenous auxin (2,4-D) was detected in these cultures. The fact that root-derived calli tend to be more determined to rhizogenesis should be faced at the same time as a challenge and an opportunity of comparison between the GM and conventional hybrids, as well as to better understand maize *in vitro* morphogenesis. Further studies are required to investigate the environmental parameters of control for proliferation of induced cultures, as well as their possible maturation to organogenic or embryogenic states. This study corroborates the use of *in vitro* cultures as a novel approach to perform comparisons between GM maize and conventional counterparts, providing a sensitive low complexity model for detection of emergent properties of genetic modification, as reflected on altered ontogenetic and morphogenetic responses of GM maize cells to environmental stimuli *in vitro*.

REFERENCES

AL-ABED, D.; RUDRABHATLA, S.; TALLA, R.; GOLDMAN, S. Split-seed: a new tool for maize researchers. **Planta**, v. 223, p. 1355-1360, 2006.

BHASKARAN, S.; SMITH, R.A. Regeneration in cereal tissue culture a review. **Crop Sci.**, v. 30, p. 1328-1336, 1990.

BOLKER, B.M.; BROOKS, M.E.; CLARK, C.J.; GEANGE, S.W.; POULSEN, J.R.; STEVENS, M.H.H.; WHITE, J.S.S. Generalized linear mixed models: A practical guide for ecology and evolution. **Trends Ecol. Evol.**, v. 24, p. 127-135, 2009.

BURNHAM, K.P.; ANDERSON, D.R. Multimodel inference: understanding AIC and BIC in model selection. **Sociological Methods & Research**, v. 33, p. 261-304, 2004. Disponível em: https://doi.org/10.1177/0049124104268644.

CERA, Center for Environmental Risk Assessment. **GM Crop Database, MON-ØØ81Ø-6 (MON810)**. ILSI Research Foundation, Washington D.C., 2016. Disponível em: http://cera-gmc.org/GmCropDatabaseEvent/MON810/short. Acesso em: 03 dez. 2016.

CONGER, B.V.; NOVAK, F.J.; AFZA, R.; ERDELSKY, K.E. Somatic embryogenesis from cultured leaf segments of *Zea mays*. **Plant Cell Rep.**, v. 6, p. 345-347, 1987.

CUMMING, G.; FINCH, S. Inference by eye: Confidence intervals, and how to read pictures of data. **American Psychologist**, v. 60, p. 170-180, 2005.

CUMMING, G.; FIDLER, F.; VAUX, D.L. Error bars in experimental biology. **Journal of Cell Biology**, v. 177, p. 7-11, 2007. Disponível em: http://doi.org/10.1083/jcb.200611141.

DUNCAN, D.R.; WILLIAMS, M.E.; ZEHR, B.E.; WIDHOLM, J.M. The production of callus capable of regeneration from immature embryos of numerous *Zea mays* genotypes. **Planta**, v. 165, p. 322-332, 1985.

EMONS, A.M.C.; SAMALLO-DROPPERS, A.; VAN DER TOOM, C. The influence of sucrose, mannitol. L-proline, abscisic acid and gibberellic acid on the maturation of somatic embryos of *Zea mays* L. from suspension cultures. **Plant Physiol.**, v. 142, p. 597-604, 1993.

EMONS, A.M.C.; KIEFT, H. Somatic embryogenesis in maize (*Zea mays* L.), in: BAJAJ, Y.P.S. (ed), **Biotechnology in Agriculture and Forestry**, v. 31. Berlin: Springer, 1995, p. 24-39.

FRAME, B.R.; SHOU, H.; CHIKWAMBA, R.K.; ZHANG, Z.; XIANG, C.; FONGER, T.M.; PEGG, S.E.E.; LI, B.; NETTLETON, D.S.; PEI, D.; WANG, K. Agrobacterium tumefaciens-mediated transformation of maize embryos using a standard binary vector system. **Plant Physiol.**, v. 129, p. 13-22, 2002.

GEORGE, E.F.; HALL, M.A.; DE KLERK, G.J. (eds.). **Plant Propagation by Tissue Culture**. Dordrecht, The Netherlands: Springer, 2008.

GREEN, C.E.; PHILIPS, R.L. Plant regeneration from tissue culture of maize. **Crop. Sci.**, v. 15, p. 417-421, 1975.

HODGES, T.K.; KAMO, K.K.; IMBRIE, C.W.; BECWAR, M.R. Genotype specificity of somatic embryogenesis and regeneration in maize. **BioTechnology**, v. 4, p. 219-223, 1986.

HUANG, X.Q.; WEI, Z.M. High-frequency plant regeneration through callus initiation from mature embryos of maize (*Zea Mays* L.). **Plant Cell Rep.**, v. 22, p. 293-800, 2004.

HURVICH, C.M.; TSAI, C-L. Regression and Time Series Model Selection in Small Samples. **Biometrika**, v. 76, p. 297-307.

IKEUCHI, M.; SUGIMOTO, K.; IWASE, A. Plant callus: mechanisms of induction and repression. **Plant Cell**, v. 25, n. 9, p. 3159-3173, 2013.

JAMES, C. **Executive Summary of Global Status of Commercialized Biotech/GM Crops: 2016**. ISAAA Brief, 52. Ithaca, NY, 2016.

MCCULLAGH, P.; NELDER, J.A. **Generalized Linear Models**, Second Edition, London: Chapman and Hall, 1989.

MOREL, G.; WETMORE, R.H. Fern callus tissue culture. **American Journal of Botany**, v. 38, n. 2, p.141-143, 1951.

MURASHIGE, T.; SKOOG, F. A revised medium for rapid growth and bio assays with tobacco tissue cultures. **Physiologia Plantarum**, v. 15, p. 473-497, 1962.

O'CONNOR-SANCHEZ, A.; CABRERA-PONCE, J.L.; VALDEZ-MELARA, M.; TÉLLEZ-RODRÍGUEZ, P.; PONS-HERNÁNDEZ, J.L.; HERRERA-ESTRELLA, L. Transgenic maize plants of tropical and subtropical genotypes obtained from calluses containing organogenic and embryogenic-like structures derived from shoot tips. **Plant Cell Reports**, v. 21, p. 302-312, 2002.

RHODES, C.R.; GREEN, C.E.; PHILLIPS, R.L. Factors affecting tissue culture initiation from maize tassels. **Plant Science**, v. 46, p. 225-232, 1986.

R CORE TEAM. **R: A Language and Environment for Statistical Computing**. R Foundation for Statistical Computing. Vienna, Austria, 2017.

SPRINGER, W.D.; GREEN, C.E.; KOHN, K.A. A histological examination of tissue culture initiation from immature embryos of maize. **Protoplasma**, v. 101, p. 269-281, 1979.

VASIL, V.; LU, C.; VASIL, I.K. Histology of somatic embryogenesis in cultured immature embryos of maize (*Zea mays* L.). **Protoplasma**, v. 127, p. 1–8, 1985.

VASIL, L.K. Developing cell and tissue culture systems for the improvement of cereal and grass crops. **Journal of Plant Physiology**, v. 128, p. 193-218, 1987.

WANG, A.S. Callus induction and plant regeneration from maize mature embryos. **Plant Cell Rep.**, v. 6. p. 360-362, 1987.

ZHONG, H.; SRINIVASAN, C.; STRICKLEN, M.B. In-vitro morphogenesis of corn (*Zea mays* L.). I. Differentiation of multiple shoot clumps and somatic embryos from shoot tips. **Planta**, v. 187, p. 483-489, 1992.

6. CAPÍTULO III – MAINTENANCE/PROLIFERATION OF *IN VITRO* CULTURES OF TRANSGENIC MAIZE AG-5011YG (EVENT MON810) AND ITS CONVENTIONAL NEAR-ISOGENIC MAIZE AG-5011

ABSTRACT

Plant transformation may cause unintended emergent properties that alter the transformed cell phenotype, producing so called off-target effects. This study aimed at evaluating morphophysiological and developmental parameters of a GM maize hybrid (AG-5011YG, event MON810) and its conventional near-isogenic hybrid (NIH) (AG-5011), during long-term *in vitro* maintenance of pre-established friable callus cultures, as affected by multiple environmental control variables in multiple experiments. Growth rate and morphophysiological comparisons of GM and conventional calli subcultured from maintenance medium (20 μM 2,4-D) to media supplemented with ABA (2 μM) and 0, 2 or 20 μM 2,4-D, evidenced stronger responses of the GM callus to 2,4-D reduction, with lower friability and higher rhizogenesis rates. Subculturing maintenance calli to a range of 2,4-D concentrations in suspension cultures (from 0 to 20 μM) produced a linear reduction in growth rate for both NIHs, but the GM NIH showed significantly lower growth rate regardless of 2,4-D concentration. Increases in 2iP concentration relative to 2,4-D proved to influence growth rates and cell vitality in cell suspension cultures, with a positive effect for the GM NIH and a negative effect for the conventional NIH, indicating a differential cell response to 2iP. Suspension cultures provide optimal growth conditions for maintenance/proliferation within the *in vitro* model, reaching up to 3.5- and 2.0-fold biomass increases in 21 days, for the conventional and GM NIHs, respectively. To maintain calli in an undifferentiated state while improving suspension culture growth rates, 2,4-D concentration in maintenance medium can be reduced up to 5 μM and 10 μM, for conventional and GM NIHs, respectively. Additional efforts are required to elucidate the specific molecular mechanisms behind the altered responses of the GM hybrid's cells to exogenous growth regulators *in vitro*, such as 2,4-D and 2iP. These results are further evidence of the potential an *in vitro* culture model has for comparisons between GM maize and conventional maize counterparts, expanding the body of evidence built from a low complexity, high resolution model for detection of emergent properties of plant genetic modification.

6.1 INTRODUCTION

Genetically modified (GM) maize (*Zea mays spp. mays*) event MON810 (Monsanto Company, YieldGard® maize, unique identifier MON-ØØ81Ø-6 (CERA, 2016)) is a GM maize widely employed for the production of insect resistant GM maize hybrids (James, 2016; CERA, 2016). In order to establish an interactive model for the screening of unintended effects from plant genetic transformation, we previously initiated *in vitro* cultures of GM hybrid AG-5011YG (event MON810) and its conventional near-isogenic hybrid AG-5011, bearing in mind that an *in vitro* model would have good qualities of environmental control, reproducibility and scalability.

Within the context of tissue culture, culture maintenance/proliferation is used as source of plant cell and calli biomass, which can be continually subcultured and multiplied in an "unorganized" state, or re-determined by environmental stimuli (physical growth conditions, growth regulators, etc) during an additional maturation stage into organogenesis or somatic embryogenesis (George *et al*., 2008).

During culture maintenance, a myriad of physico-chemical conditions of the culture system, as well as subculture frequency, largely determine ontogenetic and morphogenetic features of *in vitro* established cultures (George *et al*., 2008). Specifically, differences in the regenerative capacity of maize genotypes can be overcome by manipulation of growth regulator concentration in the culture medium (Vasil 1987; Zhong *et al.*, 1992). The potential of the synthetic auxin 2,4-D in combination with cytokinins for maize *in vitro* morphogenesis was previously demonstrated, allowing for the establishment of cell and tissue cultures and plant regeneration, independently of the explant genotype (Zhong *et al.*, 1992).

The objective of this study was to evaluate and compare growth rates, cell vitality, callus friability rates, and morphogenesis of a GM maize hybrid (AG-5011YG) and its conventional near-isogenic hybrid (AG-5011), both in semi-solid media and in liquid media (suspension cultures). The main hypotheses tested were: maize isogenic hybrid (transgenic and conventional), 2,4-D concentration, and the balance between 2iP and 2,4-D affect culture growth rates, cell vitality, callus friability and morphogenic potential, either in an interactive or independent fashion.

6.2 MATERIAL AND METHODS

6.2.1 Calli source, culture media and in vitro experimental practices

Fast growing, friable, rhizogenesis-determined calli (Type III - Emons *et al*., 1993)) derived from maize seedling root segments of a GM maize hybrid (AG-5011YG) and its conventional NIH (AG-5011), which were previously induced *in vitro* (Capítulo II), were subcultured to maintenance medium consisting of MS salts (Murashige and Skoog, 1962), Morel vitamins (Morel and Wetmore, 1951), sucrose (3%), mannitol (2%), enzymatic casein hydrolisate (200 mg/L), L-proline (10 mM) - modified from Emons *et al.* (1993) - and 2,4-D (20 μM), for several passages, with subcultures every four weeks. All culture media had pH adjusted to 5.8, and semi-solid media were gelled with Phytagel (0.2%), prior to sterilization at 121 ºC and 1.5 atm for 20 min. All manipulations of cultures took place in aseptic conditions in a laminar flow hood, using aseptic technique and sterilized tools and materials.

The rhizogenesis-determined Type III callus was selected as a model for subsequent maintenance/proliferation, morphogenesis and embryogenesis experiments, due to several potential advantages: i) abundance of explant source (*in vitro* germinated plantlet roots); ii) high induction frequency (~70-90%, for GM and conventional NIHs, respectively); iii) maintenance/proliferation of friable callus of undifferentiated nature at high 2,4-D concentrations (20 μM); iv) potential opportunity for additional studies on somatic embryogenesis recalcitrance in maize (Emons *et al.*, 1993), based on plantlet root explants; and v) potential for studies about the emergent properties of plant genetic modification on *in vitro* ontogenesis and morphogenesis of maize hybrids.

6.2.2 Callus maintenance/proliferation on semi-solid media with reduced 2,4-D concentration

Type III maize calli maintained with 2,4-D (20 μM) were used to evaluate the combined effects of maize near-isogenic hybrid and 2,4-D concentration on callus growth rate and morphogenesis during maintenance/proliferation of *in vitro* cultures in semi-solid media. For this experiment, calli were inoculated in sterile plastic Petri dishes containing 25 ml maintenance medium, supplemented with ABA (2 μM - in an attempt to inhibit rhizogenesis of Type III calli in media with reduced 2,4-D concentrations (Emons *et al*., 1993)), 2,4-D at maintenance level (20 μM - high level stimulus) or reduced levels (2 μM - low level stimulus

- and 0 µM - absence of stimulus), subcultured 3 times on the same media, with 3-week long subcultures, at 25 ºC in the dark. At the third subculture calli fresh weight (range from 201 to 449 mg) was measured using paper plates over an analytic scale inside the laminar flow hood, and calli were immediately placed on fresh medium afterwards. In total, 278 calli were inoculated between the six combinations of NIH and 2,4-D concentrations. After 21 days of the third subculture, every callus was re-weighed, and evaluated regarding friability and rhizogenic response.

6.2.3 Callus and cell maintenance/proliferation in suspension cultures under orbital agitation

Root-derived, fast growing, friable, rhizogenesis determined calli (Type III) subcultured in semi-solid maintenance/proliferation medium for several passages, were transferred to 250 ml flasks containing 50 ml of liquid maintenance medium, in order to start suspension cultures. Suspension cultures were kept in an orbital shaker-incubator (New Brunswick™ Innova® 40R) at 90 rpm and 25 ºC, and subcultured every 3-4 weeks, by filtration of the biomass (cell clusters and calli bigger than 500 µm) and transfer to flasks containing fresh medium. These cultures were employed as source of material for the following suspension culture experiments.

6.2.3.1 Effect of 2,4-D concentration and maize NIH on the growth rate of suspension cultures

Cell clusters and calli from maintenance suspension cultures (clusters and calli bigger than 500 µm), of GM and conventional maize NIHs, were aseptically filtered and used as inoculum in an experiment to determine the effect of 2,4-D concentration (0, 5, 10 and 20 *µM*) on biomass growth rate of suspension cultures, after a three week subculture. Three flasks containing 50 ml of medium were inoculated with 2 g of cell clusters/calli for every combination of NIH and 2,4-D concentration, in a total of 24 flasks. Suspension cultures were kept in an orbital shaker-incubator (New Brunswick™ Innova® 40R) at 90 rpm and 25 ºC. After 3 weeks, the course biomass in every culture flask (cell clusters and calli > 500 µm) was filtered and weighed in an analytical scale.

6.2.3.2 Growth curves of maize NIHs' suspension cultures on dedifferentiation medium and differentiation medium

With the objective of quantifying time-dependent growth-curves of GM and conventional NIHs' suspension cultures, cell clusters and calli from maintenance suspension cultures (clusters and calli > 500 µm) were used as starter in a suspension culture growth-curve experiment, in which cell proliferation and cell vitality were recorded throughout the course of one subculture (21 days). Additionally, in order to evaluate the growth curves in contrasting culture conditions, two different culture media were devised: i) dedifferentiation medium (regular maintenance medium, with the normal 2,4-D concentration (20 μM) - high auxin stimulus inducing friable, undifferentiated callus cultures), and ii) differentiation medium (maintenance medium with reduced 2,4-D (2 μM) + 2iP (1 μM) - low auxin allowing for differentiation, but still limiting rhizogenesis in maize Type III calli, and low cytokinin, possibly inducing differentiation (Zhong *et al.*, 1992; Emons *et al.*, 1993; George *et al.*, 2008)). Six flasks containing 50 ml of medium were inoculated with 2 g of cell clusters and calli for every combination of NIH and culture medium, in a total of 24 flasks. Suspension cultures were kept in an orbital shaker-incubator (New Brunswick™ Innova® 40R) at 90 rpm and 25 ºC. Aliquots of 500 ul were removed from one replicate of each tested condition on each collection day (days 1, 3, 7, 11, 16 and 21), and used for cell counting and viability analysis.

6.2.3.3 Effect of [2iP]:[2,4-D] balance on maize NIHs' suspension culture growth rate

Fine suspension cultures (cells and clusters smaller than 500 µm) were used as starter to estimate cell proliferation and vitality of the GM and conventional NIHs, subjected to a gradient of the balance of culture medium concentrations of 2iP and 2,4-D (2:2 μM; 4:2 μM; and 8:2 μM, for 2iP:2,4-D, or proportions of 1:1, 2:1 and 4:1, respectively), over one subculture period (21 days). Three flasks containing 50 ml of medium were inoculated with 10 ml of cell suspension (cells and clusters smaller than 500 µm), for every combination of NIH and 2iP:2,4-D proportion, in a total of 18 flasks. Cell suspension cultures were kept in an orbital shaker-incubator (New Brunswick™ Innova® 40R) at 90 rpm and 25 ºC, and 1000 ul aliquots were collected from every replicate for cell counting after 21 days.

6.2.3.4 Cell counting, cell concentration estimation and viability analysis

Cell proliferation and vitality in suspension cultures were evaluated by counting cells in a Neubauer chamber, with recorded values representing the average count of 10 technical replicates for each flask. Cell viability was assessed by means of staining with fluoroscein diacetate (FDA) (Jones & Senft, 1984) and visualization in an Olympus IX 81 inverted fluorescence microscope. Total cells were counted on visible light and viable cells were counted under blue light to elicit FDA fluorescence. Photographs were taken with a CCD camera coupled to the IX81 Olympus microscope, using the CellSens software (Olympus).

6.2.4 Statistical Analysis

Data were analyzed in a generalized linear model framework (Mccullagh and Nelder, 1989; Bolker *et al.*, 2009). Data on biomass growth rates, growth curves, total cell concentration, viable cell concentration, and percentage of viable cells in suspension cultures were analyzed with normal polynomial regression. Callus friability and rhizogenesis were evaluated as binary variables (yes = 1; no = 0) and analyzed with logistic regression. For every analysis, the initial statistical models included all explanatory variables, interactions, and quadratic terms (and cubic terms in the case of growth curves) for quantitative variables (e.g. 2,4-D concentration, time). Model selection was carried out by means of stepwise elimination of variables followed by inspection of the small sample-corrected Akaike Information Criterion (cAIC) (Hurvich and Tsai, 1989; Burnham and Anderson, 2004). Model assumptions about residual variance and distribution were evaluated graphically for all selected models, and the dispersion parameter - Chi-square/degrees of freedom - was additionally used to assess model fit, when applicable (Mccullagh and Nelder, 1989; Bolker *et al.*, 2009). Effects were considered significant when $P < 0.05$. Significant trend- and point-wise differences were detected by comparison of 95% confidence intervals/envelopes (Cumming and Finch, 2005; Cumming *et al.*, 2007). Analyses were carried out in the R statistical language/software (R Core Team, 2017).

6.3 RESULTS AND DISCUSSION

6.3.1 Callus maintenance/proliferation on semi-solid media with regular and reduced 2,4-D levels

Friable calli derived from root segments were successfully maintained and proliferated in maintenance/proliferation medium containing 20 μM 2,4-D, and subsequently an experiment was established to assess the influence of the GM and conventional NIHs, and of reduced 2,4-D concentration on callus growth rate and morphogenetic responses during maintenance/proliferation. Friable calli were cultivated in maintenance media supplemented with either regular (20 μM - high level stimulus) or reduced 2,4-D concentrations (0 μM - absence of stimulus - and 2 μM - low level stimulus), and ABA (2 μM - aiming at inhibiting rhizogenesis in Type III calli subjected to 2,4-D reduction) (Figure 27). Calli underwent three subcultures in these media to minimize residual effects from the previously higher 2,4-D concentration, and at the third subculture all calli were weighed and then weighed again after three weeks.

The reduction in 2,4-D concentration in the culture medium from 20 μM to 2 or 0 μM affected callus growth rate in a complex manner. Callus growth rate showed a significant curvilinear trend ($P > 0.001$) across tested 2,4-D concentrations for both NIHs, but a significant interaction between 2,4-D and NIH was also evidenced, indicating different growth rate trends for GM and conventional NIHs (Figure 28).

It should be noted, however, that the presence of ABA (2 μM) in the culture medium - which was not controlled for in this particular experiment (i.e. all media had the same ABA concentration) - could exert an inhibitory effect on growth rates, and possibly interact with maize NIH. The trend-differences between NIHs are reflected on significantly higher growth rates observed in the conventional NIH from 0 to 2 μM 2,4-D, and in the slightly higher growth rate of the GM NIH at 20 μM (Figure 28).

Figure 27: Calli of conventional (a-c) and GM (MON810) (d-f) near-isogenic maize hybrids derived from root segments of *in vitro* germinated plantlets, maintained for several subcultures in maintenance medium supplemented with 2,4-D (20 µM), and then grown for three subcultures on media supplemented with ABA (2 µM) and 2,4-D at 0 µM (a and d), 2 µM (b and e), and 20 µM (d and h).

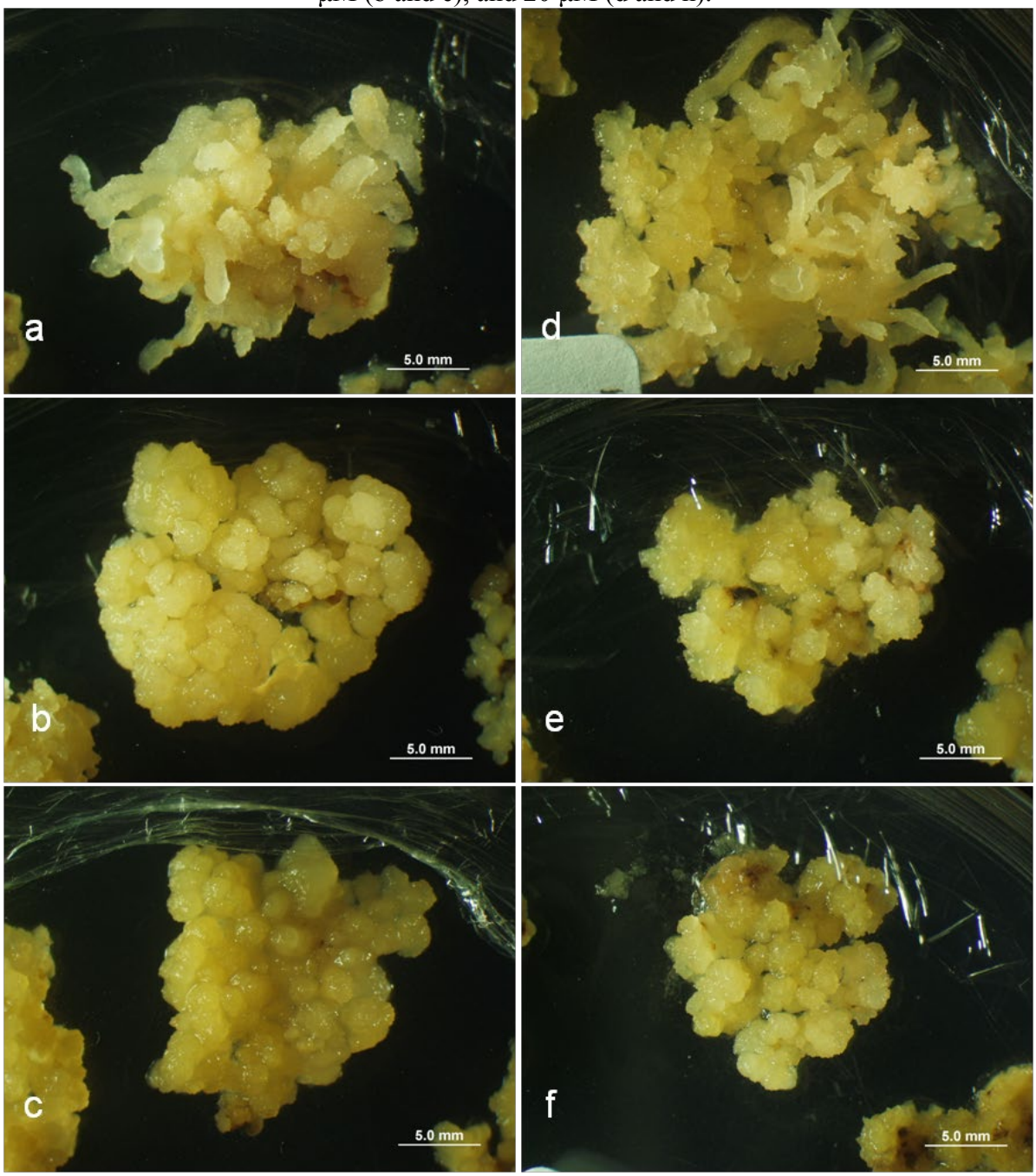

Fonte: Daniel Ferreirra Holderbaum (2019).

Figure 28: Polynomial regression model for callus growth rate of GM (GM - dashed line) and conventional (NM - solid line) near-isogenic maize hybrids, after three 3-week subcultures in media with ABA (2 µM) and regular maintenance 2,4-D concentration (20 µM) or reduced 2,4-D concentrations (0 and 2 µM). Lines depict estimated trends, shaded bands indicate 95% confidence envelopes, and black dots (NM) and triangles (GM) represent observations (slightly dislocated vertically and horizontally to improve visualization).

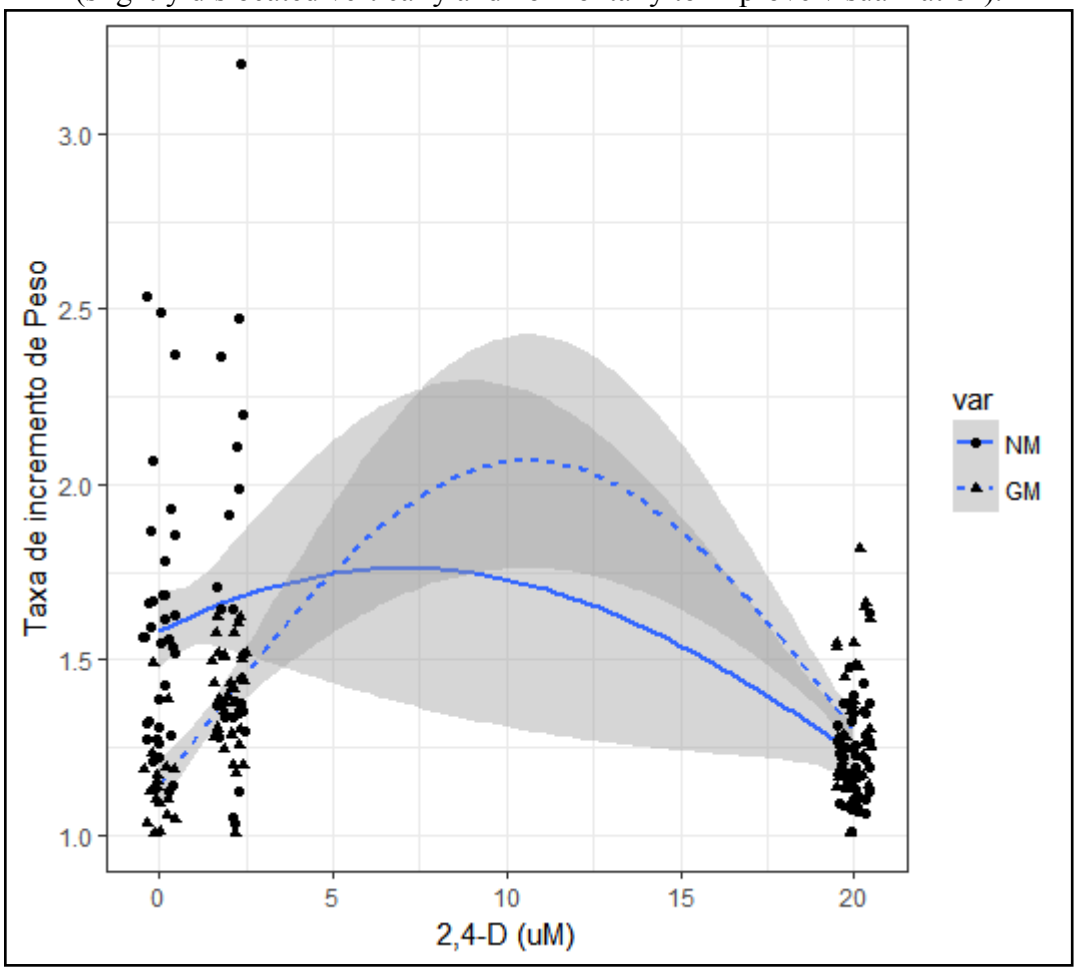

Fonte: Daniel Ferreirra Holderbaum (2019).

One important caveat of this particular experimental design and regression analysis, is that the trend estimations between 2 and 20 µM, and therefore a large portion of the tested 2,4-D gradient, are associated with great uncertainty (very large confidence intervals) due to great variability in the dependent variable (callus growth rate), and to the absence of observations in this concentration range, what reduces accuracy of estimated trends between 2 and 20 µM 2,4-D. Nonetheless, the estimates at 0, 2 and 20 µM 2,4-D are robust and reliable.

Callus friability was also significantly affected by reduced 2,4-D concentration in the culture medium. A strong curvilinear effect of 2,4-D was evidenced ($P < 0.001$), indicating calli remain friable between 5 and 20 µM 2,4-D, and friability is abruptly lost at concentrations lower than 5 µM for both NIHs (Figure 29). However, a significant interaction between NIH and 2,4-D ($P < 0.001$) indicates the loss of friability happens at higher

concentrations for GM (~4 µM) than for the conventional NIH (~2 µM), what causes significant differences in the frequency of friable callus between the two NIHs (Figure 29). After three subcultures in medium free of 2,4-D, model estimates indicate ~15% of calli remained friable for the GM NIH and ~60% for the conventional NIH.

Figure 29: Frequency of friable calli for GM (GM) and conventional (NM) near-isogenic maize hybrids, after a three 3-week subculture in media with ABA (2 µM) and regular maintenance 2,4-D concentration (20 µM) or reduced 2,4-D concentrations (0 and 2 µM). Lines depict estimated trends, shaded bands indicate 95% confidence envelopes, and dots represent observations (slightly dislocated vertically and horizontally to improve visualization).

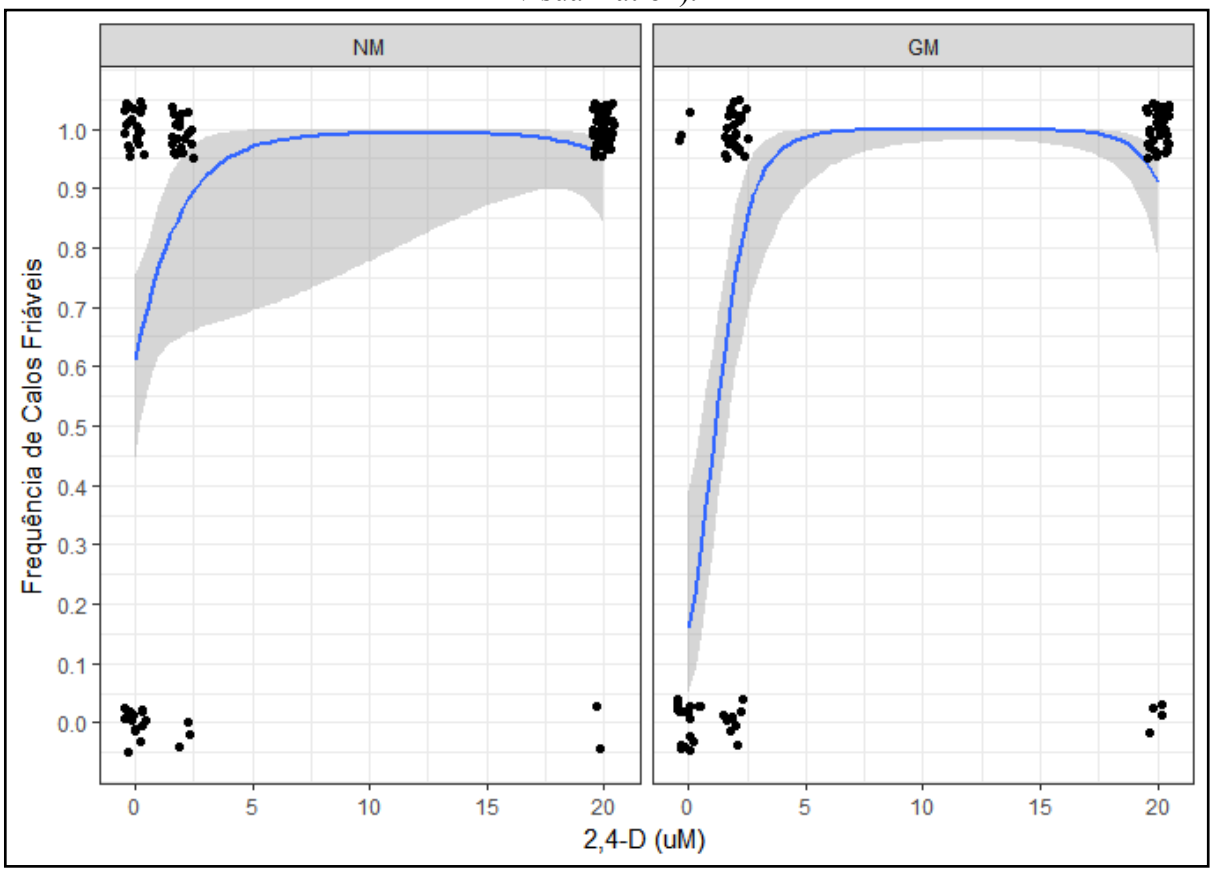

Fonte: Daniel Ferreirra Holderbaum (2019).

Rhizogenesis was strongly stimulated by reducing 2,4-D concentration in the medium, presenting significant curvilinear trends (P = 0.004) (Figure 30). Model estimates show that once 2,4-D is reduced below ~5 µM for the conventional NIH, and below ~10 µM for the GM NIH, calli start to develop roots, with ~20% conventional calli and ~50% GM calli becoming rhizogenic at 2 µM 2,4-D, and ~70% conventional calli and 60% GM calli becoming rhizogenic at 0 µM 2,4-D.

Figure 30: Frequency of rhizogenic calli of GM and conventional (NM) near-isogenic maize hybrids after three 3-week subcultures in media with regular maintenance 2,4-D concentration (20 µM) or reduced concentrations (0 and 2 µM). Lines depict estimated trends, shaded bands indicate 95% confidence envelopes, and black dots (NM) and triangles (GM) represent observations (slightly dislocated vertically and horizontally to improve visualization).

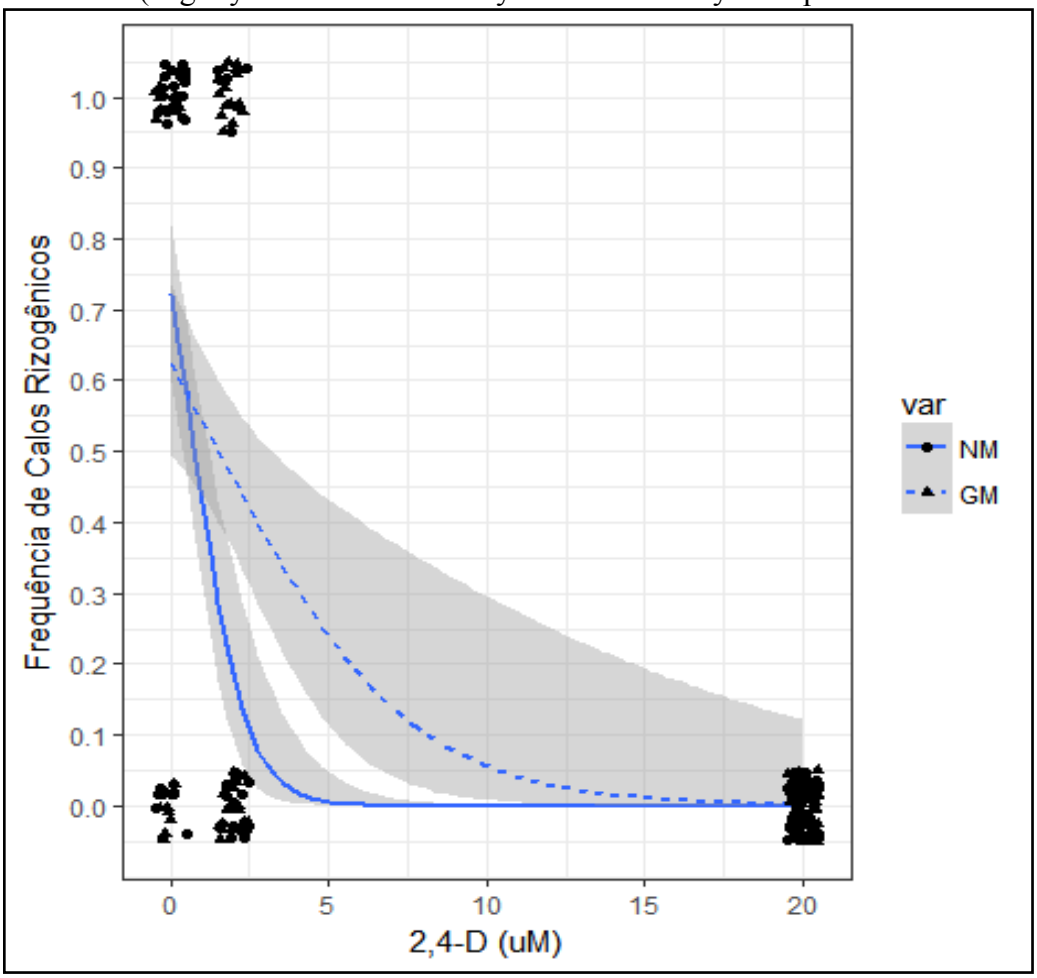

Fonte: Daniel Ferreirra Holderbaum (2019).

Friable callus transfer from medium containing 20 µM 2,4-D to medium containing either 2 or 0 µM 2,4-D had a similar effect to maintaining calli for extended periods (8 weeks) in the same induction medium without subculture: rhizogenesis was increased, with the absence of 2,4-D in the medium inducing the highest levels of rhizogenic calli. Contrary to the observed effects for callus growth rate and friability, rhizogenesis was not affected by NIH. This may indicate that unintended effects of MON810 genetic transformation are related to the *in vitro* responses of the tested GM and conventional NIHs, but are relatively small, and thus only detectable in highly undifferentiated cells/tissues, which are more readily sensitive to environmental stimuli such as changes in concentrations of the synthetic auxin 2,4-D. This hypothesis requires further testing in order to be appropriately addressed.

6.3.2 Callus and cell maintenance/proliferation in suspension cultures under orbital agitation

6.3.2.1 Effect of 2,4-D concentration and maize NIH on the growth rate of suspension cultures

The growth rate of GM and conventional NIHs was further inspected in suspension cultures, evaluating the effect of 2,4-D concentrations (0, 5, 10 and 20) on culture growth. After a 3 week incubation period, significant effects of NIH ($p<0.001$) and a quadratic effect of 2,4-D ($p=0.012$) were detected, with interaction between NIH and the quadratic parameter for 2,4-D. ($p=0.004$) (Figure 31). Overall, on all tested 2,4-D concentrations, the conventional hybrid showed significantly greater growth rates than the GM hybrid. For both NIHs, the increase in 2,4-D concentration in culture media is followed by a significant decrease in growth rate, but the decrease was more pronounced for the GM NIH, which depicted a proper curvilinear trend, while the conventional NIH showed a roughly linear trend. This result corroborates previous findings (Capítulos I e II), evidencing developmental differences in the responses of the tested NIHs to 2,4-D *in vitro*.

Figure 31: Growth rate of GM (solid line) and conventional (dashed line) near-isogenic maize hybrids suspension cultures, as a function of 2,4-D concentration in liquid media. Lines depict estimated trends, grey shaded bands indicate 95% confidence envelopes, and dots (NM) and triangles (GM) represent observations (slightly dislocated horizontally to avoid overlapping).

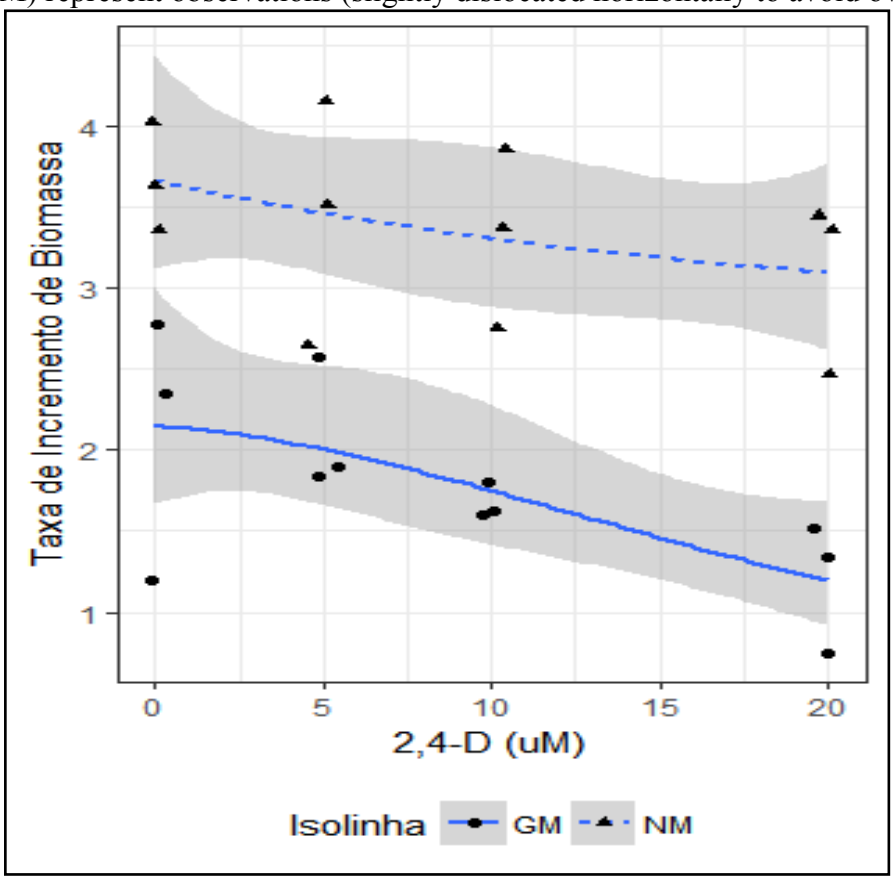

Fonte: Daniel Ferreirra Holderbaum (2019).

6.3.2.2 Maize NIH suspension cultures growth curves on dedifferentiation medium and differentiation medium

In evaluating the growth dynamics of conventional and GM NIHs, estimated as the increase in total cell concentration in suspension cultures through time, a significant cubic trend ($p<0.001$) was evidenced for both hybrids, showing great resemblance to a classical sigmoid growth dynamic (Figure 32), with an initial lag phase, then exponential growth, and stabilization. The two tested culture media (dedifferentiation medium - maintenance medium (which is supplemented with 20 µM 2,4-D) - and differentiation medium - maintenance medium with reduced 2,4-D (2 µM) + 2iP (1 µM)) had no significant effect on the growth curves of the NIHs. Furthermore, there was a significant interaction between maize hybrid and a quadratic term for time, indicating both NIH show a curvilinear trend for growth through time, but that the growth rates are different. At the first days of culture both NIHs show similar values, but the different growth rates result in significant differences from circa

day 13 onwards, with the conventional hybrid showing greater number of total cells in suspension.

Figure 32: Growth dynamics for GM (GM-solid line) and conventional (NM-dashed line) near-isogenic maize hybrids suspension cultures, as a function of days after inoculation (Tempo), averaged between both tested culture media. Lines depict estimated growth curves, grey shaded bands indicate 95% confidence envelopes, and dots (GM) and triangles (NM) represent observations (slightly dislocated horizontally to avoid overlapping).

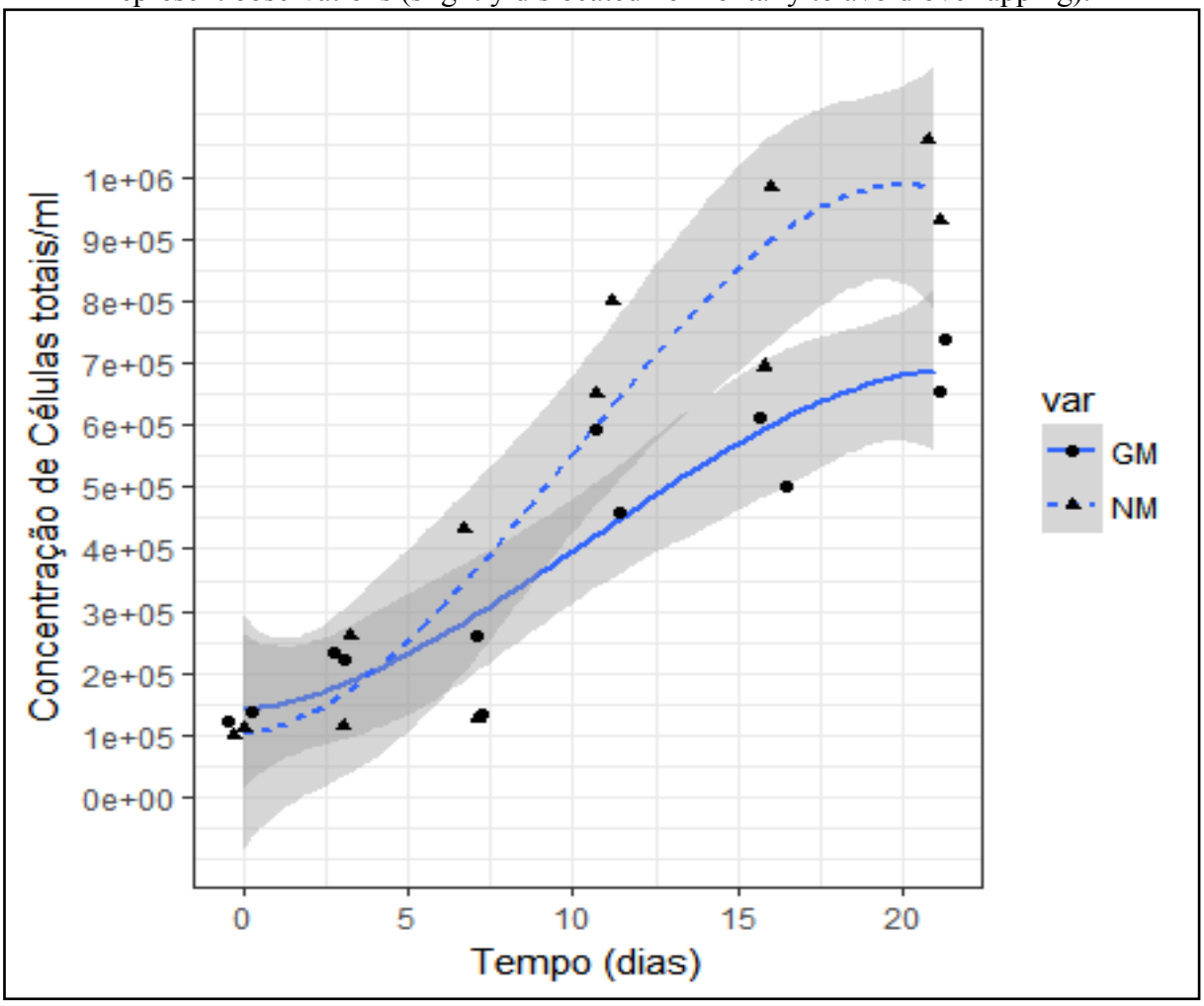

Fonte: Daniel Ferreirra Holderbaum (2019).

The concentration of viable cells in suspension cultures was significantly influenced by NIH and culture time. Overall, a linear increase in viable cell concentration was observed throughout the culture period ($p<0.001$), and on average the conventional NIH showed higher concentrations of viable cells ($p=0.025$), although the linear trends for GM and conventional NIHs were not significantly different (Figure 33).

Figure 33: Viable cell concentration estimated in GM (GM-solid line) and conventional (NM-dashed line) near-isogenic maize hybrids cell suspension cultures, as a function of days after inoculation (Tempo), averaged between both tested culture media. Lines depict estimated trends, grey shaded bands indicate 95% confidence envelopes, and dots (GM) and triangles (NM) represent observations (slightly dislocated horizontally to avoid overlapping).

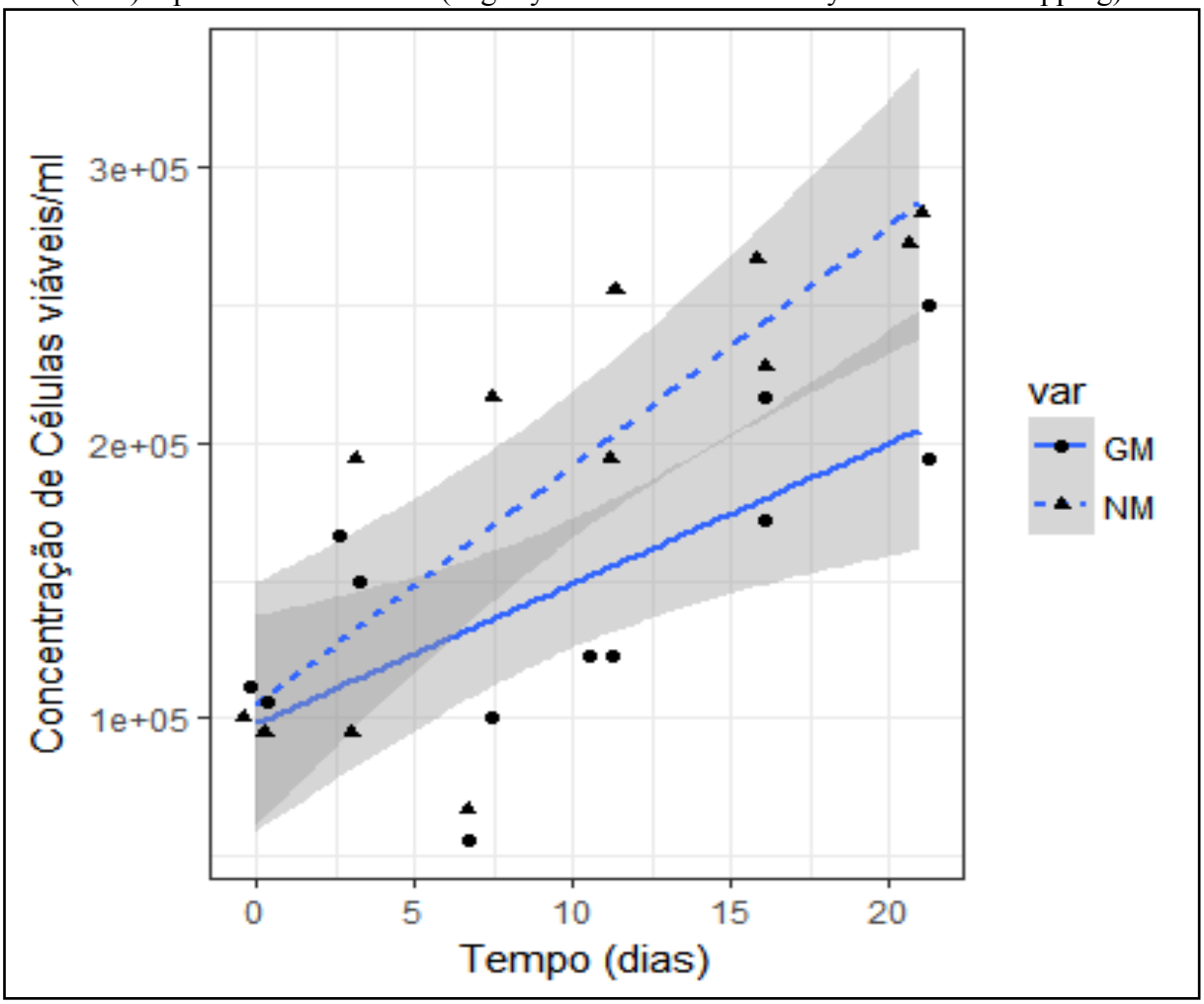

Fonte: Daniel Ferreirra Holderbaum (2019).

The percentage of viable cells in cell suspensions of GM and conventional NIHs showed a significant quadratic trend for both NIHs ($p<0.001$), and interaction between NIH and the quadratic term for the time effect ($p=0,031$), indicating the curvilinear trends are different, although no significant differences were observed between GM and NM NIHs at any specific time-points (Figure 34).

Figure 34: Percentage of viable cells estimated in GM (GM - solid line) and conventional (NM - dashed line) near-isogenic maize hybrids cell suspension cultures, as a function of days after inoculation (Tempo), averaged between both tested culture media. Lines depict estimated trends, grey shaded bands indicate 95% confidence envelopes, and dots (GM) and triangles (NM) represent observations (slightly dislocated horizontally to avoid overlapping).

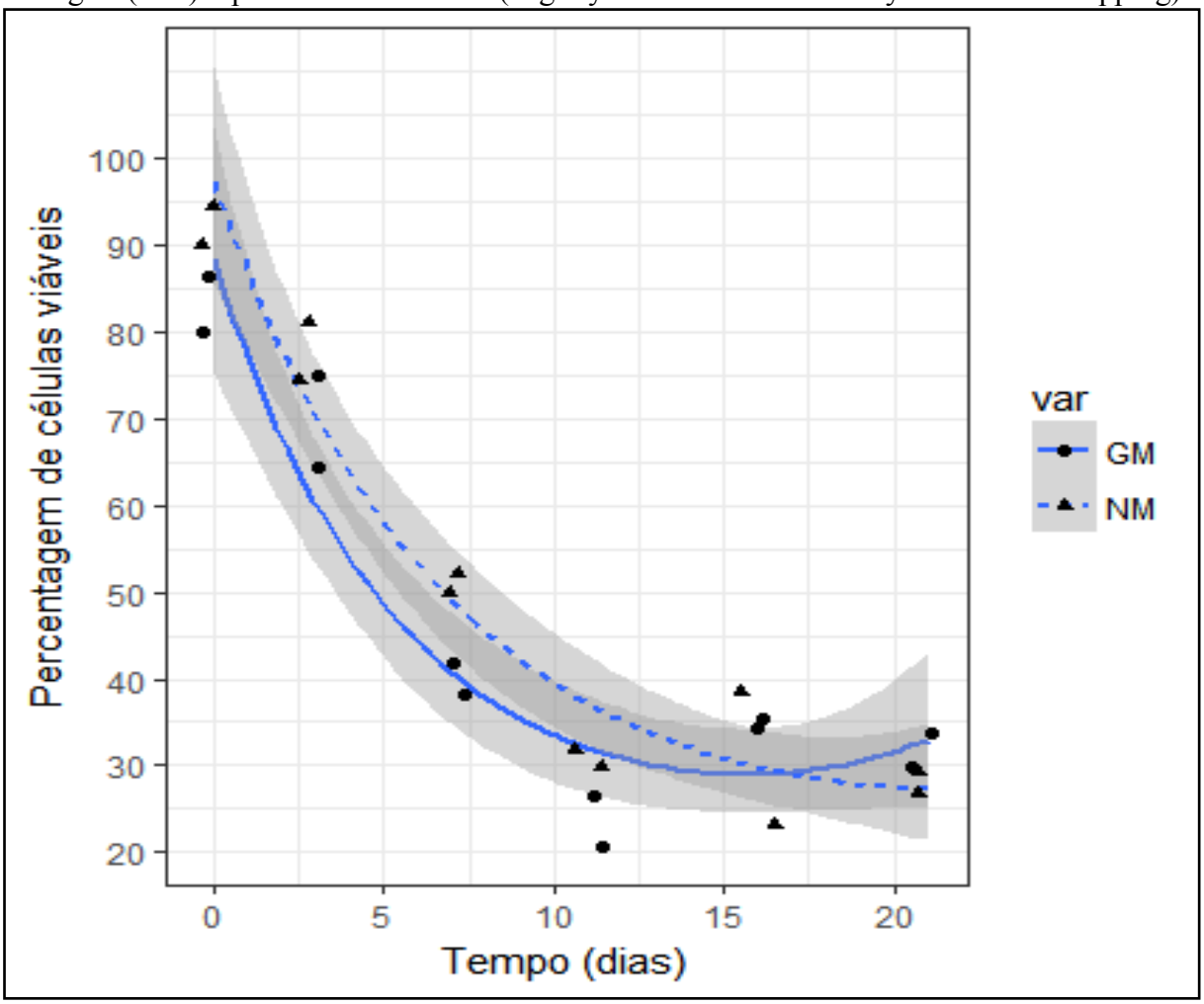

Fonte: Daniel Ferreirra Holderbaum (2019).

6.3.2.3 Effect of [2iP]:[2,4-D] balance on maize NIHs' cell suspension culture growth rate and cell viability

Cell suspension cultures were further employed to inspect the effects of NIH and of the balance between 2iP and 2,4-D (synthetic analogues of cytokinins and auxins, respectively) on growth rates and cell vitality parameters. For growth rate, only a marginally significant effect of the balance between 2iP and 2,4-D concentrations was verified (p=0,067), with a linear decrease in total cell concentration following an increment in 2iP concentration in relation to 2,4-D (Figure 35).

Figure 35: Total cell concentration in cell suspension cultures, as a function of the balance between 2iP and 2,4-D concentrations, 21 days after inoculation, averaged between both NIHs. The line depicts the estimated trend, the grey shaded band indicates a 95% confidence envelope, and dots represent observations (horizontally dislocated to avoid overlapping).

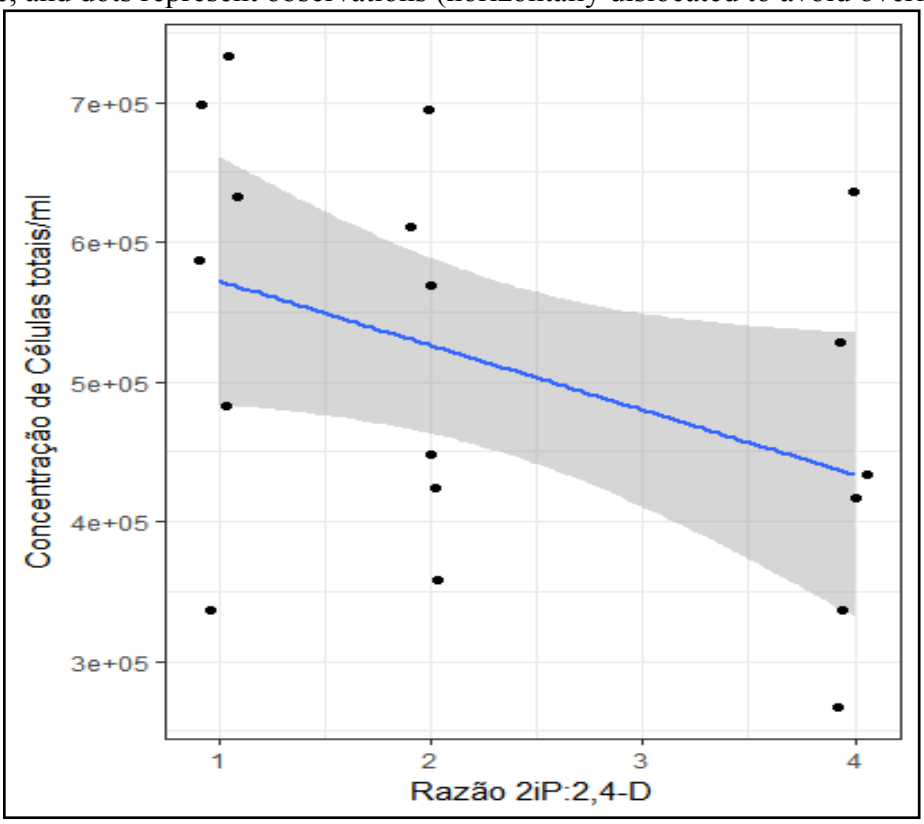

Fonte: Daniel Ferreirra Holderbaum (2019).

The concentration of viable cells, on the other hand, was significantly affected by the interaction between NIH and the balance of 2iP and 2,4-D (p=0.001), evidencing that the GM and conventional hybrids presented inverted trends: while the GM hybrid increased viable cell concentration with increasing 2iP in relation to 2,4D, the opposite was observed for the conventional hybrid, which also presented a higher magnitude of the linear change (Figure 36). This points to differential responses from the GM and conventional NIHs to 2iP, what was also established for 2,4-D previously. It is possible that the differential responses of the GM NIH to 2,4-D and 2iP are intrinsically related, since these substances act as analogues to endogenous auxins and cytokinins, respectively, and their balance is crucial in plant ontogenesis and morphogenesis *in vitro*.

Figure 36: Viable cell concentrations estimated in GM (GM) and conventional (NM) near-isogenic maize hybrids suspension cultures, as a function of the proportion between 2iP and 2,4-D concentrations, 21 days after inoculation. Lines depict estimated trends, grey shaded bands indicate 95% confidence envelopes. Dots represent observations (slightly dislocated horizontally to avoid overlapping).

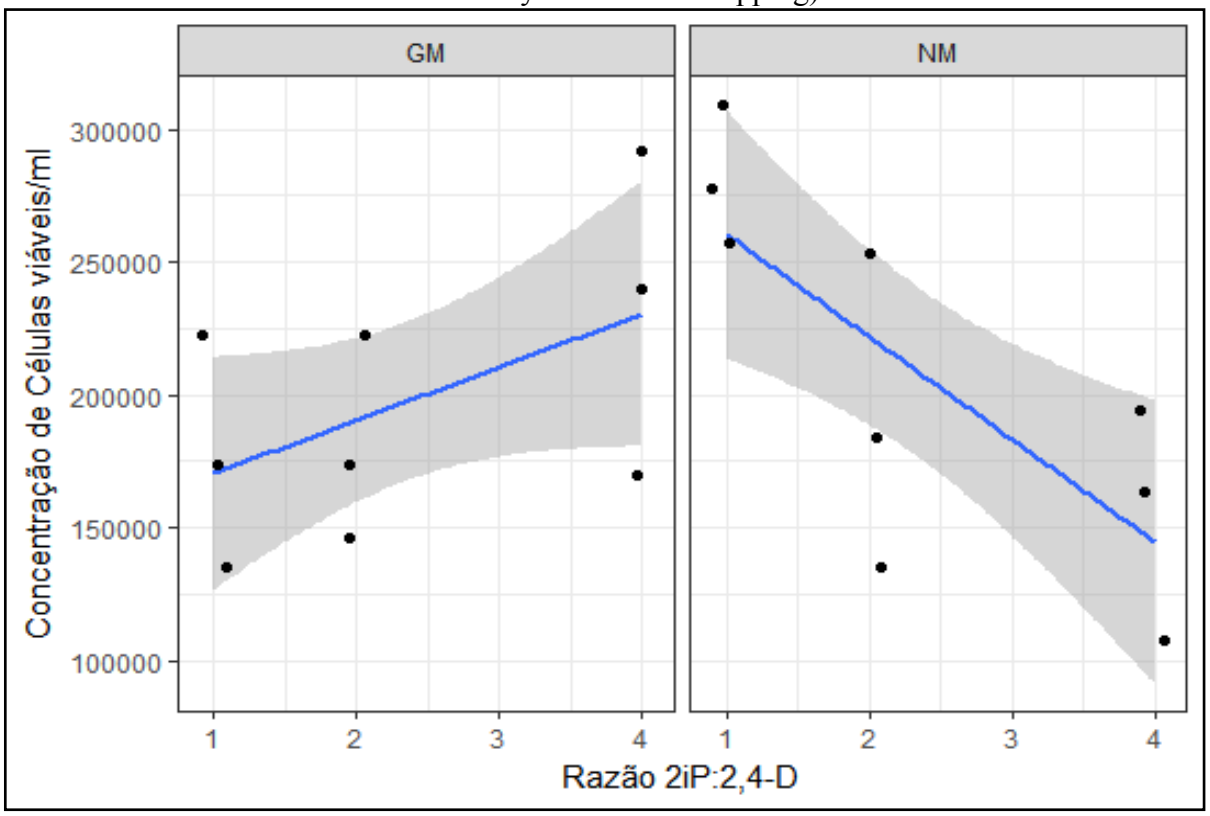

Fonte: Daniel Ferreirra Holderbaum (2019).

The percentage of viable cells showed quadratic curvilinear trends (p=0.042) for both NIHs, but also a significant interaction between NIH and a linear term for the proportion of 2iP and 2,4-D in the medium (p=0.003). This indicates the GM hybrid showed a substantial increase of viable cells in media containing higher concentrations of 2iP, while the conventional NIH presented a slight decrease in the percentage of viable cells (Figure 37).

Figure 37: Percentage of viable cells estimated in GM (GM) and conventional (NM) near-isogenic maize hybrids suspension cultures, as a function of the proportion between 2iP and 2,4-D concentrations, 21 days after inoculation. Lines depict estimated trends, grey shaded bands depict 95% confidence envelopes, and dots represent observations (slightly dislocated horizontally to avoid overlapping).

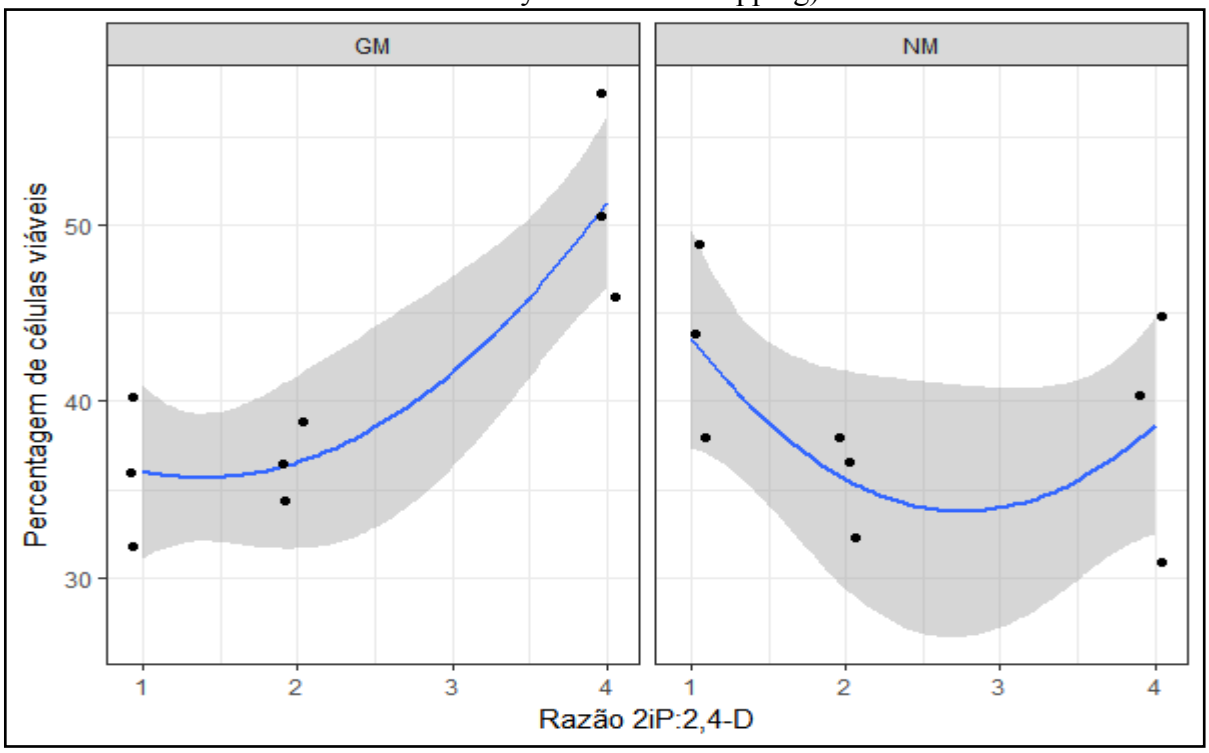

Fonte: Daniel Ferreirra Holderbaum (2019).

This study reports the investigation and optimization of maintenance conditions for previously established *in vitro* cultures, derived from seedling root segments of GM maize hybrid AG-5011YG (MON810) and its conventional near-isogenic hybrid AG-5011. Additionally, this represents additional experimental efforts to detect emergent properties of plant genetic transformation, by means of comparative *in vitro* development of callus and suspension cultures of a GM maize hybrid and its conventional NIH.

Transfer of friable callus from medium containing 20 µM 2,4-D to medium with low 2,4-D (0 and 2 µM) had a similar effect to maintaining calli for extended periods (8 weeks) in induction medium without subculture: rhizogenesis was increased, with the absence of 2,4-D in the medium inducing the highest levels of rhizogenic calli, while media with 2 *µM* 2,4-D also allowed the expression of rhizogenesis, but at lower levels. All three observed endpoints (callus growth rate, friability and rhizogenesis) evidenced significant effects from NIH.

Even for highly responsive explants such as immature embryos, the genotypic dependence of maize *in vitro* regenerative potential is well known (Vasil, 1987; Zhong *et al.*, 1992; Bhaskaran and Smith, 1990). Genotypic differences in *in vitro* regenerative capacity of

maize can be overcome by manipulating the concentration of growth regulators in the culture medium, however, to the best of our knowledge, differences in developmental parameters of a GM and a conventional NIH cultured *in vitro* were not previously reported in the scientific literature.

It was established that cell suspension cultures are the most effective means of culture maintenance and proliferation for *in vitro* cultures of the evaluated GM and conventional maize hybrids, with an approximate 3.5 fold growth rate for the conventional NIH and 2.0 fold growth rate for the GM NIH, in a period of 21 days, in culture medium free of growth regulators. The increase in 2,4-D concentrations corresponded to linear decreases in growth rates for both NIHs, but this comes with the possibility of maintaining cells and calli in an undifferentiated, unorganized state, while absence of growth regulators allows strong expression of rhizogenesis.

Growth curves were estimated for both NIHs, confirming the previously evidenced different growth rates between NIHs. Additionally, according to the estimated growth curves, suspension cultures should be subcultured at the minimum every 3 weeks, to avoid losses in cell vitality.

The proportion between 2iP and 2,4-D concentrations in the culture medium showed opposite results for cell vitality parameters of the GM and conventional NIHs in cell suspension cultures, bringing further evidence that the tested NIHs respond differently not only to 2,4-D (an auxin analogue), but also to 2iP (a cytokinin analogue). In general, the manipulation of the balance between auxins and cytokinins have shown good results for the generation of embryogenic and organogenic maize cultures, and the fact that we observed decreased growth rates with increasing 2iP concentration in the medium points to the possibility that 2iP have the potential to induce cell differentiation, and thus decrease multiplication (George *et al.*, 2008) in the tested material. Zhong *et al.* (1992) showed that cytokinins, usually in combination with 2,4-D) are key growth regulators for maize *in vitro* morphogenesis, allowing regeneration independently of the genotype used for culture initiation.

6.4 CONCLUSIONS

This is the first study to evaluate growth and morphogenetic parameters for maintenance/proliferation of an *in vitro* model comparing a GM maize hybrid and its conventional near-isogenic hybrid. Reducing the regular maintenance/proliferation 2,4-D levels altered growth rates and morphophysiological responses of GM and conventional maize calli cultured on semi-solid media, and the GM hybrid required higher 2,4-D concentrations to attain similar observed effects for callus growth rate, friability and rhizogenesis. 2,4-D also modulated growth in suspension cultures, reducing growth rates with increasing 2,4-D concentrations. However, the conventional NIH showed significantly higher suspension culture growth rates than the GM NIH, regardless of 2,4-D concentration, corroborating the previously observed altered cell responses to 2,4-D. Time dependent growth curves for total and viable cells in suspension cultures were estimated for both NIHs, with significant differences appearing at the end of the 21-day subculture period. Combinations of a fixed 2,4-D and variable 2iP concentrations greatly influenced growth rates and cell vitality in cell suspension cultures, with the GM NIH presenting increased growth and cell vitality with increasing 2iP concentration, and the conventional NIH presenting opposite responses, suggesting altered cell responses of the GM NIH to 2iP, but with positive results compared to the conventional NIH. Suspension cultures are ideal for culture proliferation within the developed *in vitro* model, with maximum observed biomass fold-changes of ~3.5 and ~2.0 for conventional e GM NIHs, respectively, in a 21-day subculture period in culture medium free of 2,4-D, while increasing 2,4-D concentrations tend to decrease growth rates linearly for the both NIHs. In parallel, decreasing the 2,4-D concentration in culture media below ~5 μM tends to greatly reduce callus friability and induce rhizogenesis in both NIHs, so that a balance might be achieved between conservation of callus friability and high growth rates in maintenance media containing at least 5 μM 2,4-D. This study provides a substantial amount of information to optimize maintenance/proliferation of *in vitro* cultures of a pair of GM and conventional maize NIHs, contributing to the establishment of a reliable, high resolution *in vitro* model for detection of emergent properties of plant genetic modification. Additional research efforts are required to elucidate the specific molecular mechanisms behind the altered cell responses of the GM hybrid to the synthetic plant growth regulators 2,4-D and 2iP.

REFERENCES

BHASKARAN, S.; SMITH, R.A. Regeneration in cereal tissue culture a review. **Crop Sci.**, v. 30, p. 1328-1336, 1990.

BOLKER, B.M.; BROOKS, M.E.; CLARK, C.J.; GEANGE, S.W.; POULSEN, J.R.; STEVENS, M.H.H.; WHITE, J.S.S. Generalized linear mixed models: A practical guide for ecology and evolution. **Trends Ecol. Evol.**, v. 24, p. 127-135, 2009.

BURNHAM, K.P.; ANDERSON, D.R. Multimodel inference: understanding AIC and BIC in model selection. **Sociological Methods & Research**, v. 33, p. 261-304, 2004. Disponível em: https://doi.org/10.1177/0049124104268644.

CERA, Center for Environmental Risk Assessment. **GM Crop Database, MON-ØØ81Ø-6 (MON810)**. ILSI Research Foundation, Washington D.C., 2016. Disponível em: http://cera-gmc.org/GmCropDatabaseEvent/MON810/short. Acesso em: 03 dez. 2016.

CUMMING, G.; FINCH, S. Inference by eye: Confidence intervals, and how to read pictures of data. **American Psychologist**, v. 60, p. 170-180, 2005.

CUMMING, G.; FIDLER, F.; VAUX, D.L. Error bars in experimental biology. **Journal of Cell Biology**, v. 177, p. 7-11, 2007. Disponível em: http://doi.org/10.1083/jcb.200611141.

EMONS, A.M.C.; SAMALLO-DROPPERS, A.; VAN DER TOOM, C. The influence of sucrose, mannitol. L-proline, abscisic acid and gibberellic acid on the maturation of somatic embryos of *Zea mays* L. from suspension cultures. **Plant Physiol.**, v. 142, p. 597-604, 1993.

GEORGE, E.F.; HALL, M.A.; DE KLERK, G.J. (eds.). **Plant Propagation by Tissue Culture**. Dordrecht, The Netherlands: Springer, 2008.

HURVICH, C.M.; TSAI, C-L. Regression and Time Series Model Selection in Small Samples. **Biometrika**, v. 76, p. 297-307.

JAMES, C. **Executive Summary of Global Status of Commercialized Biotech/GM Crops: 2016**. ISAAA Brief, 52. Ithaca, NY, 2016.

JONES, K.H.; SENFT, J.A. An Improved Method to Determine Cell Viability by Simultaneous Staining with Fluorescein Diacetate-Propidium Iodide. **The Journal of Histochemistry and Cytochemistry**, v. 33, p. 77-79, 1985.

MCCULLAGH, P.; NELDER, J.A. **Generalized Linear Models**, Second Edition, London: Chapman and Hall, 1989.

MOREL, G.; WETMORE, R.H. Fern callus tissue culture. **American Journal of Botany**, v. 38, n. 2, p.141-143, 1951.

MURASHIGE, T.; SKOOG, F. A revised medium for rapid growth and bio assays with tobacco tissue cultures. **Physiologia Plantarum**, v. 15, p. 473-497, 1962.

VASIL, L.K. Developing cell and tissue culture systems for the improvement of cereal and grass crops. **Journal of Plant Physiology**, v. 128, p. 193-218, 1987.

ZHONG, H.; SRINIVASAN, C.; STRICKLEN, M.B. In-vitro morphogenesis of corn (*Zea mays* L.). I. Differentiation of multiple shoot clumps and somatic embryos from shoot tips. **Planta**, v. 187, p. 483-489, 1992.

7. CAPÍTULO IV - INDUCTION OF SOMATIC EMBRYOGENESIS IN ROOT-DERIVED *IN VITRO* CULTURES OF TRANSGENIC MAIZE AG-5011YG (MON810) AND ITS CONVENTIONAL NEAR-ISOGENIC MAIZE AG-5011.

ABSTRACT

Plant genetic transformation processes may produce emergent properties beyond the intended genetic modification, possibly resulting in off-target effects that alter the transformed cell phenotype. In order to advance a previously established *in vitro* model for the study of off-target effects of plant transformation, this study aimed at inducing somatic embryogenesis using callus cultures derived from seedling root segments of a GM maize hybrid (Ag-5011YG) and its conventional near-isogenic hybrid (AG-5011) (NIH), comparing the two NIHs with regards to their embryogenic and overall morphogenic potential. Somatic embryogenesis was successfully induced and modulated by the combined effects of varying TDZ, ABA and glutathione concentrations in the culture medium, as well as by lighting conditions and the tested GM and conventional NIHs. It is noteworthy that by controlling these parameters, a strong rhizogenic determination of the selected model callus (Type III callus) was overcome, although embryos did not reach full maturity, nor any embryos were converted into plantlets as of yet. Overall, no significant differences were observed for embryogenic competence between the GM and conventional NIHs, although the GM NIH showed slightly better responses. Further investigations are necessary to precisely and effectively control somatic embryogenesis in the tested *in vitro* model, which was idealized and established as an alternative for the study of emergent properties of plant genetic transformation. The results presented here complement two previous investigations, which concerned the initiation and maintenance/proliferation, respectively, of *in vitro* cultures of commercial GM maize hybrid AG-5011YG (MON810) and its conventional near-isogenic hybrid AG-5011, bringing further evidence that the established interactive *in vitro* model is not only a valuable tool for the investigation of emergent properties of plant genetic transformation, but also relevant for maize developmental physiology studies.

7.1 INTRODUCTION

Maize (*Zea mays spp. mays*) GM event MON810 (Monsanto Company, YieldGard® maize, GM event MON810, unique identifier MON-ØØ81Ø-6 (CERA, 2016)) is a GM maize widely employed for the production of insect resistant GM maize hybrids (James, 2016; CERA, 2016). It was obtained by biolistic insertion of a recombinant genetically engineered construct (GEC) in the genome of highly *in vitro* regenerable maize hybrid Hi-II (a cross between inbred lines A188 and B73) (CERA, 2016). Amongst hundreds of commercial GM events, MON810 has the third highest number of regulatory approvals in the world (James, 2016).

Previously we reported the initiation (Chapter II) and maintenance/proliferation optimization (Chapter III) of *in vitro* cultures of GM maize hybrid AG-5011YG (event MON810) and its conventional near-isogenic hybrid (NIH) AG-5011. The established *in vitro* cultures were successfully employed as a model for the comparison of ontological and morphological endpoints between the two NIHs. Here, we report an investigation to try and induce somatic embryogenesis in the established cultures, comparing the NIHs over their embryogenic response to environmental stimuli, while attempting to re-determine the strongly rhizogenesis-determined calli (Type III maize calli) into an embryogenetic pathway.

Plant hormones, or more commonly their synthetic analogues, are used to regulate and control physiological processes in somatic cells derived from explants introduced *in vitro*, in order to initiate and maintain plant cell and tissue cultures (George *et al*., 2008). Known differences in the regenerative capacity of maize genotypes can be overcome by manipulation of growth regulator concentration in the culture medium (Vasil 1987; Zhong *et al.*, 1992).

The objective of this study was to evaluate somatic embryogenesis induction, number of somatic embryos per embryogenic callus, callus friability and rhizogenesis of a GM maize hybrid (AG-5011YG) and its conventional NIH (AG-5011), under the influence of culture lighting regime, ABA, TDZ and glutathione. The main hypotheses tested were: NIH (GM or conventional), ABA, culture lighting regime, TDZ concentration and glutathione affect somatic embryogenesis induction, number of somatic embryos, callus friability and rhizogenesis, either independently or in an interactive manner.

7.2 MATERIAL AND METHODS

7.2.1 Calli source

Previous to somatic embryogenesis experiments, friable, unorganized but rhizogenesis determined calli and cell clusters (Type III callus) derived from seedling root segments, of GM maize hybrid (AG-5011YG) and its conventional near-isogenic hybrid (AG-5011), were maintained in suspensions cultures based on MS salts (Murashige and Skoog, 1962), Morel vitamins (Morel and Wetmore, 1951), sucrose (3%), mannitol (2%), casein hydrolisate (200 mg/L), L-proline (10 mM), and 2,4-D (10 μM) (improved maintenance (IM) medium - modified from Emons *et al.* (1993), and based on previous results observed in this *in vitro* model (Capítulo III)), with subcultures every three-four weeks.

Type III maize callus was selected for maintenance and embryogenesis induction experiments due to the following features: abundance of explant source (plantlet roots), high induction frequency and maintenance/proliferation of callus of undifferentiated nature at 2,4-D concentrations above 10 µM for GM and conventional NIHs, and strong morphogenetic determination to rhizogenesis, making it interesting for studies about GM and conventional NIHs *in vitro* development and morphogenesis, as well as for general studies on somatic embryogenesis recalcitrance in maize tissues (Emons *et al.*, 1993).

7.2.2 Induction of somatic embryogenesis based on lighting regime, TDZ concentration and ABA

Type III calli derived from plantlet root segments were used in a multifactorial experiment to evaluate the combined effects of maize NIH, culture lighting regime, ABA and TDZ concentrations on somatic embryogenesis induction, number of somatic embryos, callus friability and rhizogenesis. Calli were inoculated in sterile plastic Petri dishes containing 25 ml IM medium free of mannitol and 2,4-D, supplemented with a higher sucrose dose (6%), and combinations of ABA (0 and 10 μM) and TDZ (0, 1 and 5 μM). Additionally, culture media treatments were crossed with two lighting conditions (24 h dark or 16 h light/8 h dark photoperiod, with light intensity of 60 $\mu mol.m^{-2}.s^{-1}$ from cool white fluorescent lamps). Cultures were kept at 25±2 ºC. All manipulations of cultures took place in aseptic conditions

in a laminar flow hood, using aseptic technique and sterilized tools and materials. After six weeks, induction of somatic embryogenesis (regarded as the existence of smooth, globular, club-like transition-stage, or early-coleoptilar structures (Clark and Sheridan, 1986)), number of embryos per embryogenic calli, callus friability and rhizogenic response were recorded using a stereomicroscope.

7.2.3 Optimization of somatic embryogenesis by supplementation of glutathione to 2iP- and ABA-containing medium

Type III calli maintained in suspension cultures with either IM medium or IM medium with reduced 2,4-D concentration (1 μM), were used in a factorial experiment to evaluate the potential of glutathione to improve somatic embryogenesis in the GM and conventional NIHs. Calli were inoculated in sterile plastic Petri dishes containing 25 ml IM medium free of mannitol and 2,4-D, and supplemented with sucrose (6%), ABA (10 μM) and TDZ (1 μM), with or without addition of glutathione (0 μM vs. 1000 μM). Cultures were kept at 25 ºC in the dark. After four weeks calli were inspected for induction of somatic embryogenesis (regarded as the existence of smooth, globular, club-like transition-stage, or early-coleoptilar structures (Clark and Sheridan, 1986)), number of embryo per embryogenic calli, callus friability and rhizogenic response, using a stereomicroscope.

7.2.4 Statistical Analysis

Data were analyzed in a generalized linear model framework (Mccullagh and Nelder, 1989; Bolker *et al.*, 2009). Data on embryogenesis induction were evaluated as binary variables (yes = 1; no = 0) and analyzed with logistic regression. Data on number of embryos per embryogenic callus were analyzed with Poisson regression. For every analysis, the initial statistical models included all explanatory variables, interactions, and quadratic terms for quantitative variables (e.g. TDZ concentration). Model selection was carried out by means of stepwise elimination of variables followed by inspection of the small sample-corrected Akaike Information Criterion (cAIC) (Hurvich and Tsai, 1989; Burnham and Anderson, 2004). Model assumptions about residual variance and distribution were evaluated graphically for all models, and the dispersion parameter - Chi-square/degrees of freedom - was additionally used to assess model fit, when applicable (Mccullagh and Nelder, 1989; Bolker *et al.*, 2009). Effects were considered significant when $P < 0.05$. Significant trend- and point-

wise differences were detected by comparison of 95% confidence intervals/envelopes (Cumming and Finch, 2005; Cumming *et al.*, 2007). Analyses were carried out in the R language/software (R Core Team, 2017).

7.3 RESULTS AND DISCUSSION

7.3.1 Effects of TDZ, ABA and lighting regime on somatic embryogenesis induction in a GM maize hybrid (AG-5011YG, MON810) and its conventional near-isogenic hybrid (AG-5011)

7.3.1.1 Somatic embryogenesis induction

Somatic embryogenesis was successfully induced in this experiment, which tested the combined effects of NIH, TDZ, ABA and lighting regime, although induction frequencies were mostly low, and embryo maturation was not accomplished (Figure 38). A significant three-way interaction was evidenced between ABA, lighting regime, and a quadratic term for TDZ concentration ($p=0.025$). This means that embryogenesis induction on both NIHs shows a curvilinear dose-response to TDZ concentration, but only in the presence of ABA and in the dark; otherwise TDZ does not seem to promote embryogenesis (Figures 39 and 40).

Previous studies on maize somatic embryogenesis found beneficial effects of ABA supplementation, indicating that this growth regulator is particularly important in preventing early root development in immature maize somatic embryos (Emons *et al*., 1993). Other studies showed the relevance of cytokinins in maize somatic embryogenesis (Vasil 1987; Zhong *et al.*, 1992), and TDZ was successfully employed to induce somatic embryogenesis in rice (Gairi & Rashid, 2004).

It should be noted, also, that due to a small number of embryogenic calli, and the lack of observations between 1 and 5 μM TDZ, there is substantial uncertainty related to the exact values of estimated curvilinear trends within this concentration range, as depicted by the enlarged confidence envelopes. Nonetheless, this is the first experiment within this thesis in which somatic embryos developed with consistency.

Figure 38: Representative maize somatic embryos formed on root-derived calli, in culture media containing sucrose (6%), ABA (10 μM) and TDZ (1 μM), with 24 h darkness lighting regime.

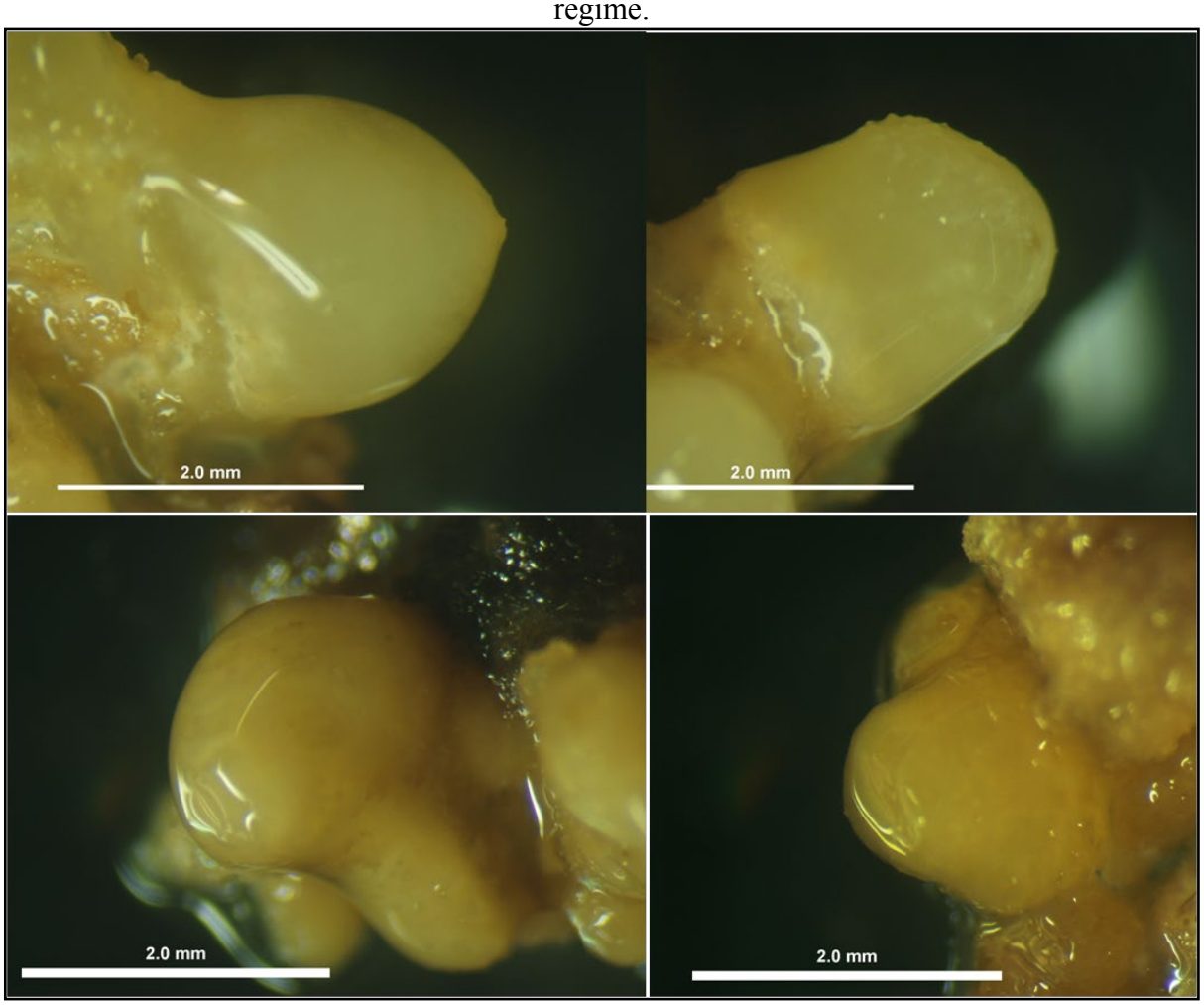

Fonte: Daniel Ferreira Holderbaum (2019).

Figure 39: Trends of somatic embryogenesis induction frequency on root-derived calli of a GM maize hybrid (AG-5011YG - GM, solid line, black dot) and its conventional near-isogenic hybrid (AG-5011 - NM, dashed line, black triangle), in culture media supplemented with a range of TDZ concentrations (0, 1 and 5 μM), abscisic acid (ABA, 0 or 10 μM), and cultured in 24 h darkness (Escuro) or 18 h light/6 h dark photoperiod (Luz). Lines depict estimated trends, shaded bands indicate 95% confidence envelopes, and dots and triangles represent observations (dislocated vertically and horizontally to diminish overlap).

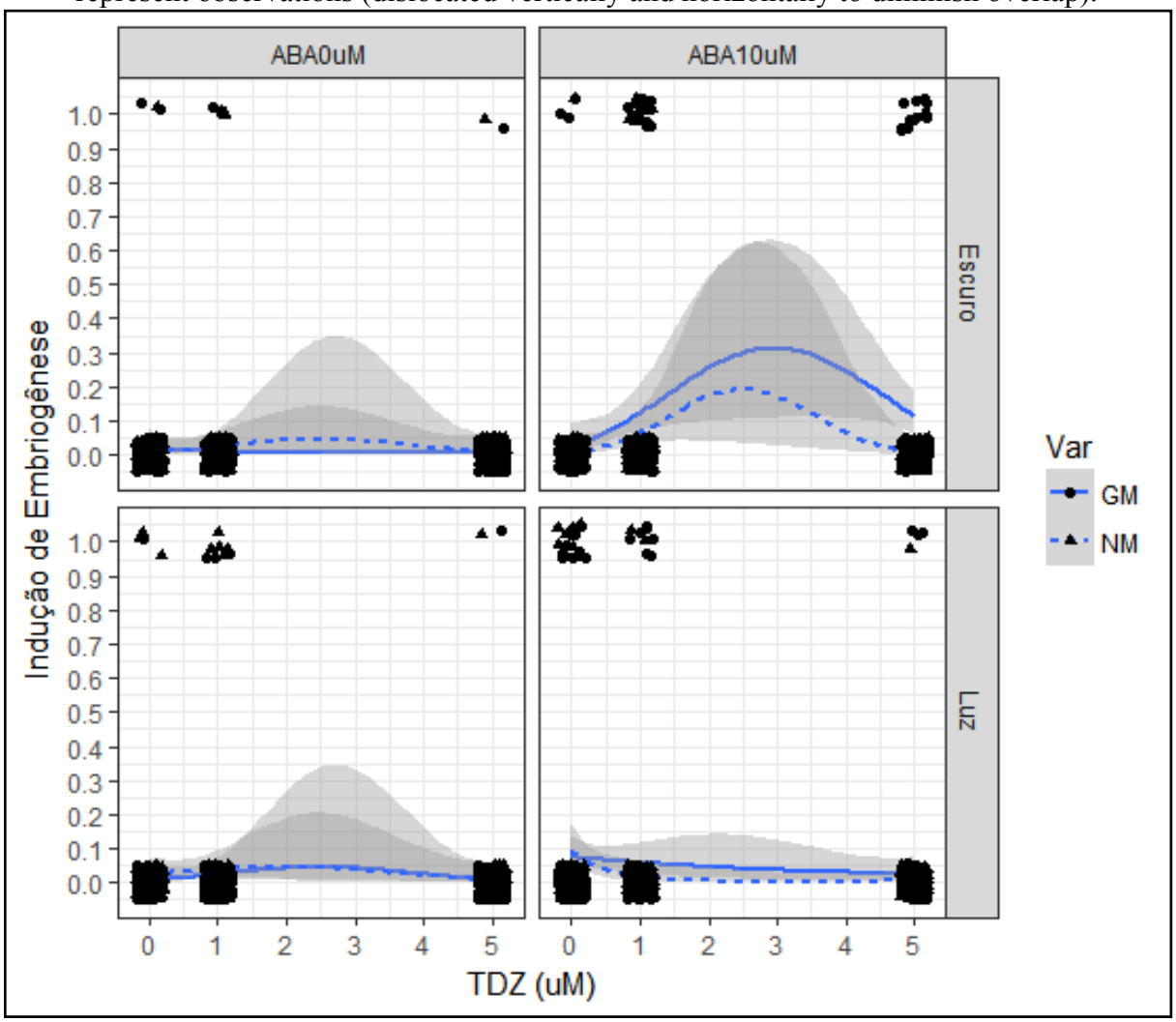

Fonte: Daniel Ferreira Holderbaum (2019).

Figure 40: Trends of somatic embryogenesis induction frequency in culture media supplemented with a range of TDZ concentrations (0, 1 and 5 μM), abscisic acid (ABA, 0 μM - solid line, black dot - or 10 μM - dashed line, black triangle), and cultured in 24 h darkness (Escuro) or 16 h light/8 h dark photoperiod (Luz). Lines depict estimated trends, which are averaged between the two tested NIHs; shaded bands indicate 95% confidence envelopes, and black dots and triangles represent observations (dislocated vertically and horizontally to diminish overlap).

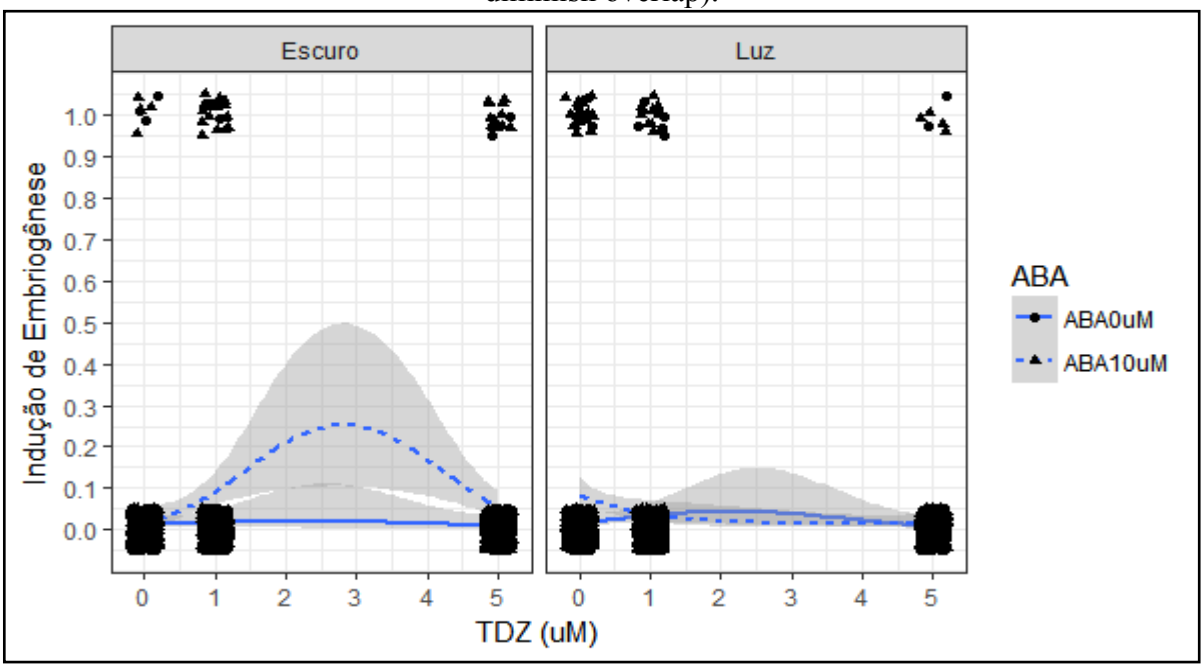

Fonte: Daniel Ferreira Holderbaum (2019).

7.3.1.2 Embryo count

For embryo count, or the number of embryos per embryogenic calli, a significant three-way interaction was evidenced between NIH, ABA and lighting regime (p=0.011), as well as an interaction between ABA and a quadratic term for TDZ (p=0.027). In other words, the number of embryos per embryogenic calli was significantly increased by supplementation of the culture media with 10 μM ABA, but only in cultures kept in the dark and in the GM NIH (Figure 41). Also, the number of embryos showed a curvilinear dose-response to TDZ only in the presence of ABA (Figure 42).

Figure 41: Trends for number of embryos per embryogenic calli, obtained from root-derived calli of a GM maize hybrid (AG-5011YG - GM, solid line, black dot) and its conventional near-isogenic hybrid (AG-5011 - NM, dashed line, black triangle), in culture media supplemented with a range of TDZ concentrations (0, 1 and 5 μM), abscisic acid (ABA, 0 or 10 μM), and cultured in 24 h darkness (Escuro) or 18 h light/6 h dark photoperiod (Luz). Lines depict estimated trends, shaded bands indicate 95% confidence envelopes, and black dots and triangles represent observations (dislocated horizontally to diminish overlap).

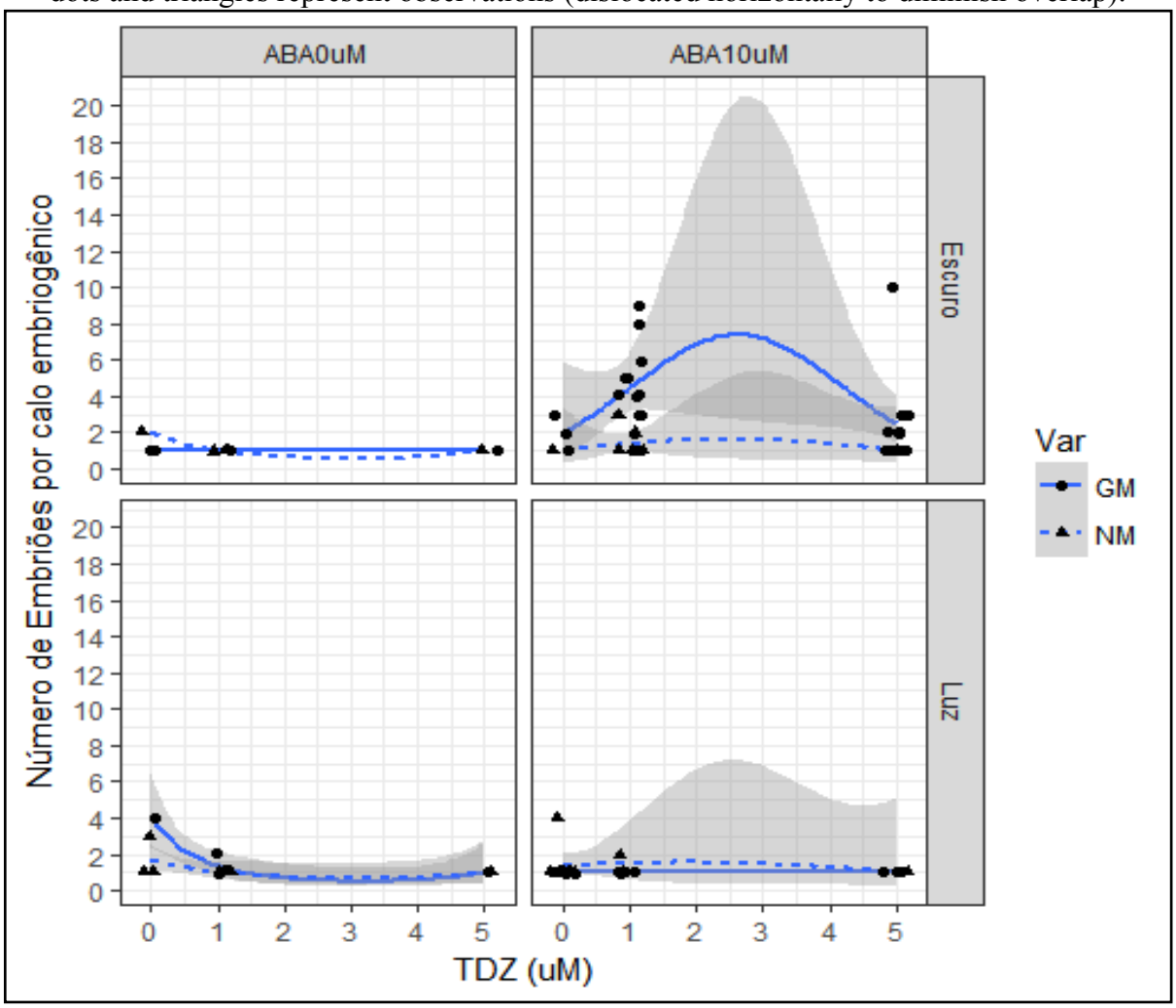

Fonte: Daniel Ferreira Holderbaum (2019).

Figure 42: Trends for number of somatic embryos per embryogenic calli in culture media supplemented with a range of TDZ concentrations (0, 1 and 5 μM), and abscisic acid (ABA, 0 μM (solid line, black dot) or 10 μM (dashed line, black triangle)). Trends are averaged between near-isogenic hybrids and lighting conditions. Lines depict estimated trends, shaded bands indicate 95% confidence envelopes, and black dots and triangles represent observations (dislocated horizontally to diminish overlap).

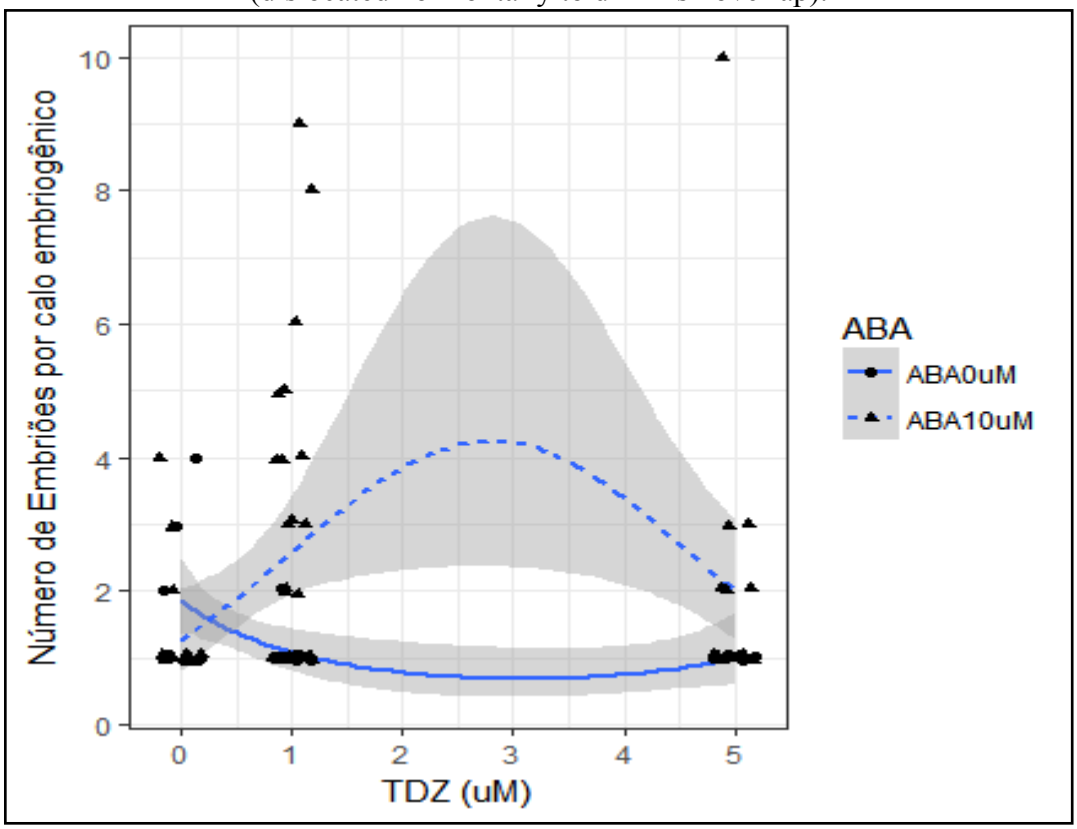

Fonte: Daniel Ferreira Holderbaum (2019).

7.3.1.3 Callus friability

The frequency of friable calli was influenced by TDZ concentration ($p<0.031$), in a linear decreasing trend along increasing TDZ concentration. Additionally, NIH showed a significant effect ($p=0.042$), with the conventional hybrid presenting significantly more friable calli than the GM hybrid across the TDZ gradient (Figure 43). It should be noted that the frequency of friable calli in this experiment (~8% to ~18%) is quite low compared to induction and maintenance conditions. Furthermore, we observed embryogenic calli, in general, are not friable, but more structured and with smoother surface.

Figure 43: Trends for frequency of friable calli of GM maize hybrid (AG-5011YG - GM, solid line) and its conventional near-isogenic hybrid (AG-5011 - NM, dashed line), in culture media supplemented with a range of TDZ concentrations (0, 1 and 5 μM). Trends are averaged between tested abscisic acid and lighting conditions. Lines depict estimated trends and shaded bands indicate 95% confidence envelopes.

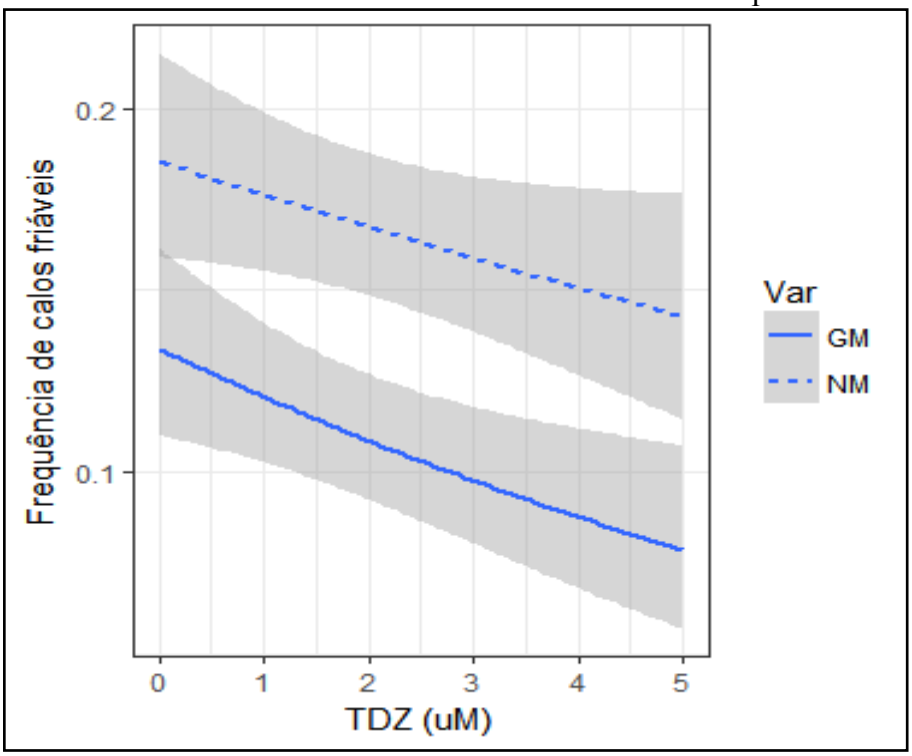

Fonte: Daniel Ferreira Holderbaum (2019).

7.3.1.4 Rhizogenesis

Rhizogenesis was significantly affected by all four tested factors, with evidence for a significant four-way interaction between NIH, ABA, TDZ and lighting regime (p=0.024) (Figure 44). Overall, TDZ has the effect of reducing rhizogenesis in a linear fashion when in combination with ABA, and in a curvilinear fashion in the absence of ABA in the culture medium. Furthermore, there are substantial differences in rhizogenesis between the GM and conventional NIHs in media free of ABA, particularly when cultures are exposed to light, but these differences become smaller or disappear altogether in the presence of ABA.

Besides well known developmental inhibitory effects of ABA, previous studies have shown TDZ's inhibitory effect on maize root growth (Devlin *et al.*, 1989), what is in agreement with results observed in this study.

Figure 44: Trends for frequency of rhizogenesis in root-derived calli of a GM maize hybrid (AG-5011YG - GM, solid line, black dot) and its conventional near-isogenic hybrid (AG-5011 - NM, dashed line, black triangle), in culture media supplemented with a range of TDZ concentrations (0, 1 and 5 μM), abscisic acid (ABA, 0 or 10 μM), and cultured in 24 h darkness (Escuro) or 18 h light/6 h dark (Luz). Lines depict estimated trends and shaded bands indicate 95% confidence envelopes.

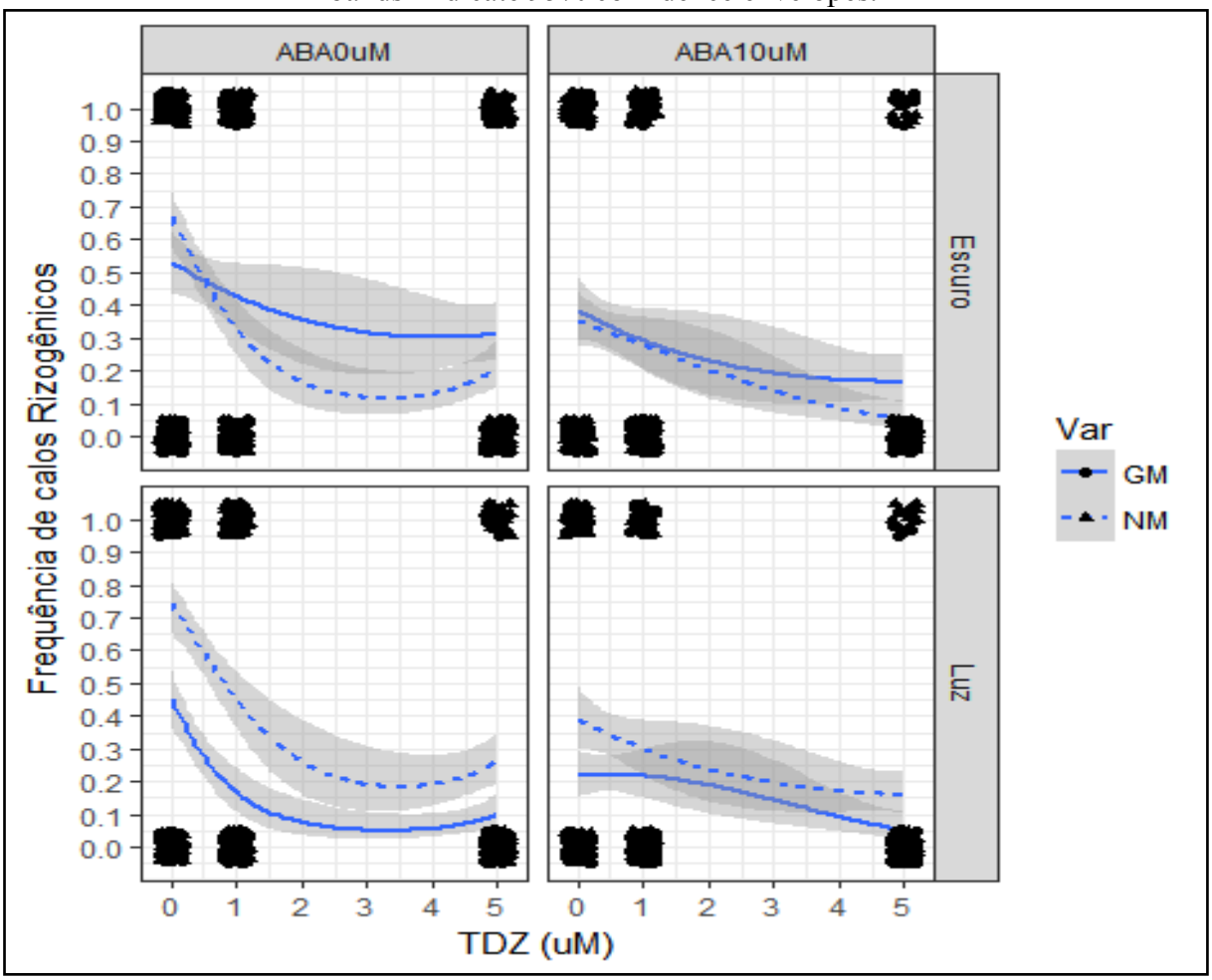

Fonte: Daniel Ferreira Holderbaum (2019).

7.3.2 Glutathione is synergic to TDZ and ABA in stimulating somatic embryogenesis in a GM maize hybrid (AG-5011YG, MON810) and its conventional near-isogenic hybrid (AG-5011)

7.3.2.1 Somatic embryogenesis induction

Embryogenic calli were observed in media with and without glutathione (1000 μM) (Figure 45), but the combination of TDZ (1 μM), ABA (10 μM) and Glutathione (1000 μM) significantly increased the frequency of embryogenic calli in comparison to the medium free of glutathione ($p<0.001$) (Figures 46 and 47).

Figure 45: Maize embryogenic callus induced in culture medium supplemented with glutathione (1000 μM) (A), and without glutathione (B).

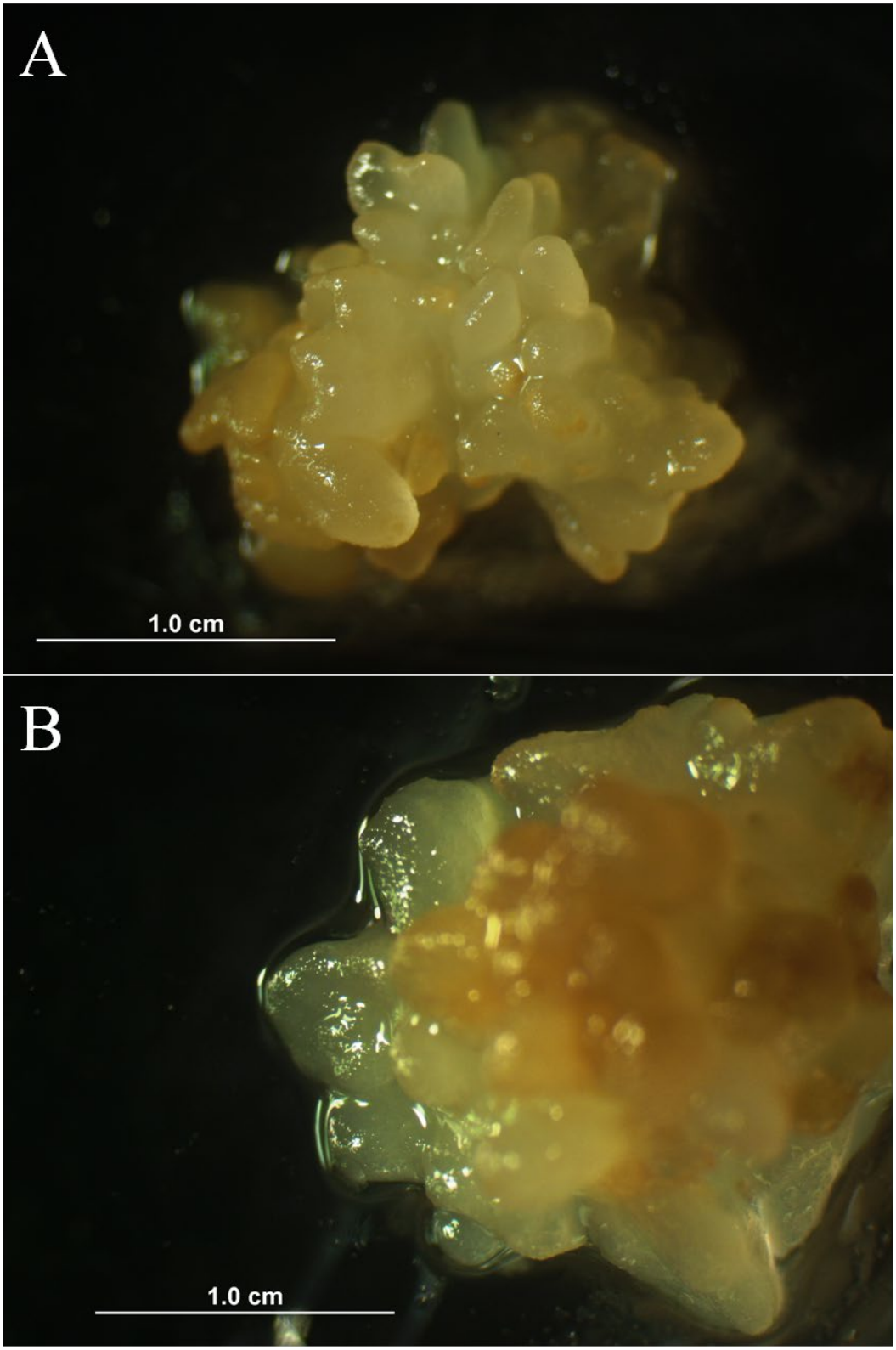

Fonte: Daniel Ferreira Holderbaum (2019).

Figure 46: Frequency of somatic embryogenesis in root-derived calli of a GM maize hybrid (AG-5011YG - GM) and its conventional near-isogenic hybrid (AG-5011 - NM), subcultured from two different maintenance media (M - IM medium with reduced 2,4-D (1 μM); P - regular IM medium, with 10 μM 2,4-D), to IM media free of mannitol and 2,4-D, and supplemented with sucrose (6%), thidiazuron (TDZ, 1 μM) and abscisic acid (ABA, 10 μM), combined with 0 μM or 1000 μM glutathione (GLU). Dots and triangles represent means, error bars represent 95% confidence intervals.

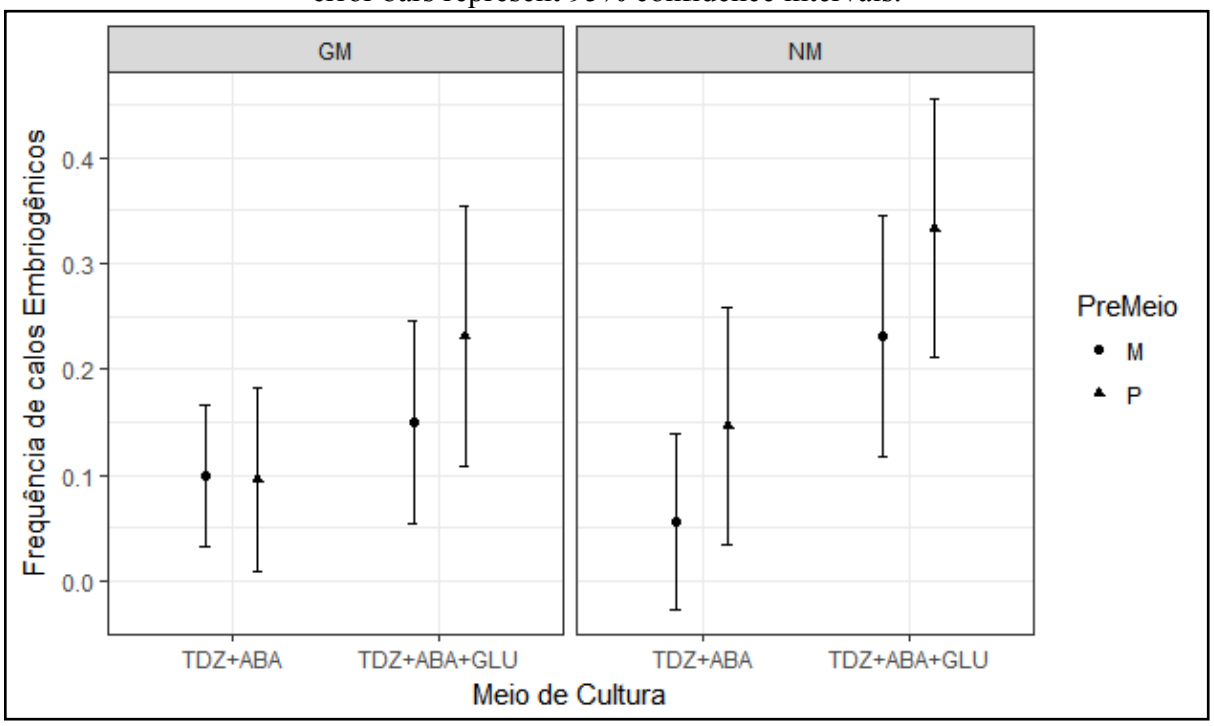

Fonte: Daniel Ferreira Holderbaum (2019).

Also, there is marginal evidence (p=0.067) that transferring calli from a maintenance medium with medium-high 2,4-D concentration (10 μM) to the embryogenic medium is more advantageous than transferring calli from maintenance medium with low 2,4-D levels (1 μM) (Figure 47).

Glutathione exists in reduced (GSH) and oxidized (GSSG) states. GSH has been successfully employed to improve somatic embryogenesis in different plant species, being a thiol tripeptide involved in cell division and differentiation (Belmonte *et al.*, 2005; Caprestano *et al.*, 2015). When added to culture medium, GSH creates a reduced state favoring cell proliferation and early somatic embryogenesis (Stasolla, 2010), what is corroborated by results obtained for maize in this study.

Figure 47: Frequency of somatic embryogenesis in root-derived calli cultured in IM media free of mannitol and 2,4-D, and supplemented with sucrose (6%), thidiazuron (TDZ, 1 μM) and abscisic acid (ABA, 10 μM), combined with 0 μM or 1000 μM glutathione (GLU), averaged for all conditions of NIH and previous culture media. Dots represent means, error bars represent 95% confidence intervals.

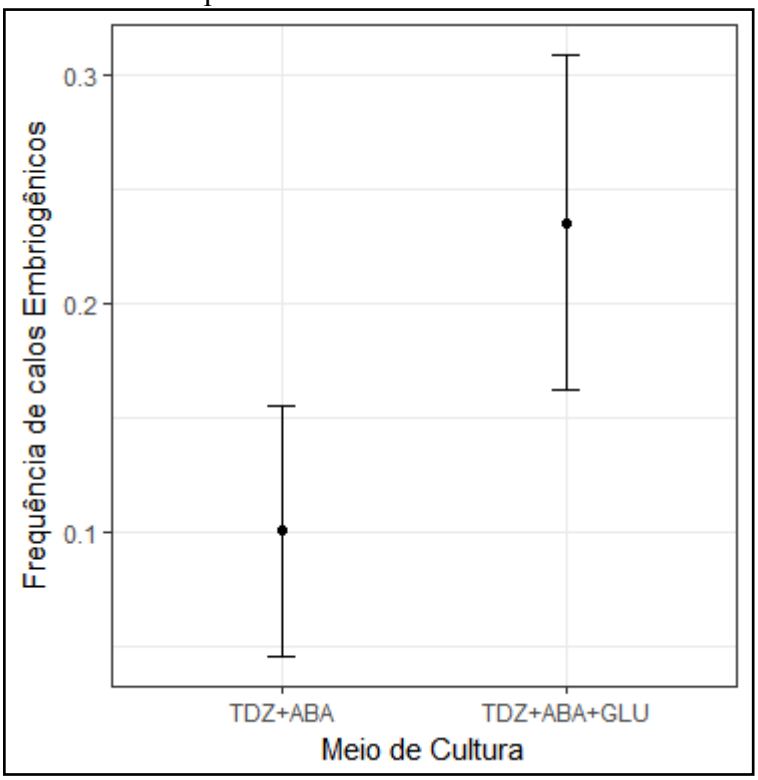

Fonte: Daniel Ferreira Holderbaum (2019).

7.3.2.2 Embryo count

For the number of embryos per embryogenic calli, no significant effects were evidenced for any of the tested factors or their interactions (Figure 48). A marginally significant interaction was observed between NIH and pre-medium (the maintenance medium from which calli were transferred to embryogenesis media - maintenance media supplemented with either 1 or 10 μM 2,4-D), suggesting that 2,4-D levels on maintenance medium might have a residual effect that plays a role in somatic embryogenesis, particularly if there is no auxin in the embryogenesis medium, as was the case in this experiment.

Figure 48: Number of embryos per embryogenic calli, in root-derived calli of a GM maize hybrid (AG-5011YG - GM) and its conventional near-isogenic hybrid (AG-5011 - NM), subcultured from two different maintenance media (M - IM medium with reduced 2,4-D (1 *μM)*; P - regular IM medium, with 10 *μM* 2,4-D), to IM media free of mannitol and 2,4-D, and supplemented with sucrose (6%), thidiazuron (TDZ, 1 *μM*) and abscisic acid (ABA, 10 *μM*), combined with glutathione (GLU) concentrations of 0 *μM* (TDZ+ABA) or 1000 *μM* (TDZ+ABA+GLU). Dots and triangles represent means, error bars represent 95% confidence intervals.

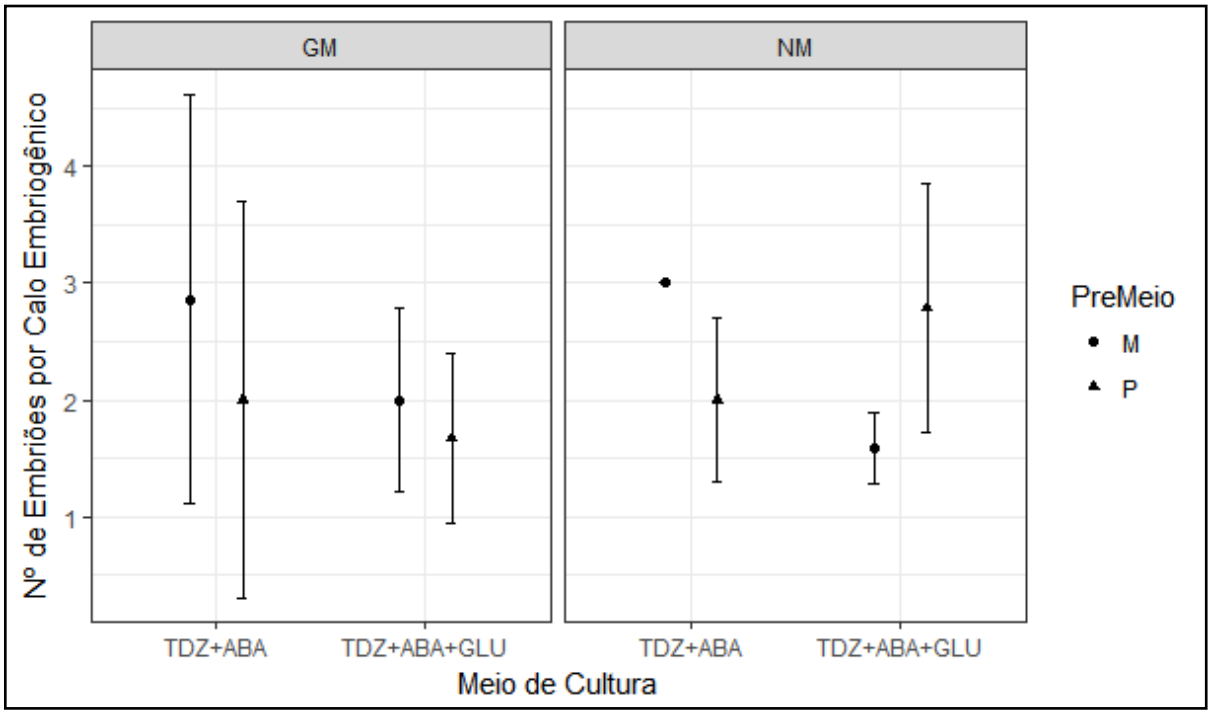

Fonte: Daniel Ferreira Holderbaum (2019).

7.4 CONCLUSIONS

This study reports the first documented experimental effort to induce somatic embryogenesis using callus cultures of a GM maize hybrid and its conventional NIH, comparing the two NIHs with regards to their embryogenic and overall morphogenic potential. Somatic embryogenesis was successfully induced and modulated by the combined effects of lighting regime, TDZ, ABA and glutathione in the culture medium, and it was also influenced by the tested GM and conventional NIHs. The best conditions for somatic embryogenesis induction in the evaluated calli include incubation in complete darkness (light strongly suppresses embryogenesis in all tested conditions and treatments), and supplementation of IM medium free of mannitol and 2,4-D with extra sucrose (6%), TDZ (1 µM), ABA (10 µM) and glutathione (1000 µM). It is worth noting that by controlling these parameters, a strong rhizogenic determination of the selected model callus (Type III maize callus) was overcome and permitted induction of somatic embryogenesis, although embryos

did not reach full maturity, nor any embryos were converted into plantlets. Additional studies are necessary to fine-tune concentrations of sucrose, TDZ, ABA, and glutathione in somatic embryogenesis medium, in order to optimize somatic embryogenesis induction and maturation in the tested maize *in vitro* model. The results presented here complement two previous investigations, which concerned the initiation (Capítulo II) and maintenance/proliferation (Capítulo III) of *in vitro* cultures of the commercial GM maize hybrid AG-5011YG (MON810) and its conventional near-isogenic hybrid AG-5011, expanding the developed *in vitro* culture model for investigation of emergent properties in genetically modified plants.

REFERENCES

BELMONTE, M.F.; DONALD, G.; REID, D.M. YEUNG, E.C.; STASOLLA; C. Alterations of the glutathione redox state improve apical meristem structure and somatic embryo quality in white spruce (Picea glauca). **Journal of Experimental Botany**, v. 56, n. 419, p. 2355-2364, 2005.

BOLKER, B.M.; BROOKS, M.E.; CLARK, C.J.; GEANGE, S.W.; POULSEN, J.R.; STEVENS, M.H.H.; WHITE, J.S.S. Generalized linear mixed models: A practical guide for ecology and evolution. **Trends Ecol. Evol.**, v. 24, p. 127-135, 2009.

BURNHAM, K.P.; ANDERSON, D.R. Multimodel inference: understanding AIC and BIC in model selection. **Sociological Methods & Research**, v. 33, p. 261-304, 2004. Disponível em: https://doi.org/10.1177/0049124104268644.

CAPRESTANO, C.A.; GUERRA, M.P.; WINKELMANN, T. Effect of glutathione on the early differentiation of Cyclamen persicum somatic embryos. **DGG-Proceedings**, v. 5, p. 12-5, 2015.

CERA, Center for Environmental Risk Assessment. **GM Crop Database, MON-ØØ81Ø-6 (MON810)**. ILSI Research Foundation, Washington D.C., 2016. Disponível em: http://cera-gmc.org/GmCropDatabaseEvent/MON810/short. Acesso em: 03 dez. 2016.

CLARK, J.K.; SHERIDAN, W.F. Developmental profiles of the maize embryo-lethal mutants *dek22* and *dek23*. **The Journal of Heredity**, v. 77, p. 83-92, 1986.

CUMMING, G.; FINCH, S. Inference by eye: Confidence intervals, and how to read pictures of data. **American Psychologist**, v. 60, p. 170-180, 2005.

CUMMING, G.; FIDLER, F.; VAUX, D.L. Error bars in experimental biology. **Journal of Cell Biology**, v. 177, p. 7-11, 2007. Disponível em: http://doi.org/10.1083/jcb.200611141.

DEVLIN, R.M.; ZBIEC, I.L.; NOWICKA, S.E. The effect of TDZ on some plant growth systems. **Proc. Plant Growth Regul. Soc.**, v. 16, p. 99-103, 1989.

EMONS, A.M.C.; SAMALLO-DROPPERS, A.; VAN DER TOOM, C. The influence of sucrose, mannitol. L-proline, abscisic acid and gibberellic acid on the maturation of somatic embryos of *Zea mays* L. from suspension cultures. **Plant Physiol.**, v. 142, p. 597-604, 1993.

GAIRI, A.; RASHID, A. TDZ-induced somatic embryogenesis in non-responsive caryopses of rice using a short treatment with 2,4-D. **Plant Cell, Tissue and Organ Culture**. v. 76:, n. 1, p. 29-33, 2004. Disponível em: https://doi.org/10.1023/A:1025864605846.

GEORGE, E.F.; HALL, M.A.; DE KLERK, G.J. (eds.). **Plant Propagation by Tissue Culture**. Dordrecht, The Netherlands: Springer, 2008.

HURVICH, C.M.; TSAI, C-L. Regression and Time Series Model Selection in Small Samples. **Biometrika**, v. 76, p. 297-307.

JAMES, C. **Executive Summary of Global Status of Commercialized Biotech/GM Crops: 2016**. ISAAA Brief, 52. Ithaca, NY, 2016.

MOREL, G.; WETMORE, R.H. Fern callus tissue culture. **American Journal of Botany**, v. 38, n. 2, p.141-143, 1951.

MURASHIGE, T.; SKOOG, F. A revised medium for rapid growth and bio assays with tobacco tissue cultures. **Physiologia Plantarum**, v. 15, p. 473-497, 1962.

STASOLLA, C. Glutathione redox regulation of *in vitro* embryogenesis. **Plant Physiology and Biochemistry**, v. 48, n. 5, p. 319-327, 2010.

VASIL, L.K. Developing cell and tissue culture systems for the improvement of cereal and grass crops. **Journal of Plant Physiology**, v. 128, p. 193-218, 1987.

ZHONG, H.; SRINIVASAN, C.; STRICKLEN, M.B. In-vitro morphogenesis of corn (*Zea mays* L.). I. Differentiation of multiple shoot clumps and somatic embryos from shoot tips. **Planta**, v. 187, p. 483-489, 1992.

8. CAPÍTULO V - COMPARISON OF HISTOCHEMICAL FEATURES AND PROTEOMIC PROFILES OF *IN VITRO* CULTURED CALLI OF A TRANSGENIC MAIZE (EVENT MON810) AND ITS CONVENTIONAL NEAR-ISOGENIC COUNTERPART

ABSTRACT

In order to establish an interactive model for the screening of emergent properties of plant genetic transformation, we previously initiated and maintained *in vitro* cultures of GM hybrid AG-5011YG (event MON810) and its conventional near-isogenic hybrid AG-5011, considering that an *in vitro* model would have good qualities of environmental control, reproducibility and scalability. Here, we apply the established *in vitro* model to investigate unintended changes in histochemical features and proteomic profile of a transgenic maize hybrid maintained *in vitro*, as compared to the conventional near-isogenic hybrid maintained in the same conditions. Marked histochemical differences were detected between the tested NIHs, and 197 proteins showed significant ($p<0.05$) differential regulation, with 106 down-regulated proteins (ranging from 0.66 to 0.03 fold-change), 90 up-regulated proteins (ranging from 1.5 to 9.3 fold-change), and one unique protein in the GM maize. The observed off-target effects include complex differential regulation of multiple proteins associated to several biological processes, molecular functions, and cellular components, most notably carbohydrate and energy metabolism, macromolecule metabolism, stress responses and responses to stimulus, growth regulator biosynthesis, cell growth and plant morphogenesis. Additionally, tryptophan, glutathione, AIA and ABA biosynthesis-related proteins presented evidence of significant differential regulation, allowing for the establishment of a causal link between the differential proteomic regulation and previously observed altered responses of the GM NIH to growth regulators *in vitro*. Furthermore, the presence of an exclusive MAPKKK-like protein in the GM maize proteome fosters the hypothesis that, not only the constitutive expression of recombinant Cry1Ab protein in the GM maize represents additional metabolic costs, it may also induce immune responses in the transgenic plant that were unaccounted for until now. These findings strongly suggest the occurrence of emergent properties derived from the integration and expression of MON810 recombinant gene construct in the GM maize.

8.1 INTRODUCTION

Plant transformation arises from the joint application of recombinant DNA (rDNA) technology and plant tissue culture techniques, which are implemented to obtain genetically modified (GM) plants. It represents a useful tool in plant research, and holds great promise in plant breeding, but so far, GM plants remain a controversial topic worldwide.

Maize (*Zea mays spp. mays*) GM event MON810 (Monsanto Company, YieldGard® maize, unique identifier MON-ØØ81Ø-6 (CERA, 2016)) is a GM maize event widely employed for the production of insect resistant GM maize hybrids (James, 2016; CERA, 2016). It was obtained by biolistic insertion of a recombinant gene expression cassette in the genome of highly *in vitro* regenerable maize hybrid Hi-II (CERA, 2016). MON810 recombinant construct contains the Cauliflower Mosaic-Virus (CaMV) 35S promoter, a maize *hsp70* (*heat shock protein70*) intron, and a truncated *Bacillus thuringiensis* (Bt) *cry1Ab* gene that codes for the insecticidal δ-endotoxin Cry1Ab; the *nopaline synthase* termination sequence was part of the original designed construct, but was lost in a truncation event during the construct's insertion into HI-II maize genome (Rosati *et al.*, 2008; CERA, 2016).

Before approval for cultivation and commercialization, normally a new GM event must undergo a risk assessment where not only the recombinant construct integration, stability and expression must be demonstrated, but also possible genetic and phenotypic unintended effects must be evaluated, in comparison to the most similar conventional counterpart available (Bartsch *et al.*, 2010). For maize, the appropriate comparators are near-isogenic lines (NILs) (Cellini *et al.*, 2004), and, in the specific case of maize hybrids, near-isogenic hybrids.

NILs are obtained by initially crossing two contrasting lines for a target locus (i.e. a recombinant construct) and then consecutively backcrossing the progeny with the receptor parental line, until the target locus is introgressed; thus, after 6-8 backcrossings, the genotype of produced seeds will be more than 99% similar to the backcrossed parental line, and additionally contain the target locus. NILs are defined as two or more homozygous lines that share the same genetic makeup except for one selected locus, and possibly a few additional loci genetically linked to the target locus (Zeven and Waninge, 1986). Likewise, the production of near-isogenic GM and conventional maize hybrids demands the previous production of GM and conventional NILs, so that crosses between GM NILs produce GM NIHs, and the cross between conventional NILs produces conventional hybrids.

Based on this premise, the objective of this study was to apply a previously established interactive *in vitro* model to investigate unintended changes, or emergent properties, in histochemical features and proteomic profile of a transgenic maize (AG-5011YG) maintained *in vitro*, as compared to the conventional near-isogenic hybrid (AG-5011) maintained in the same conditions.

8.2 MATERIAL AND METHODS

8.2.1 Calli source culture medium and in vitro experimental practices

Friable, rhizogenesis determined calli (Type III) (Emons *et al.*, 1993) of GM maize hybrid (AG-5011YG) and its conventional NIH (AG-5011), previously established *in vitro* using seedling root segments as explants (Chapter II), were maintained in culture medium based on MS salts (Murashige and Skoog, 1962), Morel vitamins (Morel and Wetmore, 1951), sucrose (3%), mannitol (2%), casein hydrolisate (200 mg/L), L-proline (10 mM), and 2,4-D (20 μM) - maintenance medium (Capítulo III) - for several subcultures, and used in the experiment herein described. All manipulations of cultures took place in aseptic conditions in a laminar flow hood, using aseptic technique and sterilized tools and materials. Callus samples from both hybrids were periodically tested for Cry1Ab presence using a lateral flow strip kit for detection of Cry1Ab protein (Envirologix Quickstix AS-003-CRLS kit).

8.2.3 Reduction of 2,4-D concentration in culture medium and callus sample collection

Prior to histochemical and proteomic analyses, calli growing in maintenance medium were transferred to sterile plastic Petri dishes containing 25 ml maintenance medium with reduced 2,4-D (2 μM), and subcultured 3 times on the same medium, at 25 ºC in the dark. At the end of the third subculture three biological samples of 200 mg of calli from GM and conventional NIHs were collected in liquid nitrogen and then frozen at -70 ºC until total protein extraction. Three additional callus samples of each NIH were collected and prepared for histochemical analyses.

8.2.4 Histochemistry

Friable, morphologically similar calli from GM and conventional NIHs grown in medium with 2 μM 2,4-D for 3 subcultures, were sampled to assess histochemical features. Histological preparations and histochemical procedures were carried out based on Steiner *et al.* (2015). Callus samples were fixed by vacuum infiltration of paraformaldehyde (2,5 %) in sodium phosphate buffer (0.1 M, pH 7.2) for 24 h. After vacuum infiltration samples were washed thrice with phosphate buffer (0.1 M, pH 7.2) for 30 min, and then dehydrated in a gradual ethylic series (30%, 50%, 70%, 90% and 100%), with three 15 min immersions in each solution. Sample pre-infiltration was initially carried out in a 1:1 solution of 100% ethanol:historesine (Leica, Heidelberg, Germany) for 12 h; subsequently, samples were infiltrated in pure historesine for 24 h. Inclusion was carried out for 24 h at room temperature using historesine supplemented with polymerizer (Leica, Heidelberg, Germany) (Gerrits and Smid, 1983). Longitudinal and transversal sections (5 μm) were obtained in a RM 2135 rotating microtome (Leica, Nussloch, Germany) with tungsten blades, and placed on glass slides with a drop of water, kept over a heating plate (40 ºC). Specimens were stained with 0.5 % toluidine blue (TB-O) (O'Brien *et al.*, 1964) to identify phenols and acidic polysaccharides. An acidified ethanolic solution containing 0.4 % Coomassie Brilliant Blue (CBB) was used to stain total proteins (Fisher, 1968); Periodic acid-Schiff stain (PAS) was used to stain neutral polysaccharides (Gahan, 1984). Permanent glass slides were mounted using Canada Balsam and glass cover slips. Images were captured with a DM500 microscope (Leica) attached to a OPTHD 14mp photomicrography system.

8.2.5 Total Protein Extraction

For total protein extraction, a previously described protocol was used (Balbuena *et al.*., 2011). The extraction buffer consisted of 7 M urea, 2 M thiourea, 2% triton X-100, 1% dithiothreitol (DTT), 1 mM phenylmethanesulfonyl fluoride (PMSF), and 5 μM pepstatin. Three biological samples (200 mg FW each sample) were pulverized in liquid nitrogen, using a mortar and pestle. Then, in microtubes, 1 mL of extraction buffer was added to the sample powder. Samples were vortexed and incubated on ice for 30 min, followed by centrifugation at 16,000 g for 20 min at 4 °C. The supernatants were collected, and protein concentration was measured using a 2-D Quant Kit (GE Healthcare, Piscataway, NJ, USA).

8.2.6 Protein digestion

Before the trypsin digestion step, pooled samples were desalted on 5000 MWCO Vivaspin 500 membranes (GE Healthcare, UK) using 50 mM ammonium bicarbonate (Sigma-Aldrich) pH 8.5, as buffer. Membranes were filled to maximum capacity with ammonium bicarbonate and centrifuged at 15,000 g for 20 min at 8 °C. This procedure was repeated at least three times, resulting in approximately 50 µL per sample. The methodology used for protein digestion was as previously described (Calderan-Rodriguez *et al.*, 2014). For each sample, 25 µL of 0.2% (v/v) RapiGest® (Waters, Milford, CT, USA) was added, and samples were briefly vortexed and incubated in an Eppendorf Thermomixer® at 80 °C for 15 min. Then, 2.5 µL of 100 mM DTT (Bio-Rad Laboratories, Hercules, CA, USA) was added, and the tubes were vortexed and incubated at 60 °C for 30 min under agitation. Next, 2.5 µL of 300 mM iodoacetamide (GE Healthcare) was added, and the samples were vortexed and then incubated in the dark for 30 min at room temperature. The digestion was performed by adding 20 µL of trypsin solution (50 ng/µL; V5111, Promega, Madison, WI, USA) prepared in 50 mM ammonium bicarbonate, and samples were incubated at 37 °C overnight. For RapiGest® precipitation, 10 µL of 5% (v/v) trifluoroacetic acid (TFA, Sigma-Aldrich) was added and incubated at 37 °C for 90 min, followed by a centrifugation step of 30 min at 16,000 g. Samples were the transferred to Total Recovery Vials (Waters).

8.2.7 Protein Mass spectrometry analysis

A nanoAcquity UPLC connected to a Synapt G2-Si HDMS mass spectrometer (Waters, Manchester, UK) was used for ESI-LC-MS/MS analysis. The chromatography step was performed by injecting 1 µL of digested samples to normalize them before the relative quantification of proteins. To ensure standardized molar values for all conditions, normalization among samples was based on stoichiometric measurements of total ion counts of scouting runs prior to analyses. Runs consisted of three technical replicates per pooled sample. During separation, samples were loaded onto the nanoAcquity UPLC 5 µm C18 trap column (180 µm × 20 mm) at 5 µL/min during 3 min and then onto the nanoAcquity HSS T3 1.8 µm analytical reversed phase column (100 µm × 100 mm) at 600 nL/min, with a column temperature of 60 °C. For peptide elution, a binary gradient was used, with mobile phase A

consisting of water (Tedia, Fairfield, Ohio, USA) and 0.1% formic acid (Sigma-Aldrich) and mobile phase B consisting of acetonitrile (Sigma-Aldrich) and 0.1% formic acid. Gradient elution started at 7% B and was held for 3 min, then ramped from 7% B to 40% B up to 90.09 min, and from 40% B to 85% B until 94.09 min, being maintained at 85% until 98.09 min, then decreasing to 7% B until 100.09 min and kept at 7% B until the end of experiment at 108.09 min. Mass spectrometry was performed in positive and resolution mode (V mode), 35,000 FWHM, with ion mobility, and in data-independent acquisition (DIA) mode; IMS wave velocity was set to 600 m/s; the transfer collision energy ramped from 19 V to 45 V in high-energy mode; cone and capillary voltages of 30 V and 2800 V, respectively; and a source temperature of 70 °C. In TOF parameters, the scan time was set to 0.5 s in continuum mode with a mass range of 50 to 2000 Da. The human [Glu1]-fibrinopeptide B (Sigma-Aldrich) at 100 fmol/μL was used as an external calibrant and lock mass acquisition was performed every 30 s.

8.2.8 Gene Ontology Enrichment Analysis

Down-regulated accessions and up-regulated accessions were used to extract peptide sequences with FaBox 1.4.1 FASTA sequence extractor (http://users-birc.au.dk/biopv/php/fabox/fasta_extractor.php). Then, the obtained FASTA files with peptide sequences were imported to OmicsBox 1.1.164 and enrichment analysis carried out according to the recommended workflow for Gene Ontology Annotation. Gene ontology graphs and charts were produced in OmicsBox 1.1.164. The Sequence Filter, Nodescore Filter and Nodescore Alpha parameters were tuned to obtain simplified gene ontologies while retaining relevant information, following the software's user manual recommendations.

8.2.9 Statistical Analysis

T-tests were employed to compare the GM and conventional hybrids with regards to protein levels, and comparisons with $p < 0.05$ were considered significant.

8.3 RESULTS AND DISCUSSION

8.3.1 Characterization of cultures

After 3 consecutive subcultures in basal medium containing 2 μM 2,4-D (10 fold less than the concentration in regular maintenance medium, where calli remained highly friable and without signs of differentiation), most calli from both hybrids remained friable, but some calli were presenting the formation of roots, with a significantly increased frequency of rhizogenesis in GM maize calli (see Capítulo III).

8.3.2 Histochemistry

Friable calli grown during three subcultures in culture medium with 2 μM 2,4-D were used to assess histochemical features. Calli sections from GM and conventional NIHs stained with TB presented a large cell-nucleus ratio, but nuclei were better defined in conventional than GM NIH, while PAS revealed the presence of a few more starch grains in GM and similar amounts of acidic polysaccharides (Figure 49). CBB staining for total protein, on the other hand, evidenced marked differences between the GM and conventional NIH: the GM NIH specimens reacted much more intensely with CBB, indicating a higher amount of total protein in the cytoplasm of GM NIH cells grown with 2 μM 2,4-D, compared to conventional NIH cells (Figure 49). Additionally, cells from conventional NIH calli were notably smaller than cells from GM calli and presented fewer vacuoles.

On average, GM and conventional calli grown on medium with 2 μM 2,4-D presented different morphological and cellular characteristics, with less friable, more rhizogenic calli for the GM maize. We observed cells from GM calli were overall bigger than cells from conventional calli and presented less conspicuous nuclei in TB-O stained specimens, and that acidic polysaccharides were more abundant in the cell wall of conventional cells stained with PAS, what is in agreement with the observation that the frequency of friable calli was lower in GM than conventional calli.

Figure 49: Histological sections of conventional (a, c, e) and GM (b, d, f) maize calli grown in basal medium supplemented with 2 µM 24-D. Toluidine blue (TB-O) stained sections (a and b); Periodic acid-Schiff (PAS) stained sections; Coomassie Brilliant Blue (CBB) stained sections (e and f); arrows indicated acidic polysaccharides in cell walls; n=nucleus; v=vacuole; s=starch grains; Bars have 100 µm.

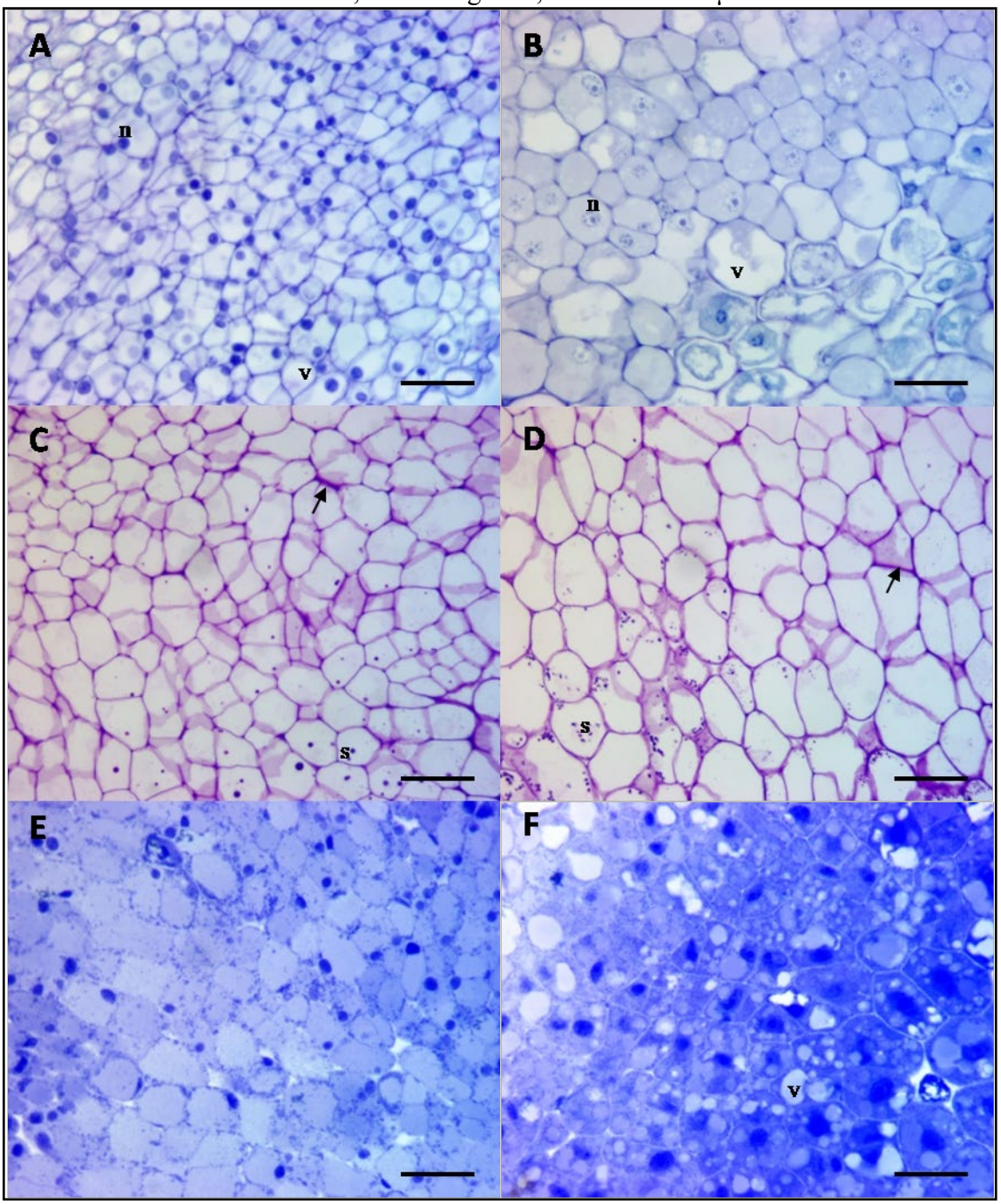

Fonte: Daniel Ferreira Holderbaum (2019).

8.3.3 Proteomic analysis

In total, 197 proteins showed significant ($p<0.05$) differential regulation in GM maize as compared to the conventional maize, being 106 down-regulated (ranging from 0.66

to 0.03 fold-change, with 50 proteins showing 0.5 or lower fold-change), 90 up-regulated (ranging from 1.5 to 9.3 fold-change, where 57 proteins had fold-change higher than 2), and one unique protein in GM maize (Table 1 of Apêndices). Gene ontology (GO) enrichment analysis revealed a high number of biological processes, cellular components and molecular functions where down-regulated (Figure 50) and up-regulated (Figure 51) proteins are involved, at multiple GO levels, evidencing a highly complex web of off-target effects on the GM-maize proteome, under highly controlled *in vitro* model conditions (Tables 2, 3 e 4 of the Apêndices).

Figure 50: Number of GO Annotations for down-regulated proteins, according to GO level (0-15) and domain (P: Biological Process; F: Molecular Function; C: Cellular component).

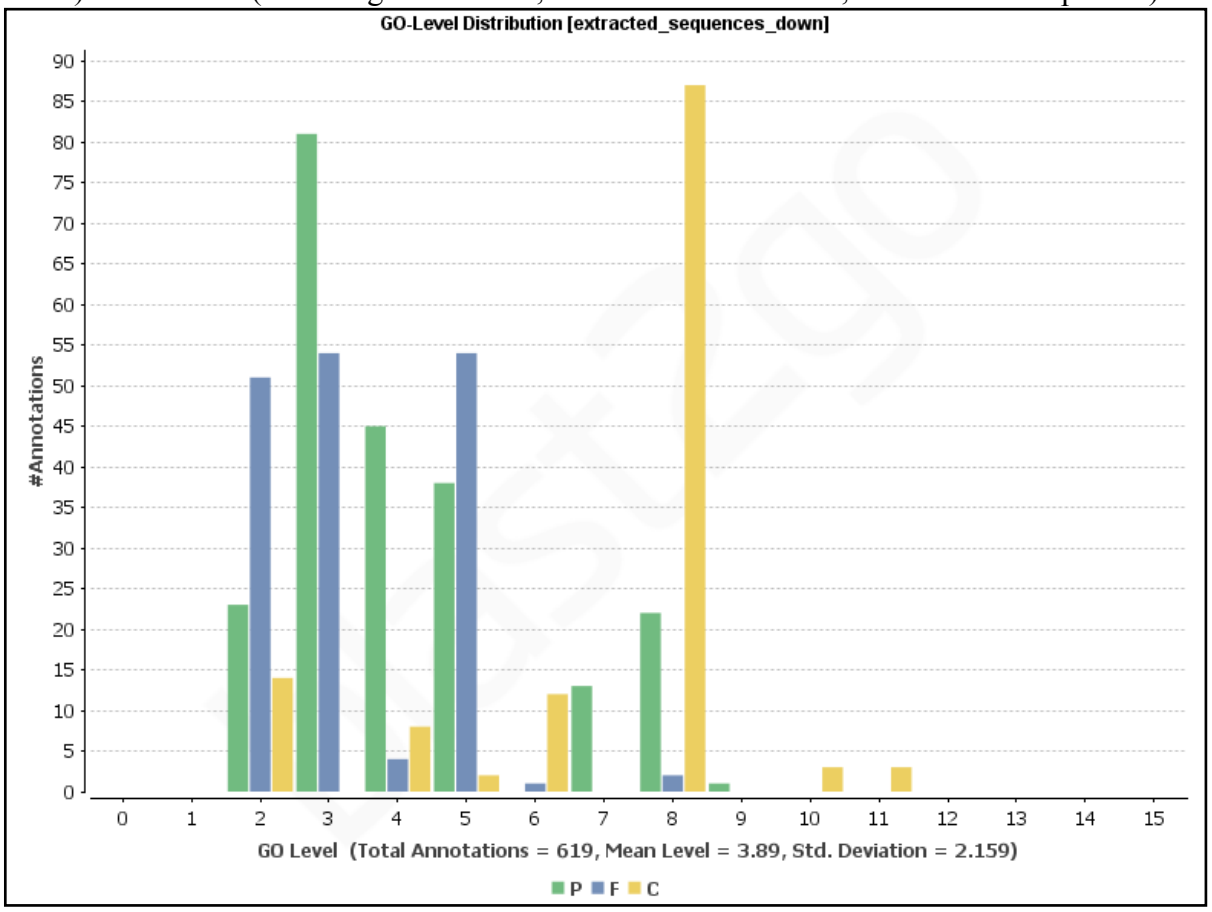

Fonte: Daniel Ferreira Holderbaum (2019).

Figure 51: Number of GO Annotations for up-regulated proteins, according to GO level (0-15) and domain (P: Biological Process; F: Molecular Function; C: Cellular component).

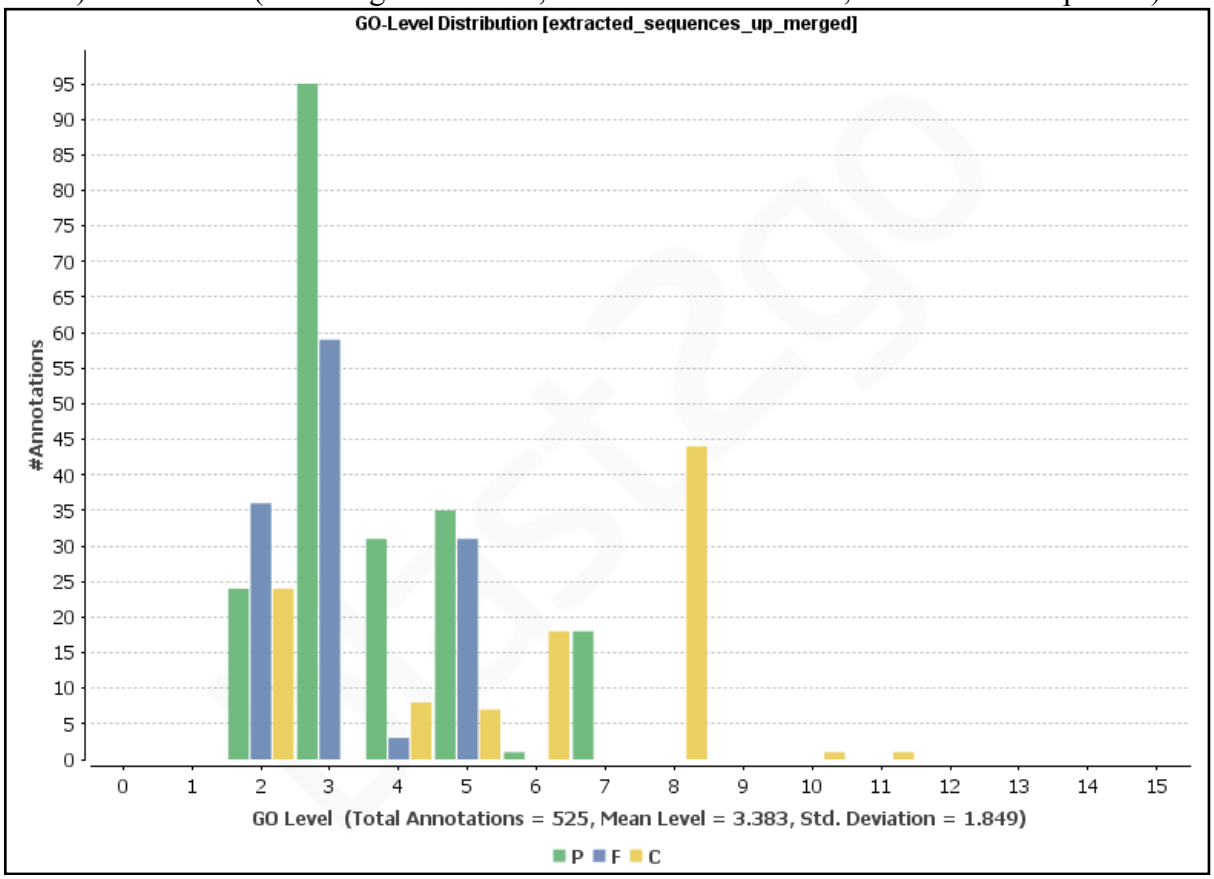

Fonte: Daniel Ferreira Holderbaum (2019).

For down-regulated proteins, multiple biological processes were annotated, and important relations were evidenced between the multiple GO levels, indicating possible molecular chain-reactions starting with down-regulation of translation-related proteins at the lowest level, affecting proteins related to biosynthetic processes, protein metabolic processes, and varied cellular processes (Figure 52).

Among biological processes, carbohydrate metabolic processes, nucleobase-containing compound metabolic processes, catabolic processes, generation of precursor metabolites and energy, response to stress, and cellular component organization, are all influenced by down-regulated proteins (Figure 52). Importantly, one protein involved in tryptophan metabolism and auxin synthesis (E.C. 1.2.3.7 - indole-3-acetaldehyde oxidase) (Seo *et al.*, 1998) was down-regulated 0.49-fold (about 50% of levels found in conventional maize). Additionally, glutathione metabolism featured 3 down-regulated enzymes (EC: 1.1.1.42, EC: 1.1.1.49 and EC: 6.3.2.2), and starch and sucrose metabolism showed 6 down-regulated enzymes (EC: 2.7.1.1, EC: 2.7.1.2, EC: 2.7.1.4, EC: 2.7.7.9, EC: 3.2.1.21 and EC: 5.4.2.2).

A somewhat similar biological process GO tree was obtained based on up-regulated proteins, though with some marked differences (Figure 53). Here, the most affected biological processes included cellular protein modification, which affects protein metabolism, which then affects primary metabolite metabolism, biosynthesis, response to stress, response to stimulus, catabolism, nucleobase-containing compound metabolism, and cellular component organization.

Figure 52: Annotated gene ontologies, including GO name, number and percentage of sequences, for biological processes with down-regulated proteins in GM maize. Color intensity represents nodescores.

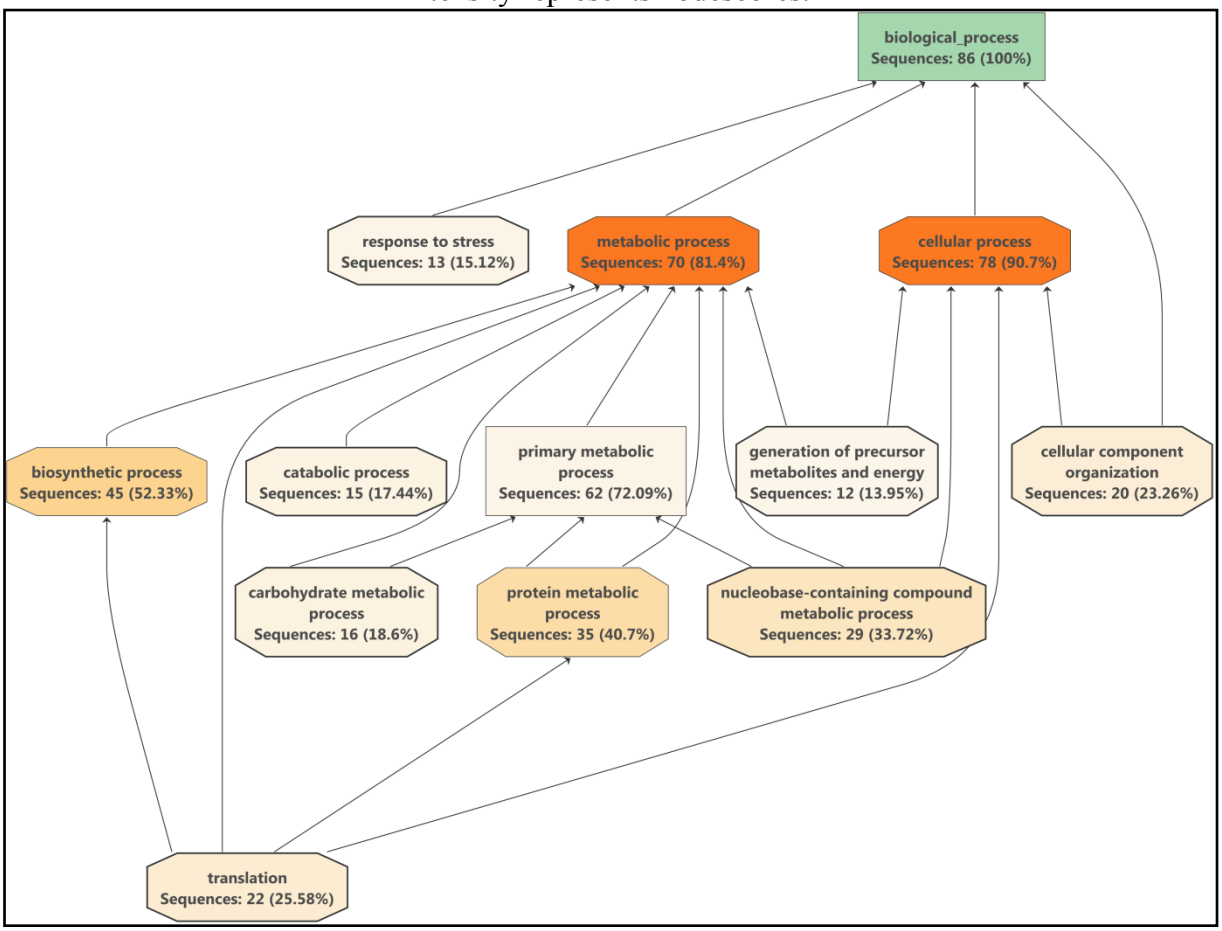

Fonte: Daniel Ferreira Holderbaum (2019).

Notably, three enzymes involved in tryptophan metabolism were up-regulated (EC: 1.2.4.2 - dehydrogenase (succinyl-trasferring), EC: 1.2.3.1 - oxidase, and EC: 1.2.3.7 - oxidase); starch and sucrose metabolism presented 5 up-regulated enzymes (EC: 3.2.1.21 - gentiobiase, EC: 3.2.1.26 - invertase, EC: 3.2.1.48 - alpha-glucosidase, EC: 5.3.1.9 - isomerase, EC: 3.2.1.39 - endo-1,3-beta-D-glucosidase); glycolysis/gluconeogenesis also had

5 up-regulated enzymes (EC: 2.7.1.11 - phosphohexokinase, EC: 5.3.1.1 - isomerase, EC: 5.3.1.9 - isomerase, EC: 1.2.4.1 - dehydrogenase (acetyl-transferring), EC: 2.7.1.40 - kinase); and glutathione metabolism had one up-regulated protein (EC: 1.11.1.11 - peroxidase).

Figure 53: Annotated gene ontologies, including GO name, number and percentage of sequences, for biological processes with up-regulated proteins in GM maize. Color intensity represents nodescores.

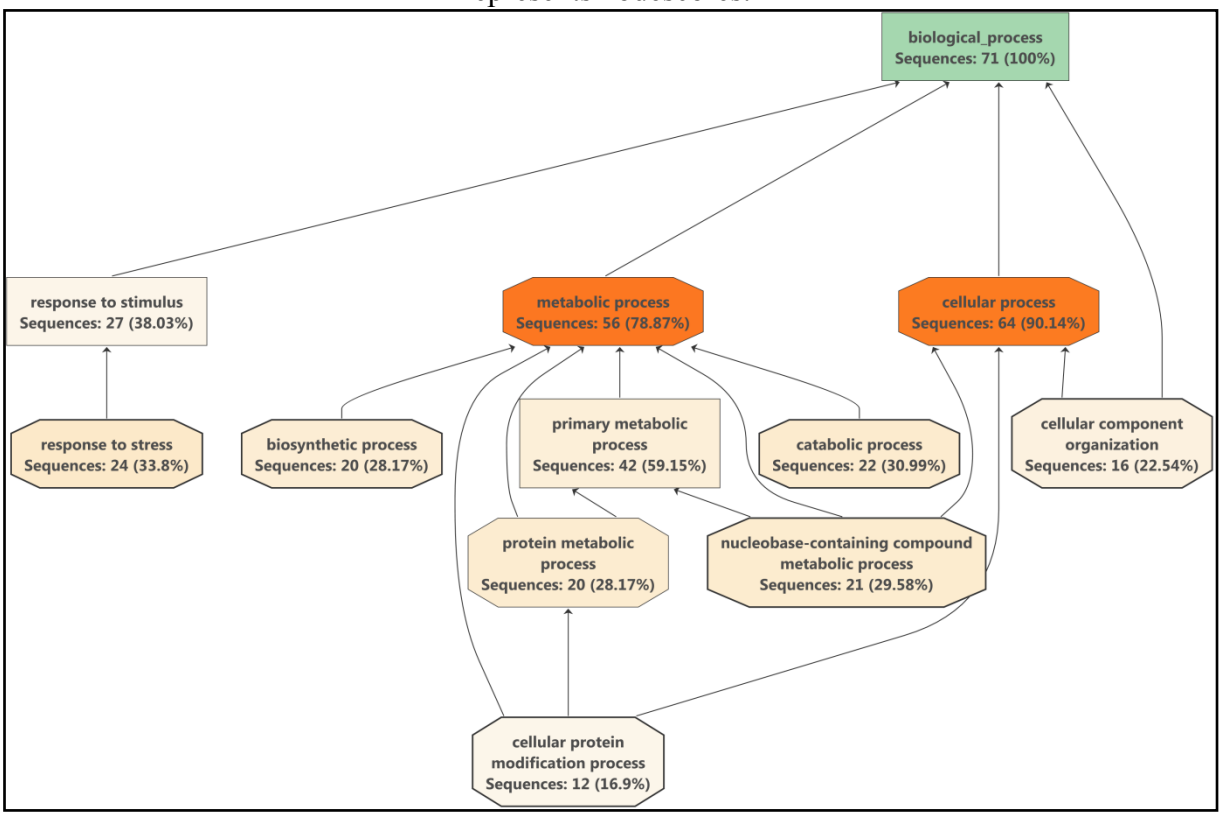

Fonte: Daniel Ferreira Holderbaum (2019).

Regarding molecular functions, 94 down-regulated proteins were annotated, with binding proteins being a major down-regulated GO (70 proteins), including nucleotide binding proteins (33) at the lowest level, nucleoside phosphate binding proteins (33), organic cyclic compound binding proteins (48), heterocyclic compound binding proteins (48), and small molecule binding proteins (33) (Figure 54). Structural molecule activity had 22 down-regulated proteins, and catalytic activity had 51 down-regulated proteins, including 22 hydrolase activity proteins.

The obtained molecular function GO tree for up-regulated proteins (Figure 55) also depicts binding proteins (52) and catalytic activity proteins (53) as major affected GOs. For catalytic activity, hydrolase activity proteins were the most prevalent (23 proteins). For binding proteins, the same GOs affected by down-regulated proteins were also affected by up-regulated proteins, being 21 nucleotide binding proteins, 21 nucleoside phosphate binding proteins, 22 organic cyclic compound binding proteins, 22 heterocyclic compound binding proteins, and 21 small molecule binding proteins.

Figure 54: Annotated gene ontologies, including GO name, number and percentage of sequences, for molecular functions with down-regulated proteins in GM maize. Color intensity represents nodescores.

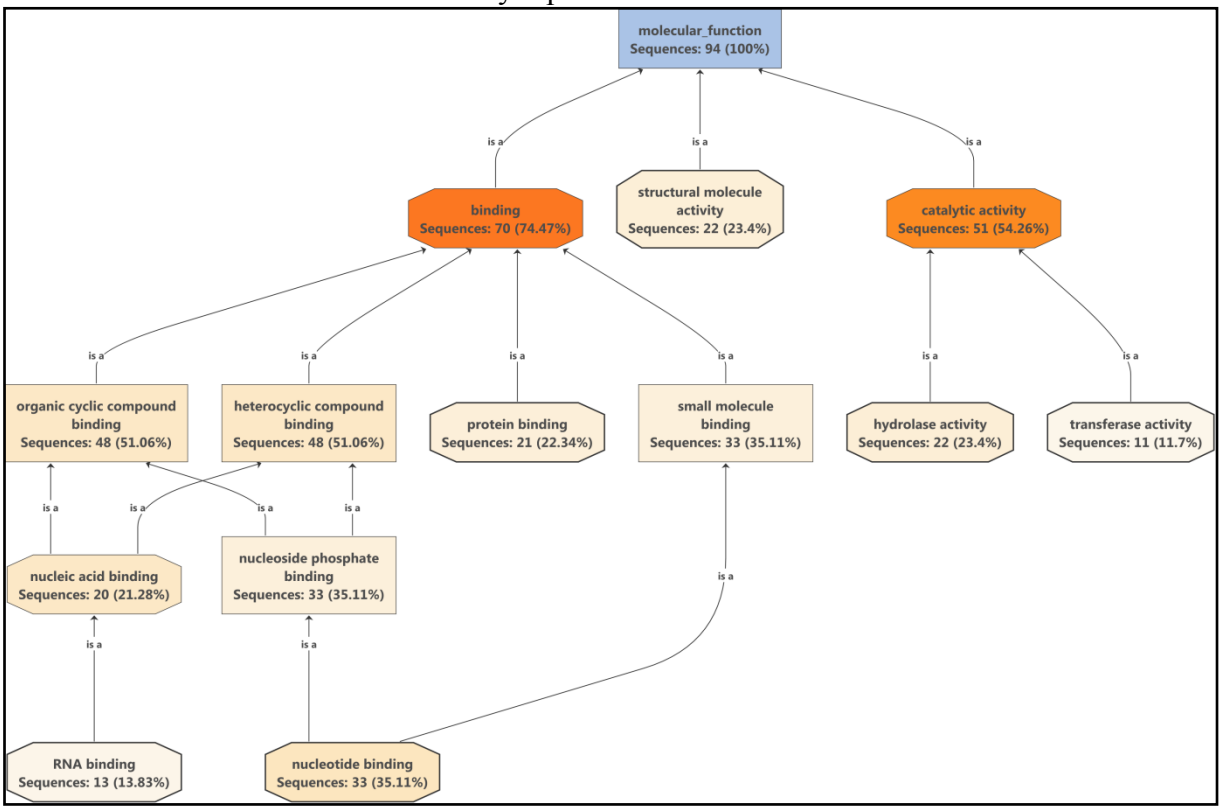

Fonte: Daniel Ferreira Holderbaum (2019).

Figure 55: Annotated gene ontologies, including GO name, number and percentage of sequences, for molecular functions with up-regulated proteins in GM maize. Color intensity represents nodescores.

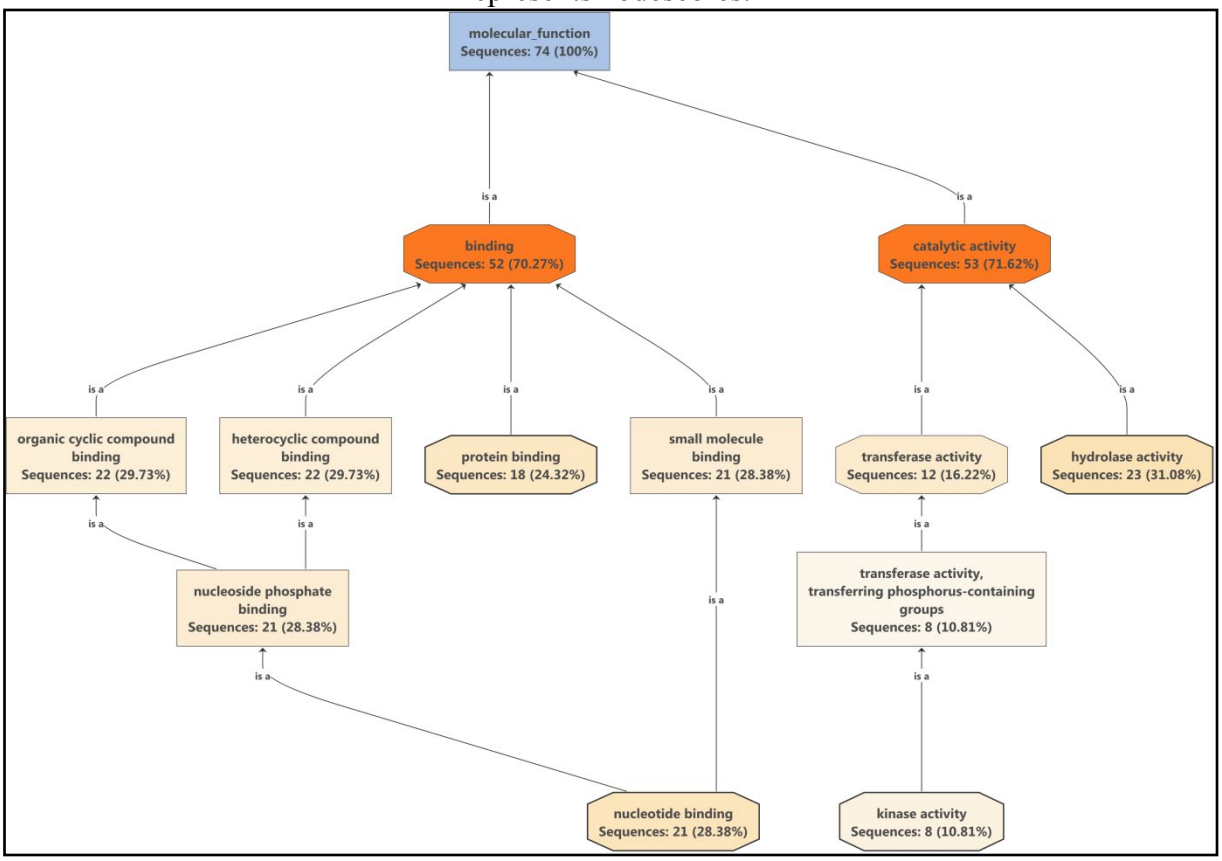

Fonte: Daniel Ferreira Holderbaum (2019).

For cellular component GOs (Figure 56), 84 down-regulated proteins were annotated, including proteins located at the nucleus (13), plastids (13), mitochondrion (14), ribosome (18), and cytosol (27). A total of 61 down-regulated proteins had cellular component GOs annotated to organelles, including membrane-bounded organelles (41 proteins), non-membrane-bounded organelles (22 proteins), and intracellular organelles (61 proteins). Cytoplasm was also an important cellular component GO, with a total of 67 down-regulated proteins. Additionally, intracellular ribonucleoprotein complex (18 proteins), ribonucleoprotein complex (18 proteins), macromolecular complex (18 proteins), and the cell membrane (14 proteins) were also marked as relevant cellular component GOs.

The cellular component GOs for up-regulated proteins (Figure 57) included the cytosol (10 proteins), plastids (11 proteins), nucleus (10 proteins), the cytoplasm (34 proteins), cell-wall (9 proteins), intracellular organelles (29 proteins), membrane-bounded organelles (28 proteins), external encapsulating structure (9 proteins), cell periphery (16 proteins), cell membrane (17 proteins), and extracellular region (13 proteins).

Figure 56: Annotated gene ontologies, including GO name, number and percentage of sequences, for cellular components with down-regulated proteins in GM maize. Color intensity represents nodescores.

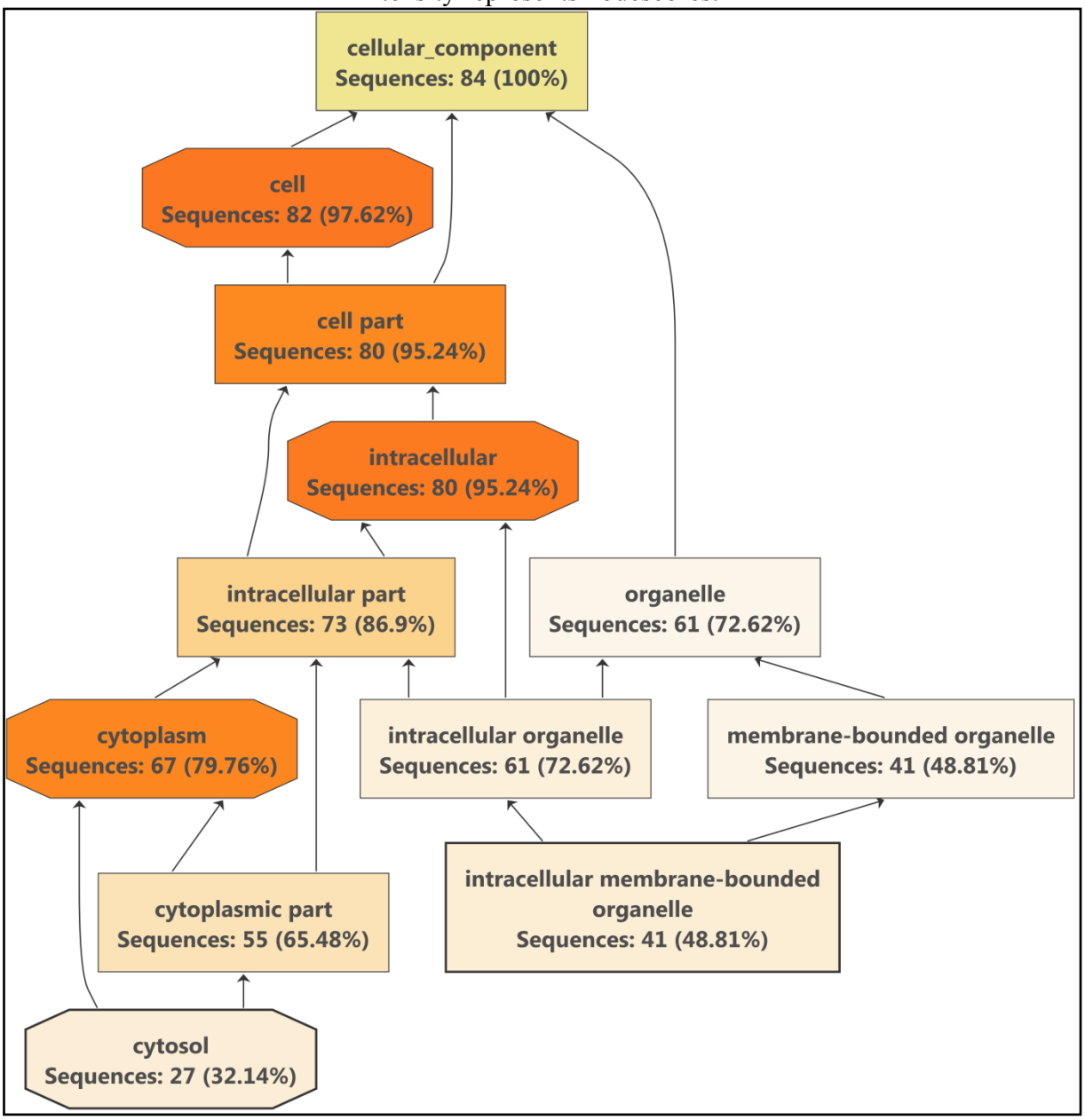

Fonte: Daniel Ferreira Holderbaum (2019).

Figure 57: Annotated gene ontologies, including GO name, number and percentage of sequences, for cellular components with up-regulated proteins in GM maize. Color intensity represents nodescores.

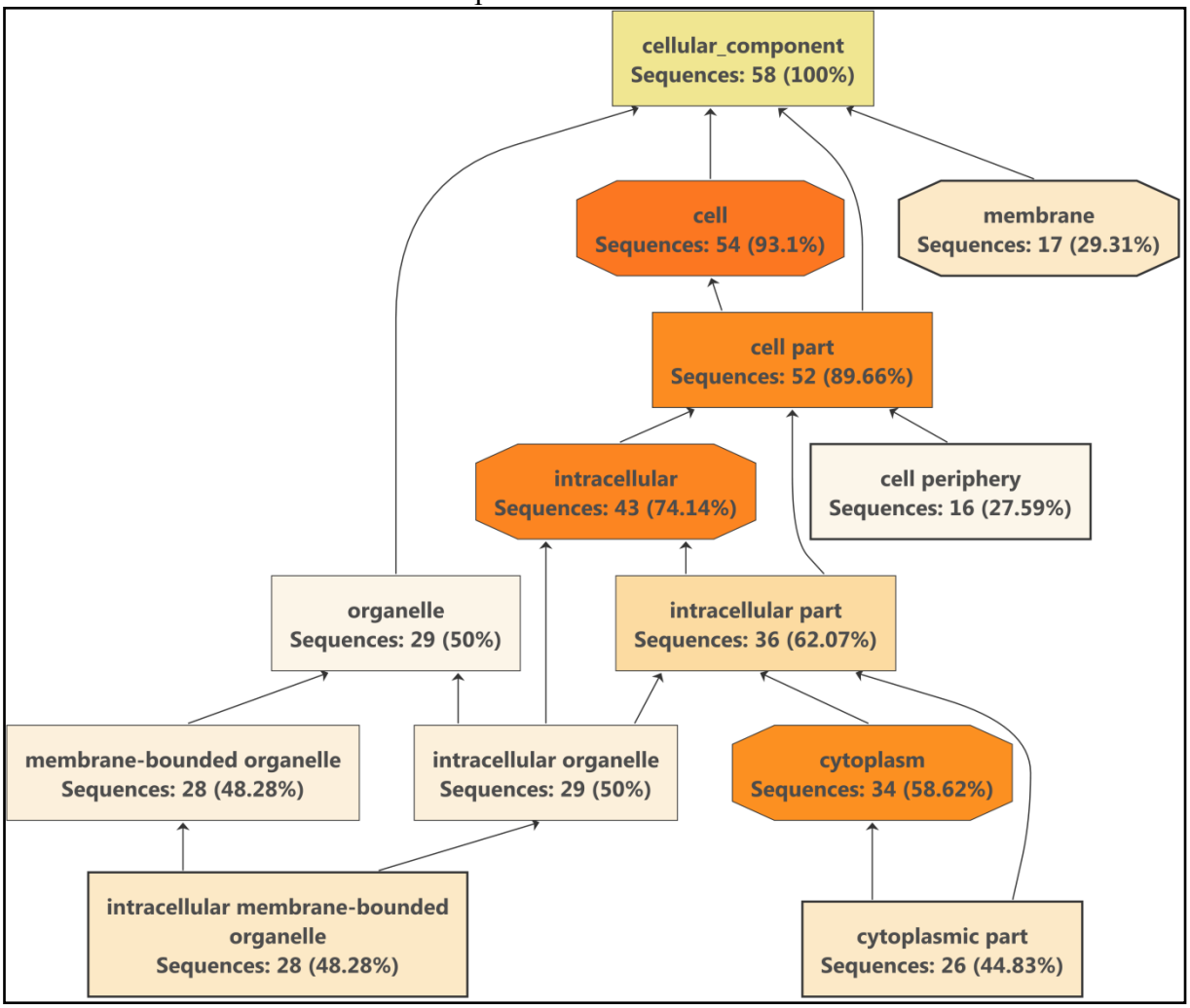

Fonte: Daniel Ferreira Holderbaum (2019).

Only one maize protein was detected exclusively on the transgenic maize (sequence name A0A1D6NEL8, mitogen-activated protein kinase kinase kinase A-like, E.C: 2.7.11). Mitogen-activated protein kinases (MAPKs) are serine/threonine-specific protein kinases found in plants, animals and yeast, that are activated in response to extracellular signals and phosphorylate substrates such as transcription factors, other kinases, and cytoskeletal-associated proteins (Seger & Krebs 1995; Widmann *al et*. 1999; Ligterink & Hirt 2001). MAPKs have been found to act in plant responses to exogenous factors such as elicitors (Zhang, Du & Klessig 1998), cold (Jonak *al et*. 1996) and hormones, including auxin (Kovtun *al et*. 1998).

MAPK cascades are evolutionarily conserved signaling hubs that regulate innate immune responses in plants and animals (Meng and Zhang, 2013). The recognition of nonself

by pattern recognition receptors on the cell surface activates a MAPK phosphorylation relay, where initial activation of a MAP kinase kinase kinase (MAPKKK) leads to the phosphorylation and activation of a downstream MAP kinase kinase (MAPKK), which subsequently phosphorylates a downstream MAPK. The activated MAPK then phosphorylates its target proteins, ultimately reprogramming gene expression (Pitzschke *et al*., 2009; Rasmussen *et al*., 2012; Meng and Zhang, 2013; Pitzschke, 2015; Xu *et al*, 2018).

Interestingly, pore-forming toxins, such as Cry proteins, are important virulent factors produced by several pathogenic bacteria, representing a fundamental threat to the host after infection; as a consequence, general host defense-responses have evolved against PFTs (Cancino-Rodezno *et al.*, 2013). One pathway activated in different organisms in response to a variety of pore-forming toxins is the mitogen activated protein kinase p38 pathway (MAPK p38), that activates a complex cascading defense response (Cancino-Rodezno *et al.*, 2013).

Considering that i) MAPK cascades function in defense responses in plants; ii) that Cry toxins were shown to activate MAPK cascades in different organisms; and iii) that a MAPKKK was exclusively detected in the GM maize in this study, we hypothesize that the constitutive expression of the recombinant Cry1Ab protein in the GM maize elicits the production of a MAPKKK-like protein, in a plant immune-response to the transgenic protein of bacterial origin. Further studies are necessary to corroborate or refute this hypothesis.

Experiments designed to assess unintended effects of plant genetic modification are benefited by *in vitro* approaches, because it allows for highly controllable environmental conditions of luminosity, temperature, nutrient and water supply, while also making possible to test specific and highly standardized treatments, while increasing statistical power by decreasing residual variance (Coll *et al*., 2008; 2009) .

Previous studies have inspected the transcriptomic (Barros *et al*., 2010; Coll *et al*., 2008; 2009; 2010) and proteomic profiles (Zolla *et al*., 2008; Barros *et al*., 2010; Balsamo *et al*., 2011; Coll *et al*., 2011; Agapito-Tenfen *et al*., 2013) of MON810 maize hybrids and their respective conventional counterparts, with analyzed plants being cultivated under varied conditions (field, greenhouse and *in vitro* grown whole plants). Adding to this increasing body of evidence, this is the first study to investigate proteomic profile effects of plant genetic transformation using an *in vitro* model of plant cell, tissue and organ development.

Zolla *et al.*, (2008) evaluated environmental effects as well as those resulting from genetic transformation on the proteome of GM maize and conventional NIH kernels,

considering a minimum of 2 fold variation with 99 % confidence intervals. They found that ~100 proteins were differentially modulated by environmental changes, 43 proteins had their expression levels altered in transgenic maize compared to its NIH, and that the GM and conventional NIH responded differently within the same environment. Zolla *et al.* (2008) attributed the observed effects to a genome rearrangement derived from random gene insertion in maize's genome.

Other authors (Balsamo *et al*., 2011; Barros *et al*., 2010; Coll *et al*., 2008; 2009; 2010; 2011) remarked that the presence of the transgenic construct had no substantial effects on the analyzed characteristics, and yet other studies that compared transcriptopic or proteomic profiles (Zolla *et al*., 2008; Agapito Tenfen *et al*., 2013; La Paz *et al*., 2014) between GM MON810 maize hybrids and non-GM counterparts, are in agreement with the unintended emergent properties observed in the *in vitro* development of maize cells/tissues/organs in this study.

Agapito-Tenfen *et al.* (2013) investigated the proteomic profiles of a pair of GM (MON810) and conventional brazilian maize hybrids (NIHs) cultivated in different locations in south Brazil. They found the environment was the major source of variation in proteomic profiles, while differential production of proteins between GM and conventional NIHs accounted for 3.1% of analyzed proteins. Additionally, they observed changes that were specific to the GM or conventional NIHs and to different agroecosystems. Contrary to the conclusions of studies by Coll *et al.* (2008, 2009, 2010, 2011) and other authors (Barros *et al.*, 2010; Balsamo *et al.*, 2011), Agapito-Tenfen *et al.* (2013) considered the observed differences in proteomic profiles of GM and conventional maize as indications of unintended effects of the MON810 GM character in a maize hybrid, and that such effects are environmentally modulated. Finally, these authors emphasized the detected changes in proteomic profiles should be further scrutinized in order to address their biological importance.

Of special relevance to this study is the fact that Agapito-Tenfen *et al.* (2013), and also Coll *et al.* (2008) reported changes in protein expression levels in GM MON810 hybrids, related to biological functions of carbohydrate and energy metabolism. Changes in the levels of proteins related to energy metabolism are expected to influence plant development and growth, all results that were observed in the present study of *in vitro* cultures of a GM MON810 maize and its conventional NIH.

La Paz *et al.* (2014) assessed the extent to which the introduction of a transgene may alter expression of endogenous genes in several pairs of GM MON810 and conventional NIHs. Additionally, for an in-depth analysis, high-throughput deep sequencing coupled with

microarrays was used to compare the transcriptomes of immature embryos of the MON810 variety DKC6575 and its conventional NIH Tietar, grown under controlled environmental conditions. Gene expression analysis revealed 140 differentially expressed genes mainly involved in carbohydrate metabolism, protein metabolism and chromatin organization. The differentially expressed genes and physiological data suggested a slight but significant delay in seed and plant maturation of MON810 plants, what goes in agreement with results for *in vitro* developmental parameters observed in the present study, although La Paz *et al.* (2014) noted the observed transcriptomic changes were not associated to undesirable changes in the global phenotype or plant behavior. Additionally, La Paz *et al.* (2014) concluded that gene expression was modulated by the genetic background in which the transgene was introduced through conventional breeding programs.

The findings herein presented point to emergent properties of the presence and expression of a transgenic DNA sequence in the model GM maize AG-5011YG (event MON810), within the *in vitro*-interactive model. The observed emergent properties include complex differential regulation of multiple proteins, associated to several biological processes, cellular components and molecular functions, most notably carbohydrate and energy metabolism, macromolecule metabolism, stress responses and responses to stimuli, growth regulator biosynthesis, cell growth and plant morphogenesis. Additionally, tryptophan, glutathione, AIA, and ABA biosynthesis-related proteins presented evidence of significant differential regulation, and one MAPKKK-like protein was detected exclusively and consistently in the GM-maize, pointing to a possible plant immune response to the production of the transgenic Cry1Ab protein. The evidenced differential regulation of proteins in this study provide compelling evidence to explain the mechanisms behind previously evidenced differences between the tested GM and conventional near-isogenic hybrids, with regards to developmental and morphogenetic responses to environmental stimuli *in vitro*, such as 2,4-D, 2iP and ABA concentrations (Chapters II, III and IV) .

8.4 CONCLUSIONS

This is the first study to evaluate histochemical and proteomic features of calli from a near-isogenic pair of maize hybrids, AG-5011YG (transgenic event MON810) and AG-5011 (conventional NIH), cultured within an *in vitro* interactive model. Building upon

morphogenetic and developmental results obtained previously (Capítulos II, III and IV), the histochemical and proteomic analyses presented in this study provide compelling molecular evidence of hundreds of off-target effects on protein regulation in the transgenic hybrid, with impacts on multiple molecular functions, cellular components and biological processes, particularly carbohydrate and energy metabolism, macromolecule metabolism, responses to stress and stimuli, and plant growth regulator biosynthesis, what is in agreement with the complex differential ontogenetic and morphogenetic responses observed for the tested NIHs within the *in vitro* model, where the GM NIH predominantly produced weaker responses to environmental stimuli *in vitro*. The complex web of differential regulation of multiple proteins is reflected on differential responses to environmental stimuli - such as exogenous growth regulators - between the GM and conventional hybrids, altering morphogenetic capacity and growth rate of the GM maize cultures *in vitro*.

REFERENCES

AGAPITO-TENFEN, S.Z.; GUERRA, M.P.; WIKMARK, O.G.; NODARI, R.O. Comparative proteomic analysis of genetically modified maize grown under different agroecosystems conditions in Brazil. **Proteome Sci.**, v. 11, p. 46, 2013.

BALBUENA, T.S.; JO, L.; PIERUZZI, F.P.; DIAS, L.L.; SILVEIRA, V.; SANTA-CATARINA, C., JUNQUEIRA, M., THELEN, J.J.; SHEVCHENKO, A.; FLOH, E.I. Differential proteome analysis of mature and germinated embryos of Araucaria angustifolia. **Phytochemistry**, v. 72, n. 4-5, p. 302-311, 2011. Disponível em: http://dx.doi.org/10.1016/j.phytochem.2010.12.007.

BALSAMO, G.M.; CANGAHUALA-INOCENTE, G.C.; BERTOLDO, J.B.; TERENZI H.; ARISI, A.C. Proteomic analysis of four Brazilian MON810 maize varieties and their four non-genetically-modified isogenic varieties. **J. Agr. Food Chem.**, v. 59, p. 11553-11559, 2011.

BARROS, E.; LEZAR, S.; ANTTONEN, M.J.; VAN DIJK, J.P.; RÖHLIG, R.M.; KOK, E.J.; ENGEL, K.H. Comparison of two GM maize varieties with a near-isogenic conventional variety using transcriptomics, proteomics and metabolomics. **Plant Biotechnol. J.**, v. 8, p. 436-451, 2010.

BARTSCH, D.; DEVOS Y.; HAILS, R.; KISS, J.; KROGH, P.H.; MESTDAGH, S.; NUTI, M.; SESSITSCH, A.; SWEET J.; GATHMANN, A. Environmental impact of genetically modified maize expressing Cry1 proteins. In: KEMPKEN, F.; Jung, C. (eds.). **Genetic Modification of Plants: Agriculture, Horticulture and Forestry**. Springer, 2010.

CALDERAN-RODRIGUES, M.; JAMET, E.; CALDERAN-RODRIGUES BONASSI, M.; GUIDETTI-GONZALEZ, S.; CARMANHANIS BEGOSSI, A.; VAZ SETEM, L.;

FRANCESCHINI, L.; GUIMARÃES FONSECA, J.; LABATE, C. Cell wall proteomics of sugarcane cell suspension cultures. **Proteomics**, v. 14, p. 738-749, 2014.

CANCINO-RODEZNO, A.; ALEXANDER, C.; VILLASEÑOR, R.; PACHECO, S.; PORTA, H.; PAUCHET, Y.; SOBERÓN, M.; GILL, S.S.; BRAVO, A. The mitogen-activated protein kinase p38 is involved in insect defense against Cry toxins from Bacillus thuringiensis. **Insect Biochem. Mol. Biol.**, v. 40, n. 1, p. 58-63, 2010. Dispínivel em: http://doi.org/10.1016/j.ibmb.2009.12.010.

CELLINI, F.; CHESSON, A.; COLQUHOUN, I.; CONSTABLE, A; DAVIES, H.V.; ENGEL, K.H.; GATEHOUSE, A.M.; KÄRENLAMPI, S.; KOK, E.J.; LEGUAY, J.J.; LEHESRANTA, S.; NOTEBORN, H.P.; PEDERSEN, J.; SMITH, M. Unintended effects and their detection in genetically modified crops. **Food and Chemical Toxicology**, v. 42, p. 1089-1125, 2004.

CERA, Center for Environmental Risk Assessment. **GM Crop Database, MON-ØØ81Ø-6 (MON810)**. ILSI Research Foundation, Washington D.C., 2016. Disponível em: http://cera-gmc.org/GmCropDatabaseEvent/MON810/short. Acesso em: 03 dez. 2016.

COLL, A.; NADAL, A.; PALAUDELMÀS, M.; MESSEGUER, J.; MELÉ, E.; PUIGDOMÈNECH, P.; PLA, M. Lack of repeatable differential expression patterns between MON810 and comparable commercial varieties of maize. **Plant Mol Biol.**, v. 68, p. 105-117, 2008.

COLL, A.; NADAL, A.; COLLADO, R.; CAPELLADES, G.; MESSEGUER, J.; MELÉ, E.; PALAUDELMÀS, M.; PLA, M. Gene expression profiles of MON810 and comparable conventional maize varieties cultured in the field are more similar than are those of conventional lines. **Transgenic Res.**, v. 18, p. 801–8. 2009.

COLL, A.; NADAL A.; COLLADO, R.; CAPELLADES, G.; KUBISTA, M.; MESSEGUER, J; PLA, M. Natural variation explains most transcriptomic changes among maize plants of MON810 and comparable conventional varieties subjected to two N-fertilization farming practices. **Plant Mol. Biol.**, v. 73, p. 349–362, 2010.

COLL, A.; NADAL, A.; ROSSIGNOL, M.; PUIGDOMÈNECH, P.; PLA, M. Proteomic analysis of MON810 and comparable non-GM maize varieties grown in agricultural fields. **Transgenic Res.**, v. 4, p. 939-949, 2011.

EMONS, A.M.C.; SAMALLO-DROPPERS, A.; VAN DER TOOM, C. The influence of sucrose, mannitol. L-proline, abscisic acid and gibberellic acid on the maturation of somatic embryos of *Zea mays* L. from suspension cultures. **Plant Physiol.**, v. 142, p. 597-604, 1993.

FISHER, D.B. Protein staining of ribboned epon sections for light microscopy. **Histochemie**, v. 16, p. 92-96, 1968.

GAHAN, P.B. Plant histochemistry and cytochemistry: an introduction. Orlando: Academic Press, 1984.

GEORGE, E.F.; HALL, M.; DE KLERK, G-J. (Eds.) (2008) Plant Propagation by Tissue Culture. GEORGE, E.F.; HALL, M.A.; DE KLERK, G.J. (eds.). **Plant Propagation by Tissue Culture**. Dordrecht, The Netherlands: Springer, 2008.

GERRITS, P.O.; SMID, L. A new, less toxic polymerization system for the embedding of soft tissues in glycol methacrylate and subsequent prepairing of serial sections. **Journal of Microscopy**, v. 132, p. 81-85, 1983.

JAMES, C. **Executive Summary of Global Status of Commercialized Biotech/GM Crops: 2016**. ISAAA Brief, 52. Ithaca, NY, 2016.

JONAK, C.; KIEGERL, S.; LIGTERINK, W.; BARKER, P.; HUSKISSON, N.S.; HIRT, H. Stress signaling in plants: a mitogen-activated protein kinase pathway is activated by cold and drought. **Proceedings of the National Academy of Sciences USA**, v. 93, p. 11274–11279, 1996.

KOVTUN, Y.; CHIU, W.; ZENG, W.; Sheen, J. Suppression of auxin signal transduction by a MAPK cascade in higher plants. **Science**, v. 395, p. 716–720, 1998.

LA PAZ, J.L.; PLA, M.; CENTENO, E.; VICIENT, C.M.; PUIGDOMÈNECH, P. The use of massive sequencing to detect differences between immature embryos of MON810 and a comparable conventional maize variety. **PLoS ONE**, v. 9(6), e100895. Disponível em: https://doi.org/10.1371/journal.pone.0100895.

LIGTERINK, W.; HIRT, H. Mitogen-activated protein (MAP) kinase pathways in plants: versatile signaling tools. **International Review of Cytology**, v. 20, p. 209-275, 2001.

MENG, X.; ZHANG, S. MAPK cascades in plant disease resistance signaling. **Annu. Rev. Phytopathol.**, v. 51, p. 245-266, 2013.

MOREL, G.; WETMORE, R.H. Fern callus tissue culture. **American Journal of Botany**, v. 38, n. 2, p.141-143, 1951.

MURASHIGE, T.; SKOOG, F. A revised medium for rapid growth and bio assays with tobacco tissue cultures. **Physiologia Plantarum**, v. 15, p. 473-497, 1962.

O'BRIEN, T.P.; FEDER, N.; MCCULLY, M.E. Polychromatic staining of plant cell walls by toluidine blue O. **Protoplasma**, v. 59, n. 2, p. 368-373, 1964.

PITZSCHKE, A.; SCHIKORA, A.; HIRT, H. MAPK cascade signaling networks in plant defence. **Curr. Opin. Plant Biol.**, v. 12, p. 421-426, 2009.

PITZSCHKE, A. Modes of MAPK substrate recognition and control. **Trends Plant Sci.**, v. 20, p. 49-55, 2015.

RASMUSSEN, M.W.; ROUX, M.; PETERSEN, M.; MUNDY, J. MAP kinase cascades in Arabidopsis innate immunity. **Front. Plant Sci.**, v. 3, 169, 2012. Disponível em: http://doi.org/10.3389/fpls.2012.00169.

ROSATI A.; BOGANI, P.; SANTARLASCI, A.; BUIATTI, M. Characterization of 3′ transgene insertion site and derived mRNAs in MON810 Yieldgard maize. **Plant Mol. Biol.**, v. 67, p. 271-281, 2008.

SEGER, R.; KREBS, E.G. The MAPK signaling cascade. **FASEB Journal**, v. 9, p. 726-735, 1995.

STEINER, N.; FARIAS-SOARES, F.L.; SCHMIDT, E.C.; PEREIRA, M.L.T.; SCHEID, B.; ROGGE-RENNER, G.D.; BOUZON, Z.L. SCHMIDT, D.; MALDONADO, S.; GUERRA, M.P. Toward establishing a morphological and ultrastructural characterization of proembryogenic masses and early somatic embryos of Araucaria angustifolia (Bert.) O. Kuntze. **Protoplasma**, v. 253, n. 2, p. 487-501, 2016.

WIDMANN, C.; GIBSON, S.; JARPE, M.B.; JOHNSON, G.L. Mitogen-activated protein kinase: conservation of a three-kinase module from yeast to human. PHYSIOLOGICAL REVIEWS, v. 79, p. 143-180, 1999.

XU, H.Y.; ZHANG, C.; LI, Z.C.; WANG, Z.R.; JIANG, X.X.; SHI, Y.F.; TIAN, S.N.; BRAUN, E.; MEI, Y.; QIU, W.L.; LI, S.; WANG, B.; XU, J.; NAVARRE, D.; REN, D.; CHENG, N.; NAKATA, P.A.; GRAHAM, M.A.; WHITHAM, S.A.; LIU, J.Z. The MAPK Kinase Kinase GmMEKK1 Regulates Cell Death and Defense Responses. **Plant Physiology**, v. 178, n. 2, p. 907-922, 2018. Disponível em: http://doi.org/10.1104/pp.18.00903.

ZEVEN, A.C.; Waninge, J. The degree of phenotypic resemblance of the near-isogenic lines of the wheat cultivar Thatcher with their recurrent parent. **Euphytica**, v. 35, p. 665-676, 1986.

ZHANG, S.; DU, H.; KLESSIG, D.F. Activation of a tobacco SIP kinase by both a cell wall-derived carbohydrate elicitor and purified proteinaceous elicitins from *Phytophthora* sp. **Plant Cell**, v. 10, p. 435-449, 1998.

ZOLLA, L.; RINALDUCCI, S.; ANTONIOLI, P.; RIGHETTI, P.G. Proteomics as a complementary tool for identifying unintended side effects occurring in transgenic maize seeds as a result of genetic modifications. **J. Proteome Res.**, v. 7, p. 1850-1861, 2008.

9. CONCLUSÃO

Este estudo é pioneiro na realização de um *screening* ontogenético, morfogenético e do proteoma de culturas *in vitro* de um milho híbrido geneticamente modificado (AG-5011YG, evento MON810) quanto à ocorrência de propriedades emergentes da transformação genética de plantas.

Isto foi realizado através do desenvolvimento de um modelo interativo de cultura de células, tecidos e órgãos vegetais *in vitro*, no qual um milho híbrido GM (evento MON810) e seu híbrido quase-isogênico (HQI) convencional foram comparados. Múltiplas variáveis estudadas, incluindo fonte de explante, tipo de explante, regime de iluminação, consistência do meio de cultura, e gradientes de concentração dos reguladores de crescimento 2,4-D, 2iP, TDZ e ABA, modularam efetivamente as respostas morfofisiológicas dos HQIs GM e convencional ao longo da indução de culturas de calos, manutenção/proliferação em meio semi-sólido ou culturas em suspensões, morfogênese, e indução de embriogênese somática.

A possibilidade de ocorrência de propriedades emergentes, ou efeitos não-alvo (*off-target*) em plantas GM é uma preocupação no tocante ao uso de plantas GM na agricultura (Cellini *et al.*, 2004). Até o presente, a maioria dos eventos de plantas GM aprovados para cultivo e consumo animal e humano, tais como o milho MON810, foram obtidos pela inserção não-direcionada de um cassete de expressão gênica (CEG) recombinante no genoma de células vegetais cultivadas *in vitro*, e a natureza aleatória do processo pode dar origem a conseqüências genéticas não-intencionais (La Paz *et al.*, 2014; Quétier, 2016; Zolla *et al.*, 2008; Agapito-Tenfen *et al.*, 2013; Fan *et al.*, 2011; Weinhold *et al.*, 2013), com possíveis efeitos fenotípicos imprevisíveis e de magnitude e importância desconhecidas.

A avaliação de efeitos não-alvo da transformação genética de plantas é beneficiada por abordagens *in vitro*, pois estas permitem maior controle ambiental do suprimento de água e nutrientes, temperatura e luz, enquanto tornam possível testar tratamentos altamente específicos e padronizados, deste modo facilitando o poder estatístico pela diminuição da variância residual (Coll *et al.*, 2008; 2009) .

Diversos estudos inspecionaram perfis transcriptômicos (Barros *et al.*, 2010; Coll *et al.*, 2008; 2009; 2010) e proteômicos (Zolla *et al.*, 2008; Barros *et al.*, 2010; Balsamo *et al.*, 2011; Coll *et al.*, 2011; Agapito-Tenfen *et al.*, 2013) de milhos híbridos MON810 e seus respectivos híbridos quase-isogênicos (HQIs) convencionais, com as plantas sendo analisadas sob condições variadas (cultivo de plantas a campo, em estufa e *in vitro*). De acordo com nosso conhecimento, este é o primeiro estudo a investigar propriedades emergentes no perfil

proteômico de uma planta transgênica utilizando um modelo *in vitro* de desenvolvimento de células, tecidos e órgãos vegetais.

Após a realização de uma série de experimentos *in vitro* envolvendo a indução, manutenção e proliferação de calos e indução de embriogênese somática em milho, uma quantidade substancial de evidências foi levantada mostrando respostas diferenciais entre os híbridos GM e convencional testados. As diferenças incluíram respostas ontogenéticas e morfogenéticas em geral mais fracas do HQI GM, como um menor potencial para indução de calos e para friabilidade dos calos sob o efeito de 2,4-D, e menores taxas de crescimento de culturas em suspensões líquidas, independentemente de [2,4-D]; contudo, respostas opostas foram observadas nos HQIs quanto a proliferação e viabilidade de células em suspensões celulares submetidas a um aumento da razão [2iP]:[2,4-D] no meio de cultura, indicando que o HQI GM tem respostas mais fracas à auxina e mais fortes à citocinina. Junto a estas respostas diferenciais a 2,4-D e 2iP, foi observada a regulação diferencial de 197 proteínas, incluindo proteínas com funções em rotas metabólicas de reguladores de crescimento. Adicionalmente, enquanto uma forte determinação à rizogênese das culturas (calo do Tipo III (Emons *et al.*, 1993)) pôde ser superada pelo uso de uma combinação de ABA (10 μM), TDZ (1 μM) e glutationa (1000 μM), não foram observadas diferenças significativas entre os híbridos GM e convencional quanto ao potencial para embriogênese somática neste modelo.

A análise do perfil protéico dos híbridos GM e convencional mantidos *in vitro,* aliada à caracterização de ontologias gênicas baseadas nas proteínas diferencialmente expressas, revelou a regulação diferencial de proteínas associadas a diversos processos biológicos, funções moleculares e componentes celulares, mais notavelmente metabolismo de carboidratos e energia, metabolismo de macromoléculas, respostas a stress, respostas a estímulos, e biossíntese de reguladores de crescimento. Vale ressaltar que proteínas relacionadas à biossíntese de triptofano, glutationa, AIA e ABA mostraram regulação diferencial significativa, estando diretamente relacionadas em tratamentos experimentais nos quais foram observadas diferenças ontogenéticas e morfogenéticas significativas entre os híbridos quase-isogênicos GM e convencional.

Em conjunto, os experimentos realizados indicam alterações nas respostas celulares do milho GM (MON810) a reguladores de crescimento exógenos, moduladas por uma complexa regulação diferencial do proteoma do milho, com conseqüências detectáveis para a taxa de crescimento e competência morfogenética *in vitro*. A combinação dos resultados

obtidos para indução de culturas, manutenção, proliferação, e indução de embriogênese somática, baseados no registro de características ontogenéticas, morfogenéticas e bioquímicas, evidenciam diferenças significativas entre o milho GM AG-5011YG (MON810) e seu HQI convencional AG-5011.

Com base na análise de alto rendimento do perfil protéico, foi possível acessar e delinear características-chave de uma complexa rede de ontologias gênicas refletindo a regulação diferencial de proteínas, com especial ênfase em processos biológicos, e um forte elo causal entre a modulação do perfil protéico observada, e as respostas ontogenéticas e morfogenéticas do modelo *in vitro*.

Estes resultados são parcialmente congruentes com a hipótese de que a expressão constitutiva e em níveis elevados do transgene *cry1Ab* no milho GM MON810 afeta a homeostase do sistema, redirecionando energia, moléculas orgânicas e outros recursos para a produção de grandes quantidades de proteína recombinante (Grover *et al.*, 2003; Muños-Mayor *et al.*, 2008; Agapito-Tenfen *et al.*, 2013, Holderbaum *et al*., 2015), por fim alterando a regulação protéica em uma ampla gama de processos biológicos.

As alterações observadas no proteoma dos HQIs GM e convencional refletem em respostas ontogenéticas e morfogenéticas diferenciais, em um ambiente altamente controlado. Portanto, o modelo *in vitro* desenvolvido permitiu a detecção de propriedades emergentes em um milho GM, comparado à sua contraparte quase-isogênica convencional. Com base neste quadro, e considerando o alto grau de similaridade entre linhas quase-isogênicas (híbridos quase-isogênicos, neste caso), sugere-se que as respostas diferenciais entre os milhos GM e convencional estão relacionadas à presença e atividade do cassete de expressão recombinante de MON810 no milho transgênico.

A ampla gama de efeitos observados no proteoma, bem como suas conseqüências ontogenéticas e morfogenéticas *in vitro*, podem estar relacionadas a custos biológicos extras decorrentes da expressão constitutiva da proteína Cry1Ab recombinante, e, adicionalmente, a presença de uma proteína exclusiva no milho GM, similar a MAPKKK, levanta a hipótese de uma possível resposta imune da planta à proteína Cry1Ab (uma toxina bacateriana formadora de poros) produzida em suas células (Pitzschke *et al*., 2009; Rasmussen *et al*., 2012; Meng and Zhang, 2013; Pitzschke, 2015; Xu *et al*, 2018). De todo modo, o conjunto de evidências aqui apresentadas e confrontadas indica que a integração e atividade do cassete de expressão gênica recombinante de MON810 influenciam significativamente o desenvolvimento do híbrido AG-5011YG, de acordo com o modelo *in vitro*.

Portanto, os resultados obtidos sugerem que o modelo *in vitro* desenvolvido é útil e eficiente para o estudo de conseqüências não-intencionais da modificação genética de plantas, aglutinando múltiplas características desejáveis de um bom modelo interativo (controle ambiental, reprodutibilidade, escalabilidade, e alta resolução de efeitos), com o emprego de modelos estatísticos e visuais avançados e estratégias modernas de construção de perfis metabólicos, auxiliando sobremaneira na empreitada de detectar e identificar propriedades emergentes em plantas transgênicas.

O teste final deste modelo deve ser sua validação, que pode ser efetivada ao se prospectar as variáveis-indicadoras-chave do modelo - tais como, neste caso, taxa de crescimento, resposta a estímulos, metabolismo de carboidratos e energia, metabolismo de macromoléculas, respostas a estresse, biossíntese de reguladores de crescimento, e níveis de proteínas MAPK - e escrutiná-las em plantas do mesmo par quase-isogênico (transgênico e convencional) cultivadas *in vivo*.

Concluindo, este modelo interativo e iterativo de cultura de células, tecidos e órgãos vegetais *in vitro* representa uma abordagem inovadora, factível, reproduzível, e de alta resolução de efeitos em comparações entre contrapartes GM e convencional de milhos híbridos, fornecendo uma plataforma de alta sensibilidade para detecção de propriedades emergentes da transformação genética de plantas, conforme refletidas em alterações nas respostas ontogenéticas e morfogenéticas do milho GM a estímulos ambientais controlados *in vitro*. Recomendamos que mais modelos interativos *in vitro* sejam empregados visando aumentar nossa habilidade de detecção de efeitos *off-target* da transformação genética de plantas, e buscar usos mais seguros da biotecnologia vegetal.

REFERÊNCIAS

AGAPITO-TENFEN, S.Z.; GUERRA, M.P.; WIKMARK, O.G.; NODARI, R.O. Comparative proteomic analysis of genetically modified maize grown under different agroecosystems conditions in Brazil. **Proteome Sci.**, v. 11, p. 46, 2013.

BALSAMO, G.M.; CANGAHUALA-INOCENTE, G.C.; BERTOLDO, J.B.; TERENZI H.; ARISI, A.C. Proteomic analysis of four Brazilian MON810 maize varieties and their four non-genetically-modified isogenic varieties. **J. Agr. Food Chem.**, v. 59, p. 11553-11559, 2011.

BARROS, E.; LEZAR, S.; ANTTONEN, M.J.; VAN DIJK, J.P.; RÖHLIG, R.M.; KOK, E.J.; ENGEL, K.H. Comparison of two GM maize varieties with a near-isogenic conventional variety using transcriptomics, proteomics and metabolomics. **Plant Biotechnol. J.**, v. 8, p. 436-451, 2010.

BÍBLIA, N. T., JOÃO 12:24. In Bíblia Sagrada, Nova Versão Transformadora, letra grande, 1ª Ed. São Paulo: Mundo Cristão, 2016. 1600 p.

CELLINI, F.; CHESSON, A.; COLQUHOUN, I.; CONSTABLE, A; DAVIES, H.V.; ENGEL, K.H.; GATEHOUSE, A.M.; KÄRENLAMPI, S.; KOK, E.J.; LEGUAY, J.J.; LEHESRANTA, S.; NOTEBORN, H.P.; PEDERSEN, J.; SMITH, M. Unintended effects and their detection in genetically modified crops. **Food and Chemical Toxicology**, v. 42, p. 1089-1125, 2004.

COLL, A.; NADAL, A.; PALAUDELMÀS, M.; MESSEGUER, J.; MELÉ, E.; PUIGDOMÈNECH, P.; PLA, M. Lack of repeatable differential expression patterns between MON810 and comparable commercial varieties of maize. **Plant Mol Biol.**, v. 68, p. 105-117, 2008.

COLL, A.; NADAL, A.; COLLADO, R.; CAPELLADES, G.; MESSEGUER, J.; MELÉ, E.; PALAUDELMÀS, M.; PLA, M. Gene expression profiles of MON810 and comparable conventional maize varieties cultured in the field are more similar than are those of conventional lines. **Transgenic Res.**, v. 18, p. 801–8. 2009.

COLL, A.; NADAL A.; COLLADO, R.; CAPELLADES, G.; KUBISTA, M.; MESSEGUER, J; PLA, M. Natural variation explains most transcriptomic changes among maize plants of MON810 and comparable conventional varieties subjected to two N-fertilization farming practices. **Plant Mol. Biol.**, v. 73, p. 349–362, 2010.

EINSTEIN, A. On the Method of Theoretical Physics, p. 183. The Herbert Spencer Lecture, palestra ministrada em Oxford (10 Junho de 1933).

EMONS, A.M.C.; SAMALLO-DROPPERS, A.; VAN DER TOOM, C. The influence of sucrose, mannitol. L-proline, abscisic acid and gibberellic acid on the maturation of somatic embryos of *Zea mays* L. from suspension cultures. **Plant Physiol.**, v. 142, p. 597-604, 1993.

FAN, J.; LIU, X.; XU, S.X.; XU, Q.; GUO, W. T-DNA direct repeat and 35S promoter methylation affect transgene expression but do not cause silencing in transgenic sweet orange. **Plant Cell Tissue and Organ Culture**, v. 107, p. 225-232, 2011.

GROVER, A.; AGGARWAL, P.K.; KAPOOR, A.; KATIYAR-AGARWAL, S.; AGARWAL, M.; CHANDRAMOULI, A. Addressing abiotic stresses in agriculture through transgenic technology. **Curr. Sci. India**, v. 84, p. 355-367, 2003.

HOLDERBAUM, D.F.; CUHRA, M.; WICKSON, F.; ORTH, A.I.; NODARI, O.R.; BØHN, T. Chronic responses of *Daphnia magna* under dietary exposure to leaves of a transgenic (event MON810) Bt–maize hybrid and its conventional near-isoline. **Journal of Toxicology and Environmental Health, Part A**, v. 78, p. 993-1007, 2015.

LA PAZ, J.L.; PLA, M.; CENTENO, E.; VICIENT, C.M.; PUIGDOMÈNECH, P. The use of massive sequencing to detect differences between immature embryos of MON810 and a comparable conventional maize variety. **PLoS ONE**, v. 9(6), e100895. Disponível em: https://doi.org/10.1371/journal.pone.0100895.

MENG, X.; ZHANG, S. MAPK cascades in plant disease resistance signaling. **Annu. Rev. Phytopathol.**, v. 51, p. 245-266, 2013.

MUÑOZ-MAYOR, A.; PINEDA, B.; GARCIA-ABELLÁN, J.O.; GARCIA-SOGO, B.; MOYANO, E.; ATARES, A.; VICENTE-AGULLÓ, F.; SERRANO, R.; MORENO, V.; BOLARIN, M.C. The HAL1 function on Na + homeostasis is maintained over time in salt-treated transgenic tomato plants, but the high reduction of Na + in leaf is not associated with salt tolerance. **Physiol Plantarum**, v. 133, p. 288-297, 2008.

PITZSCHKE, A.; SCHIKORA, A.; HIRT, H. MAPK cascade signaling networks in plant defence. **Curr. Opin. Plant Biol.**, v. 12, p. 421-426, 2009.

PITZSCHKE, A. Modes of MAPK substrate recognition and control. **Trends Plant Sci.**, v. 20, p. 49-55, 2015.

QUÉTIER, F. The CRISPR-Cas9 technology: Closer to the ultimate toolkit for targeted genome editing. **Plant Science**, v. 242, p. 65-76, 2016.

RASMUSSEN, M.W.; ROUX, M.; PETERSEN, M.; MUNDY, J. MAP kinase cascades in Arabidopsis innate immunity. **Front. Plant Sci.**, v. 3, 169, 2012. Disponível em: http://doi.org/10.3389/fpls.2012.00169.

WEINHOLD, A.; KALLENBACH, A.; BALDWIN, T. Progressive 35S promoter methylation increases rapidly during vegetative development in transgenic *Nicotiana attenuata* plant. **BMC Plant Biology**, v. 13:99, 2013.

WILHELM, R. I Ching: O livro das mutações. Prefácio de C.G. Jung. Trad, Alayde Mutzenbecher e Gustavo Alberto Corrêa Pinto. São Paulo: Ed. Pensamento, 1998.

XU, H.Y.; ZHANG, C.; LI, Z.C.; WANG, Z.R.; JIANG, X.X.; SHI, Y.F.; TIAN, S.N.; BRAUN, E.; MEI, Y.; QIU, W.L.; LI, S.; WANG, B.; XU, J.; NAVARRE, D.; REN, D.; CHENG, N.; NAKATA, P.A.; GRAHAM, M.A.; WHITHAM, S.A.; LIU, J.Z. The MAPK Kinase Kinase GmMEKK1 Regulates Cell Death and Defense Responses. **Plant Physiology**, v. 178, n. 2, p. 907-922, 2018. Disponível em: http://doi.org/10.1104/pp.18.00903.

ZOLLA, L.; RINALDUCCI, S.; ANTONIOLI, P.; RIGHETTI, P.G. Proteomics as a complementary tool for identifying unintended side effects occurring in transgenic maize seeds as a result of genetic modifications. **J. Proteome Res.**, v. 7, p. 1850-1861, 2008.

APÊNDICES

Tabela 1: Lista de Proteínas diferencialmente expressas, antes da análise de enriquecimento de ontologias gênicas. Valores de Fold_chage maiores que 1,0 indicam sobre-expressão, e menores do que 1,0 indicam sub-expressão.

Accession	Peptide count	Confidence score	Anova (p)	Description	Fold_change Transgenic/Isogenic
A0A1D6KP53	3	13.8	0.0162	Uncharacterized protein	9.30
A0A1D6E5T4	2	14.9	0.0274	Uncharacterized protein	9.15
K7V364	9	50.7	0.0094	Uncharacterized protein	7.79
A0A1D6J4U6	4	18.3	0.0127	Uncharacterized protein	7.44
B4FWD0	2	11.5	0.0170	Minor allergen Alt a 7	7.38
K7VUA7	2	10.4	0.0100	Cysteine-type peptidase	6.98
A0A1D6MUJ3	3	15.2	0.0061	Uncharacterized protein	5.99
A0A1D6KX49	3	32.1	0.0227	Uncharacterized protein	5.65
B4FGU5	2	11.4	0.0009	Uncharacterized protein	5.48
B4FFW5	4	31.8	0.0057	Uncharacterized protein	5.42

A0A1D6N0K3	10	60.1	0.0003	Uncharacterized protein	5.27
K7TN25	2	14.1	0.0077	Uncharacterized protein	4.98
B4FH43	5	32.8	0.0028	Uncharacterized protein	4.66
A0A1D6J0T5	2	8.8	0.0075	Uncharacterized protein	4.46
A0A1D6H6W8	4	20.6	0.0475	Uncharacterized protein	4.45
A0A1D6DVI6	7	40.2	0.0276	Uncharacterized protein	4.38
B4FRK0	2	19.5	0.0015	Uncharacterized protein	4.32
A0A1D6LJ10	4	25.2	0.0009	Uncharacterized protein	4.04
B4FJE0	3	15.9	0.0138	Uncharacterized protein	4.04
B4FQC6	6	33.4	0.0024	Glucose-6-phosphate isomerase	3.92
C0P3K5	3	27.7	0.0008	Uncharacterized protein	3.91
A0A1D6MPD4	7	44.0	0.0127	Uncharacterized protein	3.85

A0A1D6IKV5	5	28.1	0.0007	Uncharacterized protein	3.66
Q94KS8	10	80.5	0.0001	Beta-expansin 1a	3.62
A0A1D6FWU8	5	28.0	0.0426	Uncharacterized protein	3.44
B6SN61	4	33.7	0.0476	Grx_C2.1-glutaredoxin subgroup I	3.30
A0A096UAZ3	2	10.8	0.0006	Uncharacterized protein	3.25
G0YVY8	10	91.5	0.0126	Pathogenesis-related protein 1	3.17
K7UTZ8	2	10.8	0.0278	4-methyl-5-thiazole monophosphate biosynthesis protein	3.10
A0A1D6LLS5	12	71.5	0.0015	Uncharacterized protein	3.08
A0A1D6KF26	10	44.5	0.0162	Uncharacterized protein	3.03
Q4FZ50	3	19.0	0.0030	Cysteine proteinase inhibitor	3.01
B4FXZ3	3	27.1	0.0307	Grx_C2.2-glutaredoxin subgroup I	2.98
A0A1D6KWA8	3	14.1	0.0410	Uncharacterized protein	2.95

A0A1D6P3I8	4	19.5	0.0042	Uncharacterized protein	2.94
A0A1D6PWB5	4	20.8	0.0416	Uncharacterized protein	2.89
A0A1D6N932	8	52.0	0.0008	Uncharacterized protein	2.67
A0A1D6LL73	2	11.2	0.0456	Uncharacterized protein	2.56
A0A1D6JDW4	3	14.7	0.0010	Uncharacterized protein	2.51
B6ST82	2	18.3	0.0396	Putative uncharacterized protein	2.47
P49174	8	59.6	0.0065	Beta-fructofuranosidase. cell wall isozyme	2.47
C1K9J1	25	249.7	0.0004	Heat shock protein 90	2.42
A0A1D6EK96	5	22.7	0.0459	Uncharacterized protein	2.28
K7UYX0	4	18.1	0.0296	Ubiquitin carboxyl-terminal hydrolase isoform 1	2.25
A0A1D6JZU3	4	31.5	0.0035	Uncharacterized protein	2.21

C0PBM0	5	23.4	0.0025	Uncharacterized protein	2.19
A0A1D6ECA8	2	15.2	0.0047	Uncharacterized protein	2.11
A0A1D6HTN9	7	60.3	0.0014	Uncharacterized protein	2.09
A0A1D6PZF6	4	18.2	0.0477	Uncharacterized protein	2.08
A0A1D6HLD1	4	19.8	0.0064	Uncharacterized protein	2.08
A0A1D6K996	12	66.5	0.0194	Uncharacterized protein	2.07
B4FY73	8	61.0	0.0010	Uncharacterized protein	2.06
A0A1D6KAJ0	7	32.9	0.0171	Uncharacterized protein	2.05
A0A1D6GTT1	4	17.8	0.0098	Uncharacterized protein	2.04
B6TSD7	11	90.1	0.0031	Peroxidase	2.01
A0A1D6JG12	8	74.9	0.0021	Uncharacterized protein	2.01
A0A1D6HDK1	11	120.1	0.0115	Uncharacterized protein	2.01
A0A1D6FS51	3	13.6	0.0387	Uncharacterized protein	1.98

B4FHR5	3	13.8	0.0082	RAB. member of RAS oncogene family-like 3	1.98
B4FG39	4	23.0	0.0023	Peroxidase	1.95
A0A1D6L727	8	47.9	0.0093	Uncharacterized protein	1.95
A0A1D6GMR6	12	57.2	0.0347	Uncharacterized protein	1.92
A0A1D6HW24	6	30.4	0.0264	Uncharacterized protein	1.91
B6TMI9	12	85.6	0.0218	Peroxidase	1.86
K7V8K5	17	130.0	0.0233	Peroxidase	1.86
A0A1D6MDU2	2	13.4	0.0013	Uncharacterized protein	1.83
A0A1D6HLQ4	8	43.5	0.0296	Uncharacterized protein	1.81
A0A1D6IDT6	3	14.5	0.0040	Uncharacterized protein	1.79
A0A1D6EX96	13	65.6	0.0018	Uncharacterized protein	1.78
A0A1D6K177	9	42.9	0.0074	Uncharacterized protein	1.77
Q4W1F6	3	23.4	0.0123	Thioredoxin H-type	1.76

A0A1D6QSE2	2	13.6	0.0358	Uncharacterized protein	1.76
A0A1D6GNH6	3	13.1	0.0144	Uncharacterized protein	1.71
Q08277	11	77.8	0.0050	Heat shock protein 82	1.71
A0A1D6MTS1	6	32.9	0.0250	Uncharacterized protein	1.70
C0HHC4	3	23.6	0.0004	Nucleoside diphosphate kinase	1.67
B6TYM9	2	10.2	0.0096	Vignain	1.65
B4G031	8	79.0	0.0106	Uncharacterized protein	1.64
B4FEC3	4	19.4	0.0436	Pyruvate kinase	1.63
A0A1D6GES4	6	28.0	0.0078	Uncharacterized protein	1.62
A0A1D6H186	5	23.2	0.0002	Uncharacterized protein	1.60
B6SKN3	2	11.9	0.0077	1.2-dihydroxy-3-keto-5-methylthiopentene dioxygenase	1.59
A0A1D6GN91	3	14.9	0.0183	Uncharacterized protein	1.59
B6TNF1	13	94.7	0.0102	Calnexin	1.58

A0A1D6P2B1	3	13.8	0.0104	Uncharacterized protein	1.57
A0A1D6H976	2	10.3	0.0315	Uncharacterized protein	1.55
Q42420	6	53.7	0.0010	Proteinase inhibitor	1.55
B6U3Y1	9	65.5	0.0039	Versicolorin reductase	1.52
A0A1D6GGY2	4	19.2	0.0094	Uncharacterized protein	1.52
A0A1D6FEG7	2	8.3	0.0252	Uncharacterized protein	1.50
A0A1D6NEL8	3	13.9	0.0000	Uncharacterized protein	-
A0A1D6MR41	14	73.6	0.0002	Uncharacterized protein	0.03
B4FLZ9	2	10.3	0.0007	Uncharacterized protein	0.04
K7UZU9	8	64.0	0.0001	Uncharacterized protein	0.11
B6SUP5	7	40.3	0.0058	Cytochrome P450 CYP74A19	0.13
B6SJ08	3	18.9	0.0003	60S ribosomal protein L18	0.16

B6SS31	14	136.5	0.0048	Putative uncharacterized protein	0.19
A0A1D6DUP7	6	31.0	0.0008	Uncharacterized protein	0.21
C0P3L1	7	37.8	0.0001	Uncharacterized protein	0.21
B6T7L9	14	123.4	0.0003	14-3-3-like protein	0.21
A0A1D6EM17	10	48.9	0.0236	Uncharacterized protein	0.22
B4FHX7	2	10.7	0.0263	1.4-beta-D-glucanase	0.23
K7VXH3	2	10.0	0.0197	Uncharacterized protein	0.25
B8A312	5	28.7	0.0128	Uncharacterized protein	0.27
C4J4W3	10	53.9	0.0145	Uncharacterized protein	0.30
A0A1D6MSE3	9	65.7	0.0019	Uncharacterized protein	0.30
Q71RX2	3	16.9	0.0000	Isopentenyl pyrophosphate isomerase	0.31
B4FFA5	9	53.3	0.0386	Purple acid phosphatase	0.34
B6TGT0	2	12.2	0.0269	60S ribosomal	0.34

				protein L2	
A0A1D6DU44	2	12.5	0.0080	Uncharacterized protein	0.35
K7UQL4	3	14.7	0.0127	Uncharacterized protein	0.35
B6T4R3	22	217.6	0.0036	UTP--glucose-1-phosphate uridylyltransferase	0.36
A0A1D6H6G9	5	22.7	0.0192	Uncharacterized protein	0.37
A0A1D6EIB6	16	97.1	0.0114	Uncharacterized protein	0.37
A0A1D6NVK8	3	15.3	0.0021	Uncharacterized protein	0.38
A0A1D6E7Z4	4	21.6	0.0080	Uncharacterized protein	0.38
A0A1D6KA83	3	13.0	0.0192	Uncharacterized protein	0.39
A0A1D6DQH1	5	24.6	0.0227	Uncharacterized protein	0.39
K7UDG5	10	69.1	0.0115	Uncharacterized protein	0.41
K7U884	3	13.5	0.0428	Uncharacterized protein	0.41

B4FPM1	5	34.9	0.0079	Uncharacterized protein	0.41
B6UAD0	2	11.2	0.0016	26S proteasome non-ATPase regulatory subunit 13	0.42
B6TYG2	9	59.7	0.0148	Enoyl-[acyl-carrier-protein] reductase [NADH]	0.43
A0A1D6LFA7	13	84.2	0.0064	Uncharacterized protein	0.43
A0A1D6PUE6	3	15.0	0.0189	Uncharacterized protein	0.43
A0A1D6ENT5	11	70.0	0.0037	Uncharacterized protein	0.43
B4FAM6	3	17.7	0.0308	Uncharacterized protein	0.43
C4J093	12	86.6	0.0048	Uncharacterized protein	0.44
C0PCV2	6	62.4	0.0332	40S ribosomal protein S8	0.44
A0A1D6MAM0	2	15.5	0.0004	Uncharacterized protein	0.45
B7ZXI9	3	15.3	0.0033	Uncharacterized protein	0.45
B6SSB7	3	31.0	0.0037	Protein kinase	0.45

A0A1D6PPA4	3	13.3	0.0215	Uncharacterized protein	0.46
B6SNQ1	4	26.6	0.0067	Universal stress protein	0.47
C0PD27	7	39.5	0.0391	Isocitrate dehydrogenase [NADP]	0.47
O48557	2	10.4	0.0189	60S ribosomal protein L17	0.47
B6TPA2	7	50.9	0.0334	Putative uncharacterized protein	0.48
A0A1D6J5X9	9	83.2	0.0028	Uncharacterized protein	0.48
A0A1D6L718	9	55.4	0.0019	Uncharacterized protein	0.49
C4J6J5	3	18.7	0.0367	40S ribosomal protein S6	0.50
B6SHM7	3	18.4	0.0084	40S ribosomal protein S7	0.50
K7V3I5	15	108.6	0.0420	Tubulin beta chain	0.51
A0A1D6LPH1	7	48.9	0.0038	Uncharacterized protein	0.51
A0A1D6GBW9	3	14.3	0.0185	Uncharacterized	0.52

				protein	
A0A1D6H2L6	4	19.6	0.0046	Uncharacterized protein	0.52
K7V934	2	14.8	0.0324	Uncharacterized protein	0.53
A0A1D6E267	5	28.8	0.0137	Uncharacterized protein	0.54
C4J9R8	4	25.0	0.0200	Anaphase-promoting complex subunit 10	0.54
Q43712	15	116.3	0.0479	Calcium-binding protein	0.54
A0A1D6L2L2	8	36.5	0.0058	Uncharacterized protein	0.55
A0A1D6L4K3	6	37.3	0.0482	Uncharacterized protein	0.55
B4FCG9	4	23.6	0.0178	60S ribosomal protein L11-1	0.56
A0A1D6G5Q1	2	9.4	0.0020	Uncharacterized protein	0.56
A0A1D6DW07	11	100.7	0.0238	Uncharacterized protein	0.56
B4FP25	6	44.5	0.0002	40S ribosomal protein S19	0.57
B4G1P4	3	18.8	0.0017	GTP-binding nuclear protein	0.57

A0A1D6H687	4	22.5	0.0043	Uncharacterized protein	0.57
A0A1D6F822	7	33.8	0.0345	Uncharacterized protein	0.57
B6TB39	28	271.1	0.0046	Fructokinase-2	0.58
A0A1D6MMZ3	2	10.2	0.0011	Uncharacterized protein	0.58
A0A1D6N4X2	8	49.4	0.0262	Uncharacterized protein	0.58
A0A1D6IXD5	7	39.0	0.0058	Uncharacterized protein	0.58
B4FHX3	7	55.6	0.0236	Uncharacterized protein	0.58
A0A1D6GYI3	3	15.0	0.0237	Uncharacterized protein	0.58
P93804	17	117.8	0.0320	Phosphoglucomutase. cytoplasmic 1	0.59
B6T1R0	2	12.8	0.0105	60S ribosomal protein L22-2	0.59
A0A1D6EAC4	6	31.8	0.0059	Uncharacterized protein	0.59
B6SIG8	2	20.8	0.0202	60S acidic ribosomal protein P2A	0.59

B4FDB1	5	33.7	0.0390	Uncharacterized protein	0.60
B6SHF6	8	49.4	0.0332	Mitochondrial-processing peptidase alpha subunit	0.61
A0A1D6NAN3	5	27.5	0.0455	Uncharacterized protein	0.61
A0A1D6JQ06	4	23.7	0.0006	Uncharacterized protein	0.61
B6T3D4	4	18.8	0.0288	Methionyl-tRNA synthetase	0.61
K7TQM8	3	13.9	0.0459	DNA mismatch repair protein	0.62
A0A1D6III6	2	9.2	0.0154	Uncharacterized protein	0.62
B4FH75	3	14.3	0.0317	Dihydrodipicolinate reductase	0.62
A0A1D6IYH3	5	24.2	0.0330	Uncharacterized protein	0.62
A0A1D6LN76	5	41.5	0.0166	Uncharacterized protein	0.63
A0A1D6KIZ4	2	10.1	0.0081	Uncharacterized protein	0.63
B6TRV0	5	28.9	0.0078	Membrane steroid-binding protein 1	0.63

K7U267	6	29.7	0.0128	Glucose-6-phosphate 1-dehydrogenase	0.63
B6U118	10	69.9	0.0169	T-complex protein 1 subunit zeta	0.63
C0P4M0	11	66.9	0.0103	Uncharacterized protein	0.63
B4F9I2	3	15.2	0.0248	RuvB-like helicase	0.64
A0A1D6MAD7	3	13.2	0.0119	Uncharacterized protein	0.64
K7VI04	5	29.7	0.0081	Uncharacterized protein	0.64
B4FZC0	3	17.0	0.0363	Uncharacterized protein	0.64
A0A1D6M2S2	10	50.2	0.0030	Uncharacterized protein	0.65
B4FPZ7	3	20.9	0.0058	GrpE protein homolog	0.65
A0A1D6LQT2	4	25.4	0.0222	Uncharacterized protein	0.65
A0A1D6DVL4	5	24.9	0.0083	Uncharacterized protein	0.65
A0A1D6NVF9	4	33.3	0.0265	Uncharacterized protein	0.65

B6TKY3	6	35.8	0.0279	Putative TCP-1/cpn60 chaperonin family protein	0.65
A0A1D6H3A8	2	10.7	0.0149	Uncharacterized protein	0.65
B6TNR8	2	12.1	0.0148	40S ribosomal protein S2	0.66
K7V958	2	11.1	0.0373	Uncharacterized protein	0.66
K7WGQ3	8	48.7	0.0119	DAG protein	0.66

Fonte: Daniel Ferreira Holderbaum (2019).

Tabela 2: Lista de proteínas sobre-expressas (up-regulated) em culturas de milho transgênico em proliferção in vitro, após análise de enriquecimento de ontologias gênicas. Para ontologias gênicas, "P" indica processos biológicos, "F" indica funções moleculares, e "C" indica componentes celulares.

Nome da Seqüência	Descrição	Similaridade (%)	Ontologias gênicas
A0A096UAZ3	3-isopropylmalate dehydratase small subunit 3-like	90.04	F:catalytic activity; P:metabolic process; C:plastid
A0A1D6DVI6	probable phosphoribosylformylglycinamidine chloroplastic mitochondrial	96.28	F:nucleotide binding; P:nucleobase-containing compound metabolic process; P:biosynthetic process; C:plastid; F:transferase activity
A0A1D6E5T4	probable metal-nicotianamine transporter YSL11	87.8	P:transport; C:membrane
A0A1D6ECA8	Sec-independent translocase chloroplastic	86.12	F:transporter activity; C:plasma membrane; C:plastid; C:thylakoid; P:cellular process
A0A1D6EK96			F:protein binding; P:cellular protein modification process; F:transferase activity

A0A1D6EX96	Phospholipase A I	97.28	F:protein binding; P:lipid metabolic process; P:catabolic process; P:biosynthetic process; P:response to external stimulus; P:response to biotic stimulus; P:cellular process; F:hydrolase activity
A0A1D6FEG7	WD40 YVTN repeat-like-containing domain	97.33	F:protein binding
A0A1D6FS51	hAT transposon superfamily	88.71	F:nucleic acid binding; F:protein binding
A0A1D6FWU8	transducin family WD-40 repeat family	92.32	F:protein binding
A0A1D6GES4	DNA gyrase subunit A chloroplastic mitochondrial	93.62	F:nucleotide binding; F:DNA binding; C:nucleoplasm; C:mitochondrion; P:DNA metabolic process; P:biosynthetic process; C:plastid; P:cellular component organization; F:hydrolase activity
A0A1D6GGY2	Phytochrome C	97.18	F:obsolete signal transducer activity; F:protein binding; C:nucleus; P:nucleobase-containing compound metabolic process; P:cellular protein modification process; P:biosynthetic process; P:response to external stimulus; P:response to abiotic stimulus; F:kinase activity; F:signaling receptor activity
A0A1D6GMR6	peptidase C48 domain family	91.06	C:intracellular; P:DNA metabolic process; P:response to stress; P:cellular component organization; F:hydrolase activity
A0A1D6GN91	Tubulin-folding cofactor D	96.15	P:reproduction; F:protein binding; C:cytosol; C:cytoskeleton; P:embryo development; P:post-embryonic development; P:cellular component organization; F:enzyme regulator activity
A0A1D6GNH6	Myosin heavy chain-related	96.82	
A0A1D6GTT1	Structural maintenance of chromosomes 5	93.96	C:intracellular; P:DNA metabolic process; P:response to stress; P:cell cycle; P:cellular component organization

A0A1D6H186	D -box ATP-dependent RNA helicase D 11	90.76	F:nucleotide binding; F:RNA binding; C:vacuole; P:nucleobase-containing compound metabolic process; P:transport; P:catabolic process; F:hydrolase activity
A0A1D6H6W8	Eukaryotic initiation factor 4A-2	71.42	F:nucleotide binding; F:nucleic acid binding
A0A1D6H976	MEI2-like 1	94.34	F:nucleotide binding; F:nucleic acid binding
A0A1D6HDK1	Adenosine kinase 2	96.88	P:nucleobase-containing compound metabolic process; P:biosynthetic process; F:kinase activity
A0A1D6HLD1	PHD finger family	95.99	
A0A1D6HLQ4	hypothetical protein *ZEA*MMB73_Zm00001d018231	90.21	C:intracellular; P:DNA metabolic process; P:response to stress; P:cellular component organization; F:hydrolase activity
A0A1D6HTN9	xylanase inhibitor 1	83.98	F:binding; C:extracellular region; P:carbohydrate metabolic process; P:response to stress; P:catabolic process; P:cellular process; F:hydrolase activity
A0A1D6HW24	Pentatricopeptide repeat-containing mitochondrial	82.99	F:protein binding
A0A1D6IDT6	syntaxin-132-like	76.11	F:nucleotide binding; F:transporter activity; F:protein binding; C:cytoplasm; C:plasma membrane; P:cellular component organization; F:hydrolase activity
A0A1D6IKV5	tolB -related	82.46	P:proteolysis
A0A1D6J0T5	L-type lectin-domain containing receptor kinase	79.57	F:nucleotide binding; P:cellular protein modification process; C:membrane; F:kinase activity; F:carbohydrate binding
A0A1D6J4U6	RAE1	96.65	F:protein binding
A0A1D6JDW4	26S proteasome non-ATPase regulatory subunit 1 homolog B	94.35	F:binding; C:nucleus; C:cytosol; P:catabolic process; P:cellular process; C:membrane; F:hydrolase activity; P:protein metabolic process; F:enzyme regulator activity
A0A1D6JG12	Cysteine protease 1	93.22	F:hydrolase activity; P:protein metabolic process

A0A1D6JZU3	pathogenesis-related 1	92.32	C:nucleus; C:cytoplasm; P:cellular protein modification process; P:response to stress; P:signal transduction; F:lipid binding; P:response to biotic stimulus; P:response to endogenous stimulus; F:enzyme regulator activity; F:signaling receptor activity
A0A1D6K177	NB-ARC domain containing expressed	88.79	F:nucleotide binding; C:intracellular; P:DNA metabolic process; P:response to stress; P:cellular component organization; F:hydrolase activity; P:protein metabolic process
A0A1D6K996	ATP-dependent RNA helicase mitochondrial		C:intracellular; P:carbohydrate metabolic process; P:DNA metabolic process; P:response to stress; P:biosynthetic process; P:cellular component organization; F:hydrolase activity; P:protein metabolic process
A0A1D6KAJ0	uncharacterized protein LOC100272722 isoform X1	98.12	
A0A1D6KF26	uncharacterized protein LOC103640525 isoform X1	92.01	
A0A1D6KP53	Uridine 5 - monophosphate synthase	90.63	
A0A1D6KWA8	paladin isoform X1	95.63	C:nucleus; C:cytosol; P:cellular protein modification process; F:hydrolase activity
A0A1D6KX49	L-type lectin-domain containing receptor kinase	86.16	F:nucleotide binding; P:carbohydrate metabolic process; P:generation of precursor metabolites and energy; P:nucleobase-containing compound metabolic process; P:cellular protein modification process; P:lipid metabolic process; P:catabolic process; P:biosynthetic process; C:membrane; F:kinase activity; F:carbohydrate binding

A0A1D6L727	aldehyde oxidase1	95.46	F:nucleotide binding; F:catalytic activity; C:cytosol; P:nucleobase-containing compound metabolic process; P:lipid metabolic process; P:catabolic process; P:biosynthetic process
A0A1D6LJ10	ubiquitin receptor1	97.38	F:binding; F:hydrolase activity
A0A1D6LL73	ATP-dependent 6-phosphofructokinase 3	93.39	F:nucleotide binding; C:cytosol; P:carbohydrate metabolic process; P:generation of precursor metabolites and energy; P:nucleobase-containing compound metabolic process; P:catabolic process; P:biosynthetic process; C:plastid; F:kinase activity
A0A1D6LLS5	2-oxoglutarate mitochondrial-like	96.17	F:catalytic activity; F:binding; C:mitochondrion; C:cytosol; P:generation of precursor metabolites and energy; P:catabolic process
A0A1D6MDU2	GBF-interacting 1	89.87	F:protein binding
A0A1D6MPD4	Cysteine synthase mitochondrial	93.83	F:binding; P:biosynthetic process; C:plastid; P:cellular process; C:membrane; F:transferase activity
A0A1D6MTS1	Ubiquitin carboxyl-terminal hydrolase 13	93.23	F:protein binding; P:cellular protein modification process; P:catabolic process; F:hydrolase activity
A0A1D6MUJ3	AAA-type ATPase family	86.11	F:nucleotide binding
A0A1D6N0K3	cationic peroxidase SPC4-like	84.5	F:catalytic activity; F:binding; C:extracellular region; C:cell wall; P:response to stress; P:catabolic process; P:cellular component organization
A0A1D6N932	alpha-amylase trypsin inhibitor-like	80.55	
A0A1D6P2B1	receptor kinase 1	83.85	F:nucleotide binding; C:plasma membrane; P:cellular protein modification process; P:pollen-pistil interaction; F:kinase activity
A0A1D6P3I8	Transcription initiation factor TFIID subunit	92.05	F:protein binding; C:nucleus; P:nucleobase-containing compound metabolic process; P:biosynthetic process
A0A1D6PWB5	replication A 70 kDa DNA-binding subunit A-like isoform X2	79.53	
A0A1D6PZF6	formin 6 isoform	85.21	P:cellular protein modification process; F:hydrolase

	X1		activity
A0A1D6QSE2	porphobilinogen chloroplastic	85.46	P:cellular protein modification process; P:biosynthetic process; C:plastid; F:transferase activity
B4FEC3	pyruvate kinase isozyme chloroplastic	94.17	P:reproduction; F:binding; P:carbohydrate metabolic process; P:generation of precursor metabolites and energy; P:nucleobase-containing compound metabolic process; P:lipid metabolic process; P:catabolic process; P:biosynthetic process; C:plastid; P:post-embryonic development; F:kinase activity
B4FFW5	universal stress PHOS32	91.66	C:plasma membrane; P:response to stress; P:response to external stimulus; P:response to biotic stimulus
B4FG39	cationic peroxidase SPC4-like	81.27	F:catalytic activity; F:binding; C:extracellular region; C:cell wall; P:response to stress; P:catabolic process; P:cellular component organization
B4FGU5	putidaredoxin reductase homolog1	80.88	F:nucleotide binding; F:catalytic activity; C:cell; P:generation of precursor metabolites and energy; C:membrane; P:cellular homeostasis
B4FH43	universal stress	89.87	P:response to stress
B4FHR5	Ras-related small GTP-binding family	93.42	F:nucleotide binding; C:intracellular; P:signal transduction; F:hydrolase activity
B4FJE0	endo-1,3(4)-beta-glucanase 2	89.75	C:cell; P:carbohydrate metabolic process; P:catabolic process; P:cellular process; F:hydrolase activity
B4FQC6	glucose-6-phosphate isomerase chloroplastic	95.83	F:catalytic activity; P:carbohydrate metabolic process; P:generation of precursor metabolites and energy; P:nucleobase-containing compound metabolic process; P:catabolic process; P:biosynthetic process; C:plastid
B4FRK0	fiber Fb19	89.66	P:response to stress
B4FWD0	NAD(P)H dehydrogenase (quinone) FQR1	96.06	F:nucleotide binding; F:catalytic activity; P:nucleobase-containing compound metabolic process; P:lipid metabolic process; P:biosynthetic process
B4FXZ3	glutaredoxin subgroup I	92.91	F:catalytic activity; C:extracellular region; C:vacuole; C:Golgi apparatus; C:cytosol; C:plasma membrane; P:generation of precursor metabolites and energy;

			P:cellular homeostasis
B4FY73	germin 1-1	93.93	F:catalytic activity; F:binding; C:extracellular region; C:cell wall; P:transport; P:multicellular organism development; P:metabolic process; P:cellular process
B4G031	L-ascorbate peroxidase cytosolic	97.47	F:catalytic activity; F:binding; C:cytoplasm; P:carbohydrate metabolic process; P:response to stress; P:catabolic process; P:cellular process
B6SKN3	1,2-dihydroxy-3-keto-5-methylthiopentene dioxygenase 2	97.07	F:catalytic activity; F:binding; C:nucleus; C:cytoplasm; P:biosynthetic process; P:cellular process
B6SN61	glutaredoxin subgroup I	89.61	F:catalytic activity; C:extracellular region; C:vacuole; C:Golgi apparatus; C:cytosol; C:plasma membrane; P:generation of precursor metabolites and energy; C:plastid; P:cellular homeostasis
B6ST82	copper transport ATX1	96.09	F:binding; C:cytoplasm; P:transport; P:cellular homeostasis
B6TMI9	Peroxidase 1	83.7	F:catalytic activity; F:binding; C:extracellular region; C:cell wall; P:response to stress; P:catabolic process; P:cellular component organization
B6TNF1	calnexin homolog	95.35	F:protein binding; C:endoplasmic reticulum; P:cellular process; C:membrane
B6TSD7	peroxidase 1	87.5	F:catalytic activity; F:binding; C:extracellular region; C:cell wall; C:vacuole; P:response to stress; P:catabolic process; P:cellular component organization
B6TYM9	thiol protease SEN102-like	89.36	C:extracellular space; C:lysosome; P:catabolic process; P:cellular process; C:membrane; F:hydrolase activity; P:protein metabolic process
B6U3Y1	short-chain type dehydrogenase reductase-like	89.21	
C0HHC4	nucleoside diphosphate kinase 1	96.9	F:nucleotide binding; C:intracellular; P:nucleobase-containing compound metabolic process; P:biosynthetic process; F:kinase activity

C0P3K5	pyruvate dehydrogenase E1 component subunit beta-mitochondrial	98.68	F:catalytic activity; C:mitochondrion; P:carbohydrate metabolic process; P:generation of precursor metabolites and energy; P:nucleobase-containing compound metabolic process; P:catabolic process; P:biosynthetic process
C0PBM0	ATP-dependent RNA helicase mitochondrial	94.77	F:nucleotide binding; C:nucleus; C:mitochondrion; P:nucleobase-containing compound metabolic process; P:response to stress; P:signal transduction; P:biosynthetic process; P:response to abiotic stimulus; P:response to endogenous stimulus; P:cellular component organization; F:hydrolase activity
C1K9J1	heat shock 90	97.72	F:nucleotide binding; F:protein binding; C:cytoplasm; P:response to stress; P:cellular process
G0YVY8	pathogenesis-related 1	93.06	C:nucleus; C:cytoplasm; P:cellular protein modification process; P:response to stress; P:signal transduction; F:lipid binding; P:response to biotic stimulus; P:response to endogenous stimulus; F:enzyme regulator activity; F:signaling receptor activity
K7TN25	EXB18_ORYSJ ame: Full=Expansin-B18 ame: Full=Beta-expansin-18 ame: Full= 18 ame: Full= Flags: Precursor	85.88	P:reproduction; C:extracellular region; C:cell wall; C:membrane; P:cellular component organization
K7UTZ8	DJ-1 homolog B	78.94	F:catalytic activity; C:nucleus; C:mitochondrion; C:cytosol; P:nucleobase-containing compound metabolic process; P:response to stress; P:catabolic process; P:biosynthetic process
K7UYX0	ubiquitin carboxyl-terminal hydrolase 14	93.53	F:protein binding; P:cellular protein modification process; P:catabolic process; F:hydrolase activity
K7V364	heat shock 90-chloroplastic	93.6	F:nucleotide binding; F:protein binding; P:response to stress; C:plastid; P:cellular process

K7V8K5	Peroxidase 1	90.04	F:catalytic activity; F:binding; C:extracellular region; C:cell wall; P:response to stress; P:catabolic process; P:cellular component organization
K7VUA7	ubiquitin-like-specific protease 1D isoform X2	69.02	F:hydrolase activity; P:protein metabolic process
P49174	cell wall invertase	91.0	C:extracellular region; C:cell wall; C:endoplasmic reticulum; P:carbohydrate metabolic process; P:cellular process; F:hydrolase activity
Q08277	heat shock 90	94.0	F:nucleotide binding; F:protein binding; C:cytoplasm; P:response to stress; P:cellular process
Q42420	maize ase inhibitor	97.57	P:response to stress; P:cellular process; F:hydrolase activity; P:protein metabolic process; F:enzyme regulator activity
Q4FZ50	cysteine ase inhibitor 8-like	80.82	P:cellular process; P:protein metabolic process; F:enzyme regulator activity
Q4W1F6	thioredoxin H-type	87.89	C:cytosol; C:plasma membrane; P:transport; P:response to stress; P:metabolic process; P:response to abiotic stimulus; P:cellular homeostasis; F:enzyme regulator activity
Q94KS8	beta-expansin 1a precursor	87.86	P:reproduction; C:extracellular region; C:cell wall; C:membrane; P:cellular component organization

Fonte: Daniel Ferreira Holderbaum (2019).

Tabela 3: Proteína exclusivamente expressa em culturas de milho GM AG-5011YG (MON810) em proliferação in vitro, após análise de enriquecimento de ontologias gênicas. Para ontologias gênicas, "P" indica processos biológicos, "F" indica funções moleculares, e "C" indica componentes celulares.

Nome da Seqüência	Descrição	Similaridade (%)	Ontologias gênicas
A0A1D6NEL8	mitogen-activated kinase kinase kinase A-like	76.48	F:nucleotide binding; F:obsolete signal transducer activity; C:mitochondrion; P:cellular protein modification process; C:membrane; F:kinase activity

Fonte: Daniel Ferreira Holderbaum (2019).

Tabela 4: Lista de proteínas sub-expressas (down-regulated) em culturas de milho transgênico em proliferação in vitro, após análise de enriquecimento de ontologias gênicas. Para

ontologias gênicas, "P" indica processos biológicos, "F" indica funções moleculares, e "C" indica componentes celulares.

Nome da seqüência	Descrição	Similaridade (%)	Ontologias gênicas
A0A1D6DQH1	acetyl-coenzyme A chloroplastic glyoxysomal	93.74	F:nucleotide binding; F:catalytic activity; P:carbohydrate metabolic process; P:generation of precursor metabolites and energy; P:nucleobase-containing compound metabolic process; P:catabolic process; P:biosynthetic process; C:plastid
A0A1D6DU44	cysteine protease RD21B	92.53	C:extracellular space; C:lysosome; P:catabolic process; P:cellular process; F:hydrolase activity; P:protein metabolic process
A0A1D6DUP7	beta- insoluble isoenzyme 7	79.75	C:mitochondrion; P:carbohydrate metabolic process; F:hydrolase activity
A0A1D6DVL4	H(+)-ATPase 5	98.61	F:nucleotide binding; F:transporter activity; C:intracellular; C:plasma membrane; P:generation of precursor metabolites and energy; P:nucleobase-containing compound metabolic process; P:biosynthetic process; F:hydrolase activity; P:cellular homeostasis
A0A1D6DW07	D-3-phosphoglycerate dehydrogenase chloroplastic-like	97.39	F:nucleotide binding; F:catalytic activity; P:biosynthetic process; C:plastid; P:cellular process
A0A1D6E267	fasciclin-like arabinogalactan 8	86.11	C:membrane
A0A1D6E7Z4	26S proteasome non-ATPase regulatory subunit 6	97.6	F:protein binding; C:intracellular; P:catabolic process; P:cellular process; P:protein metabolic process

A0A1D6EAC4	probable L-ascorbate peroxidase chloroplastic	96.63	F:catalytic activity; F:binding; P:carbohydrate metabolic process; P:response to stress; P:catabolic process; C:plastid; P:cellular process; C:membrane
A0A1D6EIB6	2-isopropylmalate synthase B	93.63	P:biosynthetic process; C:plastid; P:cellular process; F:transferase activity
A0A1D6EM17	hypothetical protein *ZEA*MMB73_Zm00001d005363	93.85	C:intracellular; P:DNA metabolic process; P:response to stress; P:cellular component organization; F:hydrolase activity
A0A1D6ENT5	leucine--tRNA cytoplasmic	93.75	F:nucleotide binding; C:cytosol; P:nucleobase-containing compound metabolic process; P:translation; C:membrane; F:hydrolase activity
A0A1D6F822	AAA-type ATPase family	96.31	F:nucleotide binding; F:protein binding
A0A1D6G5Q1	hypothetical protein *ZEA*MMB73_Zm00001d012004	95.1	
A0A1D6GBW9	homeodomain-like transcription factor superfamily	98.08	F:DNA binding; C:nucleus; C:plasma membrane
A0A1D6GYI3	brahma1	95.72	F:nucleotide binding; F:chromatin binding; F:protein binding; C:nucleus; C:cytosol; P:nucleobase-containing compound metabolic process; P:biosynthetic process; P:anatomical structure morphogenesis; P:cellular component organization; F:hydrolase activity; P:regulation of gene expression, epigenetic
A0A1D6H2L6	chaperone mitochondrial	95.92	F:nucleotide binding; C:mitochondrion; P:response to stress; C:plastid; P:response to abiotic stimulus; P:cellular process; P:protein metabolic process

A0A1D6H3A8	Nuclear pore complex NUP155	98.18	F:structural molecule activity; C:nuclear envelope; P:transport
A0A1D6H687	60S ribosomal L11	98.76	F:structural molecule activity; C:cytosol; C:ribosome; P:translation; P:cellular component organization
A0A1D6H6G9	P-loop nucleoside triphosphate hydrolase superfamily with CH (Calponin Homology) domain	85.32	F:nucleotide binding; F:motor activity; F:protein binding; C:cytoskeleton; P:cellular process
A0A1D6III6	pentatricopeptide repeat-containing At5g02860	87.44	F:protein binding; C:plastid
A0A1D6IXD5	non-cyanogenic beta-glucosidase precursor	87.49	P:carbohydrate metabolic process; P:signal transduction; C:plastid; P:response to endogenous stimulus; F:hydrolase activity
A0A1D6IYH3	Zinc finger BED domain-containing DAYSLEEPER	76.74	F:DNA binding; F:DNA-binding transcription factor activity; C:intracellular; P:nucleobase-containing compound metabolic process; P:biosynthetic process
A0A1D6J5X9	Dihydrolipoyllysine-residue succinyltransferase component of 2-oxoglutarate dehydrogenase complex	98.91	C:cytoplasm; P:generation of precursor metabolites and energy; P:catabolic process; P:biosynthetic process; C:membrane; F:transferase activity; P:protein metabolic process
A0A1D6JQ06	pentatricopeptide repeat-containing At5g15280	83.21	F:protein binding; C:mitochondrion
A0A1D6KA83	hypothetical protein *ZEA*MMB73_Zm00001d030134	80.36	C:intracellular; P:DNA metabolic process; P:response to stress; P:cellular component organization; F:hydrolase activity

A0A1D6KIZ4	Discolored-paralog2	92.41	C:cytoplasm; F:enzyme regulator activity
A0A1D6L2L2	translational activator GCN1	96.67	F:protein binding; P:translation; P:cellular protein modification process; P:response to stress; F:enzyme regulator activity
A0A1D6L4K3	inosine-5 -monophosphate dehydrogenase	93.86	F:nucleotide binding; F:catalytic activity; C:mitochondrion; P:nucleobase-containing compound metabolic process; P:biosynthetic process; C:membrane
A0A1D6L718	aldehyde oxidase3	92.94	F:nucleotide binding; F:catalytic activity; C:cytosol; P:nucleobase-containing compound metabolic process; P:lipid metabolic process; P:catabolic process; P:biosynthetic process
A0A1D6LFA7	heat shock 90- mitochondrial	95.61	F:nucleotide binding; F:protein binding; C:mitochondrion; P:response to stress; P:cellular process
A0A1D6LN76	Peptidyl-prolyl cis-trans isomerase CYP20-1	76.21	F:catalytic activity; C:mitochondrion; P:cellular protein modification process
A0A1D6LPH1	40S ribosomal S14-3	98.91	F:RNA binding; F:structural molecule activity; C:cytosol; C:ribosome; P:nucleobase-containing compound metabolic process; P:translation; P:cellular component organization
A0A1D6LQT2	Isoleucine--tRNA ligase cytoplasmic	96.03	F:nucleotide binding; F:RNA binding; C:cytosol; P:carbohydrate metabolic process; P:generation of precursor metabolites and energy; P:nucleobase-containing compound metabolic process; P:translation; P:response to stress; P:catabolic process; P:response to abiotic stimulus; C:membrane; P:cellular component organization; F:hydrolase activity

A0A1D6M2S2	importin subunit beta-1	95.54	F:transporter activity; F:protein binding; C:nuclear envelope; C:cytoplasm; C:membrane; P:cellular component organization
A0A1D6MAD7	respiratory burst oxidase homolog A-like	96.84	F:nucleic acid binding; F:catalytic activity; P:response to stress; P:metabolic process; P:cellular process; C:membrane
A0A1D6MAM0	kinesin-related 3	88.02	F:nucleotide binding; F:motor activity; F:protein binding; C:cytoskeleton; P:cellular process
A0A1D6MMZ3	D -box ATP-dependent RNA helicase D 3	91.58	F:nucleotide binding; F:nucleic acid binding; C:nucleus; C:cytoplasm; P:carbohydrate metabolic process; P:generation of precursor metabolites and energy; P:nucleobase-containing compound metabolic process; P:catabolic process; P:biosynthetic process; F:hydrolase activity
A0A1D6MR41	Retrovirus-related Pol poly LINE-1	97.85	F:structural molecule activity; F:binding; C:Golgi apparatus; P:transport; C:membrane
A0A1D6MSE3	dihydrolipoyl dehydrogenase mitochondrial	97.01	F:nucleotide binding; F:catalytic activity; C:mitochondrion; P:carbohydrate metabolic process; P:generation of precursor metabolites and energy; P:nucleobase-containing compound metabolic process; P:catabolic process; P:biosynthetic process; P:cellular homeostasis
A0A1D6N4X2	60S ribosomal L5-1	97.4	F:RNA binding; F:structural molecule activity; C:cytosol; C:ribosome; P:translation; P:cellular component organization

A0A1D6NAN3	Branched-chain-amino-acid aminotransferase 5 chloroplastic	90.39	
A0A1D6NVF9	Nucleosome assembly 1	94.37	C:nucleus; C:cytoplasm; P:cellular component organization
A0A1D6NVK8	Coatomer subunit beta -3	97.53	F:structural molecule activity; F:protein binding; C:Golgi apparatus; P:transport; C:membrane
A0A1D6PPA4	Galactose oxidase kelch repeat superfamily	90.88	F:protein binding; C:mitochondrion
A0A1D6PUE6	hypothetical protein *ZEA*MMB73_Zm00001d049396	90.47	C:intracellular; P:DNA metabolic process; P:response to stress; P:cellular component organization; F:hydrolase activity
B4F9I2	ruvB 1	97.97	F:nucleotide binding; C:nucleolus; C:cytosol; P:nucleobase-containing compound metabolic process; P:response to stress; P:biosynthetic process; C:plastid; P:response to external stimulus; P:response to biotic stimulus; P:cellular component organization; F:hydrolase activity
B4FAM6	60S ribosomal L13a-4	98.37	F:RNA binding; F:structural molecule activity; C:cytosol; C:ribosome; P:translation
B4FCG9	60S ribosomal L11	99.75	F:RNA binding; F:structural molecule activity; C:cytosol; C:ribosome; P:translation; P:cellular component organization
B4FDB1	cinnamoyl- reductase 2	91.14	F:catalytic activity; F:binding
B4FFA5	probable inactive purple acid phosphatase 27	92.07	F:binding; P:metabolic process; P:cellular process; F:hydrolase activity

B4FH75	probable 4-hydroxy-tetrahydrodipicolinate reductase chloroplastic	91.02	F:nucleotide binding; F:catalytic activity; P:biosynthetic process; C:plastid; P:cellular process
B4FHX3	60S ribosomal L23	100.0	F:RNA binding; F:structural molecule activity; C:nucleolus; C:cytosol; C:ribosome; P:translation
B4FHX7	endo-1,3 1,4-beta-D-glucanase-like	86.36	F:hydrolase activity
B4FLZ9	hypothetical protein	86.35	
B4FP25	40S ribosomal S19	96.44	F:nucleic acid binding; F:structural molecule activity; C:cytosol; C:ribosome; P:DNA metabolic process; P:translation; P:cellular component organization
B4FPM1	DJ-1 homolog D	94.34	P:catabolic process; P:biosynthetic process; P:cellular process; F:hydrolase activity; P:protein metabolic process
B4FPZ7	like isoform X2	82.83	F:nucleotide binding; F:protein binding; C:mitochondrion; P:cellular process; F:enzyme regulator activity
B4FZC0	multiple organellar RNA editing factor mitochondrial-like	79.43	C:mitochondrion
B4G1P4	GTP-binding nuclear Ran-2	98.11	F:nucleotide binding; C:nucleus; C:cytoplasm; P:transport; P:signal transduction; F:hydrolase activity

B6SHF6	mitochondrial-processing peptidase subunit alpha	91.08	F:nucleotide binding; C:mitochondrion; C:cytosol; P:carbohydrate metabolic process; P:generation of precursor metabolites and energy; P:nucleobase-containing compound metabolic process; P:transport; P:catabolic process; P:biosynthetic process; C:membrane; P:cellular component organization; F:kinase activity; F:hydrolase activity; P:protein metabolic process; P:cellular homeostasis; F:carbohydrate binding
B6SHM7	40S ribosomal S7	97.32	F:structural molecule activity; C:cytosol; C:ribosome; P:nucleobase-containing compound metabolic process; P:translation
B6SIG8	60S acidic ribosomal P2A	98.08	F:RNA binding; F:structural molecule activity; C:cytosol; C:ribosome; P:translation
B6SJ08	60S ribosomal L18-3	97.64	F:RNA binding; F:structural molecule activity; C:cytosol; C:ribosome; P:translation
B6SNQ1	universal stress	90.41	P:response to stress
B6SS31	hydroxyproline-rich glyco family	91.02	
B6SSB7	cysteine-rich repeat secretory 55-like	83.91	F:kinase activity
B6SUP5	allene oxide synthase	92.14	F:catalytic activity; F:binding; P:lipid metabolic process; P:biosynthetic process; P:cellular process
B6T1R0	60S ribosomal L22-2	97.68	F:structural molecule activity; C:cytosol; C:ribosome; P:translation
B6T3D4	methionyl-tRNA synthetase	86.42	F:RNA binding; F:catalytic activity; C:cytosol; P:nucleobase-containing compound metabolic process; P:translation

B6T4R3	UDP-glucose pyrophosphorylase	97.7	C:cytoplasm; P:carbohydrate metabolic process; P:nucleobase-containing compound metabolic process; F:transferase activity
B6T7L9	14-3-3 GF14-D	96.77	F:protein binding
B6TB39	fructokinase-2	97.09	F:nucleotide binding; P:carbohydrate metabolic process; P:biosynthetic process; F:kinase activity
B6TGT0	60S ribosomal L8	98.76	F:RNA binding; F:structural molecule activity; C:cytosol; C:ribosome; P:translation
B6TKY3	T-complex 1 subunit alpha	97.86	F:nucleotide binding; F:protein binding; C:cytosol; P:cellular process
B6TNR8	40S ribosomal S2-3	96.71	F:RNA binding; F:structural molecule activity; C:cytosol; C:ribosome; P:translation
B6TPA2	hypothetical protein	90.87	C:mitochondrion
B6TRV0	membrane steroid-binding 1	82.37	F:binding; C:cell; P:generation of precursor metabolites and energy; C:membrane
B6TYG2	Enoyl-[acyl-carrier-] reductase [NADH] chloroplastic	91.8	C:cytosol; P:lipid metabolic process; P:biosynthetic process; C:plastid; P:cellular process; F:transferase activity; P:protein metabolic process
B6U118	T-complex 1 subunit zeta 1	98.28	F:nucleotide binding; F:protein binding; C:cytoplasm; P:cellular process
B6UAD0	26S proteasome non-ATPase regulatory subunit 13 homolog A	96.54	F:structural molecule activity; F:protein binding; C:nucleus; C:cytosol; P:catabolic process; P:cellular component organization; P:protein metabolic process

B7ZXI9	Phosphoinositide phosphatase SAC1	91.43	P:carbohydrate metabolic process; P:cellular protein modification process; P:lipid metabolic process; P:multicellular organism development; P:catabolic process; P:biosynthetic process; P:anatomical structure morphogenesis; P:cellular component organization; P:cell growth; F:hydrolase activity; P:cell differentiation
B8A312	glucose-6-phosphate 1-epimerase	93.55	F:catalytic activity; P:carbohydrate metabolic process; F:carbohydrate binding
C0P3L1	phosphoenolpyruvate carboxykinase1	98.38	F:nucleotide binding; C:cytosol; P:carbohydrate metabolic process; P:generation of precursor metabolites and energy; P:biosynthetic process; F:kinase activity
C0P4M0	monodehydroascorbate reductase	94.17	F:nucleotide binding; F:catalytic activity; C:cell; P:carbohydrate metabolic process; P:generation of precursor metabolites and energy; P:cellular homeostasis
C0PCV2	40S ribosomal S8	95.31	F:structural molecule activity; C:cytosol; C:ribosome; P:nucleobase-containing compound metabolic process; P:translation
C0PD27	isocitrate dehydrogenase [NADP]	97.65	F:nucleotide binding; F:catalytic activity; P:generation of precursor metabolites and energy
C4J093	Adenylate kinase 4	96.15	F:nucleotide binding; C:cytoplasm; P:nucleobase-containing compound metabolic process; F:kinase activity
C4J4W3	hsp70-Hsp90 organizing	93.89	F:protein binding; C:nucleus; C:cytoplasm; P:cellular component organization
C4J6J5	40S ribosomal S6	99.26	F:structural molecule activity; C:cytosol; C:ribosome; P:nucleobase-containing compound metabolic process; P:translation

C4J9R8	Anaphase-promoting complex subunit 10	93.73	C:nucleoplasm; P:DNA metabolic process; P:cellular protein modification process; P:cell cycle; P:catabolic process; P:biosynthetic process; P:cellular component organization
K7TQM8	DNA mismatch repair	93.25	P:reproduction; F:nucleotide binding; F:DNA binding; C:nucleus; P:DNA metabolic process; P:response to stress; P:cell cycle; P:cellular component organization
K7U267	glucose-6-phosphate 1-dehydrogenase chloroplastic	93.46	F:nucleotide binding; F:catalytic activity; C:mitochondrion; P:carbohydrate metabolic process; P:nucleobase-containing compound metabolic process; C:plastid
K7U884	Increased DNA methylation 1	99.62	F:binding
K7UDG5	proline--tRNA cytoplasmic	96.67	F:nucleotide binding; F:RNA binding; F:catalytic activity; C:cytoplasm; P:nucleobase-containing compound metabolic process; P:translation
K7UQL4	DCD (Development and Cell Death) domain	75.89	F:protein binding; C:intracellular; P:cellular protein modification process; F:transferase activity
K7UZU9	Luminal-binding 2	96.84	F:nucleotide binding; C:endoplasmic reticulum; P:cellular protein modification process; F:kinase activity
K7V3I5	tubulin beta-5 chain	99.98	F:nucleotide binding; F:structural molecule activity; C:cytoplasm; C:cytoskeleton; P:cellular process; F:hydrolase activity
K7V934	Pentatricopeptide repeat-containing mitochondrial	85.6	F:protein binding; P:nucleobase-containing compound metabolic process
K7V958			F:structural molecule activity;

			C:ribosome; P:translation
K7VI04	Glutamate--cysteine ligase chloroplastic	94.96	F:nucleotide binding; F:nucleic acid binding; F:catalytic activity; C:mitochondrion; P:response to stress; P:biosynthetic process; C:plastid; P:response to external stimulus; P:response to biotic stimulus; P:response to abiotic stimulus; P:flower development; P:cellular component organization; P:secondary metabolic process
K7VXH3	serine arginine repetitive matrix 1 isoform X1	86.74	
K7WGQ3	multiple organellar RNA editing factor chloroplastic mitochondrial	95.1	
O48557	60S ribosomal L17	97.15	F:structural molecule activity; C:ribosome; P:translation
P93804	cytoplasmic 2	97.66	F:catalytic activity; F:binding; C:cytosol; P:carbohydrate metabolic process; P:generation of precursor metabolites and energy; P:nucleobase-containing compound metabolic process; P:catabolic process; P:biosynthetic process; C:plastid; P:response to external stimulus; P:response to abiotic stimulus
Q43712	Calreticulin precursor	99.02	F:protein binding; C:endoplasmic reticulum; P:cellular process; F:carbohydrate binding
Q71RX2	isopentenyl-diphosphate Delta-isomerase I	97.09	C:ribosome; P:lipid metabolic process; F:translation factor activity, RNA binding; F:hydrolase activity

Fonte: Daniel Ferreira Holderbaum (2019).